The Role of Phosphoinositides in the Regulation of NADPH Oxidase Activation in Neutrophils

Zhimin Song

NNT : 2017SACLS152

THÈSE DE DOCTORAT
DE
L'UNIVERSITÉ PARIS-SACLAY
PRÉPARÉE A
L'UNIVERSITÉ PARIS-SUD

ÉCOLE DOCTORALE N° 568
SIGNALISATION ET RÉSEAUX INTÉGRATIFS EN BIOLOGIE
SPÉCIALITÉ DE DOCTORAT : ASPECTS MOLÉCULAIRES ET CELLULAIRES DE LA BIOLOGIE

Par

M. ZHIMIN SONG

THE ROLE OF PHOSPHOINOSITIDES IN THE REGULATION OF NADPH OXIDASE ACTIVATION IN NEUTROPHILS

Thèse présentée et soutenue à Orsay, le 12 Juillet 2017 :

Composition du Jury :

Mme **CUIF-LORDEZ Marie-hélène**, Professeure, Université Paris-Sud, Présidente du Jury
M. **ZAHRAOUI Ahmed**, Directeur de Recherche, Institut Cochin, Rapporteur
Mme **BRÉCHARD Sabrina**, Chargé de Recherche, Université du Luxembourg, Rapporteuse
Mme **JACKSON Catherine**, Directrice de Recherche, Institut Jacques Monod, Examinatrice
Mme **BACIOU Laura**, Directrice de Recherche, Université Paris-Sud, Examinatrice
Mme **DUPRÉ-CROCHET Sophie**, Maître de Conférence, Université Paris-Sud, Directrice de thèse

ACKNOWLEDGEMENTS

I would like to express my deepest gratitude to my advisor Dr. **DUPRÉ Sophie** for the continuous support of my Ph.D. study and related research. Importantly, I thank her for her excellent guidance, immense knowledge, caring, patience, and providing me with an excellent atmosphere for doing research. Her guidance helped me in all the time of research and writing of this thesis.

I would like to thank the members of my committee, Dr. **ZAHRAOUI Ahmed**, Dr. **BRÉCHARD Sabrina**, Dr. **CUIF-LORDEZ Marie-Hélène**, Dr. **JACKSON Catherine**, and Dr. **BACIOU Laura** for their advice and helpful comments on my research work.

I greatly appreciate Dr. **NÜßE Oliver** for his continuous support, sharing of ideas and knowledge, and guidance for the experiments and writing. I would like to thank other members in the phagocyte lab for their kind help and support: **HUDIK Elodie**, **BOUCHAB Leïla** and **JOLY Jérémy**. I had a wonderful time working with all the members in the Phagocyte Lab.

I wish to express my appreciation to all the colleagues in the Inserm U1174 for their knowledge and friendship, in particular Dr. **NG-BONAVENTURE Kim**, **GROSSE Brigitte**, **LAPIERRE Claudine**, Dr. **BOUCHERIE Sylviane**, **PRIGENT Sylvie**, **DOIGNON Isabelle**, **GARCIN Isabelle**, **COLLADO-HILLY Mauricette**, **FAYOL Olivier**, and Dr. **COMBETTES Laurent**.

I would like to thank all the members in LCP for their kindness and assistance, especially Dr. **ERARD Marie**, Dr. **LEDERER Florence**, Dr. **BIZOUARN Tania** and Dr. **BRUN Emilie**.

I would like to thank the members in I2BC (Platform Imagif) who have always been instrumental and supportive, in particular **LE BARS Romain**, **BESSE Laëtitia**, and **BOURGE Mickael**.

I would like to thank all the members in the group of Dr. **EL BENNA Jamel**, in particular **DANG Pham My-Chan**, for their kind assistance for blood experiment.

I would like to express my appreciation to all of my friends for the friendship and support: **SONG Yuxiang**, **CAO Jing**, **SAFYA Hanna**, **ZIEGLER Cornelia**, **MELLOUK Amine**, **VILLEMAIN Laure**, **LE GUILCHER Camille**, and all the friends from the "**La Pacaterie**" group.

I am so grateful to **CSC (Chinese Scholarship Council)** and **Université Paris-Sud** for making it possible for me to study in France.

Finally, I am continually thankful for the love and support of my parents (**SONG Baolin** and **CAO Fenghua**), my brother (**SONG Zhiguo**), my sister (**SONG Qingzhen**), and my girlfriend (**YANG Xiuna**).

TABLE OF CONTENTS

LIST OF TABLES

LIST OF FIGURES

CHAPTER ONE

CHAPTER TWO

CHAPTER THREE

CHAPTER FOUR

ABBREVIATIONS

AD	**Activation domain**
ADMIDAS	**site adjacent to MIDAS**
AIR	**Auto-inhibitory region**
AML	**Acute myeloid leukemia**
ANCA	**Anti-neutrophil cytoplasmic antibody**
bTD	**b tail domain**
CDG	**Chronic granulomatous disease**
CG	**Cathepsin G**
CIB	**Calcium-and integrin-binding protein**
CLP	**Common lymphoid progenitor**
CLR	**C-type lectin receptor**
CMP	**Common myeloid progenitor**
CR3	**Complement receptor 3**
DAG	**Diacyl glycerol**
DAMP	**Damage associated molecular pattern**
DAP12	**DNAX activation protein of 12 kDa**
DC	**Dendritic cell**
ECM	**Extracellular matrix**
EGF	**Epidermal growth factor**
ER	**Endoplasmic reticulum**
ESL-1	**E-selectin ligand 1**
FAK	**Focal adhesion-kinase**
FcR	**Fc receptor**
FPR	**Formyl peptide receptor**
GAP	**GTPase activating protein**
G-CSF	**Granulocyte colony stimulating factor**
GDI	**Guanine nucleotide dissociation inhibitor**
GEF	**Guanine nucleotide exchange factor**
GM-CSF	**Granulocyte macrophage colony-stimulating factor**
GMP	**granulocyte-macrophage progenitor**
GPCR	**G-protein-coupled receptor**
HSC	**Hematopoietic stem cell**

ICAM	**Intercellular adhesion molecule**
ICAP-1	**Cytoplasmic domain associated protein-1**
ILK	**Integrin-linked kinase**
ITAM	**Immunoreceptor tyrosine-based activation motif**
ITIM	**Immunoreceptor tyrosine-based inhibitory motif**
JAK	**Janus kinase**
JNK	**c-Jun N-terminal kinase**
LAD	**Leukocyte adhesion deficiency**
LAF-1	**Lymphocyte function-associated antigen 1**
LPS	**Lipopolysaccharide**
LTB4	**Leukotriene B4**
Mac-1	**Macrophage-1 antigen**
MBL	**Mannan-binding lectin**
MEP	**Megakaryocyte-erythroid progenitor**
MIDAS	**Metal-ion-dependent adhesive site**
MPO	**Myeloperoxidase**
MTM	**Myotubularin**
NCF	**Neutrophil cytosol factor**
NE	**Neutrophil elastase**
NETs	**Neutrophil extracellular traps**
NF-κB	**nuclear factor κB**
NGAL	**Neutrophil gelatinase-associated lipocalin**
NLR	**Nucleotide-binding oligomerization domain-like receptor**
PA	**Phosphatidic acid**
PAMP	**Pathogen associated molecular pattern**
PB1	**Phox and Bem1**
PBR	**Polybasic region**
PDGF	**Platelet derived growth factor**
PI3P	**Phosphatidylinositol 3-phosphate**
PI(3,4)P_2	**Phosphatidylinositol (3,4)-biphosphate**
PI(4,5)P_2	**Phosphatidylinositol (4,5)-bisphosphate**
PI(3,4,5)P_3	**Phosphatidylinositol (3,4,5)-trisphosphate**
PI3K	**Phosphoinositide 3-kinase**

PI4K	**Phosphoinositide 4-kinase**
PI4P	**Phosphatidylinositol 4-phosphate**
PITP	**PtdIns transfer protein**
PKC	**Protein kinase C**
PLCγ	**Phospholipase Cγ**
PR3	**Proteinase 3**
PRR	**Pathogen recognition receptor**
PRR	**Proline-rich region**
PS	**Phosphatidylserine**
PSGL-1	**P-selectin ligand 1**
PSI	**Plexin/semaphorin/intergrin**
PSM	**Phenol-soluble modulin**
PTB	**Phosphotyrosine-binding**
PTEN	**Phosphatase and tensin homolog**
PTP	**Protein tyrosine phosphatase**
PX	**Phox homology**
Rack1	**Receptor for activated C kinase 1**
RIAM	**Rap-1-mediated adaptor molecule**
RLR	**RIG-I-like receptor**
ROCK	**Rho-associated protein kinase**
ROS	**Reactive oxygen species**
Rubicon	**(RUN domain protein as Beclin-1 interacting and cysteine-rich containing**
SH3	**Src homology3**
SLE	**Systemic lupus erythematosus**
SNARE	**Soluble N-ethylmaleimide sensitive factor or N-ethylmaleimide sensitive fusion protein**
t-SNARE	**target-membrane-specific SNARE**
v-SNARE	**vesicle-membrane-specific SNARE**
SOCS	**Suppressor of cytokine signaling**
SOD	**Superoxide dismutase**
STAT	**Signal transducers and activators of transcription**
Syk	**spleen tyrosine kinase**
TLR	**Toll-like receptor**
TNF-α	**tumor necrosis factor-α**

TPR	**Tetratricopeptide repeat**
VAMP2	**Vesicle- associated membrane protein-2**
VCAM-1	**Vascular cell adhesion protein 1**
Vps34	**Vacuolar protein sorting 34**

CHAPTER ONE: Introduction

1.1 Neutrophil biology

1.1.1 The immune system

The human anti-microbial defense system includes 3 different levels: (1) anatomic and physiologic barriers; (2) innate immunity; and (3) adaptive immunity **(Figure 1)**. Failure in any of these systems will greatly increase susceptibility to infection (Turvey and Broide, 2010). The innate immune system first appeared 750 million years ago and has been notably conserved throughout the evolutionary tree of life. The innate immune system is the first line of defense against infection or self-damaged tissue injury (Hato and Dagher, 2014). Both innate and adaptive immune responses depend upon the activities of leukocytes (white blood cells) (Murphy, 2012). Neutrophils take up for 50% to 70% of all circulating leukocytes in humans (Mayadas et al., 2014). Neutrophils are highly motile and respond to a wide range of stimuli, especially pathogen- and damage-associated molecular patterns (PAMPs and DAMPs) (Jones et al., 2016). Researchers first believed that neutrophils were playing a passive role functioning only as pathogen killers. This view is not more prevailing since recent data suggest that activated neutrophils are able to also perform most of macrophages functions. Neutrophils can communicate with macrophages, dendritic cells (DCs) and cells of the adaptive immune response through direct cell-cell contacts or soluble mediators (Mayadas et al., 2014; Wright et al., 2010).

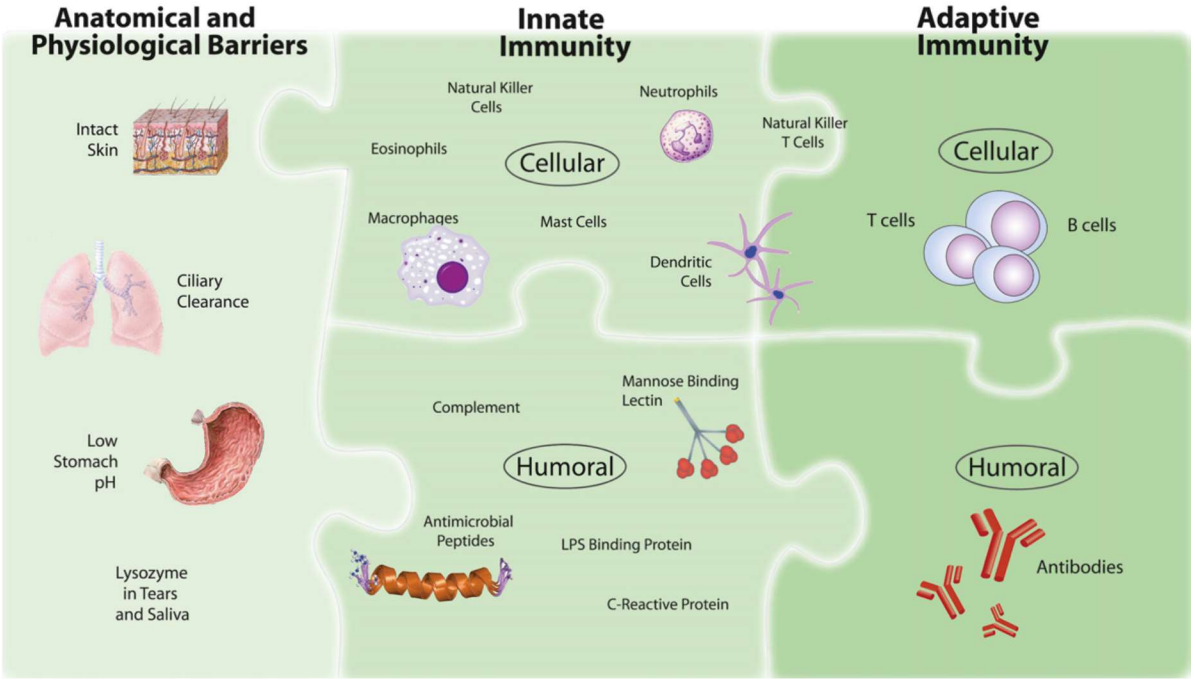

Figure 1. Integrated human immune system.

The human microbial defense system consists of 3 levels: (1) **Anatomic and physiologic barriers**. These barriers include intact skin, vigorous mucociliary clearance mechanisms, low stomach pH, and bacteriolytic lysozyme in tears, saliva, and other secretions. (2) **Innate immunity.** Hematopoietic cells including macrophages, dendritic cells, mast cells, neutrophils, eosinophils, natural killer (NK) cells, and NK T cells are involved in innate immunity. The skin and the epithelial cells lining the respiratory, gastrointestinal, and genitourinary tracts are also involved in innate immunity. Innate immunity augments the protection offered by anatomic and physiologic barriers and plays a central role in activating the subsequent adaptive immune response. (3) **Adaptive immunity.** T and B lymphocytes are the main self-defensive weapons of the adaptive immune system. Some elements are difficult to categorize, e.g. NK T cells and dendritic cells are classified as being on the cusp of innate and adaptive immunity rather than being firmly in one side (Turvey and Broide, 2010).

1.1.2 Neutrophil activation

1.1.2.1 Neutrophil production

Neutrophils come from hematopoietic stem cells (HSCs) **(Figure 2)**. HSCs reside in bone marrow and produce all blood cells. HSCs localize to niches provided by osteoblasts, where there is little blood flow and low oxygen tension. The more mature and actively dividing stem cells localize close to the abluminal side of the sinusoids, which is a special vascular structure of the bone marrow (Borregaard, 2010; Winkler et al., 2010). Neutrophils are generated at a rate of 1 to $2x10^{11}$ per day in a normal adult human. Granulocyte colony stimulating factor (G-CSF) and granulocyte macrophage colony-stimulating factor (GM-CSF) are essential to trigger neutrophil production during infections. However, they are not absolutely required. Indeed mice lacking one or both of these cytokines still have approximately 20% of the normal level of fully mature neutrophils (Borregaard, 2010; Hibbs et al., 2007; Mayadas et al., 2014). Mature neutrophils leave the bone marrow and enter the circulation.

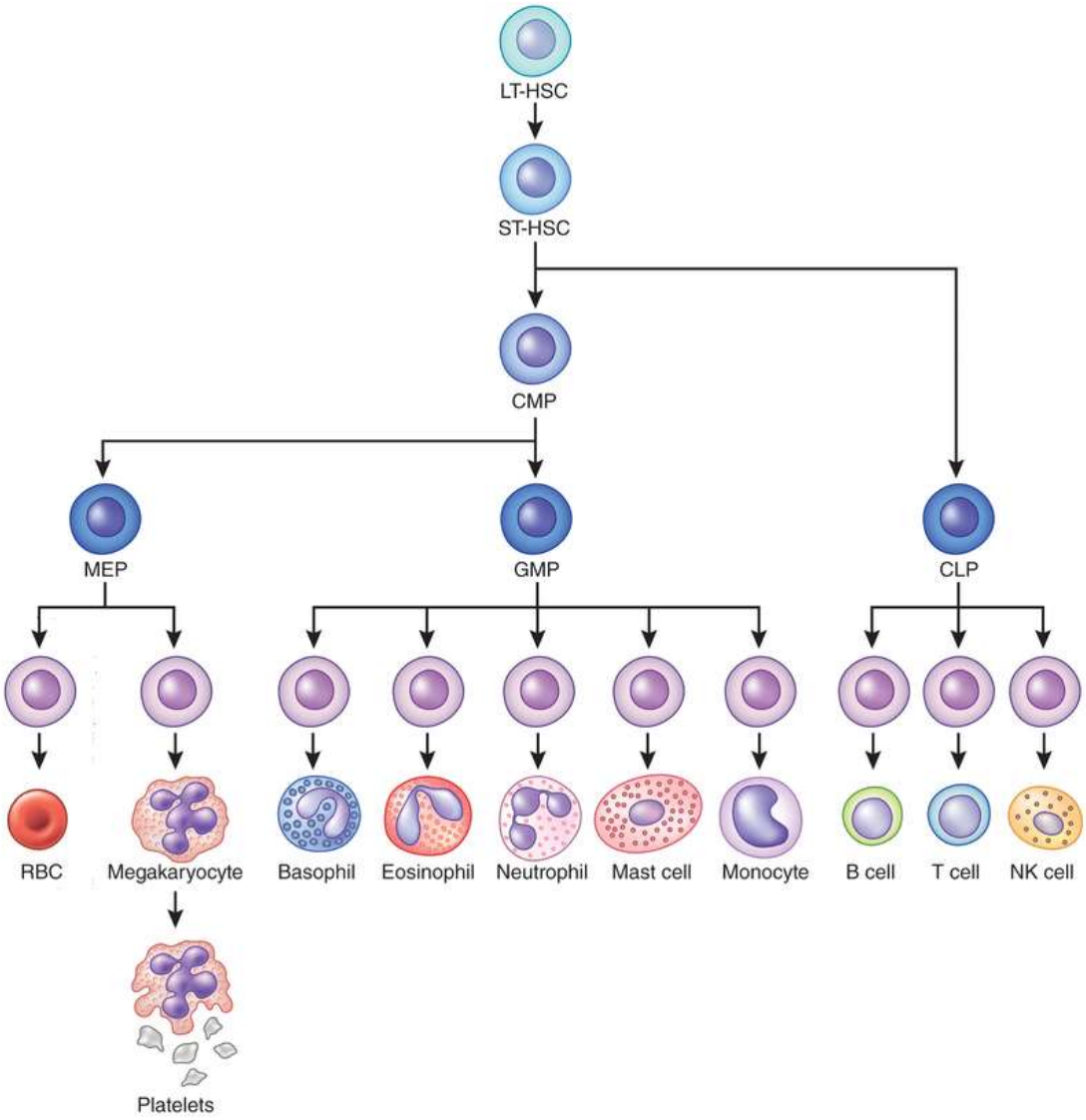

Figure 2. Differentiation of the hematopoietic lineages.

The long-term hematopoietic stem cell (LT-HSC) gives rise to short-term hematopoietic stem cells (ST-HSCs) that then give rise to the multipotent common myeloid progenitor (CMP) and common lymphoid progenitor (CLP). The CMP are the precursor of the megakaryocyte-erythroid progenitors (MEPs) and granulocyte-macrophage progenitors (GMPs). The maturation of lineage-committed erythroid progenitors is shown on the left side. MEPs give rise to erythrocytes, megakaryocytes and platelets. GMP give rise to eosinophils, basophils, neutrophils and monocytes/macrophages.CLP are the precursors of the B cells, T cells and Natural Killer (NK) cells. *Adapted from* (Sankaran and Weiss, 2015).

1.1.2.2 Neutrophil recruitment

Mature neutrophils will reach the sites of tissue inflammation or infection through postcapillary venules where the vessel wall is rather thin and the neutrophils can make contact with the endothelium. Neutrophil recruitment consists of the following steps: (1) capture, i. e. an initial attachment of the neutrophil to the endothelium, (2) rolling of the neutrophil along the endothelium, (3) firm arrest of the neutrophil with accompanying cell spreading, (4) crawling of the neutrophil along the endothelium, (5) transmigration of the neutrophil into the tissue **(Figure 3)** (Mayadas et al., 2014).

1.1.2.2.1 Rolling

TNF (tumor necrosis factor)-α, IL-1β, or IL-17 which are generated by immune cells during inflammation or infection result in stimulation of endothelial cells. Such stimulation leads to expression of P-selectin, E-selectin and members of the integrin superfamily on their luminal surface. Neutrophils constitutively express P-selectin glycoprotein ligand 1 (PSGL-1) and L-selectin, which bind other selectins on endothelial cells. PSGL-1 binding to P-selectin and E-selectin constitutes the initial contact between neutrophils and activated endothelial cells. Neutrophils also express E-selectin ligand 1 (ESL-1) and CD44, which bind both to E-selectin on endothelial cells. ESL-1 binding to E-selectin mediates the slower rolling, while CD44 binding to E-selectin contributes to a redistribution of PSGL-1 and L-selectin to form clusters. Ligands binding to PSGL-1 and CD44 activate Src family kinase (Hcr, Fgr, and Lyn), which activate DAP12 (DNAX activation protein of 12 kDa) and FcRγ (γ chain of immunoglobulin Fc receptors). DAP12 and FcRγ recruit and active spleen tyrosine kinase (Syk). Activated Syk mediates further activation of phospholipase Cγ (PLCγ), phosphoinositide 3-kinase (PI3K) and p38 mitogen-activated protein kinase (Borregaard, 2010; Hidalgo et al., 2007).

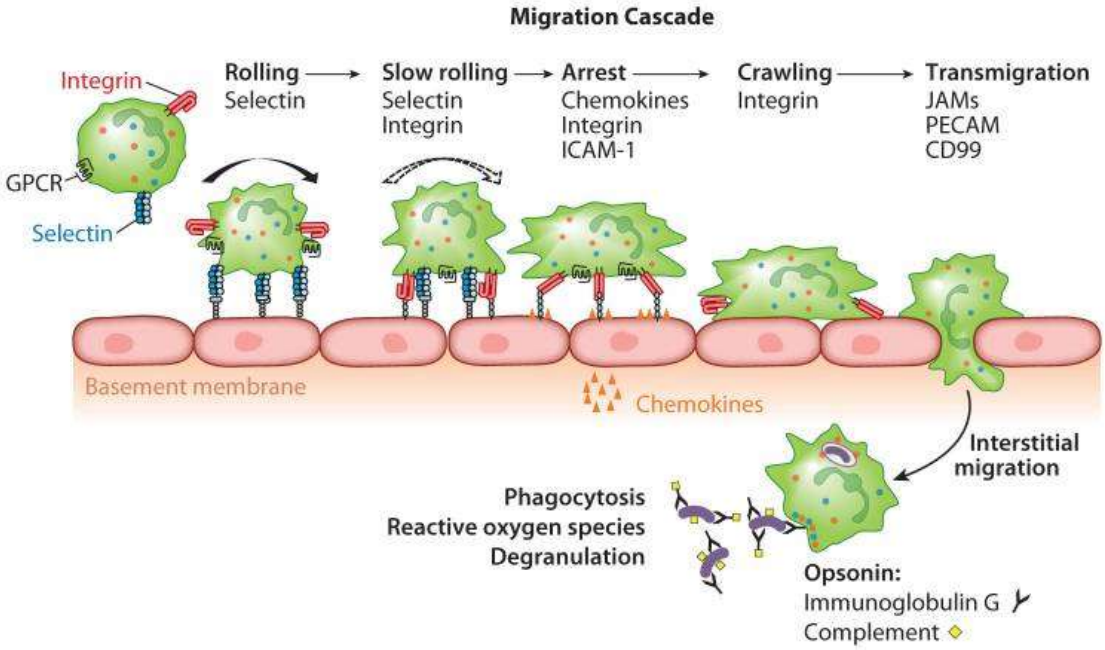

Figure 3. Neutrophils recruitment to the sites of inflammation.

Neutrophils attachment and rolling on the endothelium is mediated by the transient interaction of selectins/ligands. Selectins mediate the rolling of neutrophils along chemoattractant gradients, then integrins mediate the firm adhesion. Subsequently, the neutrophils transmigrate through the endothelium and arrive at the site of inflammation. Neutrophils kill pathogens through degranulation, phagocytosis and production of reactive oxygen species (Mayadas et al., 2014).

1.1.2.2.2 Firm adhesion

Firm adhesion is mediated by the β2 integrins LAF-1 (αLβ2) and αMβ2 (Mac-1) on neutrophils, with their ligands on endothelial cells: intercellular adhesion molecule-1 (ICAM-1) and ICAM-2. Before activation, integrins are in a bent conformation unable of binding the ligand. Then, upon inside-out activation (described below) due to selectin interaction, the conformation changes: the head of the integrin unfolds giving rise first to the "extended" conformation with a closed ligand-binding head that is of intermediate affinity for ligand binding, then to the "open extended" conformation with higher affinity for the ligand (Evans et al., 2009). As mentioned in the "Rolling" part, ligands binding between neutrophils and endothelial cells results in the activation of PLCγ in neutrophils. Activated PLCγ catalyses the hydrolysis of phosphatidylinositol (4,5) bisphosphate to produce diacyl glycerol (DAG) and inositol-3-phosphate (IP3), which actives protein kinase C (PKC) and induces a rise of intracellular Ca^{2+}. This rise in Ca^{2+} activates the guanine exchange factor CalDAG-GEF1 which activates small GTPase Rap-1. Activated Rap-1 binds Rap-1-mediated adaptor molecule (RIAM), which recruits talins to bind to β chains of integrins and twist the two integrin (α and β) chains apart inducing a conformational change in the ectodomain and ligand binding. Talins tether the integrins to the actin skeleton. The activated integrin induces then an outside-in signalling (see below part) and cytoskeletal rearrangements in neutrophils (Borregaard, 2010).

1.1.2.2.3 Tissue neutrophils

Neutrophils migrate through the endothelial cell barrier in two ways: (1) paracellular way in which neutrophils squeeze between endothelial cells, (2) transcellular way in which neutrophils penetrate the individual endothelial cell. Both ways need the neutrophil integrins LFA-1 and αMβ2 and their ligands ICAM-1 and ICAM-2 (Borregaard, 2010; Mayadas et al., 2014). After their migration into tissues, neutrophils are more active as phagocytic cells than blood neutrophils (Sorensen et al., 2001). The migration of neutrophils in tissues distant from the site of injury is not dependent on activated β2 integrins (Nauseef and Borregaard, 2014). Neutrophils migrate to the site of injury in two waves of recruitment after leaving circulation. Firstly, neutrophils adjacent to the site of injury migrate toward the infection locus, then a second 'swarm' of neutrophils are recruited more than 200 μm from the site of tissue injury. Neutrophils in the reaction centre produce leukotriene B4 (LTB4), which drives the long-distance migration (Nauseef and Borregaard, 2014).

1.1.2.3 Neutrophil receptors

Neutrophil activation is a key step in the inflammatory response. Pre-activation of neutrophils upon exposure to stimuli such as lipopolysaccharide (LPS), TNF, chemokines, growth factors (which is also called neutrophil priming) or upon adhesion induces an enhanced response to a second stimulus such as fMLF (Mayadas et al., 2014). Neutrophils express numerous surface receptors involved in the recognition of microbial infection. Some of the receptors recognize microbial structures, others are related to the activation of adaptive immune response, while others recognize the inflammatory environment (Futosi et al., 2013b). Neutrophils express several class of receptors on the surface, including G-protein-coupled receptors (GPCRs), Fc-receptors, adhesion receptors such as selectins/selectin ligands and integrins, various cytokine receptors and innate immune receptors such as Toll-like receptors and C-type lectins**.** Neutrophil receptors are summarized in **Table 1** and selected ones are described in details below.

Table 1. Neutrophil receptors

The most important neutrophil receptors (Futosi et al., 2013a).

G-protein-coupled receptors	Fc-receptors	Adhesion receptors	Cytokine receptors	Innate immune receptors
Formyl-peptide receptors • FPR1 (FPR) • FPR2 (FPRL1) • FPR3 (FPRL2) *Classical chemoattractant receptors* • BLT1 (LTB_4-rec.) • BLT2 (LTB_4-rec.) • PAFR • C5aR *Chemokine receptors* • CXCR1 (human) • CXCR2 • CCR1 • CCR2	*Fcγ-receptors* • FcγRI • FcγRIIA (human) • FcγRIIB (inhibitory) • FcγRIII (mouse) • FcγRIIIB (human) • FcγRIV (mouse) *Fcα-receptors* • FcαRI (human) *Fcε-receptors* • FcεRI • FcεRII	*Selectins and selectin ligands* • L-selectin • PSGL-1 *Integrins* • LFA-1 ($\alpha_L\beta_2$) • Mac-1 ($\alpha_M\beta_2$) • VLA-4 ($\alpha_4\beta_1$)	*Type I cytokine receptors* • IL-4R • IL-6R • IL-12R • IL-15R • G-CSFR • GM-CSFR *Type II cytokine receptors* • IFNAR (IFNα/β-rec) • IFNGR • IL-10R *IL-1R family* • IL-1RI • IL1RII (decoy) • IL-18R *TNFR family* • TNFR1 (p55) • TNFR2 (p75) • Fas • LTβR • RANK • TRAIL-R2 • TRAIL-R3	*Toll-like receptors* • TLR1 • TLR2 • TLR4 • TLR5 • TLR6 • TLR7 (?) • TLR8 • TLR9 *C-type lectins* • Dectin-1 • Mincle • MDL-1 • Mcl • CLEC-2 *NOD-like receptors* • NOD2 • NLRP3 *RIG-like receptors* • RIG-I • MDA5

1.1.2.3.1 G-protein-coupled receptors

Neutrophil express a large number of GPCRs including formyl peptide receptors (FPRs), classical chemoattractant receptors and chemokine receptors. These GPCRs strongly activate the chemotactic migration of neutrophils. Activation of the GPCRs triggers the dissociation of the Gα subunit from the Gβγ dimer and subsequently activate various signal pathways. One is the calcium signalling pathway. Gβγ dimer active phospholipase Cβ (PLCβ) leading to the generation of IP3 and DAG. IP3 triggers the release of intracellular Ca^{2+} and DAG activates some isoforms of the PKC. The other one is the phosphatidylinositol (PtdIns) 3-kinase (PI3-kinase or PI3K) pathway. Gβγ dimer stimulates PI3Kγ isoforme, which leads to the generation of PIP3. PIP3 further activate Akt and ERK. Src tyrosine kinase (Hck, Fgr and Lyn) may be involved in neutrophil GPCR signalling. The mechanism of Src-family kinase activation by neutrophil GPCRs is poorly understand, it could be mediated by the direct interaction of Src-family kinase with β-arrestins, G-protein subunits or the GPCRs themselves **(Figure 4.)** (Futosi et al., 2013b).

Formyl-peptide receptors

Human neutrophils have three FPRs: FPR1 (FPR), FPR2 (lipoxin A4 (LXA4) receptor (ALX) or FPR-like receptor (FPRL)-1) and FPR3 (FPRL-2). These receptors bind numerous agonistic ligands including N-formyl and non-formyl peptides of different composition. FPR1 and FPR2 respond to very low concentrations of bacterial formyl peptides and phenol-soluble modulins (PSMs) (Kretschmer et al., 2010; Ye et al., 2009). N-formyl peptides, encoded only by bacterial and mitochondrial genes, are the only ligand class common to all three human receptors. Formyl peptides such as fMLF, fMIFL, fMIVIL or fMIGWI that result from the degradation of larger formylated proteins, have been found in culture supernatants of several bacterial species such as *Escherichia coli*, *Staphylococcus aureus*, *L. monocytogenes* and *Helicobacter pylori*. Certain formylated mitochondrial peptides have also been found to stimulate neutrophils. Thus FPR may have a role in infection associated inflammation as well as tissue injury (Bloes et al., 2015; Ye et al., 2009).

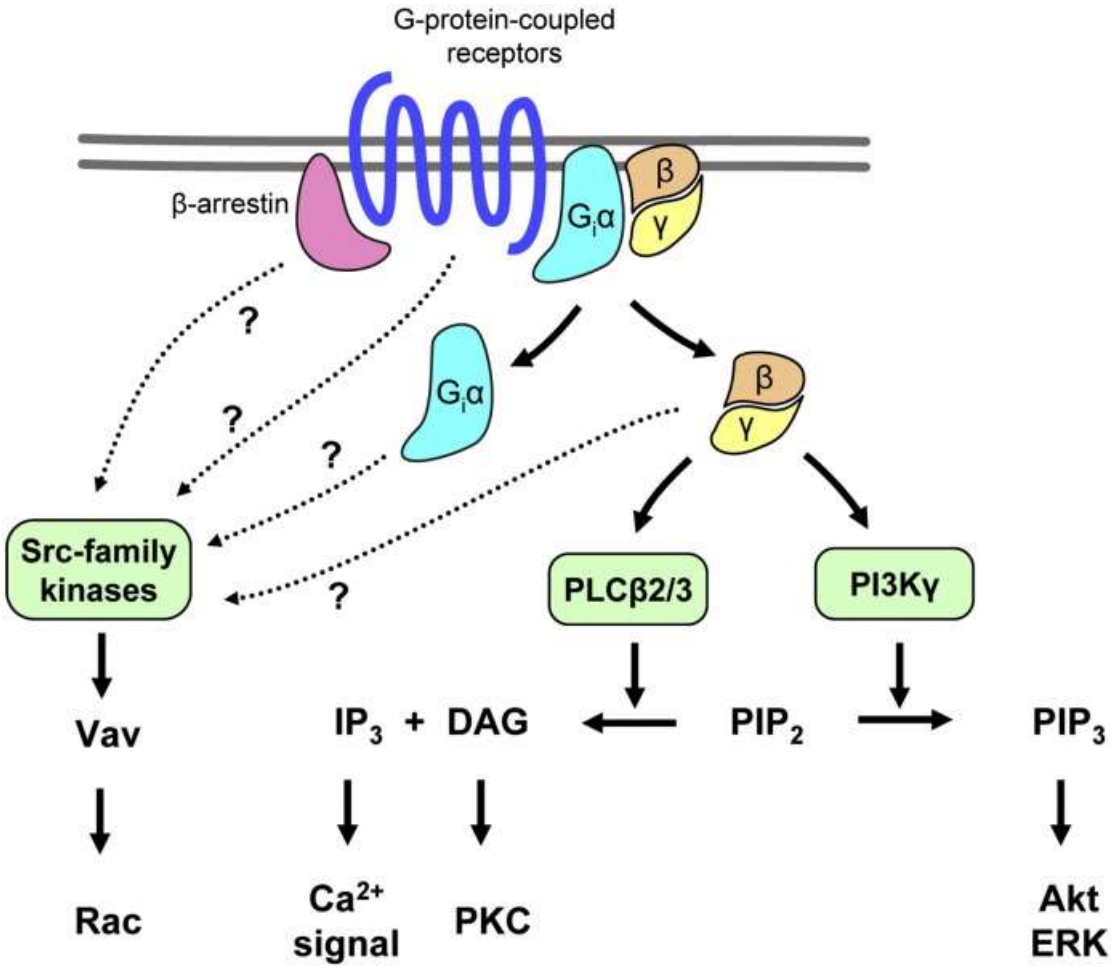

Figure 4. GPCR signaling in neutrophils.

GPCRs in neutrophils primarily dissociate Gα and Gβγ heterodimer, Gβγ activates PLCβ2/3 and PI3Kγ pathway. The activation of Src-family kinases is still poorly understand (Futosi et al., 2013a).

1.1.2.3.2 Fc-receptors (FcRs)

Neutrophil Fc-receptors participate in recognition of IgG-opsonized and immune complex-opsonized pathogens. One important role of FcRs is to trigger phagocytosis. Human neutrophils express FcγRIIA and FcγRIIIB which are low-affinity Fcγ receptors. FcγRIIA and FcγRIIIB are required in activation of human neutrophils by immune complex (Futosi et al., 2013b; Jakus et al., 2008). FcγRIIA is a single-chain transmembrane receptor with a cytoplasmic tail which bears an immunoreceptor tyrosine-based activation motif (ITAM). ITAMs are short consensus sequences of YxxL/Ix(6-12)YxxL/I (x refers to any amino acid). Crosslinking of the FcγRIIAs results in dual tyrosine phosphorylation of the ITAM sequence, which then activates the Syk tyrosine kinase. Syk tyrosine kinase initiates further downstream signalling (Mocsai et al., 2010). FcγRIIIB is an entirely extracellular molecule anchored to the plasma membrane by a GPI moiety **(Figure 5).** Neutrophils also express high-affinity FcγRI molecule, which is expressed in neutrophils activated by cytokines such as IFN-γ or G-CSF, but not in resting neutrophils. Neutrophils from patients with streptococcal pharyngitis, which is an infection of the back of the throat including the tonsils caused by group A streptococcus, express increased numbers of FcγRI, thus high-affinity FcγRI molecule is of great diagnostic value (Futosi et al., 2013b; Hoffmann, 2009).

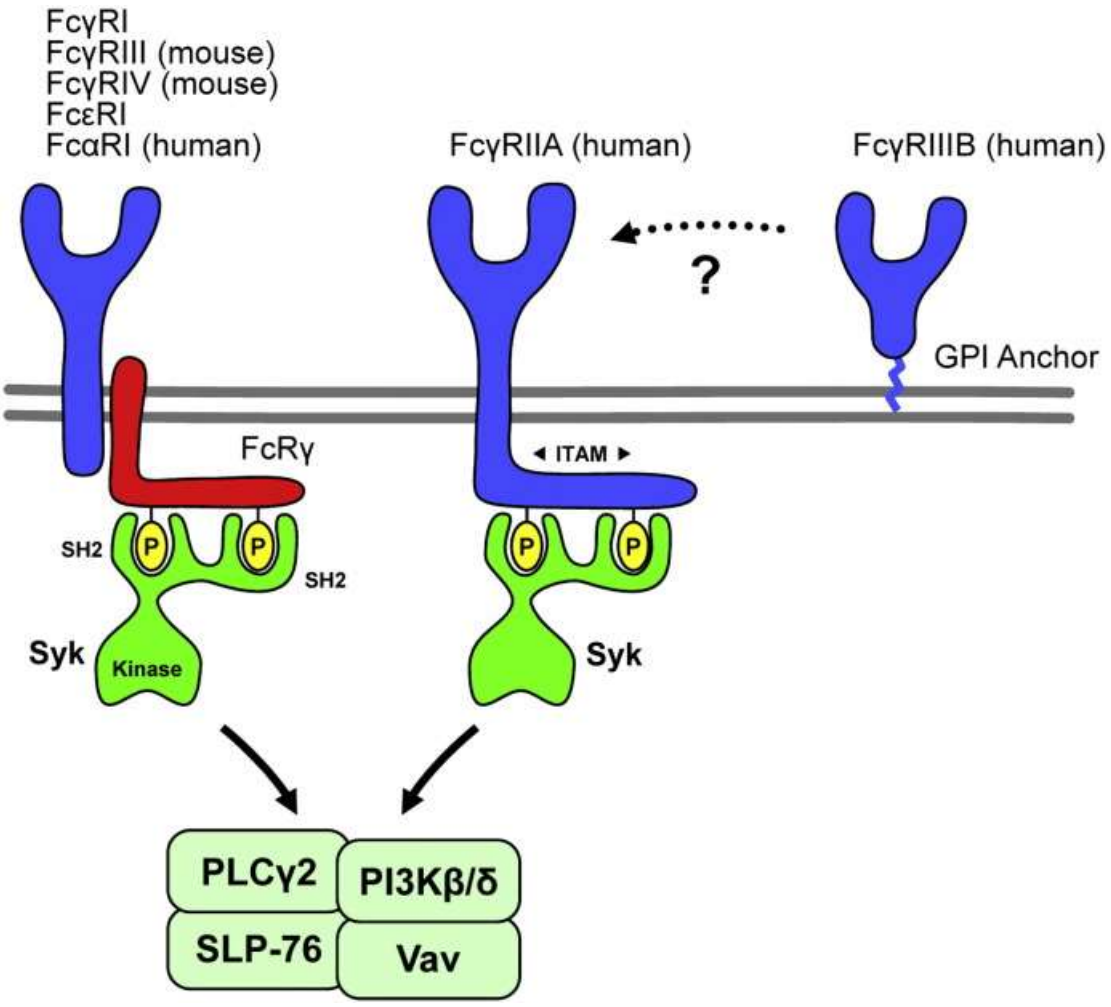

Figure 5. Neutrophil Fc-receptors.

Cytoplasmic ITAM of Fcγ-receptors bind the Syk tyrosine kinase which activates further signaling. The human FcγRIIIB receptor is linked to the membrane by a GPI anchor (Futosi et al., 2013a).

1.1.2.3.3 Neutrophil adhesion receptors

Neutrophil adhesion receptors include selectins/selectin ligands and integrins. Selectins are single-chain transmembrane glycoproteins which mediate transient interactions between neutrophils and the vessel wall. P-selectin is expressed on platelets and endothelial cells, L-selectin is expressed on leukocytes. The expression of P-selectin increases in an inflammatory environment on endothelial cells and E-selectin is expressed on endothelial cells only in inflammatory condition (Futosi et al., 2013b; Sperandio et al., 2009). More informations about selectins/selectin ligands has been given in the "Rolling" paragraph. The structure and function of integrins are discussed in the "Firm Adhesion" paragraph and the "Integrin" paragraph.

1.1.2.3.4 Cytokine receptors

Neutrophil cytokine receptors include conventional cytokine receptors, IL-1-receptor/Toll-like receptor family members, and TNF-receptor family members. Neutrophil cytokine receptors participate in intercellular communication. Conventional cytokine receptors are represented by type I (which have a conserved extracellular WSXWS motif) and type II (which do not contain the WSXWS motif) cytokine receptors. Neutrophil type I cytokine receptors include IL-4, IL-6, IL-12, IL-15, G-CSF and GM-CSF receptors. Neutrophil type II cytokine receptors include IFNα, IFNβ, IFNγ and IL-10 receptors. G-CSF and GM-CSF are involved in neutrophil differentiation, survival and activation. IL-4, IL-6, and IL-15 participate in neutrophil activation. IL-10 inhibits neutrophil chemokine and cytokine production. IFNα, IFNβ, and IFNγ delay neutrophil apoptosis, while IFNγ can upregulate the gene expression of NADPH oxidase subunit, $gp91^{phox}$, and enhance ROS production. Type I and Type II cytokine receptors activate the Janus kinase/signal transducers and activators of transcription (JAK/STAT) pathway, but also Src-family kinases, the PI3K-Akt pathway, the ERK and p38 MAP kinases, and inhibitory SOCS (suppressor of cytokine signalling) molecules (Futosi et al., 2013b). Neutrophils express IL-1 and IL-18 receptors, which are members of the IL-1-receptor/Toll-like receptor family. IL-1 mainly prolongs the survival of neutrophils, IL-18 can trigger the release of chemokine and cytokine, enhance the ROS production and delay the apoptosis of neutrophils. Neutrophils also express the TNF receptor–related Fas, TRAIL receptors (TRAIL-R2 and TRAIL-R2), RANK, and LTβ receptor. TNF-α is a major cytokine which triggers neutrophils activation and primes neutrophils for the response to additional stimuli (Futosi et al., 2013b).

1.1.2.3.5 Innate immune receptors

Neutrophil innate immune receptors (pattern recognition receptors (PRRs)) include Toll-like receptors, C-type lectins, nucleotide-binding oligomerization domain-like receptors (NOD-like receptors, NLRs), and RIG-I-like receptors (RLRs), which recognize PAMPs (**Table 1**). Neutrophils express all known TLRs except TLR3 (Hayashi et al., 2003), and there is still a debate about TLR7 (Berger et al., 2012). Various microbial structures can be recognized by neutrophil TLRs, such as bacterial lipopolysaccharide (TLR4) and peptidoglycans (TLR2) (Futosi et al., 2013b). Signalling through TLRs leads to the production of interleukin-8 (IL-8), triggers the shedding of L-selectin on their surface, primes for fMLF-mediated superoxide production, increases the rate of phagocytosis, and decreases IL-8-induced chemotaxis (Hayashi et al., 2003). Neutrophil C-type lectins include Dectin-1 (CLEC7A), Mincle (CLEC4E), MDL-1 (CLEC5A), Mcl (CLEC4D) and CLEC2 (Futosi et al., 2013b). Dectin-1 is an important phagocytic receptor for fungi and triggers ROS production in response to fungal exposure. Dectin-1 contains a C-type lectin domain, a stalk region, and a cytoplasmic tail with an ITAM motif. Dectin-1 binds exclusively to β-1,3-glucan. β-1,3-glucans are not expressed on mammalian cells, therefore they are classic pathogen-associated molecular patterns (PAMP) recognized by the innate immune system. Like other receptors (such as FcRs) with an ITAM motif, dectin-1 signalling relies on activation of Src and Syk family kinases (Huysamen and Brown, 2008; Plato et al., 2013). Dectin-1 is able to collaborate with many MyD88-coupled TLRs including TLR2, TLR4, TLR5, TLR7 and TLR9. It has been shown that collaboration between Dectin-1 and TLR2 is important in phagocytosis and MAPK activity in the control of *Candida* infections (Plato et al., 2013). Dectin-1 can also activate αMβ2 integrin via Vav proteins, this combined signalling enhances phagocytosis and ROS production of neutrophils in response to fungi (Li et al., 2011).

1.1.3 Anti-microbial function of neutrophils

Neutrophils can kill pathogens by multiple ways, including phagocytosis and formation of neutrophil extracellular traps (NETs). These process are both associated with neutrophil granules, which contains a series of anti-microbial proteins and proteolytic enzymes. In this part, granules, degranulation, antimicrobial proteins, phagocytosis and neutrophil extracellular traps are described.

1.1.3.1 Granules

There are three major granules in neutrophils azurophilic granules (primary/peroxidase-positive granules), secondary granules (specific granules) and tertiary granules (gelatinase granules). Azurophil granules are peroxidase-positive granules. The azurophil granules proteins contains the myeloperoxidase (MPO), the serine proteases: proteinase 3 (PR3), neutrophil elastase (NE), cathepsin G (CG), defensins etc (Amulic et al., 2012; Cowland and Borregaard, 2016). Both secondary granules and gelatinase granules are peroxidase-negative granules. The secondary granules contain a wide range of antimicrobial compounds including lactoferrin, neutrophil gelatinase-associated lipocalin (NGAL), hCAP-18 and lysozyme (Faurschou and Borregaard, 2003). Gelatinase granules are smaller than the secondary granules but are more easily exocytosed than specific granules. Except these granules, neutrophils also have secretory vesicles as a reservoir of membrane-associated receptors which is needed in the inflammatory response. The membrane of secretory vesicles are rich in the αMβ2 integrin, the complement receptor 1 (CR1), the FPRs, the LPS/lipoteichoic acid-receptor CD14, the FcγIII receptor CD16 and the metalloprotease leukolysin (Faurschou and Borregaard, 2003). CR1 is the best validated maker for secretory vesicles and is absent from the plasma of unstimulated neutrophils and granules (Cowland and Borregaard, 2016). Major granules proteins are summarized in **Table 2**.

Table 2. Granule proteins.

	Protein	Azurophil Granules	Specific Granules	Gelatinase Granules	Secretory Vesicles
Membrane	CD63, CD68	+	-	-	-
	CD10	-	-	-	+
	CD11b/CD18	-	++	+	+
	CD15	-	-	-	+
	CD16	-	-	-	+
	CD35	-	-	-	+
	CD66	-	+	-	-
	CD67	-	+	-	-
	CD177	-	++(*)	+(*)	-
	NOX2	-	++	+	+
	MMP-25	-	-	+	++
	NRAMP2	-	-	-	+
	fMLF-R	-	-	+	-
	SCAMP	-	+	++	+++
	VAMP2	-	-	+	++
	Syntaxin-4	-	-	-	-
Matrix	Myeloperoxidase	+	-	-	-
	BPI	+()	-	-	-
	Defensins	+()	-	-	-
	Elastase	+	-	-	-
	Azurocidin	+	-	-	-
	Cathepsin G	+	-	-	-
	Proteinase 3	+	-	-	-
	NSP4	+	-	-	-
	Cathepsin C	+	-	-	-
	AI-at	+	+	-	++
	Lysozyme	+	++	+	-
	Arginase I	-	-	+	-
	β2-microglobulin	-	+	-	-
	Collagenase	-	+	-	-
	Gelatinase	-	+()	+	-
	Haptoglobin	-	+	-	+
	hCAP-18	-	+	-	-
	Lactoferrin	-	+	-	-
	NGAL	-	+	-	-
	Ficolin I	-	-	+	-
	Pentraxin 3	-	+	-	-
	SLPI	-	+	-	-
	OLFM4	-	+(*)	-	-
	Plasma proteins	-	-	-	+

If a protein is present in present in more than one granule subset, the distribution is graded by the number of +. +() indicates that the protein is present in only a subset of the particular type of granule. (*) indicates that the protein is present in granules of only a subset of neutrophils (Cowland and Borregaard, 2016).

1.1.3.2 Degranulation

After activation of the neutrophils by soluble or particular stimuli, granules are mobilized and fuse with the plasma membrane or the phagosome (Borregaard and Cowland, 1997). Secretory vesicles are the easiest released, followed by gelatinase granules, secondary granules, and azurophil granules (Faurschou and Borregaard, 2003). The amount of actin associated with the granules decreases from the secretory vesicles to the gelatinase granules, to the secondary granules, and to the azurophil granules (Jog et al., 2007), which indicates that the presence of an actin-binding protein on the granule membrane can possibly determine the degranulation (Cowland and Borregaard, 2016). It is reported that Rac-dependent actin remodelling can control the degranulation of azurophil granules (Mitchell et al., 2008). SNARE (soluble NSF (N-ethylmaleimide sensitive factor or N-ethylmaleimide sensitive fusion proteins) attachment protein receptor) family is highly conserved and ubiquitous in vesicle budding and fusion. The t-SNARE (target-membrane-specific SNARE proteins) and syntaxin-4 are present in the plasma membrane. The v-SNARE (vesicle-membrane-specific SNARE proteins) and VAMP2 (vesicle- associated membrane protein-2) are present predominately in the membrane of secretory vesicles, followed by gelatinase granules secondary granules and none in azurophil granules (Cowland and Borregaard, 2016). SNARE plays a critical role in the process of vesicle fusion, however the relationship between cytoskeleton and SNAREs in the regulation of neutrophil degranulation is not clear, which need further investigation.

1.1.3.3 Antimicrobial Proteins

Neutrophil antimicrobial proteins are against a wide range of microbes, such as Gram positive and Gram negative bacteria, virus and fungi. There are three main types of antimicrobial proteins: cationic peptides and proteins which bind to microbial membrane, proteolytic enzymes, and proteins that deprive microorganisms of necessary nutrients (Amulic et al., 2012). Neutrophils contain cationic antimicrobial peptides such as defensins and cathelicidins, and also cationic antimicrobial proteins such as BPI and histones. Neutrophils have a broad range of proteolytic enzymes that destruct the microbessuch as lysozyme, the serine proteases (PR3, CG and NE) and azurocidin. Lysozyme destroys the bacterial wall independently of its enzymatic activity (Markart et al., 2004; Nash et al., 2006).Although azurocidin lacks protease activity, it still kills microbes (Amulic et al., 2012; Campanelli et al., 1990).

Neutrophils also contain proteins that chelate essential metals from microbes and possibly affect the growth of microbes, such as lactoferrin which inhibits the proliferation of bacteria by sequestering iron (Levay and Viljoen, 1995) and calprotectin that inhibits S. aureus growth through chelation of nutrient Mn^{2+} and Zn^{2+} (Corbin et al., 2008).

1.1.3.4 Phagocytosis

Phagocytosis is essential for tissue homeostasis and innate immune response. It is defined as the regulated uptake of particles, larger than 0.5 μm in diameter, into cytosolic membrane-bound vacuoles named phagosomes (Levin et al., 2016). Phagocytosis is mediated primarily by white blood cells, such as macrophages, neutrophils and dendritic cells (DCs). Most mechanisms of phagocytosis have been described in macrophages. Much less is known about neutrophils due to their short lives and the difficulties to make genetic modified neutrophils by either transfection or microinjection. Neutrophils can internalize both non-opsonized and opsonized particles.

1.1.3.4.1 Non-opsonic phagocytosis

Non-opsonic phagocytosis is initiated by direct recognition of phagocytic target. Pathogens express essential molecules for survival and pathogenicity which are known as PAMPs. PAMPs can be recognized by host sensors known as pathogen recognition receptors (PRRs). For example, the fungi cell wall composed of β-glucans, mannans and chitins which is recognized by immune cells as PAMPs. Neutrophils express PRRs for binding PAMPs, such as C-type lectin receptors (CLRs) and Toll-like receptors (TLRs). Human neutrophils express CLRs including Dectin-1, Dectin-2 and mincle which can recognize β-glucans and α-mannose (Gazendam et al., 2016). Zymosan is a cell wall particle of *Saccharomyces cerevisiae* yeast and is made up primarily of α-mannans and β-glucans (Di Carlo and Fiore, 1958). Dectin-1 has been reported to mediate the non-opsonic phagocytosis of yeast and zymosan in macrophage (Brown and Gordon, 2001) and also later in human neutrophils (Kennedy et al., 2007).

1.1.3.4.2 Opsonic-phagocytosis

A variety of distinct molecular and morphological processes occurs in phagocytosis, which also leads to the diversity of phagocytic mechanisms. Researchers use IgG or complement

opsonized beads to study the phagocytosis mechanism. Internalization of IgG opsonized particles requires phagocyte membrane extension, Syk tyrosine kinase and produce pro-inflammatory mediators. But internalization of Complement opsonized particles internalisation involve particle "sinking" into the cell and does not produce inflammatory mediators. Usually both process are involved in the phagocytosis of pathogens (Underhill and Ozinsky, 2002).

Fcγ-receptor mediated phagocytosis

IgG opsonized particles can be recognized by FcRs on neutrophils though binding to the Fc region of IgG. FcRs can be divided into two classes. One kind of receptors that contain ITAMs in their intracellular domains which recruit kinases and activate phosphorylation cascades, such as Fcγ RI (high affinity receptor), Fcγ RIIA and Fcγ RIIIA (low affinity receptor).

The other kind of receptors that contain ITIM (immunoreceptor tyrosine-based inhibitory motif) motifs which recruit phosphatases that inhibit signalling, such as Fcγ RIIB (Freeman and Grinstein, 2014; Underhill and Ozinsky, 2002).

Complement-receptor mediated phagocytosis

Microbes can be opsonized by complement proteins in the serum. The complement proteins are activated through antibody-dependent or antibody-independent mechanisms. Complement-opsonized particles can be recognized and internalized by specific complement receptors. Neutrophils express phagocytic complement receptors: complement receptor 1 (CR1), complement receptor 3 (CR3, αMβ2 integrin, CD11b/CD18, or Mac-1) and complement receptor 4 (CR4, αXβ2 integrin, CD11c/CD18, or gp150/95). CR1 can bind complement component c1q, c3b, c4b and mannan-binding lectin (MBL), but CR1 alone cannot mediate internalization of a particle without additional signals. αMβ2 integrin and CR4 can bind ic3b-opsonized particles (Underhill and Ozinsky, 2002). αMβ2 can mediate both non-opsonic and opsonic phagocytosis(Le Cabec et al., 2002). αMβ2 mediated phagocytosis requires additional signals such as chemokines, cytokines (e.g. TNF-α) and microbial products (e.g. LPS) (Aderem and Underhill, 1999; Underhill and Ozinsky, 2002).

1.1.3.5 Neutrophil extracellular traps

Neutrophil can kill pathogens extracellularly by releasing extracellular traps (NETs) (Brinkmann et al., 2004). NETs can be induced by bacteria, fungi, HIV parasites *etc* **(Figure 6)** (Brinkmann and Zychlinsky, 2012). NETosis is a different process from necrosis or

apoptosis. During NETosis, the nuclei swells and the chromatin decondenses. Then large strands of decondensed DNA is ejected into the extracellular space, carrying along with them some proteins (**Figure 7**) (Brinkmann et al., 2004; Brinkmann and Zychlinsky, 2007). 24 neutrophil proteins are present in NETs. Most of NETs proteins come from granules, few are from the nucleus and rare proteins are cytosolic. NETs proteins are primarily the cationic (DNA-binding) bactericidal proteins: histones, defensins, elastase, proteinase 3, heparin binding protein, cathepsin G, lactoferrin and MPO (Urban et al., 2009). The formation of NETs appears to require attachment of neutrophils to a substrate that stimulates the αMβ2 integrins (Neeli et al., 2009). Neutrophils make NETs poorly in suspension, probably preventing excessive formation of NETs in circulation and avoiding thrombus formation(Brinkmann and Zychlinsky, 2012). NETs formation depend on hydrogen peroxide generated by the NADPH oxidase and also MPO. CDG (chronic granulomatous disease) neutrophils and MPO-deficient neutrophils do not form NETs (Bianchi et al., 2009; Metzler et al., 2011). NET are a doubled-edged swords. NETs can also cause damage to the host. NETs expose self molecules extracellularly which lead to autoimmunity. NETs are involved in systemic lupus erythematosus (SLE), which is a chronic autoimmune disease affecting multiple tissues and organs. SLE produce autoantibodies, which are predominantly anti-neutrophil cytoplasmic antibodies (ANCA) (MPO and PR3 are the main targets) or directed against chromatin (Brinkmann and Zychlinsky, 2012; Villanueva et al., 2011). NETs have also been found in the airway fluids of cystic fibrosis patients. They may increase the viscosity of the sputum and decrease lung function (Marcos et al., 2010).

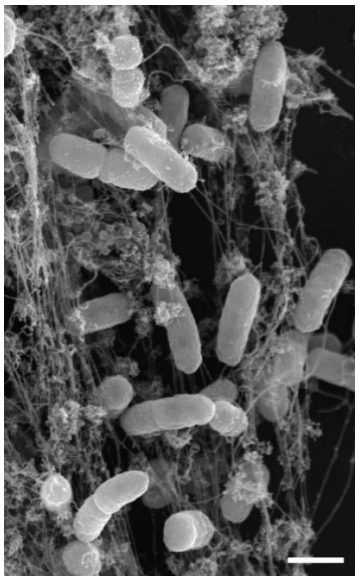

Figure 6. Bacteria caught in NETs.

Scanning electron microscopy of human neutrophils incubated with Salmonella, the bacteria are trapped in NETs. Bar, 1 μm. (Brinkmann and Zychlinsky, 2012)

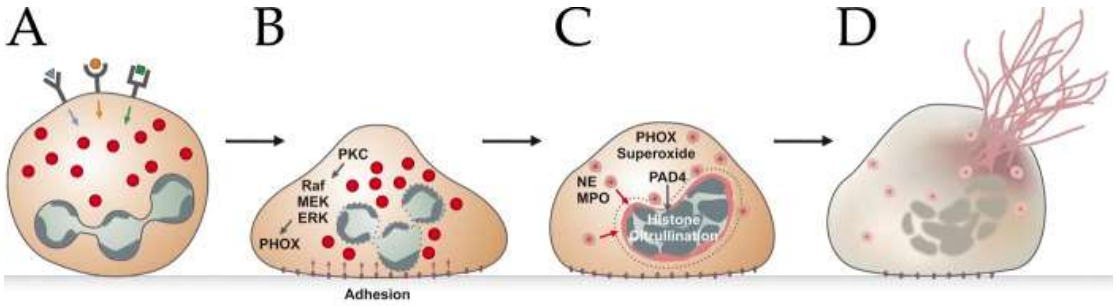

Figure 7. Schematic representation of the NETosis pathway.

After stimulation of receptors (A), neutrophils adhere to the substrate (B) and mobilize granule components, such as NE and MPO (C). Granules are shown as red circles. Histones are citrullinated and the intracellular membranes are disintegrated. In the end, the mixture of cytoplasm (granule proteins) and nucleoplasm (DNA and histones) are released into the extracellular space to form NETs (D). (Brinkmann and Zychlinsky, 2012).

1.1.4 Neutrophil and extracellular matrix

Pathogens can be recognized by a number of cells in the tissue, such as macrophages and mast cells. These cells release pro-inflammatory chemokines and cytokines, which activate the neutrophils and endothelial cells for an inflammatory response. Neutrophils firstly adhere to the vascular wall, then migrate through the endothelial cell bilayer, and subsequently through the extracellular matrix to reach the site of inflammation. During this process, neutrophils need to interact with multiple extracellular matrix proteins.

1.1.4.1 Extracellular matrix

All tissues and organs contain non cellular component, the extracellular matrix (ECM), which provides essential physical scaffolds and also regulate many cellular process such as growth, migration, differentiation, survival, homeostasis and morphogenesis (Theocharis et al., 2016). The two main ECMs are the interstitial connective tissue matrix, which surrounds cells and provides structural scaffolding for tissues, and the basement membrane, which separates the epithelium from the surrounding stroma **(Figure 8)** (Bonnans et al., 2014) . Cells can modulate the composition and structure of the ECM, in contrast, ECM can also regulate cellular process (Ayres-Sander and Gonzalez, 2012). These processes are complicated and

need to be tightly regulated to sustain tissue homeostasis, especially in response to injury. Dysregulated ECM remodeling is related with pathological conditions and can aggravate disease progression, such as in osteoarthritis, fibrosis and cancer (Bonnans et al., 2014). The mammalian core ECM, also known as core matrisome, is composed of around 300 proteins including 43 collagen subunits, three dozen or so proteoglycans, and around 200 glycoproteins (Hynes and Naba, 2012).

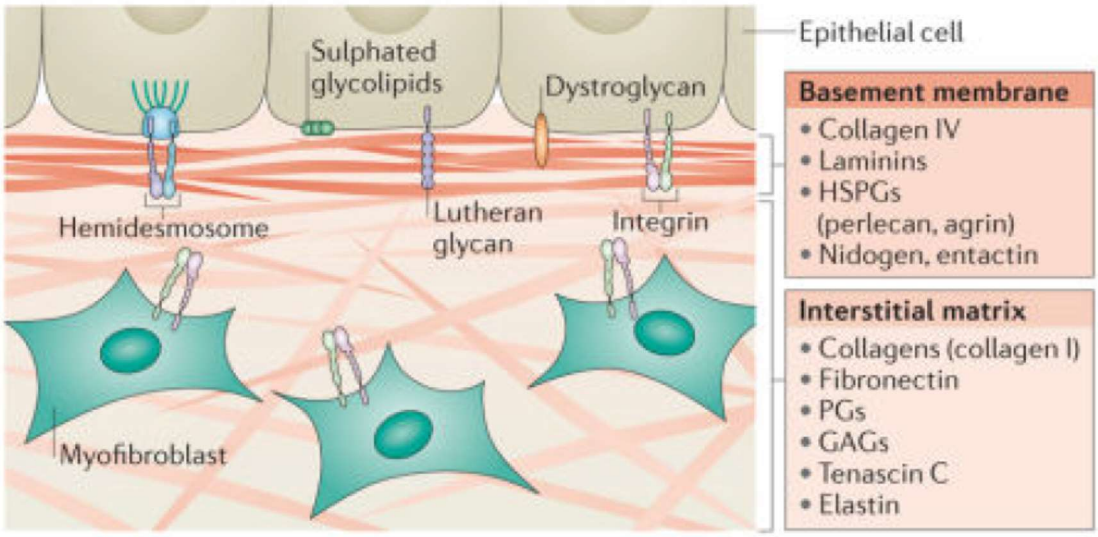

Figure 8. Two main types of ECM.

There are two main types of ECM. The interstitial connective tissue matrix and the basement membrane. The interstitial matrix surrounds cells and is mainly made up of collagen I and fibronectin. The basement membrane is more compact than the interstitial matrix and mainly consists of collagen IV, laminins, heparin sulfate proteoglycans (HSPGs) and proteins, such as nidogen and entactin. PG: Proteoglycan, GAG: Glycosaminoglycan. (Bonnans et al., 2014).

1.1.4.2 Fibrinogen

Fibrinogen together with Von Willebrand factor and vitronectin are belong to vascular ECM glycoproteins (Hynes and Naba, 2012). Fibrinogen normally present in human blood plasma at 1.5-3.5 g/L (Pulanic and Rudan, 2005) and is important for haemostasis, wound healing, inflammation and angiogenesis. Fibrinogen is soluble, but it will form a clot or insoluble gel when it is converted to fibrin by thrombin, which is activated by a cascade of enzymatic reactions induced by injury or a foreign surface (Weisel, 2005). Fibrinogen are comprised of two sets of three polypeptide chains named Aα, Bβ and γ, which form two outer D-domain and a central E-domain **(Figure 9).** There is a minor γ chain variant γ' by alternative processing of the primary mRNA transcript, γ' accounts about 8% of the total γ chain population (Mosesson et al., 2001). Fibrinogen has two integrin binding sites at Aα95-98(RGDF) and at Aα572-575(RGDS). A lot cellular interactions with fibrinogen and fibrin occur through binding to one or two of these binding sites (Henschen et al., 1983; Mosesson et al., 2001). The leukocyte αMβ2 integrin on stimulated monocytes or neutrophils has high affinity for binding fibrinogen. αMβ2 integrin binds to the fibrinogen D-domain at a site corresponding to γ-module sequences (**Figure 10**) : γ190-202(P1) and γ377-395(P2) (Ugarova et al., 1998). P1 is an integral part of the γ-module central domain, while P2 is inserted into this domain forming an antiparallel β-strand with P1. P2 is implicated as the major binding site for αMβ2 integrin. Soluble fibrinogen poorly binds to αMβ2 integrin, but fibrin or immobilized fibrinogen bind to αMβ2 with great affinity. Immobilization of fibrinogen can expose P2. (Lishko et al., 2002; Loike et al., 1992; Mosesson, 2005). Yakovlev *et al.* has hypothesized that P2 insert may be removed (pulled out) **(Figure 10)** from the γ-module. They hypothesized that P1 and P2 could be separated by this mechanism and that such separation could enhance the αMβ2-binding activity of the γ-module, thus modulating fibrinogen-leukocyte interaction during an inflammatory response (Yakovlev et al., 2000a; Yakovlev et al., 2001; Yakovlev et al., 2000b; Yakovlev et al., 2005).

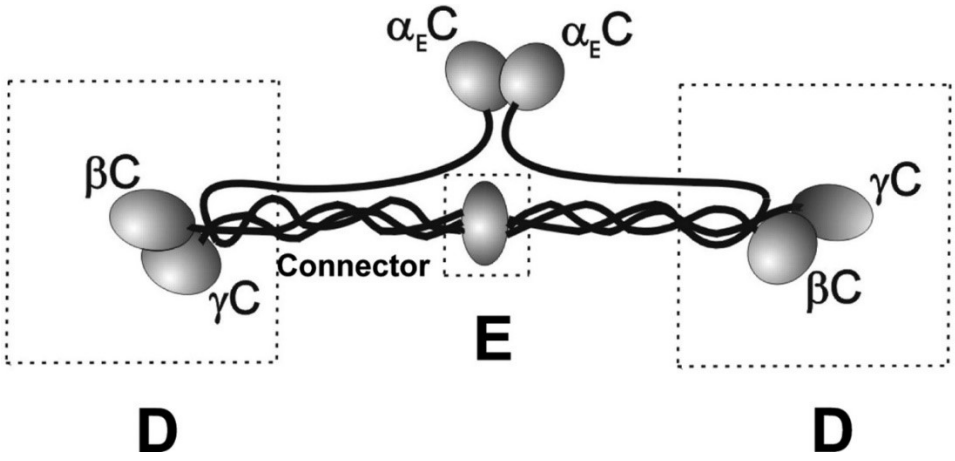

Figure 9. Schematic of the domain structure of Fibrinogen.

The D and E regions are boxed. The γC, βC, and αEC domains are shown as shaded balls. The connector is the coiled-coil region composed of segments of the α-, β-, and γ-chains. (Lishko et al., 2004).

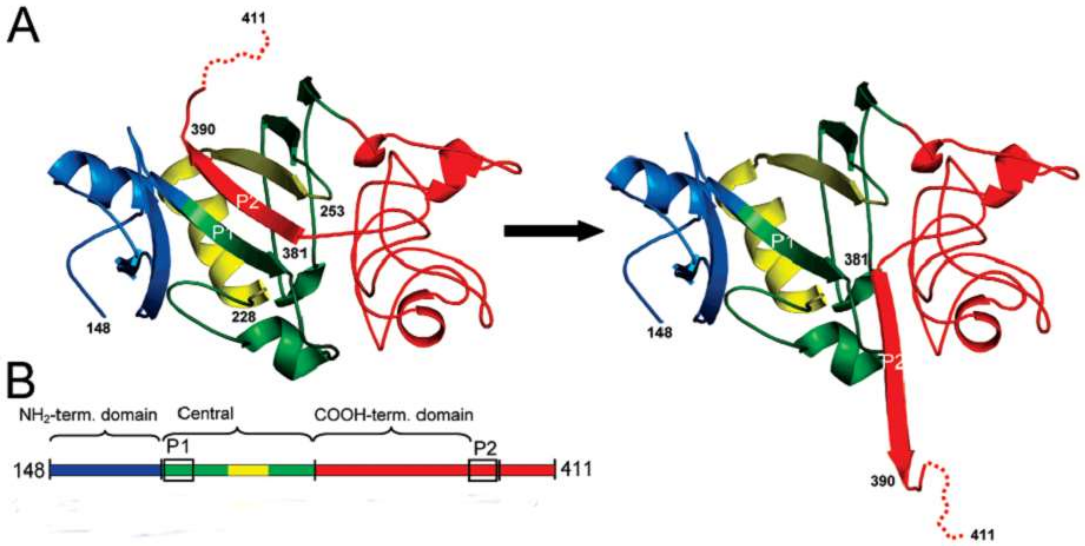

Figure 10. Pull out hypothesis.

A. Schematic ribbon diagram of the known γ-module crystal structure (residues γ148–411; left), and the hypothetical structure resulting from 'pull out' of the γ381–390 β-strand insert (P2; right). B. The NH_2-terminal domain (residues γ148−191) is colored in blue, the central domain (residues 192−286) is in green and yellow, and the COOH-terminal domain of the γ-module is in red. *Adapted from* (Yakovlev et al., 2005).

1.1.4.3 Integrins

Cell adhesion to the ECM is mediated by ECM receptors including integrins, discoidin domain receptors and syndecans (Frantz et al., 2010). Neutrophils encounter the tissue ECM and then they emigrate from the bloodstream to a site of inflammation. Cell-cell and cell-ECM adhesive events take place in extracellular matrix, integrins mediate the adhesion events and trigger signalling inside cells which leads to cell response. Integrins are expressed in metazoan, sponges and primitive bilateralia (Gahmberg et al., 2009; Hynes, 2002). Integrins are heterodimers consisting of two subunits, α and β subunits. In vertebrates, there are 18 α(α1-11, αD, αE, αL, αM, αV, αX and αIIb) and 8 β subunits (β1-8) forming 24 αβ heterodimers by noncovalent bonds(Hynes, 2002). The integrins are grouped into subgroups according to ligand-binding properties or their subunit composition **(Figure 11)**. The α and β subunits show no homology, but different α subunits or β subunits have similarities among themselves (Barczyk et al., 2010).

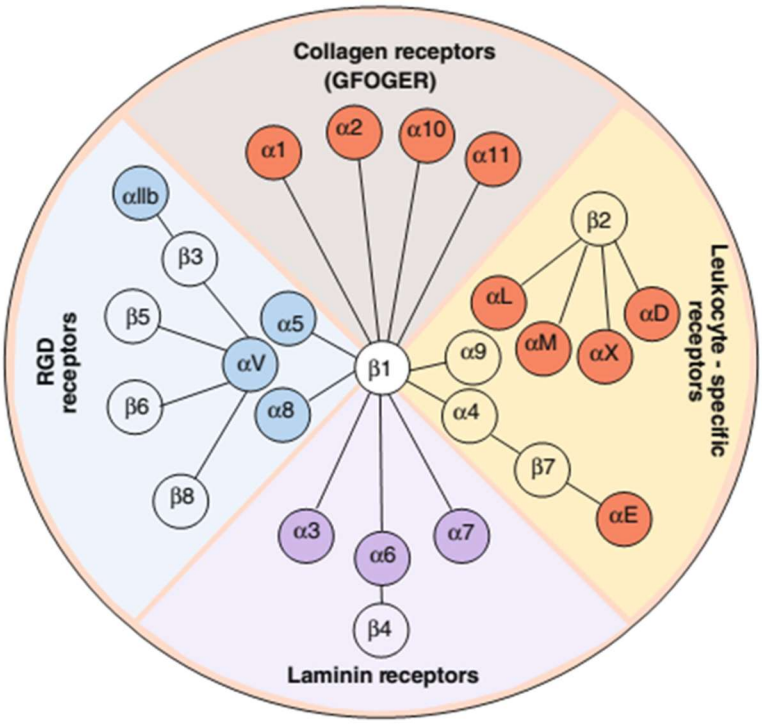

Figure 11. Representation of the integrin family.

In higher vertebrates, the integrin family has 24 members. They are classified into collagen receptors, RGD receptors, laminin receptors and leukocyte-specific receptors. (Barczyk et al., 2010).

1.1.4.3.1 Integrin structures

Both α and β subunits contain a large extracellular domain, a single-spanning transmembrane domain and a short cytoplasmic tail (except for β4) (Pan et al., 2016). The extracellular domains of α subunit contain the following domains: I-domain, β-propeller, Thigh, Calf-1 and Calf-2. Nine of the α subunit (α1, α2, α10, α11, αD, αE, αL, αM, αX) have an I-domain (around 200 amino acids) which is crucial for ligand binding. In the other α subunit, the β-Propeller domain constitute the ligand binding site. Integrin β subunits contain a I-like domain, which is crucial for ligand binding, a plexin/semaphorin/intergrin (PSI) domain, a hybrid domain, four epidermal growth factor (EGF) repeats and a membrane proximal b tail domain (bTD) (**Figure 12**) (Campbell and Humphries, 2011; Pan et al., 2016). There are around 1 mM Ca^{2+} and Mg^{2+} in blood. Ca^{2+} plays an important role in keeping integrins in inactive state. For many integrins, millimolar Ca^{2+} often has an inhibitory effect on ligand binding. For almost all integrins, removal of Ca^{2+} or addition of Mn^{2+} will remarkably increase their binding affinity and adhesiveness (Zhang and Chen, 2014). The extracellular domains of α subunits contain a MIDAS (metal-ion-dependent adhesive site) which can bind Mg^{2+} and Ca^{2+}. The β I- like domain contains an Mg^{2+} coordinating MIDAS and a site adjacent to MIDAS (ADMIDAS) which binds an inhibitory Ca^{2+}. When this ADMIDAS site binds Mn^{2+}, the conformation will change and lead to an active form of the integrin (Barczyk et al., 2010). Integrin α and β transmembrane segments are associated in the inactive resting receptor, they dissociate upon talin binding during inside-out activation(Wegener and Campbell, 2008). β integrins share homology in the cytoplasmic tail with NPXY sequences that binds proteins with phosphotyrosine-binding (PTB) domains (Bouaouina et al., 2008).

Integrin cytoplasmic domains are directly associated with several cytoskeletal proteins including α-actinin, talin, filamin, paxillin and tensin. Integrin cytoplasmic domains may also associated directly with several intracellular signaling proteins including cytohesion-1, focal adhesion-kinase (FAK) , integrin-linked kinase (ILK) ,β3-endonexin, cytoplasmic domain associated protein-1 (ICAP-1), receptor for activated C kinase 1 (Rack1) and calcium-and integrin-binding protein (CIB) (Pan et al., 2016).

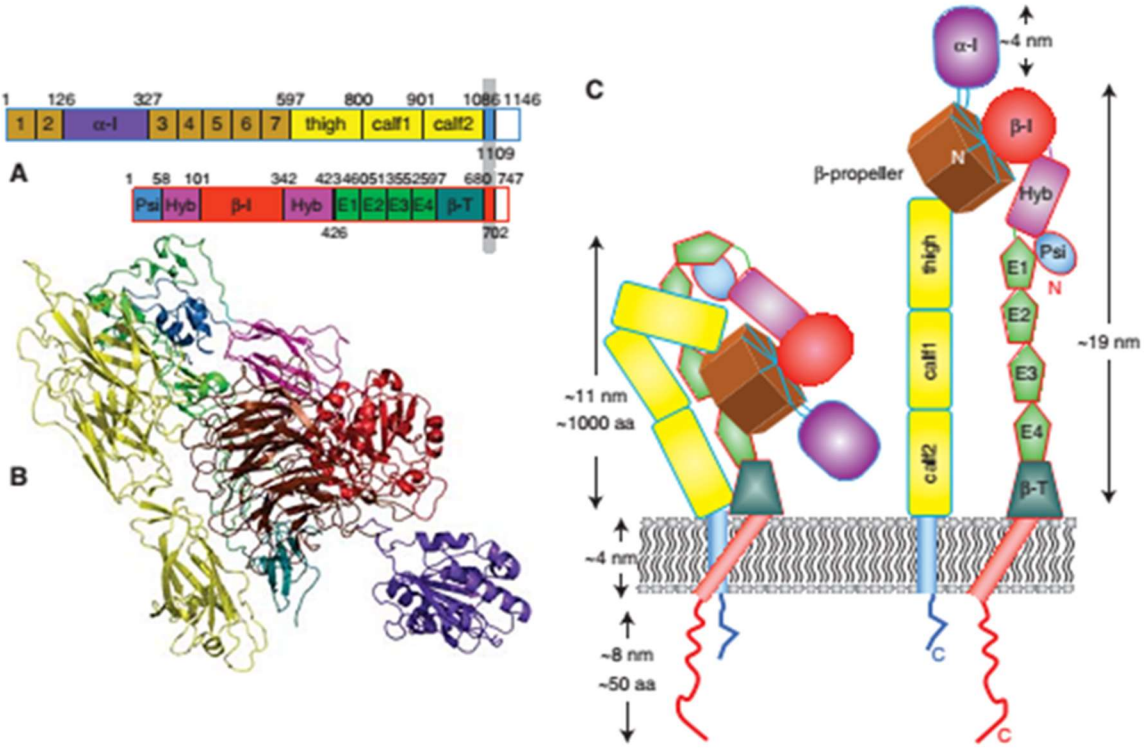

Figure 12. Integrin structure.

(A) Domain structure of αxβ2 (Upper, αx; lower, β2); (B) structure of αxβ2 using same color code as A; (C) Cartoon representation of bent and upright conformations (Campbell and Humphries, 2011).

1.1.4.3.2 Neutrophil integrins

Neutrophils express αLβ2 (LFA-1, CD11a/CD18), αMβ2, αXβ2, αDβ2 (CD11d/CD18) and low levels of α4β1, which are involved in slow rolling, adhesion, post-adhesion strengthening, neutrophil migration, ROS production, phagocytosis and polarization(Nathan et al., 1989; Zarbock and Ley, 2008). αMβ2 is the most abundant integrin on neutrophils, αDβ2 is basally expressed on the majority of circulating human neutrophils (Arnaout, 2016). αMβ2 integrin engagement is necessary for phagocytosis and ROS production (Mayadas and Cullere, 2005; Nathan et al., 1989). αMβ2 integrin is stored in neutrophil secretory, secondary and tertiary granules (Borregaard et al., 1994). αMβ2 integrin has more than 40 reported ligands, including ICAMs 1-4, vascular cell adhesion protein 1 (VCAM-1), bacterial and fungal glycoproteins, heparin, coagulation factor Xa, fibrin(ogen), fibronectin, proteinase 3 and complement C3bi (Arnaout, 2016; Ross, 2000; Zarbock and Ley, 2008).

Integrin are normally expressed in an inactive state on the cell surface, which allows the leukocytes or platelets to circulate in the blood with minimal aggregation or interaction with blood vessel walls (Arnaout, 2016). Integrin-ligand binding is regulated by the structural state of activation. When in a bent conformation the integrin is in a low-affinity state, which is modulated upon inside-out or outside-in activation. Outside-in activation involves changes in integrin conformation: Ligand binding to the external domains of integrin induce conformational changes and activates signaling patways. Outside-in signaling is important for adhesion strengthening, spreading and intraluminal crawling. During outside-in activation, Src-family kinases phosphorylate the transmembrane adapters DAP12 and FcRγ, which recruit and activate the Syk. Syk further activate different downstream molecules, such as Vav1, the regulatory subunit of Class I PI3K p85, and PLCγ2 (Mocsai et al., 2015). In most cases, the activation of integrin requires first an inside-out activation: signals originate from various cell surface receptors, such as chemokine receptors (Gahmberg et al., 2009). However integrins can be activated by immobilized fibrinogen alone without inside-out activation , resulting in ROS production, upregulation of TNF-α mRNA and induction of IL-1β (Ugarova and Yakubenko, 2001).

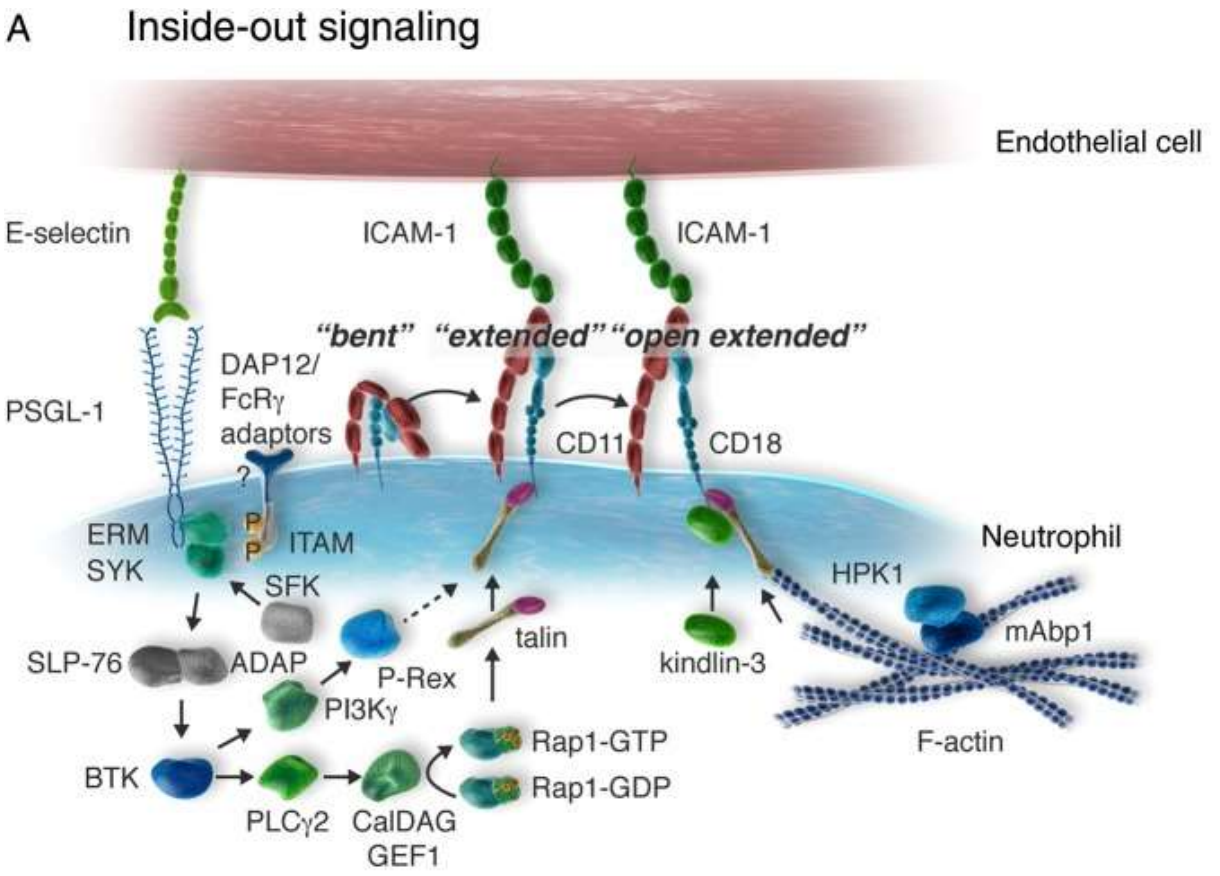
A Inside-out signaling
Endothelial cell
E-selectin
ICAM-1
ICAM-1
"bent" "extended" "open extended"
DAP12/
FcRγ
adaptors
PSGL-1
CD11
CD18
?
ERM
SYK
P
P
ITAM
Neutrophil
SFK
HPK1
talin
mAbp1
SLP-76
ADAP
P-Rex
kindlin-3
PI3Kγ
Rap1-GTP
F-actin
BTK
Rap1-GDP
PLCγ2
CalDAG
GEF1

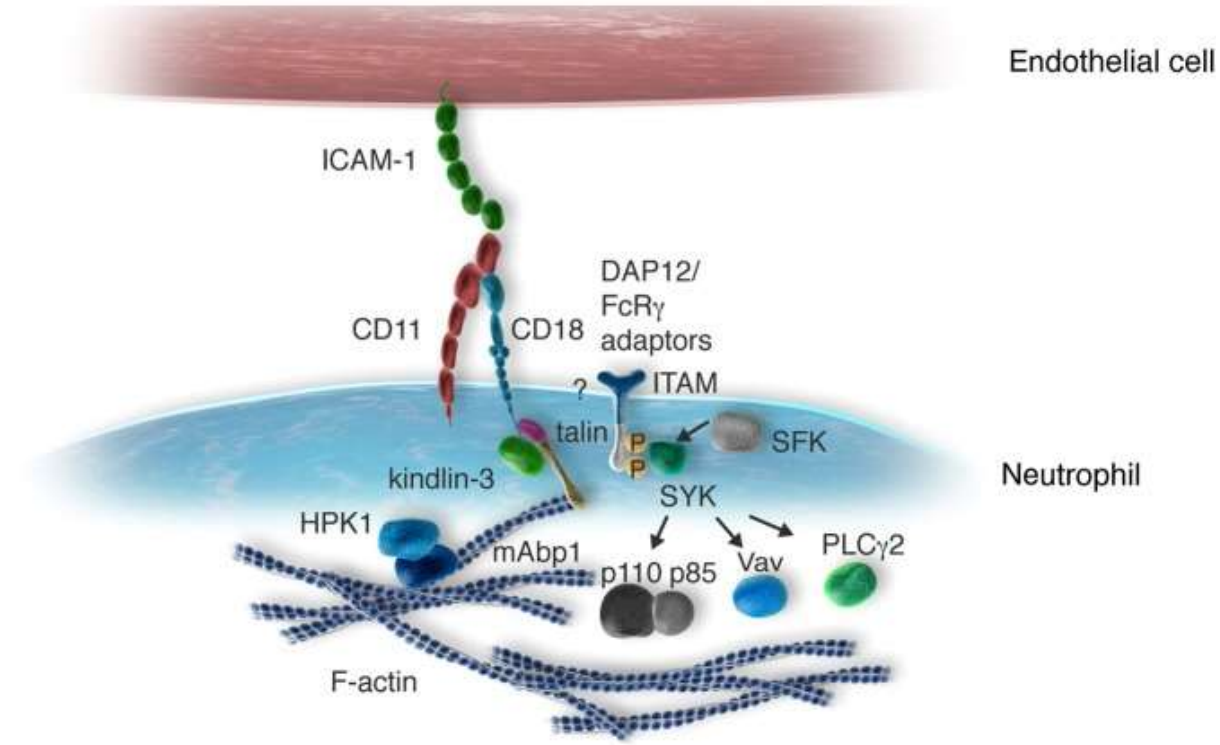
B Outside-in signaling
Endothelial cell
ICAM-1
DAP12/
FcRγ
adaptors
CD11
CD18
?
ITAM
talin
P
P
SFK
kindlin-3
Neutrophil
SYK
HPK1
mAbp1
p110 p85
Vav
PLCγ2
F-actin

Figure 13. Inside-out and Outside-in signalling of β2-integrins.

(A) Inside-out signalling of β2-integrins induces the shit of the bent conformation (low ligand binding affinity) to the extended conformation (intermediate ligand binding affinity) and the induction of the open extended conformation (high ligand binding affinity). (B) Outside-in signalling of β2-integrins is initiated upon ligand binding by clusters of high affinity integrins. Src-family kinases are involved in both signalling ways. Src-family kinases phosphorylate the ITAM motif of transmembrane adapters DAP12 and FcRγ, which recruit and activate Syk. Syk mediates different downstream signals. In inside-out activation, talin finally mediate the integrin to form open-extended conformation. In outside-in activation, Sky can activate Vav1, PLCγ2 and the regulatory subunit of Class I PI3K p85 (Mocsai et al., 2015).

1.2 Reactive oxygen species

Neutrophil produce superoxide upon activation by particulate or soluble inflammatory stimuli such as fMLF, inomycin, and LPS. Superoxide is the precursor of other reactive oxygen species (ROS). ROS production by neutrophils is an important step in human innate immune system. NADPH oxidase is the major source of ROS.

1.2.1 NADPH oxidase

The NADPH oxidase consists of membrane-associated heterodimer, cytochrome b_{558} ($gp91^{phox}$ and $p22^{phox}$), cytosolic subunits $p40^{phox}$, $p47^{phox}$ and $p67^{phox}$, and small GTPase Rac. After activation, all the subunits assemble together to form the active enzyme at the plasma membrane or at the phagosomal membrane. In mammals, there are seven isoforms of the transmembrane subunit $gp91^{phox}$ or NOX2 of the NADPH oxidase: Nox1-5, Duox1 and Duox2. Like $gp91^{phox}$, all other NOX proteins have six transmembrane domains, motifs for NADPH and FAD binding, and a conserved paired histidines for the binding to the haem groups (Nauseef, 2008).

1.2.1.1 gp91^{phox}

$gp91^{phox}$ (β subunit of the cytochrome b_{558}) is encoded by the gene CYBB, which is located on the X chromosome at position 21.1. The human $gp91^{phox}$ is synthesized as a 58 kDa core protein that is subsequently glycosylated to form a 65 kDa protein gp65 in the endoplasmic reticulum (ER). Gp65 binds to the hem and forms the heterodimer with $p22^{phox}$. The heterodimer then traffics to Golgi, and $gp91^{phox}$ is further glycosylated to the mature 91 kDa form (three N-linked glycosylation sites, Asn^{132}, Asn^{149}, Asn^{240}). (Casbon et al., 2012; DeLeo, 2000; Groemping and Rittinger, 2005; Kleniewska et al., 2012; Yu, 1999). $Gp91^{phox}$ consists of 570 amino acids. 300 amino acids in the N-terminal are predicted to form six trans-membrane α-helices, and the cytosolic domain in the C-terminal contains the FAD and NADPH binding sites. $Gp91^{phox}$ have conserved paired histidines for binding to the heme groups (**Figure 14**). Electrons are transferred from NADPH to FAD and then to the heam groups to reduce O_2 to $O_2^{\cdot -}$. The 3D structure of only a fragment of $gp91^{phox}$, the Cytochrome b_{245} heavy chain, has been resolved (Table 1). All the other information about the 3D

structures of the NADPH oxidase subunits are summarized in **Table 3** from Protein Data Bank (PDB). It has been shown that $gp91^{phox}$ is phosphorylated in activated neutrophils by PKC and this phosphorylation increase diaphorase activity (catalyze the reduction of NADPH) of the $gp91^{phox}$ flavoprotein cytosolic domain and its binding to Rac2, $p67^{phox}$, and $p47^{phox}$ (Raad et al., 2008).

1.2.1.2 $p22^{phox}$

$P22^{phox}$ (α subunit of the cytochrome b_{558}) is encoded by the gene *CYBA*, which is located on chromosome 16q24 (Dinauer et al., 1990). $p22^{phox}$ consists of 195 amino acids and is a 22 kDa protein. $p22^{phox}$ associates with $gp91^{phox}$ in a 1:1 complex and contributes to its maturation and stabilization. The N-terminal portion of $p22^{phox}$ contains at least two trans-membrane α-helices (possibly three or four). The C-terminal cytoplasmic portion of $p22^{phox}$ is devoid of any secondary structure and contains a proline-rich region (PRR) which is consist of PxxP (x indicates any amino acid) motif (**Figure 14**). This motif can bind the Src homology3 (SH3) domain of $p47^{phox}$ (Groemping and Rittinger, 2005; Nobuhisa et al., 2006; Ogura et al., 2006; Stasia, 2016). Phosphorylation of Thr147 which is close to the PRR region of $p22^{phox}$ enhances NADPH oxidase activity and regulates the $p22^{phox}$-$p47^{phox}$ interaction at the membrane (Lewis et al., 2010).

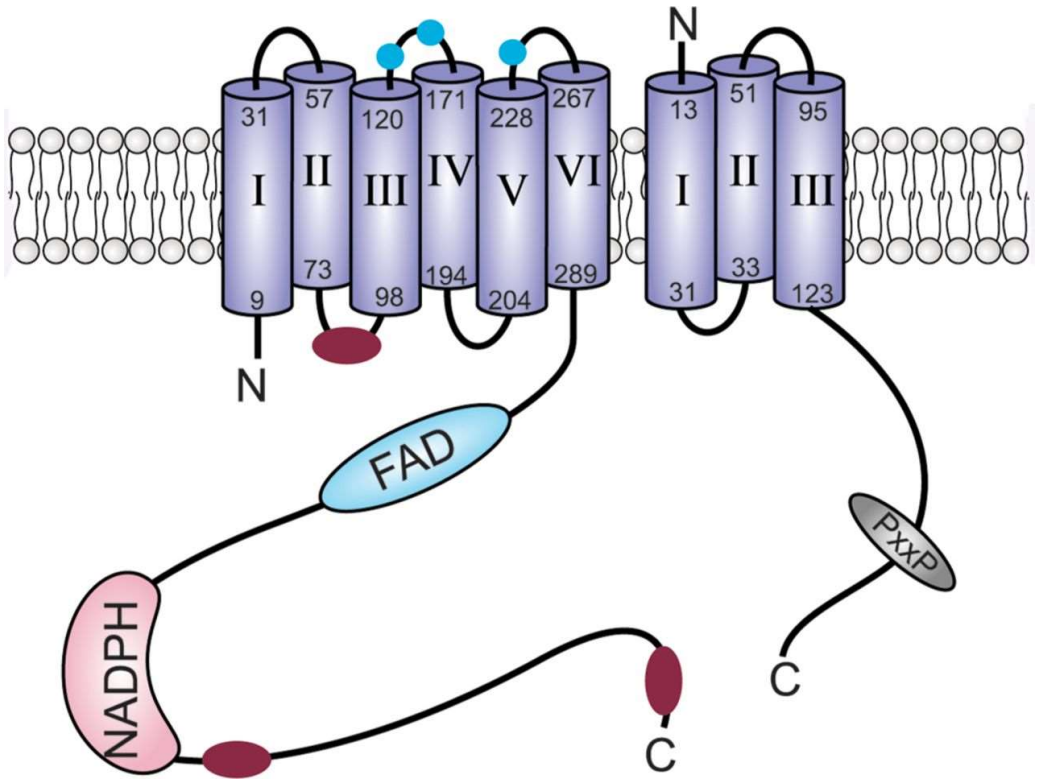

Figure 14. Model of the cytochrome b_{558}

The predicted transmembrane helices of $gp91^{phox}$ and $p22^{phox}$ are indicated. The three Asp residues at positions 132, 149, and 240 are glycosylation sites indicated by cyan dots. The regions that are believed to interact with $p47^{phox}$ in the active state is in red. The FAD-binding sites in gp91phox are shown in cyan and NADPH-binding sites are shown in pink. The consensus PxxP motif in the cytoplasmic region of $p22^{phox}$ that interacts with $p47^{phox}$ is indicated in grey. (Groemping and Rittinger, 2005).

Table 3. PDB entries for structure of the NADPH oxidase subunits.

Subunit	PDB code	Protein	Method	Released year	Reference DOI
gp91^{phox}	3A1F	Cytochrome b-245 heavy chain	X-ray Diffraction	2010	
p22^{phox}	1WLP	p22phox-p47phox complex	Solution NMR	2005	10.1074/jbc.M505193200
	1OV3	p22phox-p47phox complex	X-ray Diffraction	2003	10.1016/S0092-8674(03)00314-3
p40^{phox}	2DYB	p40phox	X-ray Diffraction	2007	10.1038/sj.emboj.7601561
	1Z9Q	SH3 domain of p40phox	Solution NMR	2006	
	1W6X	SH3 domain of p40phox	X-ray Diffraction	2005	10.1074/jbc.M412897200
	1W70	SH3 domain of p40phox complexed with c-terminal polyproline region of p47phox	X-ray Diffraction	2005	10.1074/jbc.M412897200
	1OEY	Heterodimer of p40phox and p67phox PB1 domains	X-ray Diffraction	2003	
	1H6H	Structure of the px domain from p40phox bound to phosphatidylinositol 3-phosphate	X-ray Diffraction	2001	10.1016/S1097-2765(01)00372-0
p47^{phox}	1KQ6	P47phox PX domain	X-ray Diffraction	2003	
	1UEC	Crystal structure of autoinhibited form of tandem sh3 domain of p47phox	X-ray Diffraction	2003	10.1111/j.1356-9597.2004.00733.x
	1NG2	Structure of autoinhibited p47phox	X-ray Diffraction	2003	10.1016/S0092-8674(03)00314-3
	1O7K	Human p47 PX domain complex with sulphates	X-ray Diffraction	2002	10.1093/emboj/cdf519
	1K4U	Solution structure of the c-terminal SH3 domain of p67phox complexed with the c-terminal tail region of p47phox	Solution NMR	2002	10.1093/emboj/cdf428

Subunit	PDB code	Protein	Method	Released year	Reference DOI
$p47^{phox}$	1GD5	Solution structure of the PX domain of p47phox	Solution NMR	2001	10.1038/88591
$p67^{phox}$	1WM5	Crystal structure of the N-terminal TPR domain (1-203) of p67phox	X-ray Diffraction	2005	
	1HH8	P67phox TPR domain	X-ray Diffraction	2001	10.1074/jbc.M100893200
	1E96	Structure of the Rac/p67phox complex	X-ray Diffraction	2000	10.1016/S1097-2765(05)00091-2
Rac2	2W2T	Rac2 (G12V) in complex with GDP	X-ray Diffraction	2009	10.1016/j.molcel.2009.02.023
	2W2V	Rac2 (G12V) in complex with GTPGS	X-ray Diffraction	2009	10.1016/j.molcel.2009.02.023
	2W2X	Complex of Rac2 and PlCG2 SPPH domain	X-ray Diffraction	2009	10.1016/j.molcel.2009.02.023
Rac1	3TH5	Crystal structure of wild-type Rac1	X-ray Diffraction	2012	10.1038/ng.2359

Data are form Protein data bank (PDB). Rac1 only list the crystal structure of wild-type Rac1.

1.2.1.3 The GTPase Rac

Rac is a member of the Rho-family of small GTPase. It is in an inactive state when it binds to GDP and in an active state when it binds to GTP. Guanine nucleotide exchange factors (GEFs) promote the release of GDP and allow the binding of GTP. GTPase activating proteins (GAPs) increase the rate of GTP hydrolysis and downregulate GTPase signalling. Guanine nucleotide dissociation inhibitors (GDIs) sequester the GDP-bound form of some GTPases in the cytosol and prevent them from translocating to membranes or being activated by GEFs (**Figure 15**) (Hodge and Ridley, 2016). There are two isoforms of Rac, Rac1 and Rac2. Both Rac1 and Rac2 comprise 192 amino acids and share 92% sequence homology. Rac1 is expressed ubiquitously, while Rac2 is only expressed in haematopoietic cells. Both Rac1 and Rac2 are geranylgeranylated at the C-terminus, which facilitates their interaction with membranes. In the resting state, they are kept cytosolic due to an interaction with the GDI protein RhoGDI. Purified Rac1 and Rac2 both support $O_2^{\cdot -}$ production in reconstituted cell-free systems (Groemping and Rittinger, 2005; Panday et al., 2015).

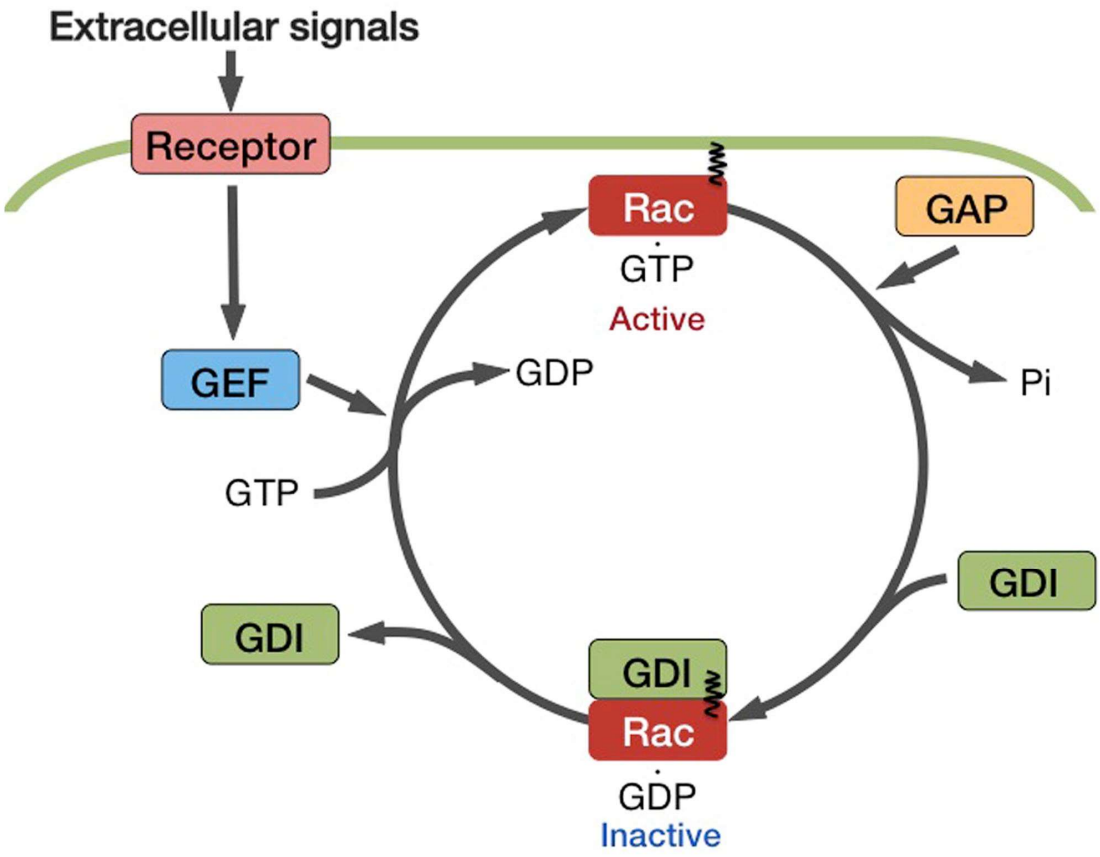

Figure 15. Mode of activation of the Rac GTPases.

Guanine nucleotide exchange factors (GEFs) promote the release of GDP from Rac and the binding of GTP. GTPase-activating proteins (GAPs) accelerate the intrinsic GTPase activity of Rac and reconvert it to the inactive GDP binding state. Guanine nucleotide dissociation inhibitors (GDIs) inhibit the exchange of GDP for GTP. (Kawano et al., 2014).

1.2.1.4 p40^{phox}

p40^{phox} is encoded by the gene *NCF4*, which is located on chromosome 22q13.1 (Zhan et al., 1996). p40^{phox} consists of 339 amino acids and is a 39 kDa protein. p40^{phox} contains a PX (Phox homology) domain, an SH3 domain and a PB1 (Phox and Bem1) domain (**Figure 16**). p40^{phox} is not needed for high-level enzyme activity on the phagocyte plasma membrane or in cell-free systems , however, p40^{phox} enhances the recruitment of p67^{phox} and p47^{phox} to the membrane in response to PMA . Furthermore, p40^{phox} is considered to play a crucial role in oxidase assembly at the phagosome (Ellson et al., 2006; Kuribayashi et al., 2002; Nunes et al., 2013; Suh et al., 2006). P40^{phox} and p67^{phox} interaction is mediated by their respective PB1 domains (p40^{phox} PB1: amino acids 237-339, p67^{phox} PB1: amino acids 352-429). p40^{phox} and p67^{phox} form a very tight complex (Groemping and Rittinger, 2005). The SH3 domain of p40^{phox} interacts with the PRR domain in C-terminus of p47^{phox}, but the interaction between p40^{phox} and p47^{phox} is very week compared with the interaction between p47^{phox} and p67^{phox} (Massenet et al., 2005). PX domain of p40^{phox} especially bind to PI3P, the details of this interaction is described in the phosphoinositides part.

1.2.1.5 p47^{phox}

p47^{phox} is encoded by the gene *NCF1*, which is located on chromosome 7q11.23 (from HGNC). p47^{phox} is composed of 390 amino acids and is a 44.7 kDa protein. p47^{phox} consists of a PX domain (amino acids 4-121), two adjacent SH3 domains (amino acids 159-214 (SH3A) and amino acids 229-284 (SH3B)), a polybasic region (PBR, a region rich in arginine and lysine residues), and at least one Proline-rich region (PRR, amino acids 363-368) (**Figure 16**). p47^{phox} PRR interacts with the second SH3 domain of p67^{phox} (p67^{phox}-SH3B) (El-Benna et al., 2009; Groemping and Rittinger, 2005).

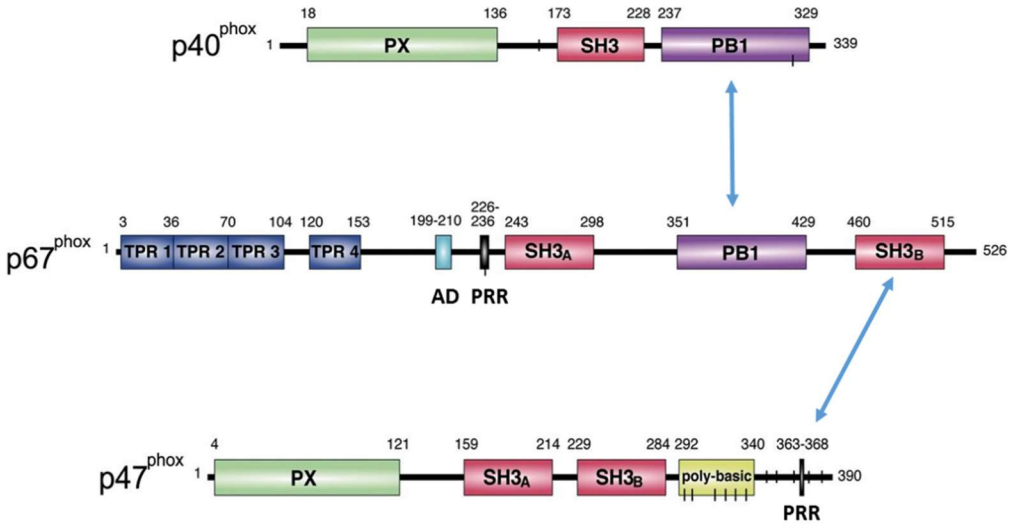

Figure 16. Domain structure of the cytosolic subunits p40^{phox}, p47^{phox} and p67^{phox}

p40^{phox} contains a Phox homology (PX) domain, an Src homology 3 (SH3) domain and a Phox and Bem1 (PB1) domain. p67^{phox} contains four tetratricopeptide (TPR) motifs, an activation domain (AD), a proline-rich region (PRR), two SH3 domains and a PB1 domain. p47^{phox} contains a PX domain, two SH3 domains, a poly-basic motif and a PRR. p67^{phox} constitutively interacts with p40^{phox} via PB1-PB1 binding. p67^{phox} also tethers to p47^{phox} via a SH3B-PRR binding. The locations of serine and threonine residues that become phosphorylated during activation are indicated by thin black bars. *Adapted from* (Groemping and Rittinger, 2005).

Auto-inhibited conformation of p47^{phox}

In the resting state, the tandem SH3s interact intramolecularly with C-terminal region of the non phosphorylated p47^{phox}, which is called auto-inhibitory region (AIR) (Groemping et al., 2003; Yuzawa et al., 2004a; Yuzawa et al., 2004b), and SH3B intramolecularly interacts with the PX domain (**Figure 17**) (Ago et al., 2003; Hiroaki et al., 2001). These domains are believed to be unmasked during activation. This enable PX domain bind to membrane anionic phospholipids (Ago et al., 2001; Karathanassis et al., 2002) and the tandem SH3s interact with the p22^{phox} C-terminus (Nobuhisa et al., 2006; Ogura et al., 2006). It seems unlikely that the second SH3B (using the same binding site) interact with the PX and the AIR at the same time. Marcoux *et al.* suggests that there are contacts between the PX and parts of the "tandem SH3s-AIR super-complex"(Marcoux et al., 2009), but the mechanism still need to be further investigated.

Phosphorylation of p47^{phox}

Multiple phosphorylation events are required in p47^{phox} to relieve auto-inhibition and allow translocation to the membrane. Neither p40^{phox} or p67^{phox} can translocate to the membrane in stimulated neutrophils from CDG patients that lack a functional p47^{phox} (Dusi et al., 1995). 11 phosphorylation sites have been mapped including serine residues 303, 304,310, 315, 320, 328, 345, 348, 359, 370 and 379. Serine residues 303, 304, 310, 315, 320 and 328 are located in the PBR and therefore are part of the auto-inhibitory segment. Serine residues 303, 304 and 328 are especially important for activation (Groemping and Rittinger, 2005). Only the mutation of serine 379 to alanine completely prevents membrane translocation and inhibits NADPH oxidase activation, mutation of serine 303 alone or 304 or 328 or 359 or 370 to alanine inhibited nearly 50% NADPH oxidase activation, and mutation of serine 315 or 320 or 348 to alanine has no effect. Double mutations show that paired phosphorylated serines (serines (303 + 304) and serines (359 + 370)) are necessary for NADPH oxidase activation (El-Benna et al., 2009). p47^{phox} is phosphorylated on selective sites by different protein kinases *in vitro* conditions. *In vivo* multiple protein kinases may participate to the p47^{phox} phosphorylation. Pro-inflammatory cytokines such as GM-CSF and TNFα induce partial phosphorylation of p47^{phox} on Ser345 by ERK1/2 or p38MAPK and promote NADPH oxidase assembly. Phosphorylation of p47^{phox} by PKC, PAK and AKT has a positive stimulatory effect on NADPH oxidase activation (El-Benna et al., 2009).

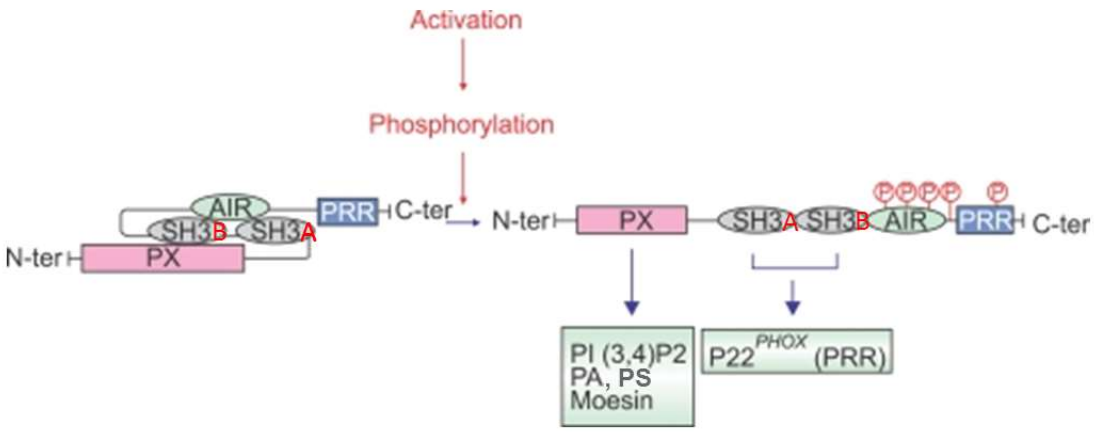

Figure 17. Conformational and domains interactions changes after p47^{phox} activation.

In resting state the two SH3 domains interact with the auto-inhibitory region (AIR) in the C-terminus and SH3B intramolecularly interacts with the PX domain to keep the protein in an auto-inhibited state. Upon activation, p47^{phox} is phosphorylated, this phosphorylation induces conformational changes allowing SH3 domains to interact with the proline-rich region (PRR) of p22^{phox} and PX domain to bind to phosphatidylinositol 3,4-biphosphate (PI(3,4P)), phosphatidic acid (PA), phosphatidylserine (PS) and moesin. *Adapted from* (El-Benna et al., 2009).

1.2.1.6 p67^{phox}

p67^{phox} is encoded by the gene neutrophil cytosol factor (NCF2), which is located on chromosome 1q25 (Francke et al., 1990). p67^{phox} consists of 526 amino acids and is a 59.8 kDa protein. p67^{phox} contains a four TPR (tetratricopeptide repeat) motif-containing domain, a PRR and two SH3 domains which are separated by a PB1 domain (**Figure 16**) (Groemping and Rittinger, 2005). p67^{phox} alone can facilitate electron flow from NADPH to the flavin center of the NADPH oxidase (Cross and Curnutte, 1995) and contains the catalytic NADPH-binding site of the NADPH oxidase (Smith et al., 1996). Rac bind to the TPR of p67^{phox}. The affinities of p67^{phox} for Rac1 and Rac2 are similar (Lapouge et al., 2000). Notably, two residues Ala^{27} and Gly^{30} of Rac in the interface of p67^{phox}-Rac complex are important for both proteins interaction and the NADPH oxidase activation. Mutation of both amino acids in Rac leads to complete failure of p67^{phox} binding and NADPH oxidase activation. Cdc42 is a close homologue to Rac but the two previous residues in Cdc42 are differents from Rac. Cdc42 can neither interact with p67^{phox} nor activate the NADPH oxidase. However introduction of the related residues from Rac to Cdc42 enable Cdc42 interact with p67^{phox} and activate the NADPH oxidase (Kwong et al., 1993; Lapouge et al., 2000). The first SH3 of p67^{phox} (p67^{phox}-SH3A) primarily increases the affinity of p67^{phox} for the oxidase complex (Maehara et al., 2009). p67^{phox} is able to bind a Cys-Gly-Cys triad in the dehydrogenase region of gp91^{phox} (Dahan et al., 2015). The Cys-Gly-Cys triad is absent in other Nox (Dahan et al., 2015) and p67^{phox}-SH3A is not involved in activation of Nox1 and Nox3 (Maehara et al., 2009), suggesting that p67^{phox} play a special role in the activation of gp91^{phox}.

1.2.1.7 NADPH oxidase assembly

Under resting conditions, p40^{phox}, p47^{phox} and p67^{phox} exist in the cytosol as a complex and associate with a 1:1:1 stoichiometry (Lapouge et al., 2002). After stimulation, p47^{phox} is phosphorylated and the cytosolic p40^{phox}-p47^{phox}-p67^{phox} complex subsequently translocates to the membrane and interacts with the membrane subunits gp91^{phox} and p22^{phox} to form the active NADPH oxidase. This activation also requires Rac GTPase. Upon activation, Rac binds GTP and translocate to the membrane along with the cytosolic complex (Groemping and Rittinger, 2005; Panday et al., 2015). The dynamics and interactions between the subunits are tricky questions. It has been found that p67^{phox} stays at the phagosome until the end of ROS production (Tlili et al., 2012). Li *et al* show that the interaction between p67^{phox} and p47^{phox} is lost after few minutes of phagosome closure (Li et al., 2009a), and Faure *et al.* find

that $p47^{phox}$ and Rac2 accumulate transiently at the phagosome and detach from the phagosome before the end of ROS production (**Figure 18**) (Faure et al., 2013). As both Rac-$p67^{phox}$ and $p67^{phox}$-$p47^{phox}$ interaction are important for NADPH oxidase activation, this raise the question: Is $p40^{phox}$ important to maintain $p67^{phox}$ during the ROS production at the phagosome? The dynamics of the NADPH oxidase cytosolic subunits in the complex may be different at the phagosome and at the plasma membrane.

Actin is also critical in facilitating the translocation of the cytosolic subunits (Stanley et al., 2014). It has been found that $p67^{phox}$, $p40^{phox}$, Rac2 associate with actin cytoskeleton both in resting and activated neutrophils. $p47^{phox}$ associate with actin cytoskeleton in resting neutrophils, but the association between $p47^{phox}$ and actin cytoskeleton in activated neutrophils is still a matter of debate (El Benna et al., 1999; el Benna et al., 1994; Nauseef et al., 1991; Stanley et al., 2014; Woodman et al., 1991). One study report that $p47^{phox}$ does not associate with cytoskeleton in activated neutrophils (Woodman et al., 1991), the others report that part of the $p47^{phox}$ translocated from cytosol to the cortical cytoskeleton (el Benna et al., 1994; Nauseef et al., 1991). A more recent study confirmed that $p47^{phox}$, Rac1 and to a less extent Rac2, but not $p67^{phox}$, directly bind to both α-actin and β-actin (Tamura et al., 2000). Later it has been found that $p40^{phox}$ can directly bind to F-actin via the PX domain (Shao et al., 2010). NADPH oxidase components are also able to indirectly associate with actin through actin binding proteins including WAVE1, moesin, and cortactin (Stanley et al., 2014).

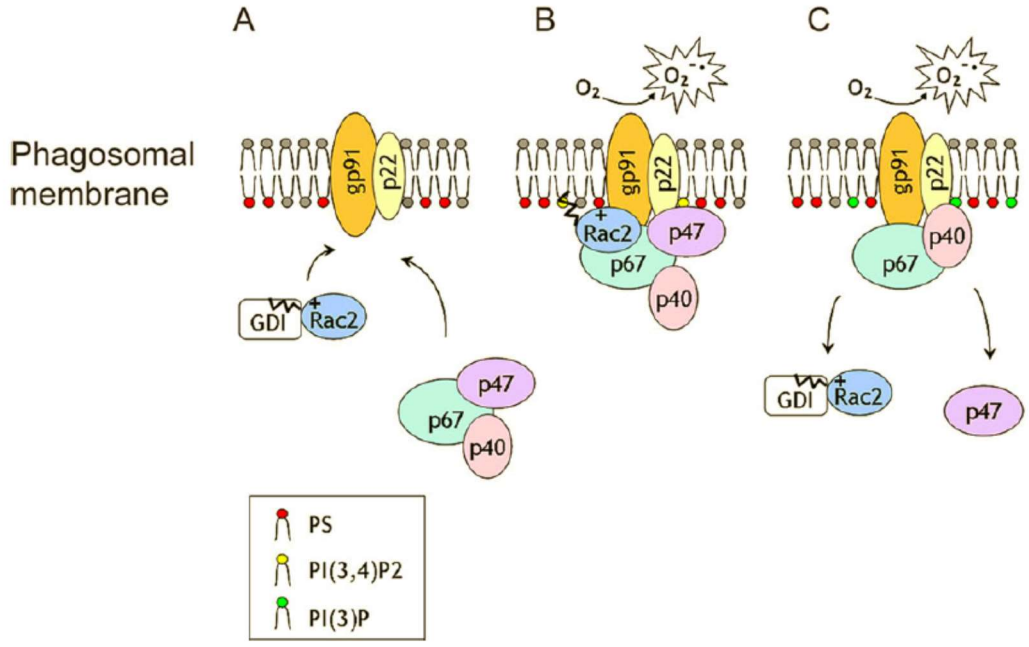

Figure 18. Model of NADPH oxidase assembly during phagocytosis.

(A) At the beginning of the NADPH oxidase activity, the cytosolic subunits complex $p40^{phox}$-$p47^{phox}$-$p67^{phox}$ and small GTPase Rac are recruited to the phagosomal membrane. (B) The activated NADPH oxidase generate $O_2^{\cdot-}$. (C) Few minutes later, Rac2 and $p47^{phox}$ detach from the phagosomal membrane, but $p67^{phox}$ and $p40^{phox}$ stay at the membrane until the termination of the ROS production. (Faure et al., 2013).

1.2.2 ROS and immunity

Reactive oxygen species play an important role in killing microbial pathogens. The major source of reactive oxygen species is from NADPH oxidase.

1.2.2.1 Reactive oxygen species

The neutrophil oxidase catalyzes the production of $O_2^{\cdot -}$, subsequently a dismutation reaction occurs to produce H_2O_2. $O_2^{\cdot -}$ and H_2O_2 are able to react with products of other microbicidal systems to generate additional ROS, such as hydroxyl radical ($OH\cdot$), singlet oxygen ($^1O_2$), hypochlorous acid (HOCl), and ozone (O_3) (**Figure 19**). They can cause deleterious modifications of proteins, nucleic acids and membrane components(Robinson, 2008). The amount of ROS produced in the phagosome is still not known. The estimated steady-state concentration of $O_2^{\cdot -}$ and H_2O_2 is respectively 25µM and 2µM in the phagosome (Winterbourn et al., 2006). *Candida albicans* and *Escherichia Coli* response differently to the exposure of H_2O_2, this raise the question of how much ROS and which kind of ROS is needed to kill the different pathogens (Dupre-Crochet et al., 2013). Compared to $O_2^{\cdot -}$ and H_2O_2, HOCl is a strong oxidant. HOCl is catalyzed by myeloperoxidase (MPO) from chloride (Cl^-) and H_2O_2. HOCl is highly cytotoxic and microbicidal. *Staphylococcus aureus* is primarily killed by HOCl inside phagosomes (Green et al., 2014).

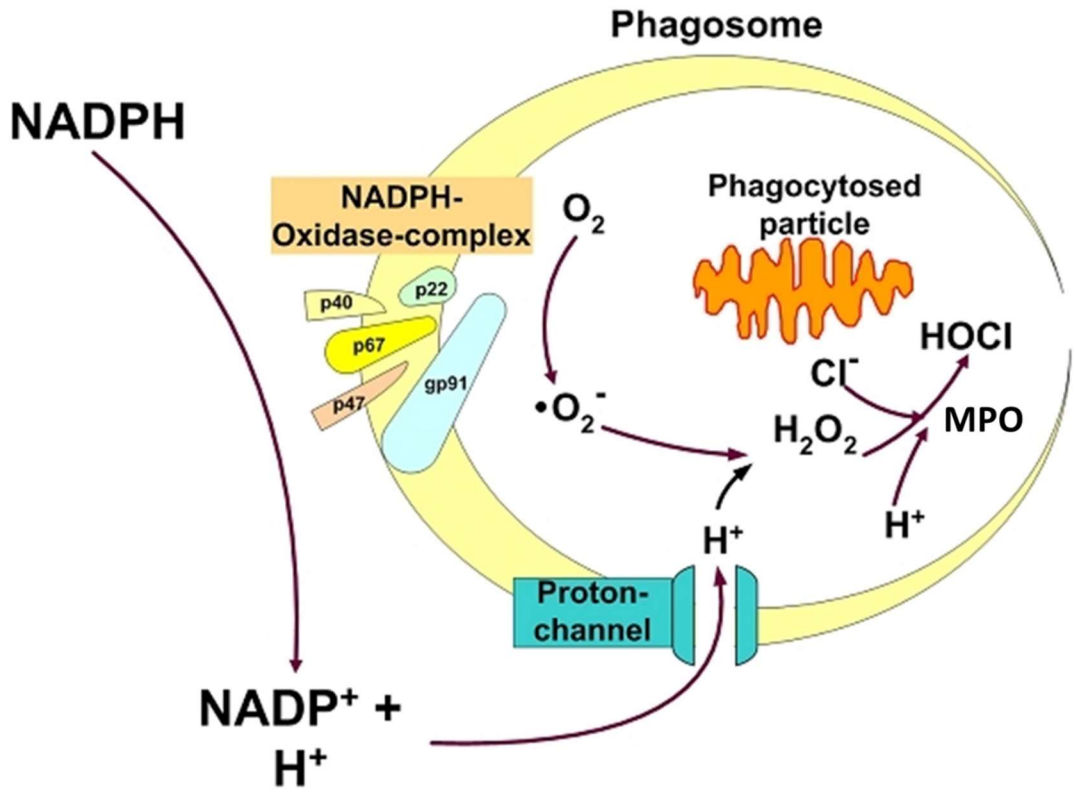

Figure 19. ROS production during phagocytosis.

The NADPH oxidase catalyzes the production of $O_2^{\cdot-}$, and generate an H^+, during the the oxidation of NADPH, that is channelled into the phagosome via a proton channel. $O_2^{\cdot-}$ is rapidly dismutated to H_2O_2, which is further transformed to HOCl by myeloperoxidase and other ROS. *Adapted from* (Riechelmann, 2004).

1.2.2.1 Chronic granulomatous disease

Chronic granulomatous disease (CGD) is a rare genetic disorder caused by defects in the phagocyte NADPH oxidase complex. The estimated incidence of CGD is approximately 1:200000. CGD is the most common clinically significant genetic disorder of neutrophil function (Dinauer, 2014). Nearly 70% of CGD cases are from X-linked recessive defects in the gene encoding $gp91^{phox}$. Only one case is from autosomal recessive defects in the gene encoding $p40^{phox}$ (Dinauer, 2014; Matute et al., 2009). CGD patients typically present in infancy or early childhood recurrent infections toward certain fungi (*Aspergillus*) and catalase positive bacteria (*Staphylococcus aureus, Burkholderia, cepacia complex, Serratia marcescens* and *Nocardia*) (Cachat et al., 2015; Dinauer, 2014). Neutrophils lacking functional $p47^{phox}$ can still produce low levels of superoxide (Vowells et al., 1996). CGD patients involving the $gp91^{phox}$, $p22^{phox}$, or $p67^{phox}$ are more clinically severe than patients involving $p47^{phox}$ (Kuhns et al., 2010). It has been shown that in X-linked *Cybb*-null (X-CGD) mice exhibited increased release of IL-1α and G-CSF elicited by tissue injury, high levels of cytokines resulted in hyper-inflammation (Bagaitkar et al., 2015). This suggests that ROS may decrease inflammation by decreasing cytokine production via modulation of NF-κB (nuclear factor kappa-light-chain-enhancer of activated B cells), which can control transcription of DNA, cytokine production and cell survival (Hoesel and Schmid, 2013).

1.2.2.2 Microbial antioxidant defense

Many pathogens have developped multiple strategies to counteract host defences and to survive inside the host cell (Flannagan et al., 2009). Microbes can disturb the assembly or activation of the NADPH oxidase to prevent killing by neutrophils. Human granulocytic anaplasmosis is a tick-borne rickettsial infection of neutrophils caused by *Anaplasma phagocytophilum* (Dumler et al., 2005). Infected neutrophils and HL-60 fail to produce ROS because of *A. phagocytophila* inhibits transcription of $gp91^{phox}$ and Rac2 (Carlyon et al., 2002) and decrease the levels of $p22^{phox}$ (Mott, 2002). Tularemia is a multisystem plague-like illness caused by *Fransicella tularensis*, which can exclude flavocytochrome b_{558} from its phagosome (McCaffrey et al., 2010). Helicobacter pylori (Hp) is a Gram-negative bacterium that induces gastritis, and a subset of infections that can lead to peptic ulceration or gastric cancer. Hp disrupts NADPH oxidase targeting such that $O_2^{\cdot -}$ is released into the extracellular space and do not accumulate inside Hp phagosomes. Nascent Hp phagosomes acquire

flavocytochrome b_{558} but do not efficiently recruit or retain $p47^{phox}$ or $p67^{phox}$ (Allen et al., 2005).

1.2.2.3 Overproduction of ROS by NADPH oxidase

The phagocyte NADPH oxidase is a double edge sword.Indeed, an excessive an inappropriate extracellular ROS production can be harmful Ischemia and reperfusion (IR)-induced tissue injuries that contribute to morbidity and mortality in a broad range of pathologies, such as trauma, myocardial infarction, ischemic stroke, circulatory arrest, and some types of hematological and respiratory diseases. ROS are produced in two stages, ischemia and reperfusion, at low and high levels, respectively. After reperfusion, inflammatory leucocytes such as macrophages and neutrophils cause further ROS production beyond the initiation of the inflammatory cascade. In this case, ROS overproduction can increase the complications related to cardiac reperfusion (Bagheri et al., 2016). Overproduction of ROS also contributes to neurotoxicity, neurodegeneration, and cardiovascular diseases. Many of the neurodegenerative diseases are due to increased ROS production and/or decreased antioxidant cell capacity to detoxify these molecules, such as in Parkinson's and Alzheimer's diseases (Infanger et al., 2006).

1.2.3 ROS and signaling

1.2.3.1 ROS signalling

ROS also affect the signalling pathways as messengers. ROS can regulate diverse physiological activities such as the response to growth factor stimulation and the generation of the inflammatory response. Dysregulated ROS signalling may contribute to human diseases (Finkel, 2011). H_2O_2 is generally regarded as the predominant intracellular redox-signalling molecule. It is small and relatively stable, highly ubiquitous, diffuse easily, and is rapidly induced when it is required with both its production and destruction. $O_2^{\cdot -}$ is quickly dismutated to H_2O_2, and its targets are limited to those within the immediate vicinity of its source due to its lack of diffusibility. •OH is unsuitable as a messenger due to its highly nonspecific oxidation. Peroxyl and alkoxyl radicals are more likely to induce irreversible oxidation events that further lead to the degradation of the damaged protein. HOCl has also

been proposed to function as signalling mediator in immune cells (Corcoran and Cotter, 2013).

ROS are produced in response to various ligands, such as growth factors, cytokines, and GPCRs. A variety of signalling pathways are perturbed by ROS, including ERK1, ERK2, JNK (c-Jun N-terminal kinase), NF-κB (nuclear factor κB), FAK (focal adhesion kinase), AP-1, Akt, Ras, Rac, and JAK-STAT (Lambeth and Neish, 2014). Local ROS generation causes reversible post-translational modification at cysteine, selenocysteine, methionine, and histidine residues of proteins. Modification of cysteine is regarded as a reversible redox switch. Oxidation of cysteine can change protein conformation, affect the active (or binding) site of the protein, or change its surface properties (Woolley et al., 2013). The pKa of most cysteine thiols in proteins is approximately 8.5 (protonated). Oxidation is possible if the cysteine residues are of low pKa (ionized). H_2O_2 oxidizes cysteines to disulfides, which can be reduced by glutaredoxins (Grxs), thioredoxins (Trxs), or glutathione (GSH). The modification is reversible or irreversible depend on different condition(Russell and Cotter, 2015). Reactive cysteines are always located in the active site of the enzyme. Oxidation of the reactive cysteines modulates the enzyme's activity. Such oxidant-sensitive proteins include protein tyrosine phosphatases (PTPs), lipid phosphatases (e.g. phosphatase and tensin homolog (PTEN)), mitogen-activated protein kinase phosphatases (MAPK-Ps or DUSPs), low-molecular weight protein tyrosine phosphatases (LMW-PTPs), and regulatory enzymes of ubiquitin and ubiquitin-like proteins (e.g. SUMO and Nedd8) (Lambeth and Neish, 2014; Russell and Cotter, 2015).

Akt is a serine/threonine-specific kinase consisting of three isoforms Akt1, Akt2 and Akt3. PI3K-Akt pathway is a proximal downstream target of RTKs (Fayard, 2005; Jiang et al., 2011). Following activation, the production of $PI(3,4)P_2$ and $PI(3,4,5)P_3$ by PI3K recruits AKT. ROS enhance Akt activation through inactivating the phosphatase PTEN by oxidation of the catalytic cysteine of PTEN. PTEN is a negative regulator of the PI3K activity (Kwon et al., 2004). Moreover, activation of Akt by H_2O_2 is also mediated by Src kinase, which is activated by H_2O_2 (Russell and Cotter, 2015).

1.2.3.2 Signalling and regulation of NADPH oxidase activation

One mechanism to produce more ROS is the upregulation of the expression of the enzyme. It may occur at the transcriptional or post-transcriptional levels, even translational level. $Gp91^{phox}$ transcription is regulated by the IFN-γ/ JAK-STAT (Janus tyrosine kinase-signal transducer and activator of transcription) pathway. $Gp91^{phox}$ promotor contains the consensus STAT1 binding site, γ-activated sequence, which is essential in mediating IFN-γ induced $gp91^{phox}$ transcription. Nox1, Nox4, $p22^{phox}$, $p47^{phox}$, and $p67^{phox}$ promotors also contains the γ-activated sequence which maybe involve in mediating IFN-γ induced transcription of these subunits. Meanwhile, Nox1, $p22^{phox}$, NOXO1, and $p67^{phox}$ contain the binding sites for AP-1 (activator protein 1), which is a transcription factor that regulates gene expression in response to a numerous of stimuli, such as cytokines, growth factors, stress, and microbial infections (Hess, 2004; Jiang et al., 2011).

Phosphorylation is essential for NADPH oxidase activation, $p47^{phox}$ is well established and the phosphorylation of $p47^{phox}$ has been described above in the "$p47^{phox}$ paragraph ". Elevation of intracellular Ca^{2+} acts also as an upstream signal to activate NADPH oxidase. It is well accepted that Ca^{2+} stimulates NADPH oxidase activity by promoting granule fusion, PKC activity and other indirect effects (Nunes et al., 2013). Rac is activated by an elevation of intracellular Ca^{2+} in a PKC-dependent way , but whether Ca^{2+}-PKC-Rac pathway is involved in NADPH oxidase activation is still not known (Jiang et al., 2011; Price et al., 2003).

1.2.4 ROS and adhesion

1.2.4.1 ROS and ECM

ECM influences the ROS production of the cells, and, ROS affect the production, assembly and turnover of the ECM during wound healing and matrix remodelling (Eble and de Rezende, 2014).

1.2.4.1.1 ECM regulates ROS production

De Renzede *et al.* observe that upon adhesion to laminin-111, aortic smooth muscle cells initially form membrane protrusion, they term these areas oxidative hot spots. They are

spatially and temporally transient during an early stage of adhesion and depend on the activity of the NOX4 (de Rezende et al., 2012). Platelet derived growth factor (PDGF) can induce ROS production at focal adhesion sites of fibroblasts (Lin et al., 2013). Do neutrophils also have oxidative hot spot when they adhere to ECM need to be further investigated. The adherence of neutrophils to various ECM proteins has been shown to result in an enhanced ROS production in response to a variety of soluble activators, such as fMLF and TNF-α (Nathan et al., 1989; Zhao et al., 2003).

1.2.4.1.2 ROS influence ECM production and deposition

ROS affect the production of ECM proteins at transcriptional, translational and posttranslational levels. Oxidation of the cysteine residues within the ECM proteins leads to activity-relevant conformational changes of these ECM proteins (Eble and de Rezende, 2014). Fibrinogen is extremely susceptible to ROS. Fibrinogen has calcium
binding sites, thus providing potential targets for site-specific oxidation of the protein. Fibrinogen is a glycoprotein, oxidation of the carbohydrate moieties could add to the incorporation of carbonyls (Shacter et al., 1994). Studies show that the lysine residues of fibrinogen are the functional groups which are most susceptible to be oxidized (Tetik et al., 2011; Upchurch Jr et al., 1998). Oxidized fibrinogen is more active to induce the expression cell adhesion molecules (P-selectin and ICAM-1) on the surface of cells in primary culture of human vascular endothelial cells (Azizova et al., 2007). Oxidized fibrinogen increases the fibrin formation and enhances platelet aggregation (Upchurch Jr et al., 1998). Behçet disease (BD) is a systemic vasculitis with redox imbalance and circulating neutrophil hyperactivation. It is reported that altered fibrinogen structure and impaired fibrinogen function (ie fibrin clot formation) are related with neutrophil activation and enhanced ROS production (Becatti et al., 2015). Enhanced neutrophils ROS production is associated with increased plasma levels of oxidative stress markers and in particular with a greater extent of fibrinogen carbonylation. Only neutrophil-derived ROS show a significant correlation with fibrinogen carbonyl content, suggesting neutrophil activation drives fibrinogen oxidation (Becatti et al., 2015).

1.2.4.2 ROS and integrins

Integrin-mediated neutrophil adhesion has been implicated in a wide array of phagocyte responses which includes ROS production. Superoxide dismutase (SOD) or catalase treatment

decreased neutrophils accumulation in the reperfused heart and prevented the marked upregulation of β2 integrins expression seen after reperfusion, suggesting that ROS is able to promote adhesion of neutrophils by triggering β2 integrins expression on the surface of neutrophils (Serrano et al., 1996). Furthermore, H_2O_2 also enhances the expression of ICAM-1 on endothelial cells and increases the ability of leukocyte adhesion to endothelial cells. These suggest that ROS may enhance the adhesive interaction between neutrophils and endothelial cells (Nagata, 2005).

Defects in adhesion molecules result in recognized primary immune deficiencies, collectively named leukocyte adhesion deficiency (LAD) syndromes. Three LAD syndromes have been described. LAD I affects the firm adhesion on leukocytes to the endothelium and is due the mutations in β2 integrin. LAD II, leads to defect in the rolling phase and is due to the absence of the selectin fucosylated ligands that are needed for initiating the rolling phase. LAD III is due to mutations in kindlin-3 which is an important component for all integrin activation (Hanna and Etzioni, 2012). LAD lead to the general phenomenon of poor inflammation due to poor recruitment of neutrophils into the site of infection or inflammation. Complement-mediated phagocytosis and ROS production are diminished in LAD I patients, but IgG-mediated phagocytosis, ROS production, and primary and secondary granule release are unaffected (Anderson and Springer, 1987; Rosenzweig and Holland, 2004). This may due to the presence of normal IgG, Fc, CR-I, and other receptors on deficient neutrophils.

1.3 Phosphoinositides

Phosphoinositides are phosphorylated derivatives of phosphatidylinositol (PtdIns). PtdIns are synthesized primarily in the endoplasmic reticulum (ER) and then transfered to other membranes either by vesicular transport or through cytosolic PtdIns transfer proteins (PITPs) (Di Paolo and De Camilli, 2006). PITPs mobilize energy-independent transfer of PtdIns, PtdCho and other lipids between membranes *in vitro*, and are therefore also supposed to transfer lipids in a ATP independent way *in vivo* (Grabon et al., 2015). PtdIns contains a glycerol backbone, two non-polar fatty acid tails, a phosphate group substituted with an inositol polar head group. It leaves five hydroxyls for phosphorylation in the inositol ring, but only three of these (positions -3, -4, and -5) are phosphorylated according to current knowledge. Reversible phosphorylation at positions 3, 4 and 5 leads to the generation of seven phosphoinositide species (**Figure 20**) (Balla, 2013; Di Paolo and De Camilli, 2006). The amounts and distribution of PPIs are summarized in **Table 4**.

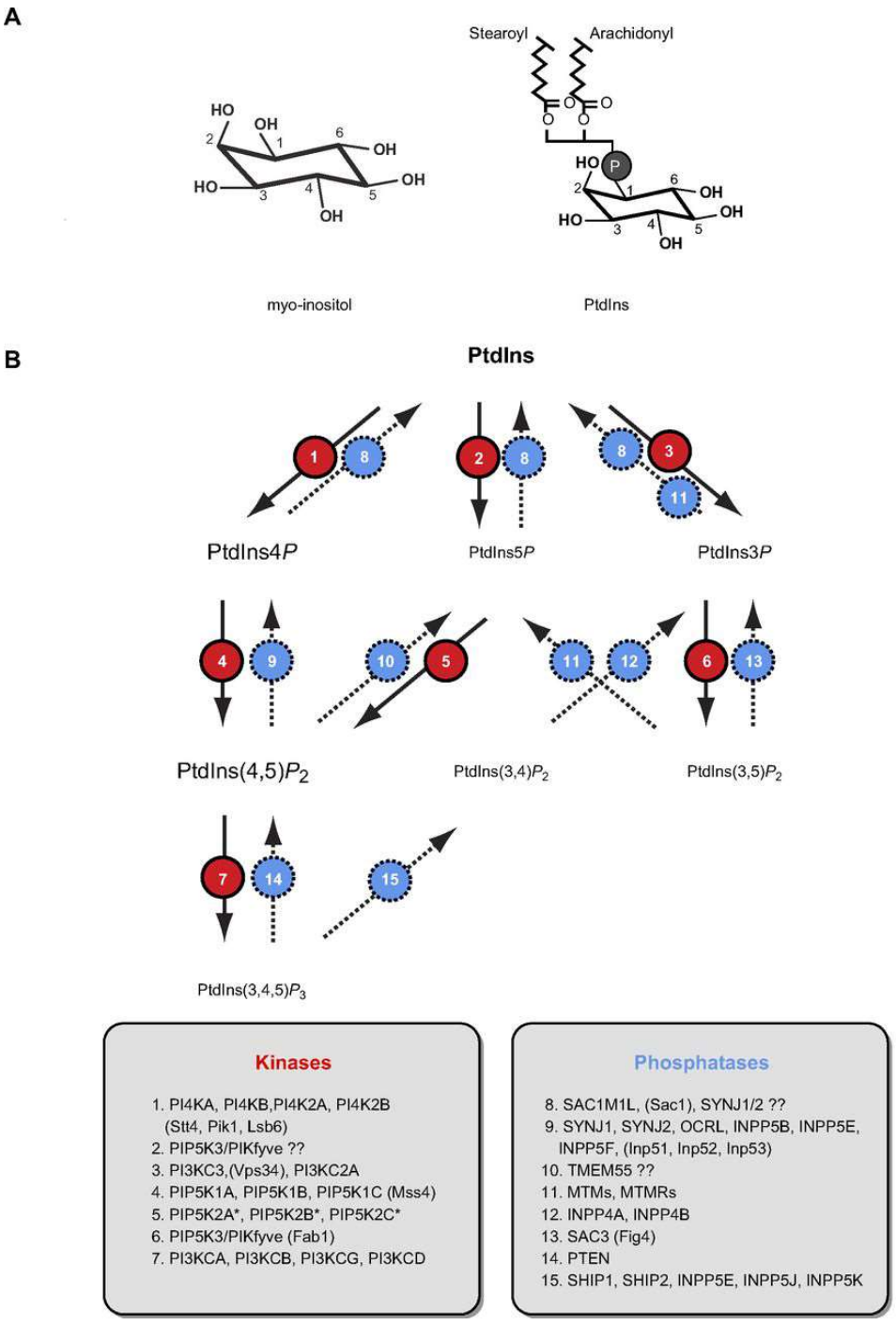

Figure 20. Structure and metabolism of phosphoinositides.

Structure of myo-inositol and phosphoinositide. B. Metabolism of phosphoinositides. The yeast enzymes are listed in parentheses. "??" indicates that there is some ambiguity. "*" indicates that PIP5K2s are 4-kinases that act on PI5P. Adapted from (Balla, 2013).

Table 4. PPIs amount and distribution in cells.

Table 4 is summarized from (Balla, 2013; Di Paolo and De Camilli, 2006; Falkenburger et al., 2010; Jeschke and Haas, 2016; Shewan et al., 2011)

	Amount	Distribution
PtdIns	~10-20 % (mol%) of total cellular phospholipids	endoplasmic reticulum (ER), Golgi complex, early endosome
PI4P and $PI(4,5)P_2$	~0.2-1 % of total cellular phospholipids	
$PI(4,5)P_2$	5000-20000 molecules/μm2 in the plasma membrane	**plasma membrane**, Golgi complex, early endosome,nucleus, **early phagosome, phagolysosome**
$PI(3,4,5)P_3$	~2-5 % of $PI(4,5)P_2$	**plasma membrane**, **early phagosome, phagolysosome**
PI3P	~20-30 % of PI4P	Golgi complex, early endosome, late endosome, multivesicular body (MVB), **early phagosome, late phagosome**
$PI(3,4)P_2$		**plasma membrane**, early endosome, **early phagosome**
$PI(3,5)P_2$		early endosome, late endosome, lysosome, MVB
PI4P		**plasma membrane**, ER, Golgi complex, early endosome, secretory granule, **early phagosome, phagolysosome**
PI5P		**plasma membrane**, late endosome, nucleus

1.3.1 Phosphoinositide kinases

Generally, most PtdIns are mono-phosphorylated by the Phosphoinositide 4-kinases (PI4Ks) at position 4 or by the Class III Phosphoinositide 3-kinases (Class III PI3K/ vps34) at position 3 in endomembranes, such as the endosomes and the Golgi/*trans*-Golgi network. PI4P is then phosphorylated to $PI(4,5)P_2$ by Phosphatidylinositol 4-Phosphate-5 kinase (PI4P5K, PIP5K, PI5K). $PI(4,5)P_2$ can then be further phosphorylated by PI(3,4,5)P3 by class I PI3Ks primarily at the plasma membrane (Balla, 2013).

The **phosphatidylinositol 4-kinases (PI4Ks)** synthesize phosphatidylinositol 4-phosphate (PI4P). All eukaryotes have two type II PI4Ks (α and β) and two type III PI4Ks (α and β) (Boura and Nencka, 2015). There are three types of **PIP Kinase (PIPK)**. Type I PIPKs are PI4P 5-kinases (**PIP5Ks**), which generate $PI(4,5)P_2$ from PI4P. Type II PIPKs are PI5P 4-kinases (**PIP4Ks**), which generate $PI(4,5)P_2$ from PI5P. Type III PIPK (PIP5K3) phosphorylate PI3P to PI(3,5)P2. Type III PIPK include a single kinase PIKfyve (Fab1 in yeast) (Balla, 2013).

Phosphoinositide 3-kinases (PI3Ks), which phosphorylate the 3′-OH position of the inositol ring of inositol phospholipids, produce three lipid products: PI3P, $PI(3,4)P_2$ and $PI(3,4,5)P_3$. There are three classes of PI3Ks in mammalian cells: class I PI3K, class II PI3K, and class III PI3K. The classification is mainly based on the presence of additional protein domains and their interactions with regulatory subunits (Cantrell, 2001; Jean and Kiger, 2014). The phosphoinositide kinases are summarized in **Table 5**. The protein names that we'll be used are common names, shown in **bold** in **Table 5**.

Table 5. Nomenclature of the phosphoinositide kinases.

Kinase	Group	Approved symbol	Approved name	Aliases	Chrosome	Yeast ortholog
PI3K	class IA catalytic	PIK3CA	phosphatidylinositol-4,5-bisphosphate 3-kinase catalytic subunit alpha	**PI3Kα**, **p110α**	3q26.32	
		PIK3CB	phosphatidylinositol-4,5-bisphosphate 3-kinase catalytic subunit beta	**PI3Kβ**, **p110β**	3q22.3	
		PIK3CD	phosphatidylinositol-4,5-bisphosphate 3-kinase catalytic subunit delta	**PI3Kδ**, **p110δ**	1p36.22	
	class IB catalytic	PIK3CG	phosphatidylinositol-4,5-bisphosphate 3-kinase catalytic subunit gamma	**PI3Kγ**, **p110γ**	7q22.3	
	class I regulatory	PIK3R1	phosphoinositide-3-kinase regulatory subunit 1	**p85α**	5q13.1	
		PIK3R2	phosphoinositide-3-kinase regulatory subunit 2	**p85β**	19p13.11	
		PIK3R3	phosphoinositide-3-kinase regulatory subunit 3	**p55γ**	1p34.1	
		PIK3R4	phosphoinositide-3-kinase regulatory subunit 4	**p150**	3q22.1	
		PIK3R5	phosphoinositide-3-kinase regulatory subunit 5	**p101**	17p13.1	
		PIK3R6	phosphoinositide-3-kinase regulatory subunit 6	**p87**	17p13.1	
	Class II	PIK3C2A	phosphatidylinositol-4-phosphate 3-kinase catalytic subunit type 2 alpha	**PI3KC 2α**	11p15.1	
		PIK3C2B	phosphatidylinositol-4-phosphate 3-kinase catalytic subunit type 2 beta	**PI3KC 2β**	1q32.1	

		PIK3C2G	phosphatidylinositol-4-phosphate 3-kinase catalytic subunit type 2 gamma	**PI3KC2δ**	12p12.3	
	Class III	PIK3C3	phosphatidylinositol 3-kinase catalytic subunit type 3	**Vps34**	18q12.3	Vps34
PI4K	Type II	PI4K2A	phosphatidylinositol 4-kinase type 2 alpha	**PI4KIIα**	10q24.2	
		PI4K2B	phosphatidylinositol 4-kinase type 2 beta	**PI4KIIβ**	4p15.2	
	Type III	PI4KA	phosphatidylinositol 4-kinase alpha	**PI4KIIIα**	22q11.21	Stt4
		PI4KB	phosphatidylinositol 4-kinase beta	**PI4KIIIβ**	1q21.3	Pik1
PIPK	Type I	PIP5K1A	phosphatidylinositol-4-phosphate 5-kinase type 1 alpha	**PIPKIα**	1q21.3	
		PIP5K1B	phosphatidylinositol-4-phosphate 5-kinase type 1 beta	**PIPKIβ**	9q21.11	
		PIP5K1C	phosphatidylinositol-4-phosphate 5-kinase type 1 gamma	**PIPKIγ**	19p13.3	Mss4
	Type II	PIP4K2A	phosphatidylinositol-5-phosphate 4-kinase type 2 alpha	PIP5K2A, **PIPKIIα**	10p12.2	
		PIP4K2B	phosphatidylinositol-5-phosphate 4-kinase type 2 beta	PIP5K2B, **PIPKIIβ**	17q12	
		PIP4K2C	phosphatidylinositol-5-phosphate 4-kinase type 2 gamma	PIP5K2C, **PIPKIIγ**	12q13.3	
	Type III	PIKFYVE	phosphoinositide kinase, FYVE-type zinc finger containing	PIP5K3, **PIKfyve**	2q34	Fab1

Table 5 is summarized from the HUGO Gene Nomenclature Committee (HGNC) and (Balla, 2013; Boura and Nencka, 2015)

1.3.1.1 Class I PI3Ks

The class I PI3K subfamily contains four members in vertebrates, only one member in worm and fly, and none in yeast (Brown and Auger, 2011; Jean and Kiger, 2014). Class I PI3K works as heterodimer including a 110 kDa catalytic subunit (p110 α, β, γ or δ), and a regulatory subunit (p85α (or its splice variants p55α and p50α), p85β, p55γ, p101 or p84/87) (**Figure 21**). Class I PI3Ks further divided into Class IA PI3Ks and Class IB PI3Ks subsets. This classification is based on sequence similarity. All the catalytic subunits contain a conserved c-terminal catalytic domain, a C2 domain which is involved in plasma membrane binding, a lipid kinase unique domain(LKU, also called "helical"), and a Ras binding domain (Ras-BD). P110α, p110β and p110γ are belong to Class IA PI3Ks catalytic subunits. P85 regulatory subunits (p85, p55, p50), which each contains two Src homology 2 domains (nSH2, cSH2) and an intervening p110-binding region (iSH2), constitutively interact with the N-terminal p85-binding region (p85BR) of the p110α, p110β and p110γ catalytic subunits. P85 acts as an adaptor to recruit the complex to phosphorylated tyrosine commonly downstream of activated receptor tyrosine kinases (RTKs) (Balla, 2013; Jean and Kiger, 2014). All p85 isoforms have a Proline rich (PR) region in N-terminal. p85α and p85β also contain a SH3 domain, a second PR region and a breakpoint cluster region-homology (BH) domain, which may have intrinsic GTPase-activating protein (GAP) activity for Rab family members. (Vanhaesebroeck et al., 2010). P110γ is belong to Class IB PI3K. p110γ has a N-terminal adaptor binding region (AdBD), which interact with the regulatory subunit p101 or p87/p84 (Balla, 2013).

1.3.1.1.1 PI3Kα

P110α is ubiquitously expressed. p85 can stabilize p110, inactive the kinase activity of p110 in basal state, and be recruited to phosphorylated tyrosine residues in receptors and adaptor molecules (Vanhaesebroeck et al., 2010). Activated RTKs recruit the p85/p110α complex through direct binding of the SH2 domain of p85 to the tyrosine phosphorylated motifs of receptors. Engagement of the SH2 domains of p85 by phosphorylated tyrosine residues renders the catalytic subunits activation and also bring them to the membrane in contact with their lipid substrates (Balla, 2013; Vanhaesebroeck et al., 2010). p85α regulatory protein can also bind directly to and enhance PTEN (Phosphatase and tensin homolog) 3'-phosphatase activity(more details about PTEN is described in 3'-phosphatase part)(Chagpar et al., 2010). So the abundance or shortage of p85α relative to p110α perhaps determine the extent of PI3K

activation, but this is not clear and still a matter of debate(Balla, 2013). P110α has a Ras binding domain, thus GTP-bound Ras can directly activate PI3Kα. Oncogenes such as Src and polyoma middle T or virus such as avian *Rous sarcoma virus* which associate with the p85/p110α complex also can strongly activate PI3Kα (Balla, 2013).

1.3.1.1.2 PI3Kβ

P110β is also broadly expressed, but is absent or expressed at low levels in B-lymphocytes and T-lymphocytes and highly expressed in myeloid cells (Vanhaesebroeck et al., 2016). P110β can be activated by both RTKs and Gβγ subunits (Balla, 2013). P110β is the major class I PI3K required for FcγR mediated phagocytosis by primary mouse macrophages (Leverrier et al., 2003). P110β was reported to associate with the autophagy-promoting Vps34–Vps15–Beclin 1–Atg14L complex and promotes the PI3P generation (Dou et al., 2010). P110β, together with P110δ also can regulate the neutrophil ROS formation in response to *Aspergillus fumigatus* Hyphae (Boyle et al., 2011). It has been shown that P110β is responsible for the ROS production by neutrophils stimulated by low concentrations of immune complex in FcγR dependent activation, while at higher concentrations of immune complex, the ROS production of neutrophils depend on both P110β and P110δ (Kulkarni et al., 2011).

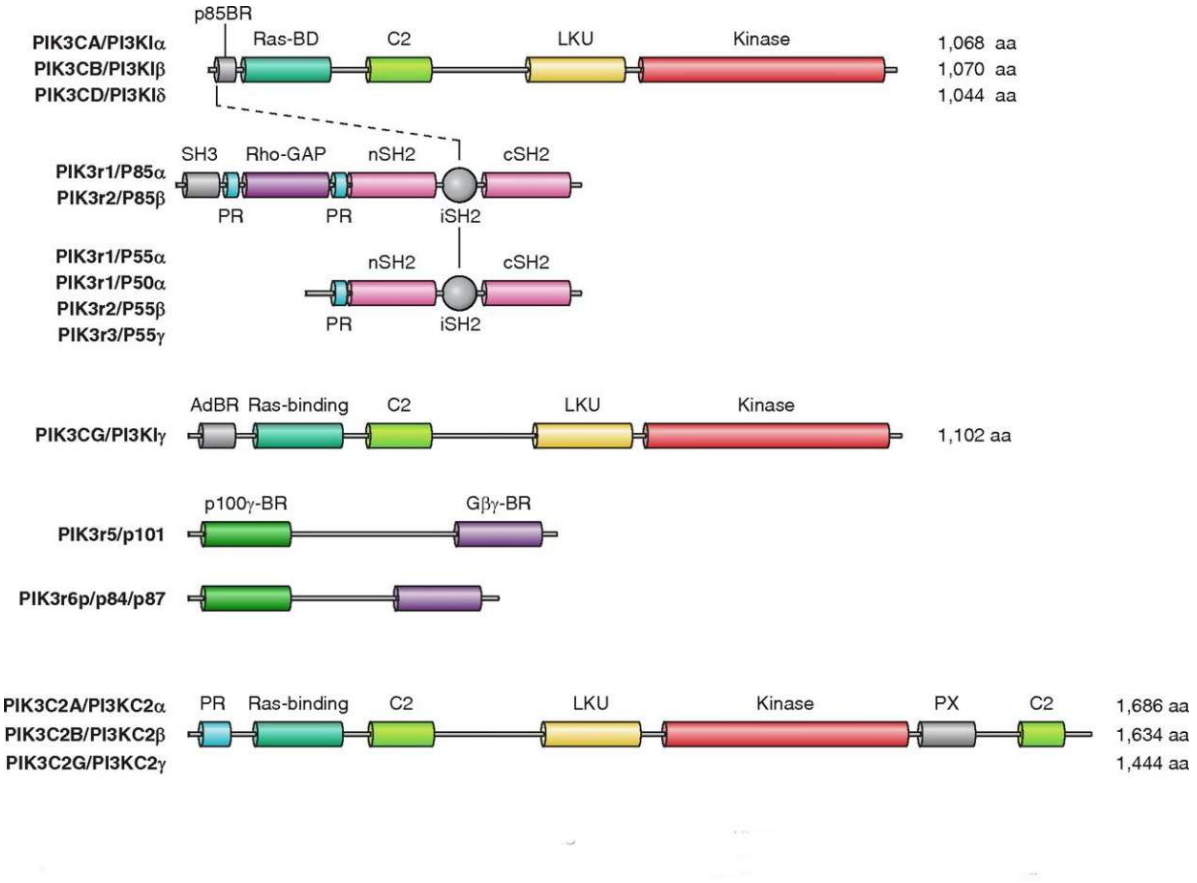

Figure 21. Domain structure of Class I and Class II PI3Ks.

PI3Ks are subdivided into three classes. Class I PI3Ks consists of PI3K1α, PI3K1β, PI3K1δ and PI3K1γ. Class I PI3Ks have 5 regulatory subunits, including p85α, p85β, p55γ, p101, and p84/87. Class II PI3Ks consist of PI3KC2α, PI3KC2β, and PI3KC2γ. (Balla, 2013).

1.3.1.1.3 PI3Kδ

P110δ is highly expressed in leukocytes, but is also intermediately expressed in other tissues, such as neurons and some epithelial cells (Vanhaesebroeck et al., 2016). P110δ can associate with the SH2-domain containing adaptors, p85α and its splice variants, p85β, and Ras (Balla, 2013; Vanhaesebroeck et al., 1997). P110δ often works together with P110γ in cell immune responses (Balla, 2013). FMLF can trigger biphasic activation of PI3K in TNF-α primed human neutrophils, the first phase is largely dependent on P110γ and the second phase is largely dependent on P110δ. The second phase is increased by the TNF-α priming and regulates parallel activation of ROS production (Condliffe, 2005). P110δ is the main PI3K isoform that is involved in Acute myeloid leukemia (AML). PI3K/Akt pathway is found to be constitutively activated in leukemic cells of AML patients and contribute to the uncontrolled survival and proliferation of immature myeloid cells and their abnormal accumulation in the bone marrow (Tzenaki and Papakonstanti, 2013). P110δ can also negatively regulate the activity of PTEN via inhibition of RhoA/ROCK (Rho-associated protein kinase) pathway (Papakonstanti et al., 2007).

1.3.1.1.4 PI3Kγ

P110γ is highly expressed in myeloid cells, and also expressed at low levels in cardiomyocytes, smooth muscle cells and endothelial cells (Balla, 2013; Vanhaesebroeck et al., 2016). The regulatory subunit p84/p87 is highly expressed in mast cells, macrophages, and the heart, while p101 is enriched in neutrophils (Balla, 2013). Loss of p101 leads to major reductions in the accumulation of $PI(3,4,5)P_3$ in mouse neutrophils (Suire et al., 2006). P110γ can be regulated in different manners. P110γ can be activated by Ras or Gβγ subunits. p101 can greatly enhance the Gβγ sensitivity of P110γ, but does not change the Ras sensitivity of P110γ. P84/p110γ complex requires Ras binding, for membrane recruitment and activation by GPCRs, but is not stimulate by Gβγ (Balla, 2013). P110γ also have a protein kinase activity and phosphorylate proteins such as MEK a activating the MAPK pathway (Balla, 2013; Stoyanova et al., 1997). The signalling pathway of four isoforms of Class I PI3K is summarized in **Figure 22**.

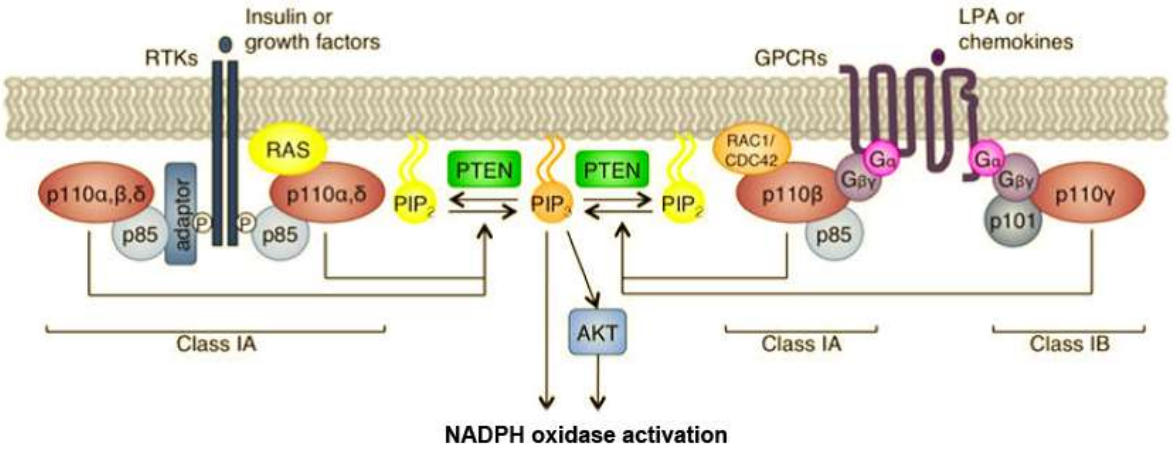

Figure 22. Class I PI3Ks signalling.

Class1A PI3Ks are heterodimers comprised of a 110 kDa catalytic subunit (p110α, p110β, and p110δ) and a p85 regulatory subunit (five isoforms exist). Class IA PI3Ks are activated by growth factor and cytokine receptors or adaptor proteins (e.g., CD19/BCAP in B cells), class IA PI3Ks are recruited to the plasma membrane by interaction with phosphorylated tyrosine on YXXM motifs of RTKs or their adaptors, or with GPCR-associated Gβγ subunits (p110β). Class IB PI3K catalytic subunit p110γ binds to p101 or p84 regulatory subunits. Class IB PI3K is activated by G protein-coupled receptors (GPCRs). Ligand like chemokine or lysophospholipid (LPA) binds to GPCR induces the dissociation of heterotrimeric G-proteins and the Gβγ subunits interact with the class IB PI3K. There they phosphorylate $PI(4,5)P_2$ to generate $PI(3,4,5)P_3$, which can activate AKT. $PI(3,4,5)P_3$ and AKT can further lead to NADPH oxidase activation. The phosphatase and tensin homolog (PTEN) lipid phosphatase removes the 3'-phosphate from $PI(3,4,5)P_3$ to inactivate class I PI3K signaling. *Adapted from* (Thorpe et al., 2015).

1.3.1.2 Class II PI3K

There are three Class II PI3K isoforms in mammalian cells, PI3KC2α, PI3KC2β, and PI3KC2γ. They do not exist in yeast, and only a single isoform is found in fly and worm (Vanhaesebroeck et al., 2010). Class II PI3Ks are larger proteins of 170-200 kDa. Class II PI3Ks do not have a regulatory subunit. Class II PI3Ks contains a Ras-binding domain, a C2 domain, a LKU and a catalytic domain like Class I PI3K, but also have a PX and a C2 domain at C-terminus and a PR segment at N-terminus (**Figure 21**). PI3KC2α and PI3KC2β are widely expressed, while PI3KC2γ is more especially expressed in liver and some other tissues depending on the species (Balla, 2013). The PX domain of PI3KC2α can bind $PI(4,5)P_2$ (Song et al., 2001; Stahelin et al., 2006) and the C2 domain at the C-terminus can bind $PI(4,5)P_2$ and $PI(3,4)P_2$ (Liu et al., 2006). Class II PI3K can phosphorylate PtdIns and PI4P at the 3-position but not $PI(4,5)P_2$ in vitro (Domin et al., 1997). It is generally accepted that class II PI3Ks do not catalyse the generation of $PI(3,4,5)P_3$. PI3P is also suggested to be the main product of class II PI3Ks for some specific processes, such as exocytosis and cell-cycle progression, but the mechanism is poorly understood (Falasca and Maffucci, 2012). The mechanisms of Class II PI3K activation are still not completely defined, especially PI3KC2γ.

1.3.1.3 Class III PI3K

Vps34 (vacuolar protein sorting 34) is originally identified in screens for genes involved in vesicular sorting in *Saccharomyces cerevisiae* (Herman and Emr, 1990). Vps34 is conservely expressed from lower eukaryotes to plants and mammals (also known as PI3KC3 in mammals)(Vanhaesebroeck et al., 2010). Vps34 has a substrate specificity which is limited to PtdIns, thus its product is PI3P in cells (Schu et al., 1993; Volinia et al., 1995). Vps34 plays an important role in vesicle traffic, including autophagy, endocytosis and phagocytosis. Vps34 can form different complex with different proteins (**Figure 23**).

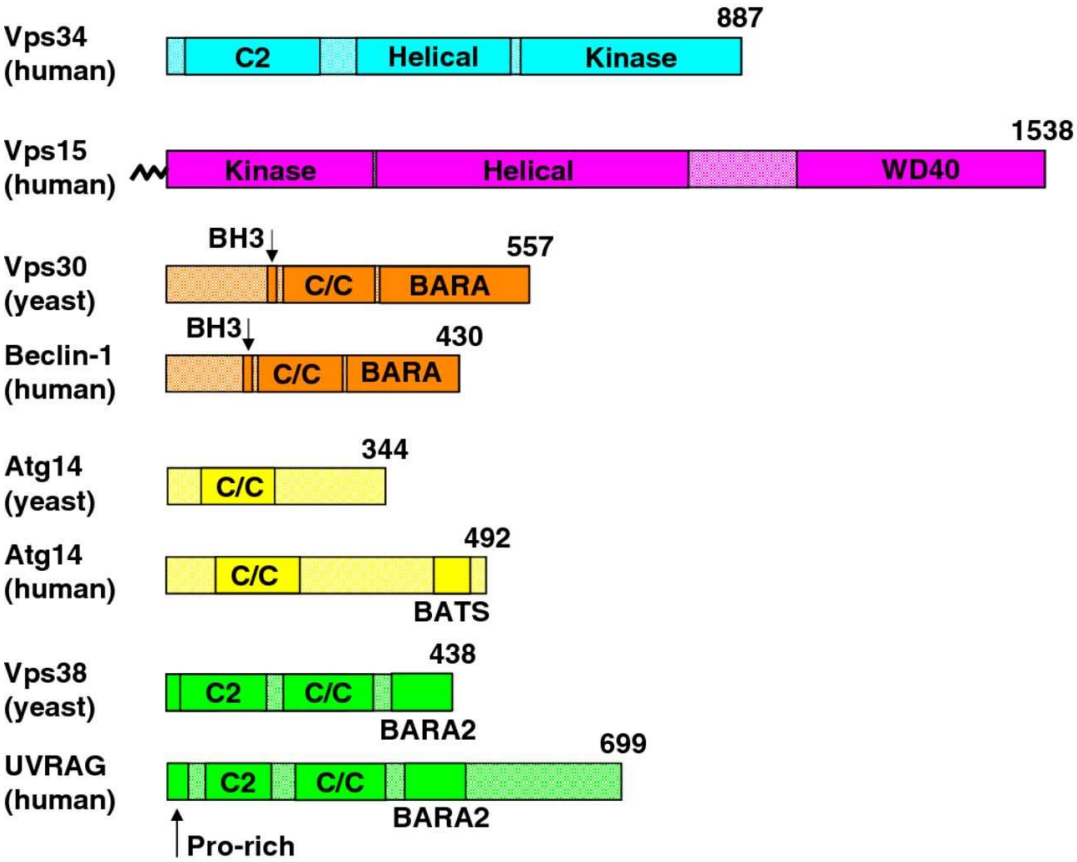

Figure 23. Protein domains of the core components of Vps34 complex I and II.

The maps shows the different domains of the following proteins: Vps34 (human); Vps15 (human); Vps30 (yeast) and Beclin-1 (human); Atg14 (yeast) and Atg14 (human); and Vps38 (yeast) and UVRAG (human). (Backer, 2016).

1.3.1.3.1 Vps34 complex

Vps34 bears a C2 domain, a helical domain and a catalytic domain. Vps15 (also known as p150 in mammals) has a N-terminal myristoylated kinase domain, a helical domain consisting of a series of internal HEAT(huntingtin, elongation factor 3, the PR65/A subunit of protein phosphatase 2A and TOR (target of rapamycin)) repeats and a C-terminal WD40 domain (**Figure 23**) (Backer, 2016). Vps34 forms a constitutive heterodimer with the serine/threonine kinase vps15, which is myristoylated to tether the vps34-vps15 complex to the intracellular membranes and also greatly stimulates the kinase activity of vps34 (Balla, 2013; Vanhaesebroeck et al., 2010). Vps15 is expressed more than vps34 in mammalian cells, thus most cellular vps34 is in interaction with vps15 (Backer, 2016; Murray et al., 2002). Beclin1 (also known as Atg6 or Vps30 in yeast) participates in Vps34 complex formation and recruits additional proteins, such as Atg14 (initially named Barkor or Atg14L in mammals) and UVRAG (UV radiation resistance-associated gene, also known as vps38 in yeast). The Vps34-vps15-Beclin-1-Atg14 complex, and the Vps34-vps15-Beclin-1-UVRAG complex is known as vps34 complex I, and vps34 complex II respectively. Beclin-1 contains a N-terminal unstructured region, a BH3 (Bcl-2 homology 3) domain, two coiled-coil domains, and a C-terminal BARA (β-α repeated, autophagy) domain (**Figure 23**) (Backer, 2016). Human Atg14 has a extended N-terminal coiled coil domain and a C-terminal BATS (Barkor/Atg14(L) autophagosome-targeting sequence) domain (**Figure 23**). The BATS domain is implicated in the targeting of Atg14 to highly curved membranes (Backer, 2016; Fan et al., 2011). UVRAG bears a N-terminal C2 domain, two coiled coil domains and a C-terminal BARA-related (BARA2) domain (**Figure 23**) (Backer, 2016). UVRAG positively regulates Vps34 activity and autophagy maturation (Liang et al., 2006). UVRAG is also required for endocytosis (Liang et al., 2008). The vps34 complex I participate in the signalling of nascent autophagosome, while the vps34 complex II is involved in endosome and autophagosome-lysosomal fusion (Backer, 2016).

1.3.1.3.2 Rubicon

Rubicon (RUN domain protein as Beclin-1 interacting and cysteine-rich containing) is a Beclin-1 binding partner. Rubicon (~124 kDa) contains 941 amino acids and has a conserved RUN domain (amino acids 49–190) near the N-terminus, a cysteine-rich domain (amino acids 837–890) near the c-terminus and a coiled-coil domain (CCD, amino acids 488–508) in the central region (**Figure 24**).

Figure 24. The different domains of the protein: Rubicon.
(Zhong et al., 2009a)

A lot of proteins can interact with Rubicon. A large region (aa 393–849) of Rubicon binds to UVRAG (Matsunaga et al., 2009b). Sun *et al.,* also showed that the Rubicon fragment aa 300-600 and aa 600-972 efficiently interact with UVRAG (Sun et al., 2010). The N-terminal region (aa 1-300) of Rubicon and also the RUN domain (aa 49-180) strongly bind to vps34. Rubicon binding of hVps34 via the RUN domain also inhibit the lipid kinase activity of vps34 (Sun et al., 2010). Yang et al has found that Beclin 1 efficiently binds to the center coiled-coil domain (CCD, aa 505-557) of Rubicon (Yang et al., 2012). $P22^{phox}$ is also able to bind to the C-terminal SR (aa558-625) of Rubicon (Yang et al., 2012). Rubicon localizes to the late endosome/lysosome, but not the autophagosome. Atg14 and UVRAG stimulate the Vps34 activity, while Rubicon downregulates its activity (**Figure 25**) (Zhong et al., 2009a; Zhong et al., 2009b). Rubicon negatively regulates the late stages of the endocytic pathway, such as maturation of endosomes and their fusion with lysosomes (Matsunaga et al., 2009a; Matsunaga et al., 2009b). It has also been found that Rubicon is recruited to LC3-positive phagosomes (LAPosomes) upon phagocytosis of unopsonized zymosan (Martinez et al., 2015; Yang et al., 2012).

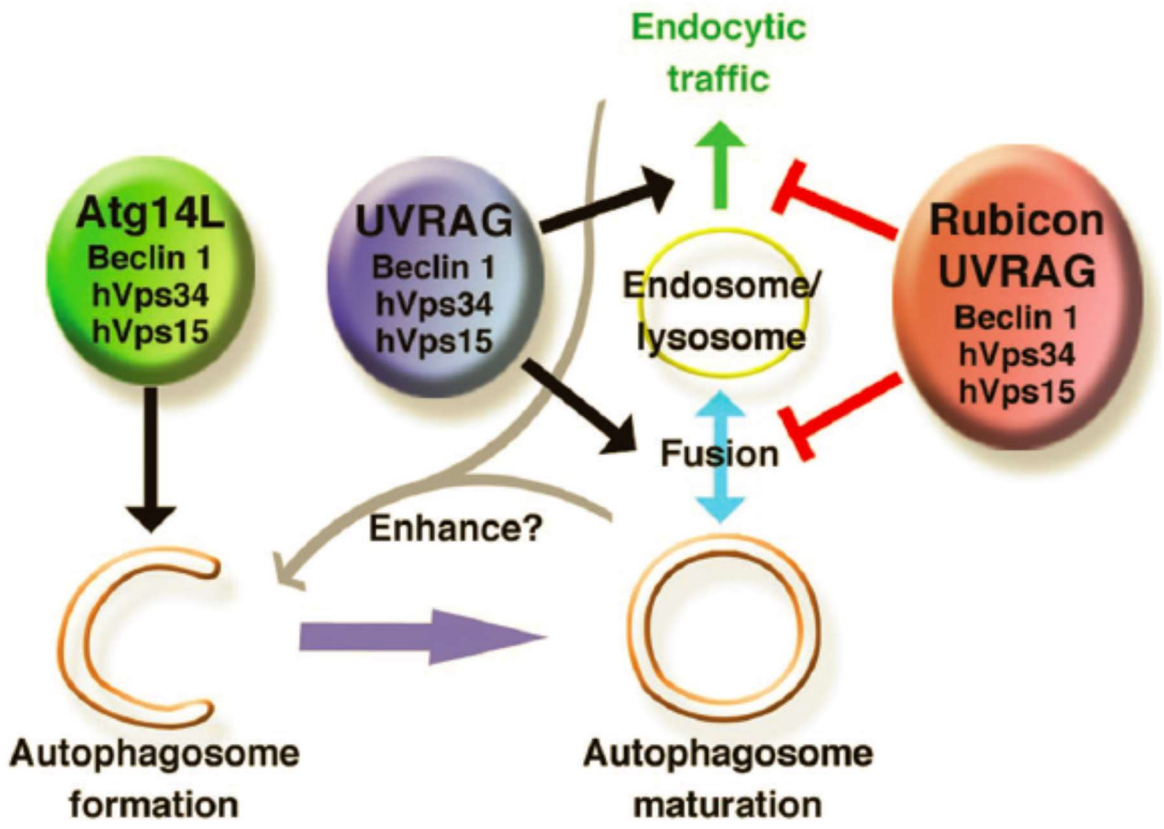

Figure 25. Model of the role of the three Beclin 1-Vps34 complexes.

The Atg14L complex are involved in autophagosome formation. The UVRAG complex functions positively in autophagosome and endosome maturation. The UVRAG-Rubicon complex functions negatively in autophagosome and endosome maturation. (Matsunaga et al., 2009a).

1.3.2 Phosphoinositide phosphatases

1.3.2.1 5-phosphatases

5-phosphatases can remove the phosphate from the 5-position from $PI(3,4,5)P_3$, $PI(4,5)P_2$, and $PI(3,5)P_2$. 5-phosphatases are divided into four types. Type I 5-phosphatases, INPP5A, dephosphorylate $Ins(1,4,5)P_3$ and $Ins(1,3,4,5)P_4$. Type II 5-phosphatases contains the synaptojanins (SYNJs), OCRL, INPP5B, INPP5J (also called proline-rich inositol polyphosphate 5-phosphatase (PIPP)), and SKIP (skeletal muscle and kidney enriched inositol polyphosphate phosphatase, also called INPP5K) (Balla, 2013). Type III 5-phosphatases include SHIP1 (INPP5D) and SHIP2 that bear a N-terminal SH2 domain. SHIP can hydrolyze $PI(3,4,5)P_3$ and $PI(4,5)P_2$ (Edimo et al., 2012; Nakatsu et al., 2010). Type IV 5-phosphatase is INPP5E. INPP5E has about a 10 times higher affinity against $PI(3,4,5)P_3$ than SHIP1, and can also remove the 5-phosphate from $PI(4,5)P_2$ and $PI(3,5)P_2$ (Balla, 2013). SHIP1 is responsible for the majority of 5-phosphatase activity in neutrophils, while SHIP2 only plays a minor role (Luo and Mondal, 2015). $PI(3,4,5)P_3$ is quickly synthesized at phagocytic cups. In macrophages, SHIP1 and INPP5E are both recruited to FcγR mediated phagocytic cups, but only SHIP1 is recruited to CR3-mediated phagocytic cups (Cox et al., 2001; Horan et al., 2007; Kamen et al., 2007). Mondal *et al.,* show that SHIP1 regulates $PI(3,4,5)P_3$ production in response to cell adhesion and plays a limited role when cells are in suspension. Loss of SHIP1 leads to reduced ROS production in neutrophils in suspension upon stimulation with fMLF, this may due to the decreased $PI(3,4)P_2$ levels. However, when SHIP1-/- neutrophils are primed with TNF-α or MIP2 (macrophage inflammatory protein 2) and adhere to fibronectin, they produce very high levels of ROS, suggesting that increased $PI(3,4,5)P_3$ signaling override the effect of decreased PI(3,4)P2 level (Luo and Mondal, 2015; Mondal et al., 2012).

1.3.2.2 4-phosphatases

The phosphatases that can remove the phosphate from the 4-position of $PI(3,4)P_2$ are called INPP4A and INPP4B, while the phosphatases that hydrolyze $PI(4,5)P_2$ are TMEM55A (Transmembrane Protein 55A) and TMEM55B. 4-phosphatases that directly work on $PI(3,4,5)P_3$ has not been reported. INPP4A and INPP4B both have a N-terminal C2 domain. The C2 domain of INPP4A prefers binding $PI(3,4)P_2$, PI3P and phosphatidylserine (PS) and the C2 domain of INPP4B binds phosphatidic acid (PA) and $PI(3,4,5)P_3$ (Balla, 2013).

1.3.2.3 3-phosphatases

The phosphoinositide 3-phosphatases consist of two major groups. The first group contains PTEN (phosphatase and tensin homolog located on chromosome TEN) and TPIP (transmembrane phosphatase with tensin homology (TPTE) and PTEN homologous inositol lipid phosphatase). The second group contains myotubularins (MTMs).

1.3.2.3.1 PTEN

A lot of cancers are related with the loss of PTEN function. PTEN is a dual-specificity protein and lipid phosphatase. PTEN shows low activity against protein and peptide substrates (Balla, 2013). The primary cellular substrate of PTEN is $PI(3,4,5)P_3$, which is hydrolyzed to $PI(4,5)P_2$ by PTEN. PTEN can also dephosphorylate $PI(3,4)P_2$, but is more active against $PI(3,4,5)P_3$ (McConnachie et al., 2003). $PI(3,4,5)P_3$ is the product of Class I PI3K. Increase in $PI(3,4,5)P_3$ recruits AKT to the membrane and results in phosphorylation and activation of AKT. The active AKT then phosphorylates a number of cytosolic and nuclear proteins that play important roles for cell survival and metabolism. This PI3K-AKT pathway is negatively regulated by PTEN (Hemmings and Restuccia, 2012). PTEN is a 403 amino acid protein that contains an N-terminal $P(4,5)P_2$-binding (PBD)/phosphatase domain, a C2 domain, a carboxyl-terminal tail (c-tail) domain, and a PDZ(PSD-95, Discs-large, ZO-1)-binding (PDZ-BD) domain (**Figure 26**) (Worby and Dixon, 2014). The C2 domain plays an important role in membrane targeting and in the regulation of the enzyme. Truncation or mutations within C2 domain make PTEN unstable (Balla, 2013).

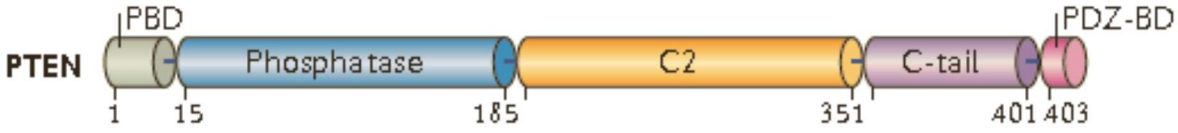

Figure 26. The protein domain of PTEN.
(Song et al., 2012)

PTEN is phosphorylated on its C2 domain (S362, T366, S370, S380, T382, T383, and S385) and C-tail domain (S398) by several kinases. Phosphorylation of the c-tail domain of PTEN stabilizes the protein and renders the protein inactive because of the interaction between the

phosphorylated C-tail domain and the C2 domain. This interaction causes dissociation of C2 domain from the membrane and blocks the association of PTEN catalytic domain with membrane localized PI(3,4,5)P_3. The conformation change also precludes the interaction between PTEN PDZ-BD with its binding partners, which leads to the disruption of downstream signal transduction pathways. On the contrary, the phosphorylation of the C2 domain of PTEN increases PTEN activity and stability by enhanced membrane targeting and reduced polyubiquitylation, which leads to the degradation of PTEN (Worby and Dixon, 2014). It is suggested that PTEN can autodephosphorylate itself (Zhang et al., 2012). PTEN is very sensitive to oxidative damage. H_2O_2 oxidizes and inactivates PTEN by creating a disulfide bond between between catalytic C124 and C71. Oxidation decreases PTEN activity, this causes sustained activation of PI3K pathway (Worby and Dixon, 2014).

1.3.2.3.2 Myotubularins

The myotubularin (MTM) family contains 14 members. Eight of them (MTM1, MTMR1-4, MTMR6-8) has 3-phosphatase activity against PI3P and PI(3,5)P_2, the other six homologs (MTMR5, MTMR9-13) are pseudophosphatases which are catalytically inactive proteins and associate mostly with and regulate the active MTM homologs (**Figure 27**).

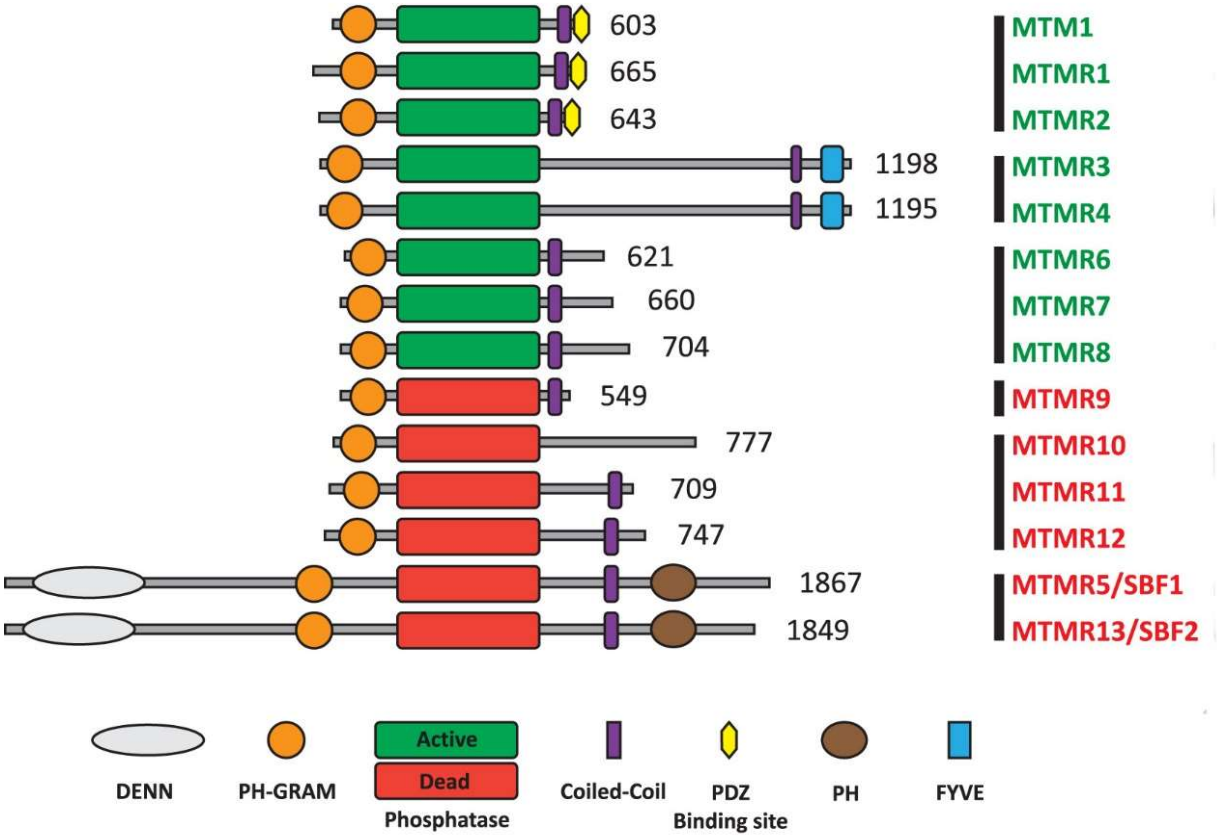

Figure 27. The protein domains of Myotubularins.
(Raess et al., 2017)

Loss of function of *MTM1* gene is implicated in X-linked centronuclear myopathy (XLCNM, OMIM: 310400), which is also called myotubular myopathy. People with XLCNM have a very severe and generalized muscle weakness, external ophthalmoplegia and respiratory distress that are usually evident at birth (Raess et al., 2017). Most of the MTM family members are expressed in a wide range of tissues, but MTMR5 and MTMR7 are exclusively expressed in the testis and brain, respectively (Balla, 2013). Myotubularins share a core domain, PH-GRAM (Pleckstrin Homology - Glucosyltransferase, Rab-like GTPase Activator and Myotubularins), which can bind to PIs. All myotubularins except MTMR10 contain a coiled-coil (CC) domain that is important for their homodimerization and/or heterodimerization. Eight active myotubularins have a catalytic domain which contains a consensus $C(X)_5R$ signature motif. MTM1, MTMR1 and MTMR2 bear a PDZ binding site which mediates protein-protein interactions. MTMR3 and MTMR4 have a FYVE (Fab1-

YOTB-Vac1-EEA1) domain. MTMR5 and MTMR13 have a PH (Pleckstrin homology) domain and a DENN domain. FYVE and PH can bind PIs, while DENN is involved in small Rab GTPase regulation (**Figure 27**) (Raess et al., 2017; Robinson and Dixon, 2006). It has been shown that MTM1 localizes to both early and late endosomes and associates with the vps34-vps15 complex in mammalian cells to control the sequential synthesis and degradation of endosomal PI3P (Cao et al., 2007). Mtm (an ortholog of MTM1 and MTMR2) in *Drosophila* is needed to regulate the endosomal PI3P generated by Class II and Class III PI3K (Velichkova et al., 2010). Mtm-1 in *Caenorhabditis elegans* is also critical for phagosome maturation via regulation of PI3P level coordinately with class II and class III PI3K (Conradt et al., 2012).

1.3.3 Phosphoinositides signalling

1.3.3.1 Phosphoinositides and NADPH oxidase

Protein–lipid interaction is an important mechanism to regulate membrane recruitment and activate proteins. Some protein domains can specificly interact with phospholipids, such as the PH (pleckstrin homology), FYVE (Fab1p, YOTB, Vac1p and EEA1), ENTH (Epsin NH2-terminal homology), ANTH, FERM, PHD, Tubby, C2 and PX domains (Seet and Hong, 2006). The protein binding domains of phosphoinositides are summarized in **Table 6**.

1.3.3.1.1 PX domain of p40^{phox}

Three crystal structures of PX-PI3P complexes have been solved, they are p40^{phox} (PDB entry 1H6H) (**Figure 28**) (Bravo et al., 2001), Grd19p (PDB entry 1OCU), and sorting nexin (SNX9; PDB entry 2RAK) (Jia et al., 2014). P40^{phox} PX domain have three β strands followed by three α helices, and a proline-rich (Pro-rich) loop between the first and second helix (Bravo et al., 2001). Four conserved residues are regarded as critical for the binding of PI3P in p40^{phox}. The first arginine (R58) forms an electrostatic interaction with the 3-phosphate group, the lysine (K92) interacts with the 1-phosphate group, the second arginine (R105) forms two hydrogen bonds with the 4- and 5-hydroxy groups of the inositol. The conserved tyrosine residue (Y59) forms a stacking interaction with the inositol group (Jia et al., 2014). A CGD patient with a mutation in the PX domain of p40^{phox} (R105Q) has also been reported. Neutrophils from this patient shows a substantial defect in intracellular superoxide production

during phagocytosis, but the ROS production stimulated by fMLF or PMA is not affected (Matute et al., 2009).

Table 6. Phosphoinositides binding domains.

PPIs	Binding domains	Full name
PI3P	PX	Phox homolog
	PH	Pleckstrin homolog
	FYVE	Fab1,YOTB,Vac1,EEA1
	BATS	Barkor/Atg14(L) autophagosome-targeting sequence
PI4P	GOLPH3	Golgi Phosphoprotein 3
	P4M	PI4P binding of SidM
	PH	Pleckstrin homolog
	PTB	Phosphotyrosine-binding
	PX	Phox homolog
	EHD	Eps15 homolog
PI5P	PHD	Plant homeodomain
$PI(3,4)P_2$	PX	Phox homolog
	PH	Pleckstrin homolog
$PI(3,5)P_2$	PH	Pleckstrin homolog
	WD40	also known as the WD or beta transduction repeats
	PROPPIN	β-propeller that binds to phosphoinositides
$PI(4,5)P_2$	ANTH	AP180 N-terminal homolog
	ENTH	Epsin N-terminal homolog
	C2	Conserved region-2
	FREM	The protein 4.1, ezrin, radixin, moesin
	PDZ	domains that occur in PSD-95, Dlg and LO-1 (previously called DHR or GLGF
	PH	Pleckstrin homolog
	PTB	Phosphotyrosine-binding
	PX	Phox homolog
	Tubby	
	EHD	Eps15 homolog
	BAR	Bin-Amphiphysin-Rvs
$PI(3,4,5)P_3$	C2	Conserved region-2
	DHR-1	DOCK- homology region 1
	PX	Phox homolog
	PH	Pleckstrin homolog
	SYLF	SH3YL1, Ysc84p/Lsb4p, Lsb3p, and plant FYVE
	GLUE	GRAM-Like Ubiquitin-binding in EAP45

Table 6 is summarized form (Balla, 2013; Idevall-Hagren and De Camilli, 2015; Kutateladze, 2010; Lemmon, 2008)

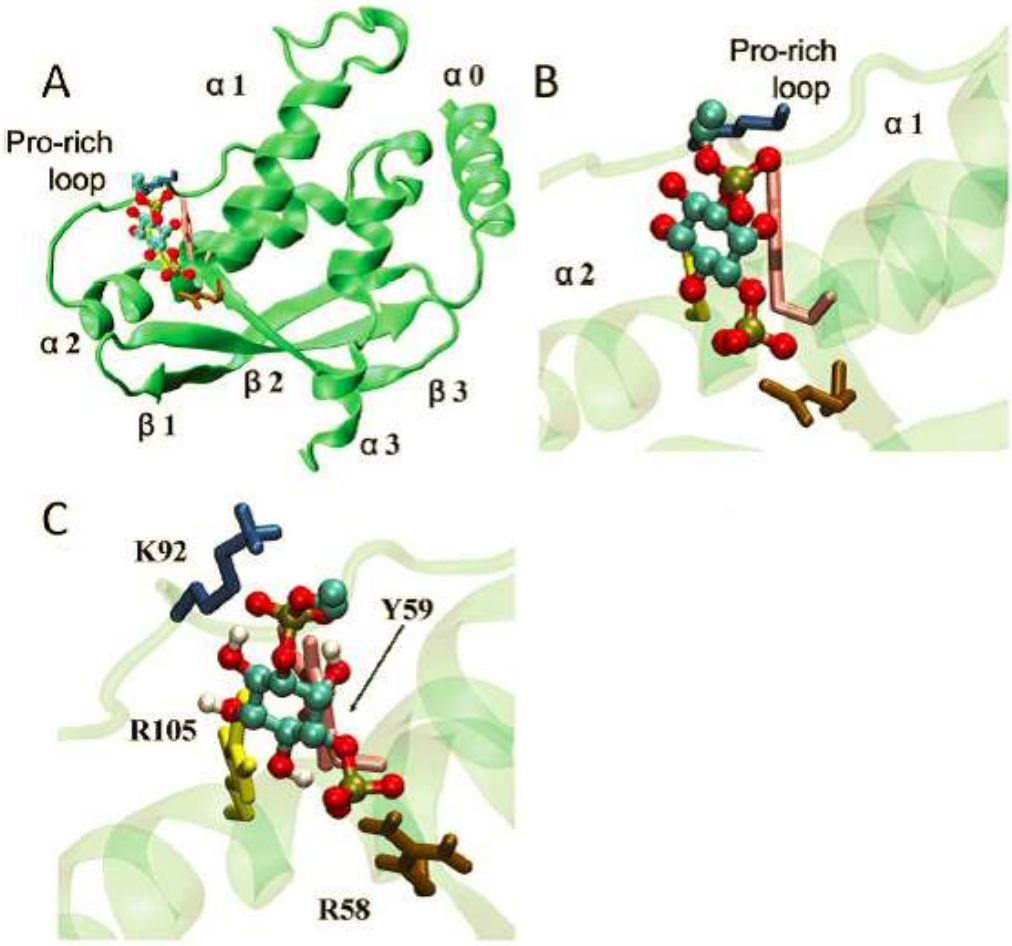

Figure 28. PI3P bound to P40^{phox} PX domain.

A and B, the crystal structure of PI3P bound to the p40^{phox} PX domain (PDB 1H6H). C. A snapshot of the p40^{phox}–PX–PI3P complex. PI3P is represented as balls-and-sticks and is colored according to atom type (C, cyan; P, orange; O, red; H, white). The four conserved residues (R58, K92, R105, and Y59 of the p40^{phox}–PX domain) are presented in a licorice representation and are colored in brown, blue, yellow, and pink, respectively. Adapted from (Jia et al., 2014).

1.3.3.1.2 PX domain of p47^{phox}

P47^{phox} PX domain consists of a three-stranded antiparallel β-sheet followed by a helical subdomain containing four α-helices and a polyproline II region. They form a phosphoinositide-binding pocket and a second anion-binding pocket (**Figure 29**). In the phosphoinositide-binding pocket, it is suggested that 3- and 4- phosphates interact with Arg43 and Arg90 (**Figure 30**), respectively. P47^{phox} PX domain binds strongly to PI(3,4)P_2, and more weakly to PI(3,5)P_2, PI3P and PI(3,4,5)P_3 (Kanai et al., 2001; Karathanassis et al., 2002). The wall of the secondary pocket are formed by the side chains of Arg70, Lys55 and His51 (**Figure 30**), which gives its basic character. The shallow nature of the second anion-binding pocket suggests that the natural ligand is likely to be a phospholipid with a small head group such as PS and PA (Karathanassis et al., 2002). Each lipid binding site functions independently but cooperatively. Low concentrations of PA has been found to greatly increase the binding of the p47^{phox} PX domain to PI(3,4)P_2-containing membranes. Point mutations in one or the other binding pocket lead to loss of binding to one lipid but not the other (Karathanassis et al., 2002; Yaffe, 2002).

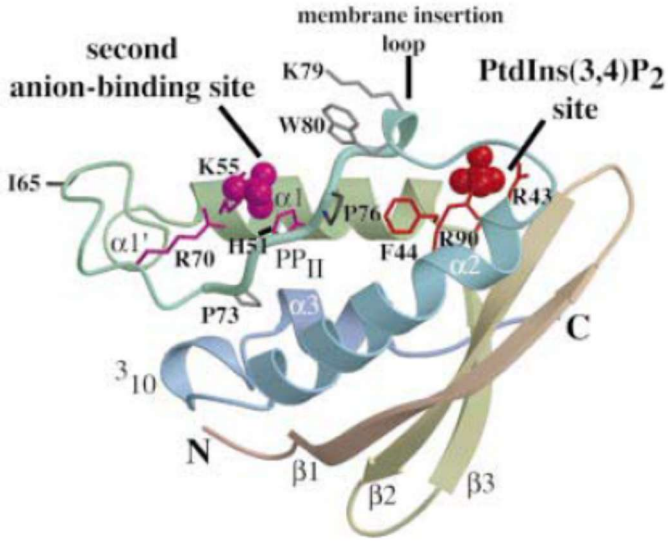

Figure 29. The structure of p47^{phox} PX domain.

The ribbon representation is coloured from red at the N-terminus to blue at the C-terminus. Residues in the phosphoinositide pocket are shown in red and those in the second anion-binding pocket are in magenta. (Karathanassis et al., 2002).

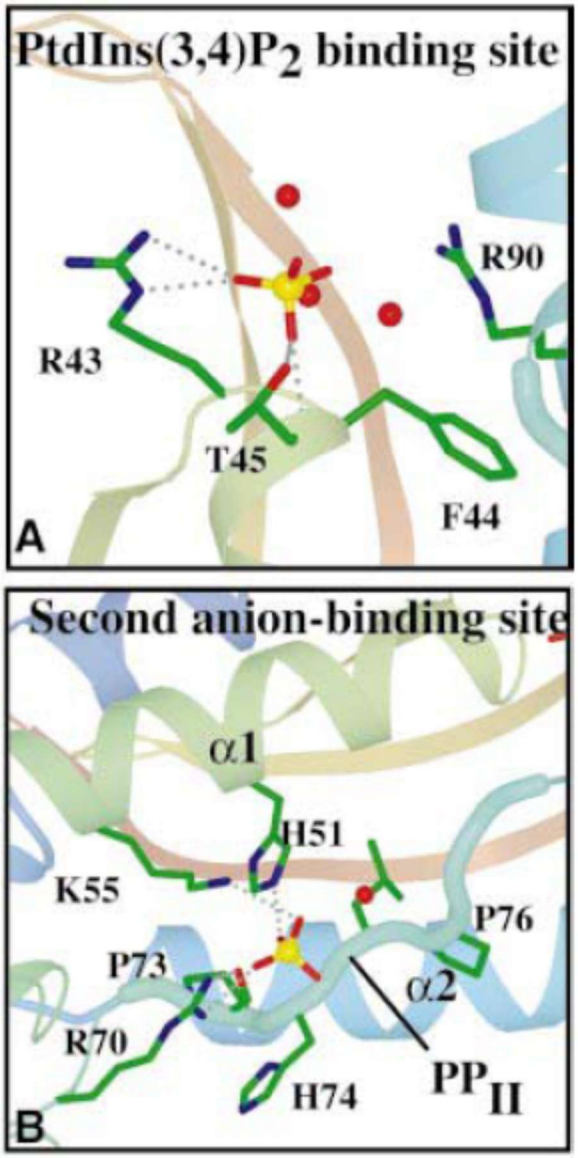

Figure 30. Binding pocket of p47^{phox} PX domain.

Dashed lines represent hydrogen bonding interactions with the protein. Ordered waters associated with the sulfates are shown as red spheres.(Karathanassis et al., 2002).

1.3.3.2 Phosphoinositides during phagocytosis

Membrane deformation is coordinately associated with characteristic phosphoinositide changes during the process of phagocytosis (**Figure 31**). PI(4,5)P_2 and PI4P are located in the inner leaflet of the plasma membrane in resting phagocytes. Increased PI(4,5)P_2 has been found to occur during the formation of the phagocytic cup due to the recruitment and activation of PIP5K (phosphorylation of PI4P at D5 position) after bounding of the particle to the plasma membrane (Botelho et al., 2000). There are perhaps other source of PI(4,5)P_2. PI(4,5)P_2 suddenly disappears after the closure of the phagosome, which is depend on several processes: 1) PLCγ hydrolyzes the PI(4,5)P_2 and thus forms DAG and I(1,4,5)P_3 (Botelho et al., 2000). 2) Class I PI3K catalyses the phosphorylation of PI(4,5)P_2 to PI(3,4,5)P_3. 3) A lot of 5-phosphatases convert PI(4,5)P_2 to PI4P, such as OCRL, INPP5B and the synaptojanins. 4) Detachment of PIP5K from internalized phagosomes facilitates the exclusion of PI(4,5)P_2 (Bohdanowicz and Grinstein, 2013; Levin et al., 2015). PI(3,4,5)P_3 levels are scare in resting cells, but it is quickly synthesized after engagement of immune receptors. PI(3,4,5)P_3 is mainly generated by Class I PI3K, which localizes to the plasma membrane. PI(3,4,5)P_3 declines sharply within 1-2 min after sealing. The breakdown of PI(3,4,5)P_3 occurs mainly through the action of 4-phosphatase INPP4A (Tridandapani et al., 2015) and 5-phosphatase SHIP (Bohdanowicz and Grinstein, 2013; Levin et al., 2015). PI3P is only detectable after phagosome sealing and stay at the phagosome for about 10 min (Vieira et al., 2001). The main source of PI3P is the phosphorylation of PtdIns by Vps34, but there may be other sources such as phosphorylation of PIs by class II PI3K or dephosphorylation of bisphosphorylated species by inositol polyphosphate phosphatases. Then,there are probably three pathways involved in the disappearance of PI3P: 1) PIKfyve phosphorylates PI3P to PI(3,5)P_2. 2) PI3P can be dephosphorylate by MTM1. 3) PI3P could be removed by lysosomal phospholipases (Bohdanowicz and Grinstein, 2013; Levin et al., 2015). It has been recently reported that PI4P is transiently enriched in the phagosomal cup and drops soon after the phagosome closure. PI4P levels drop precipitously due to the hydrolytic activity of INPP5F (Sac2) and phospholipase C. The disappearance of PI3P from early to late phagosomes is accompanied by reappearance of PI4P on maturing phagosomes (Levin et al., 2017).

A

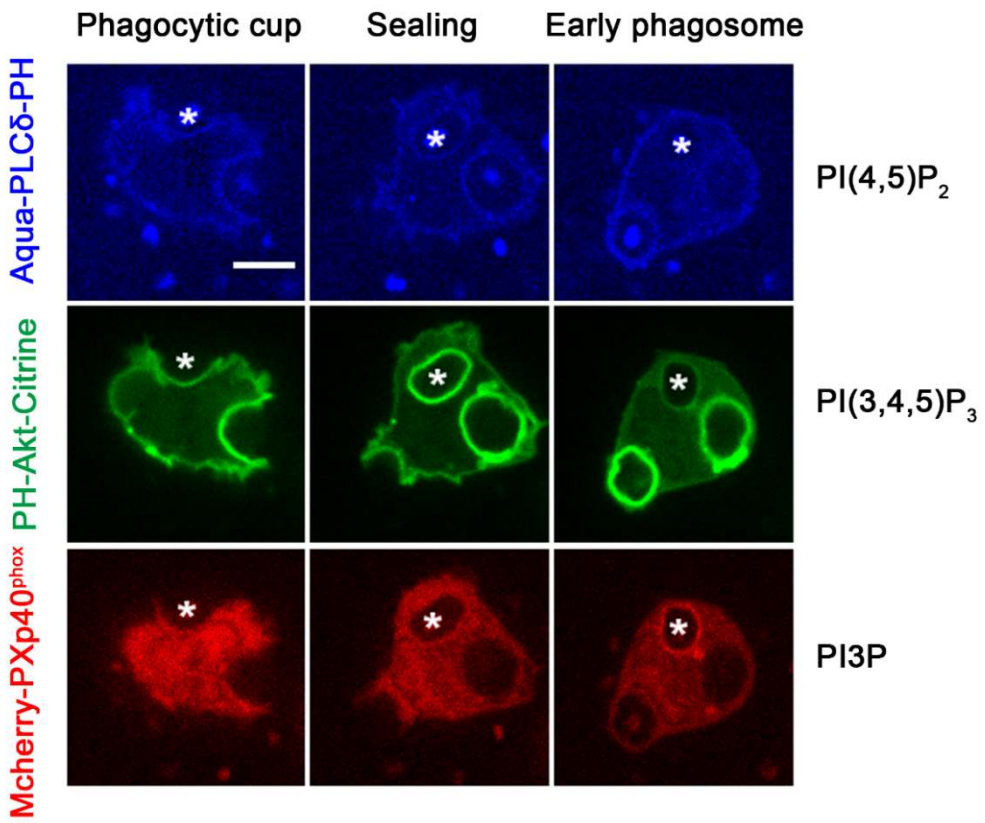

B

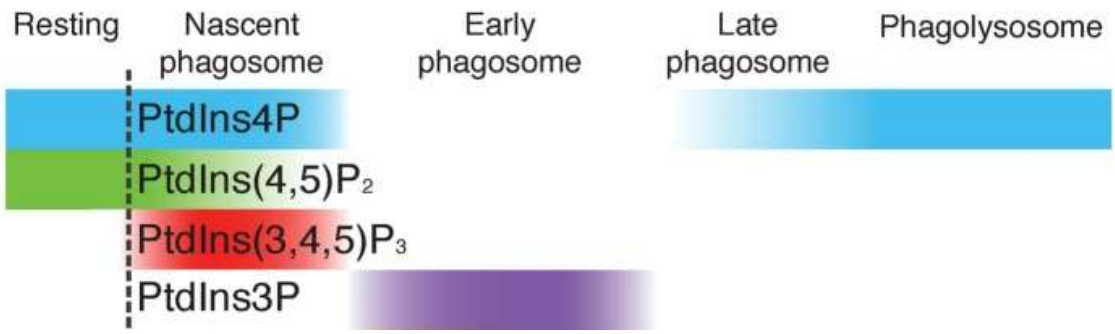

Figure 31. Phosphoinositides during phagocytosis.

A. Differentiated PLB-985 cells are transfected with Aqua-PLCδ-PH (which can bind to $PI(3,4,5)P_3$ and $PI(3,4)P_2$), PH-Akt-Citrine (which can bind to PI(4,5)P2), and mcherry-$PXp40^{phox}$ (which can bind to PI3P).The phagocytosis of zymosan (*) is followed by Spinning disk confocal microscope. Bar, 5 µm.

B. Relative timing of the acquisition by phagosomes of different phosphoinositides. Qualitative only, intended to illustrate the relative order of events. *Adapted from* (Levin et al., 2017).

1.3.3.3 Phosphoinositides during adhesion

Neutrophils can migrate to the site of infection or inflammation by responding to a variety of stimuli, including chemokines (e.g., IL-8), cytokines (e.g., TNF-α), leukotrienes (e.g.,LTB4), complement peptides (e.g., C5a, C3a), and chemicals released by bacteria directly (e.g., fMLF). This oriented migration is known as chemotaxis. $PI(3,4,5)P_3$ is quickly formed at the leading edge of neutrophils that sense a chemoattractant gradient such as fMLF. In mouse neutrophils, the formation of $PI(3,4,5)P_3$ is depend on PI3Kγ (Stephens et al., 2008). PI3Kδ is also involved in the second phase of PI3K activation in response to fMLF by TNF-α primed neutrophils (Condliffe, 2005). PI3Kδ activity is required for neutrophil spreading and polarization on a fibrinogen-coated surface (Sadhu et al., 2003). Expression of αMβ2 integrins is increased in the surface membrane when neutrophils are stimulated by fMLF or other simuli, such as GMCSF, IL-8, LTB4, TNF-α, lonomycin and so on (Sengeløv et al., 1993). fMLF causes a upregulation of αMβ2 integrins on the surfaces of neutrophils coated on fibrinogen, and also enhances the adhesion to fibrinogen. Blockade or inhibiton of PI3Kγ results in reductions of both the upregulation of αMβ2 integrins and the increased strength of adhesion and movement. This suggests that PI3Kγ plays a critical role in integrin-based adhesion (Ferguson et al., 2007; Stephens et al., 2008). ROS production by neutrophils coated on fibrinogen occurs in two phases in response to fMLF. The first phase is rapid, transient, and independent of adhesion. The second phase lasts up to 30-40 min and strictly dependent on engagement of neutrophil integrins. PI3Kγ is indispensable for the early phase, but is dispensable for the second phase of ROS production. While PI3Kα and PI3Kβ are responsible for both phase of the ROS production in response to fMLF (Fumagalli et al., 2013). Degranulation, endocytosis and exocytosis may also contribute to the changes of phosphoinositides at the plasma membrane of adherent neutrophils.

1.4 Research goals

The major goal of our research was to investigate the role of phosphoinositides in the regulation of the NADPH oxidase. Some phosphoinositides can directly bind to NADPH oxidase subunits. PI3P can specifically bind the PX domain of $p40^{phox}$, and $PI(3,4)P_2$ can bind to the PX domain of $p47^{phox}$ with great affinity than other anionic phospholipids. Thus, study whether these phosphoinositides can regulate the NADPH oxidase cytosolic subunits is critical to understand the mechanism of NADPH oxidase activation.

The synthesis of PI3P occurs on the early phagosomal membrane, however the role of PI3P in the regulation of the NADPH oxidase was still not clear. So firstly we aimed at investigating the role of PI3P in sustaining the ROS production during phagocytosis. We used neutrophil-like PLB cells and human neutrophils in our study. Pharmacological tools and molecular tools were used to modulate the PI3P level at the phagosomal membrane. We then studied the NADPH oxidase subunit localization at the phagosome and also the phagosomal ROS production. We used spinning disk microscope to follow the dynamics of fluorescent protein tagged NADPH oxidase subunits, and detected the ROS production by using live cell microscope and flow cytometer.

In the previous study, Faure *et al.* has found that few minutes after phagosome closure, $p47^{phox}$ and Rac left the phagosomal membrane (Faure et al., 2013). It has also been reported that the PX domain of $p47^{phox}$ regulated the plasma membrane but not phagosome neutrophil NADPH oxidase activation (Li et al., 2010). The role of $PI(3,4)P_2$ in the regulation of the NADPH oxidase at the plasma membrane was also poorly known. Thus we decided to study whether $PI(3,4)P_2$ could maintain the ROS production at the plasma membrane. We studied the ROS production by adherent neutrophils coated on fibrinogen in response to soluble stimuli such as bacterial peptide fMLF using chemiluminescence method. We also followed the dynamics of fluorescent protein tagged NADPH oxidase subunits by using TIRF (Total internal reflection fluorescence) microscope. Then we used pharmacological tool to modulate the PI(3,4)P2 level at the plasma membrane wether it affected the ROS production and the accumulation of the NADPH oxidase subunits at the plasma membrane.

CHAPTER TWO: Phosphoinositol 3-phosphate acts as a timer for reactive oxygen species production in the phagosome

This work has been published in Journal of Leukocyte Biology.

Doi: 10.1189/jlb.1A0716-305R

Zhi Min Song[*,†,‡], Leïla Bouchab[*,†,‡], Elodie Hudik[*,†,‡], Romain Le Bars[§], Oliver Nüsse[*,†,‡], Sophie Dupré-Crochet[*,†,‡]

*Université Paris-Sud, Université Paris-Saclay, 91405 Orsay, France, †CNRS U8000, LCP, 91405 Orsay, France, ‡INSERM U1174, 91405 Orsay, France, §Imagerie-Gif Cell Biology Pole, Institute for Integrative Biology of the Cell (I2BC), CEA, CNRS, Université Paris-Sud, Université Paris-Saclay, 91198 Gif-sur-Yvette cedex, France

Summary sentence: Modulation of the PI(3)P level at the phagosome affects ROS production by controlling the extent of $p67^{phox}$ accumulation.

Running title: PI(3)P regulates NADPH oxidase

Key words: NADPH oxidase, phagocytosis, live imaging

Abbreviations

Akt (protein kinase B), $DCFH_2$ (2, 7-dichlodihydrofluorescein), FP (fluorescent protein), FKBP (FK506 binding protein), LDH (Lactate dehydrogenase), LDR (Lyn11 targeted FRB), ND-SAFIR (NDimensional-Structure Adaptive Filtering for Image Restoration), MTM1 (Myotubular myopathy 1), PB1 (Phox and Bem1), PH (Pleckstrin Homology), PHOX (phagocyte oxidase), PI(3)P (Phosphoinositol-3-phosphate), $PI(3,5)P_2$ (Phosphatidylinositol (3,5)-bisphosphate), $PI(3,4)P_2$ (Phosphatidylinositol (3,4)-bisphosphate), $PI(3,4,5)P_3$ (Phosphatidylinositol (3,4,5)-trisphosphate), PI3K (Phosphoinositide 3-Kinase), PLB 985 (myeloid leukemia cell line), PX (Phox homology), ROS (Reactive oxygen species), Rubicon (RUN domain protein as Beclin1 interacting and cysteine-rich containing), siRNA (small interfering RNA), SR (Sarcoplasmic Reticulum), UVRAG (Ultraviolet radiation resistance-associated gene protein), Vps34 (Vacuolar Protein Sorting 34), Vps34 IN 1 (VPS34 Inhibitor 1).

Abstract

Production of reactive oxygen species (ROS) in the phagosome by the NADPH oxidase is critical for mammalian immune defense against microbial infections and phosphoinositides are important regulators in this process. Phosphoinositol 3-phosphate (PI(3)P) regulates ROS production at the phagosome via $p40^{phox}$ by an unknown mechanism. This study tested the hypothesis that PI(3)P controls ROS production by regulating the presence of $p40^{phox}$ and $p67^{phox}$ at the phagosomal membrane. Pharmacological inhibition of PI(3)P synthesis at the phagosome decreases the ROS production both in differentiated PLB-985 cells and human neutrophils. It also releases $p67^{phox}$, the key cytosolic subunit of the oxidase, and $p40^{phox}$ from the phagosome. The knockdown of the PI(3)P phosphatase MTM1 and/or Rubicon increase the level of PI(3)P at the phagosome. This increase enhances ROS production inside the phagosome and triggers an extended accumulation of $p67^{phox}$ at the phagosome. Furthermore, the overexpression of MTM1 at the phagosomal membrane induces the disappearance of PI(3)P from the phagosome, and prevents a sustained ROS production. In conclusion, PI(3)P indeed regulates ROS production by maintaining $p40^{phox}$ and $p67^{phox}$ at the phagosomal membrane.

Introduction

Neutrophils are the first line of defense against infectious pathogens. Elimination of the invading bacteria by the neutrophils depends on three primary mechanisms: 1) receptor-mediated uptake of the bacterium into a phagosome, 2) production of ROS by the NADPH oxidase and 3) fusion of neutrophil granules [1]. Chronic granulomatous disease (CGD) is a genetic disorder in which phagocytic cells are unable to kill certain pathogens due to defects in NADPH oxidase [2], leading to severe infections. The NADPH oxidase comprises two integral membrane subunits (gp91^{phox} and p22^{phox}) and three cytosolic regulatory subunits (p40^{phox}, p47^{phox} and p67^{phox}) [3]. The activation of the NADPH oxidase also requires the small GTPase Rac [4]. A key step for the activation of the NADPH oxidase is the phosphorylation of p47^{phox}. Then p47^{phox} binds to p22^{phox} and brings together p40^{phox} and p67^{phox} to initiate the active complex [5]. The activation domain of p67^{phox} regulates electron transfer from NADPH to Flavin adenine dinucleotide [6]. P67^{phox} and p40^{phox} interact *via* their PB1 (Phox and Bem1) domains [3]. P40^{phox} bears a PX (Phox homology) domain that specifically binds to phosphatidylinositol-3-phosphate (PI(3)P) [7-9]. The PX domain of p40^{phox} is required to maintain the protein at the phagosome, and a mutation in that domain that prevents PI(3)P binding, decreases phagosomal ROS production [10-13]. Previous studies have revealed that PI(3)P may play an important role in regulating the NADPH oxidase activity through its binding to p40^{phox}, but how p40^{phox} regulates NADPH oxidase activity through PI(3)P is still not understood.

The synthesis of PI(3)P occurs on the early phagosomal membrane and involves the Class III phosphoinositide 3-Kinase (PI3K): hVps34 (Vacuolar Protein Sorting 1). The knockdown of *VPS34* or *PI3KC3* reduced PI(3)P phagosomal accumulation and decreased ROS production in RAW 264.7 macrophages [14, 15]. Which other proteins regulate PI(3)P at the mammalian phagosome is still not clear. In *Caenorhabditis elegans* phagosomes, the level of PI(3)P is

regulated by the Class III PI3K ,Vps34, Class II PI3K, phosphoinositide 3-Kinase I, and the myotubularin phosphatase MTM1 [16]. Myotubularins have emerged as key regulators of PI(3)P. There are 14 myotubularin members in humans (MTM1, MTMR1-R13) characterized by a PH-glucosyltransferase Rab-like GTPase activators and Myotubularins and a Protein Tyrosine Phosphatase domain. Loss of MTM1 phosphatase activity leads to X-linked myotubular myopathy (XLMTM). MTM1 is a key regulator of the sarcoplasmic reticulum (SR) PI(3)P in muscle, regulating the SR membrane shape [17]. MTM1 also regulates PI(3)P in the early endosome, and knockdown of MTM1 blockes the trafficking of the epidermal growth factor receptor [18]. Moreover MTM1 interacts and negatively regulates hVps34-hVps15, which are, respectively, the catalytic and the regulatory subunit of the Class III PI3K [18, 19].

Another protein that could participate in the regulation of PI(3)P at the phagosomal level is Rubicon (RUN domain protein as Beclin1 interacting and cysteine-rich containing). Indeed Rubicon was reported to inhibit hVps34 [20, 21]. It localizes to the late endosome/lysosome and negatively regulates endosome and autophagosome maturation [22, 23]. Rubicon is also recruited to LC3 (microtubule associated light chain 3) positive phagosomes upon phagocytosis of unopsonized zymosan [24, 25].

Here, we report that PI(3)P regulates phagosomal ROS production by controlling the accumulation of $p40^{phox}$ and $p67^{phox}$ at the phagosome. Furthermore, our data indicate that Rubicon and MTM1 localize to the phagosome of serum opsonized zymosan and downregulate the PI(3)P level at the phagosome. Using fluorescently tagged subunits of $p40^{phox}$ and $p67^{phox}$ and a PI(3)P probe, we also observed that the time of disappearance of $p40^{phox}$ and $p67^{phox}$ at the phagosome was the same and correlated with PI(3)P decrease from the phagosomal membrane. Our results suggest that PI(3)P maintains $p40^{phox}$ at the phagosome, which, in turn, keeps $p67^{phox}$ in the NADPH oxidase complex and sustains ROS

production.

Materials and methods

Cell culture

The human myeloid leukaemia cell line PLB-985 was a generous gift from Dr. Marie-José Stasia. The stable PLB cell line expressing citrine tagged $p67^{phox}$ subunit was described previously [26, 27]. For all the experiments, PLB-985 cells were differentiated into neutrophil-like cells by adding 1.25% DMSO in exponentially growing condition for 5 or 6 days. 2000 U/ml IFN-γ (Immuno Tools, Germany) was added to the culture 24 hours before the experiments. For all experiments, differentiated cells were centrifuged 3 min at 2000 rpm and resuspended in Hepes buffer containing 140 mM NaCl, 5 mM KCl, 1 mM $MgCl_2$, 2 mM $CaCl_2$, 10 mM Hepes (pH 7.4), 1.8 mg/ml glucose and 1% heat inactivated foetal bovine serum.

Neutrophil preparation

Neutrophils were withdrawn from healthy donner whole blood by means of dextran sedimentation and Ficoll centrifugation as previously described [28].

Plasmids

The plasmids pmCherryC1 and $p67^{phox}$-citrine were constructed as previously described [26, 27]. PcitrineC1 was obtained from YFP-C1 by the same mutagenesis as previously described for pcitrineN1 [27]. The human $p40^{phox}$ cDNA was amplified from p40CDM8 (a gift from Marie-Claire Dagher, Genoble, France) by PCR using the following primers: GGTCACTCGAGCTGCTGTGGCCCAGCAGCTG (sense) and GGCTTCCGCGGTCAGCTCATGGCATC (antisense) and then inserted in XholI and SacII restriction sites in plasmid pcitrineC1 to generate the plasmid citrine-$p40^{phox}$. In order to obtain a citrine-$p40^{phox}$ resistant to siRNA, we introduced silent mutations in amino acids

P220 and L221: the mutations t660a, c661t and c663a were introduced using the Quickchange II Site Directed Mutagenesis kit (Stratagene, La Jolla, CA, USA). EGFP-p67^{phox}, obtained from citrine-p67^{phox} [27], was cut by Nhel and Agel and p67^{phox}cDNA was inserted at the same restriction sites in pmCherryC1 as described previously [26] to generate mCherry-p67^{phox}. Lyn11-targeted FRB (LDR) (Addgene plasmid # 20147) and YFP-FKBP (Addgene plasmid # 20175) were provided by Tobias Meyer [29]. MCherry-FKBP-MTM1 (Addgene plasmid # 51614) was provided by Tamas Balla [30]. MCherry-FKBP cDNA was cut from mCherry-FKBP-MTM1 plasmid, and YFP-FKBP cDNA from YFP-FKBP plasmid was replaced by mCherry-FKBP cDNA using AgeI and SalI restriction sites. P40^{phox}PX-EYFP (Addgene plasmid # 19011) expressing YFP-PXp40^{phox} was provided by Michael Yaffe [31]. PXp40^{phox} cDNA was then cut by BgII and SacII restriction sites and inserted in pmCherryC1 to get mCherry-PXp40^{phox}. EGFP-Rubicon (Addgene plasmid # 28022) was provided by Qing Zhong [20]. PH-Akt-GFP (Addgene plasmid # 51465) was provided by Tamas Balla [32]. MCherry-Dectin-1 (Addgene plasmid # 55025) was provided by Michael Davidson. All of the constructs were confirmed by sequencing.

Transient and stable transfection

Differentiated PLB cells, PLB p67^{phox}-citrine and PLB -citrine stable cell lines were transiently transfected using the 4D-Nucleofector (Lonza, Switzerland) according to the manufacturer's protocol. For each condition, using the SF Cell Line Kit and the EH-100 program, 2×10^6 to 4×10^6 cells were transfected with 1 µM siRNA or/and 3 µg of vector and incubated in culture medium without antibiotics. LDR, mCherry-FKBP, mCherry-FKBP-MTM1, EGFP-Rubicon, mCherry-Dectin-1 plasmids were transfected 4 hours before the experiment. The p40^{phox}-citrine and mCherry-p67^{phox} siRNA were transfected 4 hours or 2 days before the experiments.

A PLB-p40^{phox}-citrine stable cell line was generated by electroporation using a Bio-Rad Gene Pulser II apparatus as previously described [27]. This cell line was cultured constantly in the presence of 0.5 mg/ml of G418 to maintain the selection.

RNA interference

All the siRNAs were purchased from Eurogenetec (Eurogenetec, Belgium). For each gene knockdown, three siRNA have been tested. The sequence of the selected siRNAs were as followed. SiRNA control (SR-CL000-005), p40^{phox} siRNA (Forward sequence (FS) :5'GGG-CAU-CUU-CCC-UCU-CUC-CUU-CGU-GAA3') , p67^{phox} siRNA (FS : 5'CCA-AGG-AGU-AAG-UAC-AAA-U3'), MTM1 siRNA(FS:5'GGG-AAG-AGU-UUA-CAU-CAC-A3') ,Rubicon siRNA (FS :5'GCU-CUC-UGU-ACA-UGG-AAU-A3'). 1 µM siRNA was transiently transfected using the 4D-Nucleofector (Lonza, Switzerland) with the SF Cell Line Kit and the EH-100 program. P40^{phox} siRNA or p67^{phox} siRNA were transfected in PLB cells after 2 days of differentiation with DMSO. Then we added DMSO again to the transfected cells to allow complete differentiation and used the cells 2 days after transfection. MTM1 siRNA and/or Rubicon siRNA were transfected after 1 day of differentiation. Then we added again DMSO to the transfected cells and did the experiments 4 days after transfection.

Immunoblotting analysis

Differentiated PLB cells were incubated on ice with lysis buffer (4×10^4 cells/µl) containing Hepes-Na 25 mM, NaCl 150 mM, $MgCl_2$ 5 mM, EGTA 0.5 mM, TritonX100 0.5%, NaF 10 mM and supplemented with a protease inhibitor cocktail complete mini EDTA-free (Roche, Switzerland). Then lysates were centrifuged at 14000g at 4°C for 30 min. Protein concentration was measured using BioRad Protein assay. Samples were diluted in 6× Laemmli buffer and boiled 5 min at 95°C. Proteins were separated on a 10% SDS-PAGE gel

and transferred onto nitrocellulose membrane (BioRad, USA). The membrane was saturated with 3% milk at room temperature for 30 min (0.05% tween in PBS). The primary antibodies (rabbit anti-$p67^{phox}$ antibody 1:1000, upstate, USA; mouse anti-$p40^{phox}$ antibody 1:100, Santa Cruz, USA; rabbit anti-LDH antibody 1:5000, AbCam, UK; mouse anti-MTM1 antibody 1:1000, upstate, USA; rabbit anti-Rubicon antibody 1:1000, cell signalling, USA ; mouse anti-GFP antibody 1 :400, Roche, Germany) were incubated at 37°C for 1h. HRP-labeled secondary antibodies (anti-mouse IgG or anti-rabbit IgG 1:2000, GE healthcare, UK) were incubated at room temperature for 1h. Proteins were detected by using ECL reagent (GE healthcare, UK) and quantification was analysed by using BioD1 software (Fisher scientific, USA).

Preparation and opsonization of yeasts and zymosan

Yeasts (*Saccharomyces cerevisiae*) and zymosan particles (zymosan and Texas-red-zymosan) from *S. cerevisiae* (Sigma Aldrich, USA) were prepared as described [33]. For flow cytometry experiments, yeasts covalently labelled with $DCFH_2$ and Alexa-405 were used [34] allowing the measurement of the intraphagosomal ROS production and the percentage of phagocyting cells. For video microscopy experiments, zymosan was covalently labelled with $DCFH_2$ as described previously for yeasts [33]. Yeasts were opsonized with polyclonal rabbit anti-yeast serum (50 times diluted, 1h, 37°C) and zymosan was opsonized with total human serum (50% diluted, 1h, 37°C). For the experiment with hVps34 and wortmannin inhibitors, yeasts were opsonized with total human serum (50 % diluted, 1h, 37°C). Opsonized yeasts or zymosan were washed twice with PBS, re-suspended in Hepes buffer.

Immunofluorescence

The immunofluorescence experiments were performed as described before [27]. The cells were immunostained with mouse anti-MTM1 antibody (upstate, USA; 1:100) followed by Alexa 488 goat anti-mouse (Life Technologies, USA; 1:500). Cells were imaged at room temperature on the PIMPA platform (Leica TCS SP8 CSU) mounted on a Leica DM6000 inverted microscope equipped with a 40×plan Apo 1.1 water-immersion objective and a HyD detector driven by the LAS AF software (Leica, Germany). Texas Red Zymosan was excited at 552 nm, MTM1 was excited at 488 nm.

Flow cytometry

Flow cytometry experiments were performed with a CyFlow ML flow cytometer (Partec, Germany) to measure the intraphagosomal ROS production and the percentage of phagocyting cells. 5×10^4 differentiated PLB-985 cells or human neutrophils were used for each experiment and re-suspended in Hepes buffer. 5×10^4 $DCFH_2$-Alexa-405 yeasts were added to the cells, then, a centrifugation at 2000 rpm for 3 min at 13°C was performed, followed by an incubation at 37°C for 30 min. The cells were analysed by flow cytometry: $DCFH_2$ was excited with the 488 nm laser and Alexa-405 with 405nm laser.

Live cell microscopy and analysis of intraphagosomal ROS production

Live cell microscopy experiments were performed as described before [33]. To follow the fluorescence of DCFH2-zymosan, mCherry-FKBP or mCherry-FKBPMTM1 a Nikon Eclipse TE200 microscope equipped with a cooled CCD camera (PCO, Sensicam-QE, Germany) was used [33]. The fluorescence of DCFH2-yeast was monitored using a wide field microscope (DMi8, Leica, Germany) equipped with HC PL APO63X objective and a CMOS camera (ORCA-Flash4, Hamamatsu, Japan). Serial images were recorded every 10 s during 600 or 700 s. Time exposure for $DCFH_2$-zymosan or $DCFH_2$-yeast was 20 ms and 200 ms for

mCherry tagged proteins. Image J software was used to analyse the fluorescence intensity of $DCFH_2$-zymosan or $DCFH_2$-yeast in each phagosome every 100 s. At least ten phagosomes were collected from at least three independent experiments. The data were represented as mean±SEM.

Spinning-disk confocal microscopy

To follow fluorescent tagged-proteins during the phagocytosis of opsonized zymosan, we used a Spinning-disk confocal system (Yokogawa CSU-X1-A1, Yokogawa Electric, Japan), mounted on a Nikon Eclipse Ti E inverted microscope, equipped with a 100× plan Apo 1.4 oil immersion objective and an EM-CCD eVolve camera (Photometrics), driven by MetaMorph 7 software (Universal imaging). Cells were resuspended in Hepes buffer and allowed to adhere to coverslips. All the experiments were performed at 37°C. After adding zymosan, images were recorded with a time-lapse from 20 s to 2 min depending on the different experiments. YFP, GFP and citrine were excited at 491 nm by using a 0.3 s laser illumination. MCherry was excited at 561 nm by using a laser illumination of 0.2 s. The fluorescence was detected with a double band beamsplitter, a 525/45 nm emission filter for YFP, GFP and citrine and a 607/36 nm emission filter for mCherry. Series of 11-18 confocal z-planes (1 µm distance) were collected and the central plane of each phagosome was chosen to construct the video sequence.

Image processing and analysis

The image J software was used to analyse all the images and quantify the fluorescence. The ratio of fluorescence intensity of the fluorescent protein at the phagosome to that in the cytoplasm was calculated as described previously [27]. When the ratio was higher than 1, we considered that the fluorescent protein was accumulated at the phagosomal membrane.

After quantification, when indicated, the images were denoised with ND-SAFIR (NDimensional-Structure Adaptive Filtering for Image Restoration) INRIA/INRA 2007 [35]. The following parameters were used: pixel size, 3; quality, high; Poisson process.

In Figure 3A, 6B and S4, the images are one plane from a deconvolved stack. The deconvolution was applied after quantification. Each stack of the videos was deconvolved employing Huygens Essential package (Scientific Volume Imaging, Hilversum, the Netherlands), with the following parameters: algorithm, CMLE; signal/noise ratio, 10; quality threshold, 0.01%; maximum iterations, 100; background calculation, in/near objects.

Data analysis

To compare the ratio values between two experiments, ratio paired T-test was analysed by using graphpad prism6 software (GraphPad Software, USA). All the others values were analysed by Students' T test.

Online supplemental material

Videos: In all the videos the time zero represents the start of the video i.e. before or just at the time of phagosome closure. The following videos 1, 2, 4, 5 and 6 have been denoised by ND-SAFIR software.

Video 1. **VPS34 IN1 decreases the accumulation of mCherry-PXp40^{phox} at the phagosome.** The phagocytosis of opsonized zymosan (*) was followed in PLB-WT cells transfected with mCherry-PXp40^{phox}. Cells were incubated with 1 µM VPS34 IN1, 1 min before adding opsonized zymosan. Images were analyzed by time-lapse spinning disk confocal microscopy. Frames were taken every 30 s for 1 min 30 s and then every 1 min until 6 min. Bar, 5 µm.

Video 2. **Wortmannin releases p67^{phox}-citrine from the phagosome.**

The phagocytosis of opsonized zymosan (*) was followed in PLB-p67^{phox}-citrine cells transfected with p67^{phox} siRNA. 300 nM wortmannin was added at 1 min 23 s. Images were taken by time-lapse spinning disk confocal microscopy. Frames were taken every 1 min until 8 min 24s. Selected images are shown in Fig. 3 B. Bar, 5 μm.

Video 3. **Citrine-p40^{phox} and p67^{phox}-mCherry display identical phagosomal dynamics.** The phagocytosis of opsonized zymosan (*) was followed in differentiated PLB-citrine-p40^{phox} cells (green) transfected with p67^{phox}-mCherry (red), p40^{phox} siRNA and p67^{phox} siRNA. Images were analyzed by time lapse spinning disk confocal microscopy. Frames were taken every 30 s for 30 s and then every 1 min until 12 min 30 s. Related images are shown in Fig. 6. Bar, 5 μm.

Video 4. **Knockdown of MTM1 and Rubicon triggers an extended accumulation of YFP-p40^{phox}PX overtime.** The phagocytosis of opsonized zymosan(*) was followed in PLB-WT cells transfected with YFP-PXp40^{phox}, MTM1 siRNA and Rubicon siRNA. Images were analyzed by time-lapse spinning disk confocal microscopy. Frames were taken every 1 min for 32 min. Selected images are shown in Fig. 9 A. Bar, 5 μm.

Video 5. **LDR/mCherry-FKBP system doesn't affect the recruitment of p40^{phox}PX-EYFP at the phagosome.** The phagocytosis of opsonized zymosan(*) was followed in PLB-WT cells transfected with YFP-PXp40^{phox} (green), LDR and mCherry-FKBP (red). Before incubation with opsonized zymosan, 0.25 μg/ml rapamycin was added to trigger the accumulation of mCherry-FKBP at the plasma membrane. Images were analyzed by time-lapse spinning disk confocal microscopy. Frames were taken every 30 s for 13 min. Selected images are shown in Fig. 11 A. Bar, 5 μm.

Video 6. **MTM1 overexpression at the phagosomal membrane prevents p40^{phox}PX-EYFP recruitment.** The phagocytosis of opsonized zymosan(*) was followed in PLB-WT cells transfected with YFP-PXp40^{phox}(green), LDR and mCherry-FKBP-MTM1(red). Before incubation with opsonized zymosan, 0.25 μg/ml rapamycin was added to trigger the accumulation of mCherry-FKBP-MTM1 at the plasma membrane. Images were analyzed by time lapse spinning disk confocal microscopy. Frames were taken every 1 min for 12 min. Selected images are shown in Fig. 11 B. Bar, 5 μm.

Results

The hVps34 inhibitor, VPS34-IN1, decreases the ROS production both in differentiated PLB-985 cells and in human neutrophils.

Wortmannin decreases human neutrophil ROS response to serum–opsonized *Escherichia Coli* and *Staphylococcus aureus*. This decrease was attributed to inhibition of Class III PI3K hVpS34 [14]. There are three classes of PI3K: Class I phosphorylates phosphoinositol 4-phosphate and phosphoinositol (4.5)-bisphosphate, and Class II and III are involved in phosphoinositol phosphorylation [36]. We wanted to examine the ROS production directly inside the phagosome of neutrophil-like PLB-985 cells and human neutrophils upon inhibition of hVps34. To measure phagosomal ROS production we used $DCFH_2$-Alexa405 stained yeasts [34] and a recently described Vps34 inhibitor named VPS34-IN1 [37]. By using the $PI(3,4)P_2$ and $PI(3,4,5)P_3$ probe PH-Akt-GFP, we checked that VPS34-IN1 did not affect the accumulation of $PI(3,4,5)P_3$ and $PI(3,4)P_2$ on the nascent phagosome in PLB-985 cells. As indicated by the fluorescence ratio between the phagosome and the cytosol, the PH-Akt-GFP probe accumulated at the phagosomal cup and early phagosome in cells pretreated with or without VPS34 IN1 (Vps34 Inhibitor 1) (**Fig. 1A and B**). The addition of VPS34-IN1 significantly decreased the accumulation of the PI(3)P probe mCherry-$PXp40^{phox}$ but did not completely abolish its recruitment. A slight and transient accumulation of the PI(3)P probe can be observed between time 0 and 3 min after phagosome closure (see **Fig. 1C and Fig. 3A**; first row for the control, **Fig. 1D** and Supplemental Video 1). This may be due to hVsp34 being the major, but maybe not the only, source of PI(3)P at the phagosome. The phagocytosis and ROS production was then assessed by evaluating Alexa405 and DCF fluorescence, respectively, after 0.5 hour of $DCFH_2$-Alexa405 labelled yeast phagocytosis. There was no significant difference in the percentage of phagocyting cells with or without preincubation with VPS34 IN1 for PLB-985 cells and neutrophils (**Fig. 2A**). However

preincubation with VPS34 IN1 decreased ROS production to (means ± SEM) 66.3 ± 8.8 % in differentiated PLB phagosomes and to 64.1 ± 2.4 % in neutrophils (**Fig. 2B**). These data clearly show that hVps34 regulates the ROS production in the phagosome of differentiated PLB cells and human neutrophils.

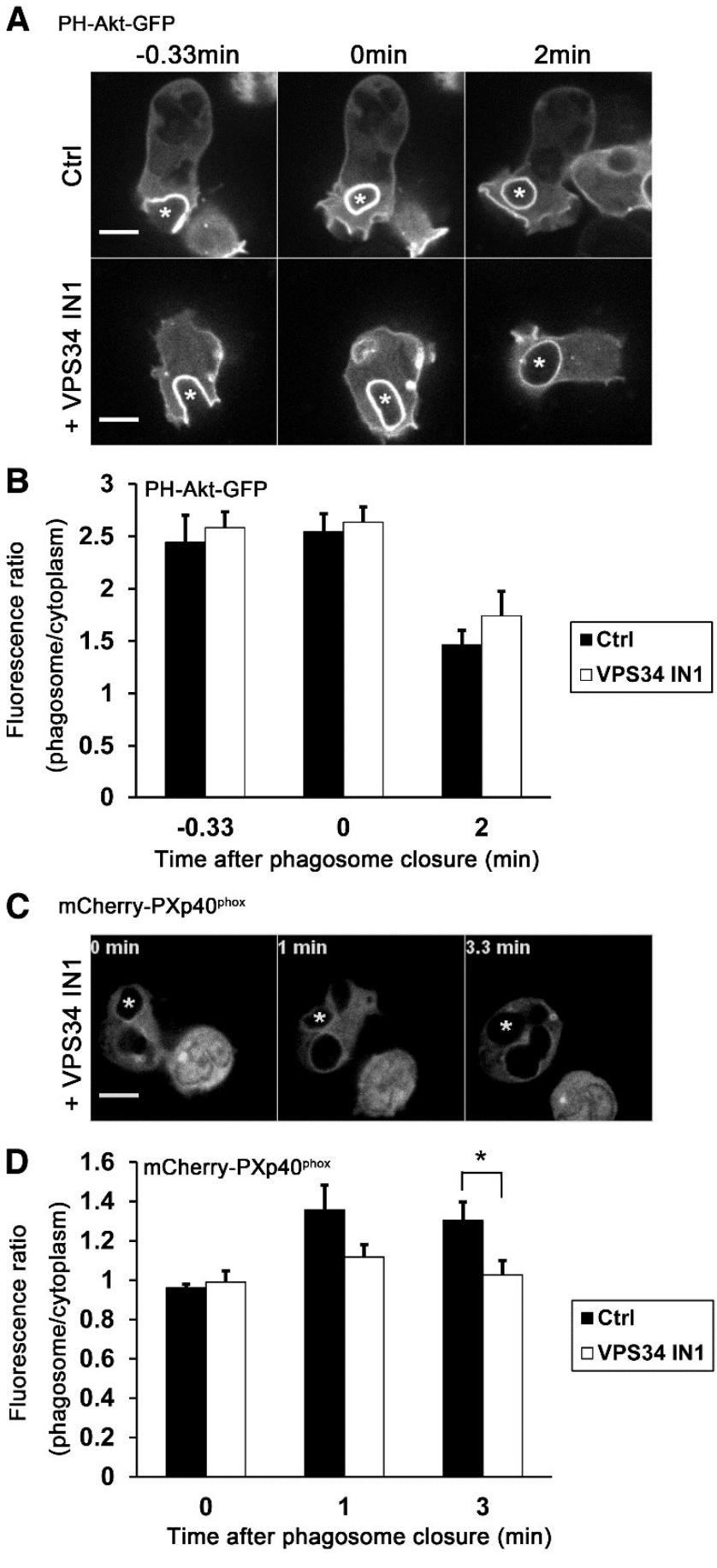
A
PH-Akt-GFP
-0.33min
0min
2min
Ctrl
+ VPS34 IN1
B
PH-Akt-GFP
Fluorescence ratio
(phagosome/cytoplasm)
3
2.5
2
1.5
1
0.5
0
-0.33
0
2
Time after phagosome closure (min)
Ctrl
VPS34 IN1
C
mCherry-PXp40phox
+ VPS34 IN1
0 min
1 min
3.3 min
D
mCherry-PXp40phox
Fluorescence ratio
(phagosome/cytoplasm)
1.6
1.4
1.2
1
0.8
0.6
0.4
0.2
0
*
0
1
3
Time after phagosome closure (min)
Ctrl
VPS34 IN1

Figure 1. VPS34-IN1 inhibits hVps34 but not Class I PI3K.

(A, C) Representative images of zymosan phagocytosis by PLB-WT cells transfected with PH-Akt-GFP (A) or mCherry-PXp40^{phox} (C and Supplemental video 1). Cells were incubated 1 min with or without 1 μM VPS34 IN1 before adding opsonized zymosan. Images were acquired by spinning disk confocal video microscopy. Time 0 represents the closure of the phagosome. The asterisks denote the position of the zymosan. (B) Quantification of the accumulation of PH-Akt-GFP at the phagosome at time -0.33, 0 and 2 min. Data are mean ± SEM. Control, *n=15*; VPS34-IN1, *n=14*. (D) Quantification of the accumulation of mCherry-PXp40^{phox} at the phagosome at time 0, 1 and 3min after closure. Data are mean ± SEM. Control, *n=10*; VPS34 IN1, *n=10*. *, $P < 0.05$, (student's *t* test). Scale bar = 5 μm.

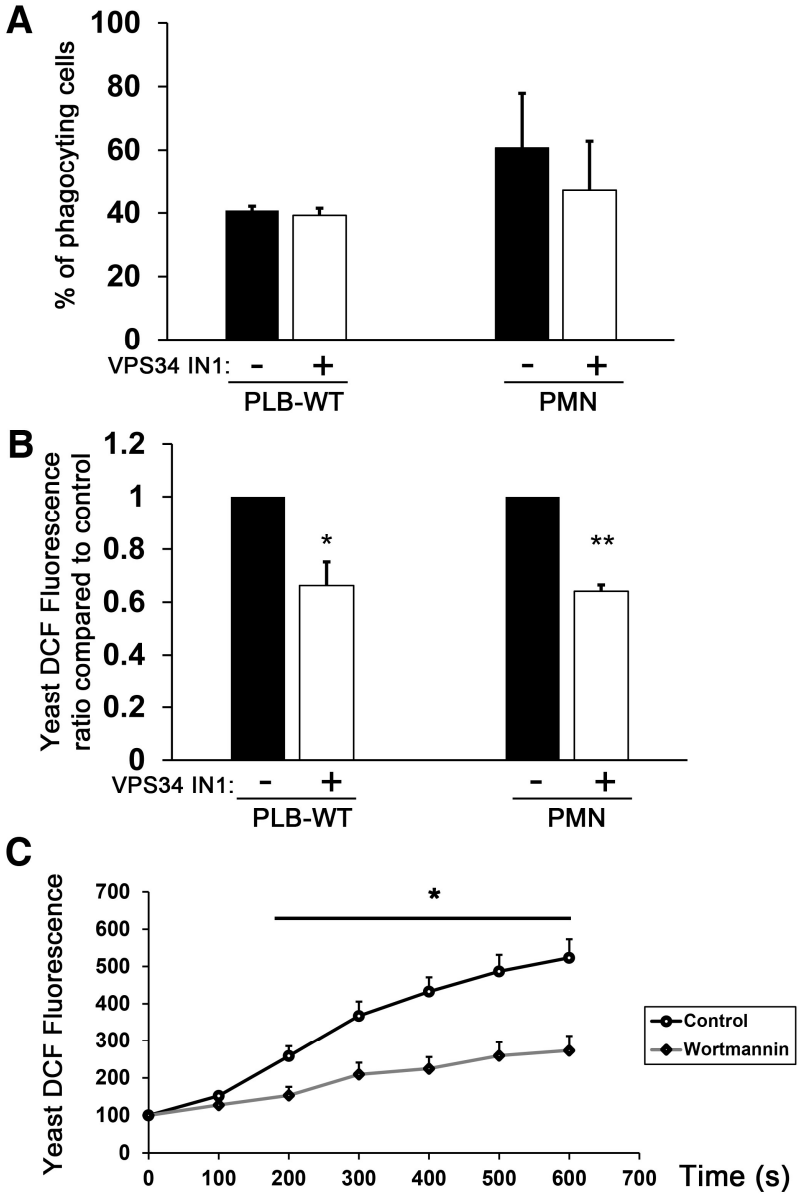

Figure 2. PI(3)P inhibitors decrease ROS production.

(A and B) PLB-985 cells or human neutrophils, pre-treated 1 min with or without 1 µM VPS34-IN1, were then allowed to phagocyte serum opsonized $DCFH_2$-Alexa405-yeast for 0.5 hour. DCF and Alexa405 fluorescence were measured by flow cytometry allowing the evaluation of respectively the percentage of phagocyting cells and the ROS production. (A) Quantification of the percentage of phagocyting cells. (B) Quantification of yeast DCF fluorescence. Results are presented as the ratio of yeast-DCF fluorescence in the presence of VPS34-IN1 to that without inhibitor Data are mean ± SEM. PLB cells, *n*=4; PMN, *n*=3; *, $P < 0.05$; **, $P < 0.01$ (ratio paired *t* test). (C) The kinetics of ROS production was assessed by videomicroscopy by quantifying $DCFH_2$-labelled yeast fluorescence in PLB-WT cells treated or not by wortmannin 1 min ± 0.5 after phagosomal closure. Data are mean ± SEM. For each condition, *n*=9. * $P < 0.05$.

Wortmannin triggers the release of p40^{phox} and p67^{phox} from the phagosome

The above data suggest that PI(3)P controls ROS production. It has been shown that the PX domain stabilizes p40^{phox} at the phagosome [11, 12], however the role of p40^{phox} and how PI(3)P controls ROS production has not been deciphered. We investigated whether the PI(3)P level at the phagosome could affect the accumulation of p40^{phox} and p67^{phox}. Because we still observed a faint mCherry-PXp40^{phox} signal at the phagosome with the VPS34-IN1 inhibitor, we, instead, used wortmannin to decrease PI(3)P. Wortmannin is a pan-PI3K inhibitor, although class II PI3K has a relatively low sensitivity to wortmannin [38, 39]. To specifically decrease specifically PI(3)P accumulation after phagosome closure, we added wortmannin just after the appearance of PI(3)P at the phagosome, i.e., 1min ± 30s after phagosome closure (**Fig. 3B**). Indeed, the addition of wortmannin after phagosome closure released the PI(3)P probe (mCherry-PXp40^{phox}) from the phagosome in a few minutes: the mean time of disappearance of mCherry-PXp40^{phox} after phagosome closure dropped from 15.4 ± 2.2 min to 5 ± 0.4 min (± SEM) (**Fig.3**). The time of disappearance is the time at which the ratio of fluorescence intensity of the phagosome to that of the cytoplasm decreases to 1. As previously shown in RAW 264.7 macrophages [40], the addition of wortmannin after phagosome closure terminates PI(3)P synthesis. We, therefore, examined whether ROS production was affected by the inhibition of PI(3)P synthesis. Using $DCFH_2$-yeasts, we followed the DCF fluorescence by video microscopy during phagocytosis. The addition of wortmannin 1min ± 0.5 after phagosome closure clearly reduced ROS production. The weak remaining ROS production could be due to the delayed inhibition of PI(3)P synthesis after addition of wortmannin (**Fig. 2C**).

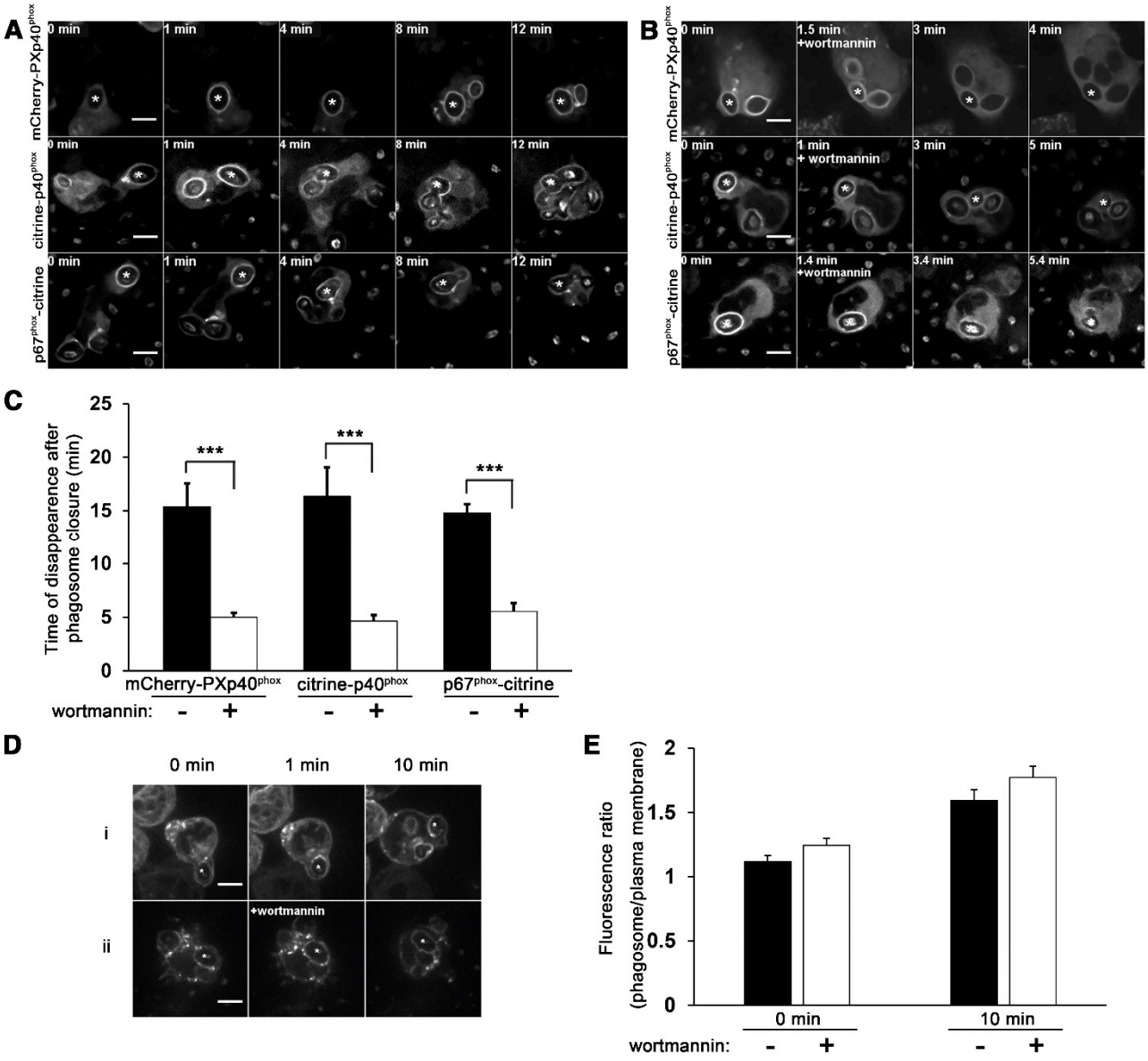
A
mCherry-PXp40phox
citrine-p40phox
p67phox-citrine
0 min
1 min
4 min
8 min
12 min
B
1.5 min +wortmannin
3 min
4 min
1 min + wortmannin
5 min
1.4 min +wortmannin
3.4 min
5.4 min
C
Time of disappearence after phagosome closure (min)
***
mCherry-PXp40phox
citrine-p40phox
p67phox-citrine
wortmannin: - + - + - +
D
0 min
1 min
10 min
i
ii
+wortmannin
E
Fluorescence ratio (phagosome/plasma membrane)
0 min
10 min
wortmannin: - + - +

Figure 3. Effects of wortmannin on phagosomal accumulation of mCherry-PXp40^{phox}, p67^{phox}-citrine and citrine-p40^{phox}.

(A) Representative images of zymosan (*) phagocytosis by transfected cells acquired by spinning disk confocal video-microscopy. PLB-WT cells were transfected with mCherry-PXp40^{phox} or citrine-p40^{phox} plus p40^{phox} siRNA and PLB-p67^{phox}-citrine cells with p67^{phox} siRNA. Time 0 represents the closure of the phagosome. (B) Same as panel A, except that wortmannin was added at 1 min ± 30s after phagosome closure. The video 2 is related to the images shown for p67^{phox}-citrine. (C) Quantification of the time of disappearance of mCherry-PXp40^{phox}/citrine-p40^{phox}/p67^{phox}-citrine at the phagosome. This time of disappearance is the time at which the ratio of fluorescence intensity at the phagosome to that of the cytoplasm decreased to 1. Data are mean ± SEM. mCherry-PXp40^{phox}, *n*=10; mCherry-PX + wortmannin, *n* =9; Citrine-p40^{phox}, *n* =11; citrine-p40^{phox} + wortmannin, *n* =11; P67^{phox}-citrine, *n* =10; p67^{phox}-citrine + wortmannin, *n* =11; *** P < 0.001 (student's *t* test). Scale bars = 5 µm. (D) Representative images of zymosan (*) phagocytosis by PLB-WT cells, transfected with mCherry-Dectin-1, at time 0, 1 and 10 min after phagosome closure. Wortmannin was added (ii) or not (i) 1min ± 0.5 after phagosome closure. (E) The graph shows the fluorescence ratio between the phagosomal and plasma membrane at the time of phagosomal closure and 10 min after. Data are mean ± SEM. Control, *n*=14; wortmannin, *n* =11. After quantification, the images shown in A, B and D have been processed with ND-SAFIR software.

To examine how the phagosomal PI(3)P decrease affected $p40^{phox}$ phagosomal accumulation, PLB-985 cells were transiently transfected with citrine-$p40^{phox}$ and a siRNA targeting only the endogenous $p40^{phox}$ (**Fig. 4A**). Silent mutations were introduced in the cDNA encoding citrine-$p40^{phox}$ to preclude hybridization between $p40^{phox}$ siRNA and citrine-$p40^{phox}$ mRNA. The $p40^{phox}$siRNA decreased the endogenous $p40^{phox}$ level to 40% and reduced ROS production (**Fig. 4A, B and E**). Imaging by confocal microscopy showed that citrine-$p40^{phox}$ disappeared from the phagosome 16.4 ± 2.7 min after phagosome closure (**Fig. 3A and C**). This time until disappearance dropped to 4.6 ± 0.6 min upon addition of wortmannin 1min ± 0.5 after phagosome closure (**Fig. 3B and C**). To observe whether the drop of PI(3)P also affected the time in with $p67^{phox}$-citrine was present at the phagosome, we studied the $p67^{phox}$-citrine accumulation at the phagosome. We used stably transfected PLB-$p67^{phox}$-citrine cells and transfected them with a siRNA targeting the 3' untranslated region of the endogenous $p67^{phox}$ mRNA. The siRNA reduced endogenous level of $p67^{phox}$ and not that of $p67^{phox}$-citrine (**Fig. 4C and D**). No difference in phagocytosis was observed in any condition (data not shown), however, phagosomal ROS production was decreased to 60% with $p67^{phox}$ targeted-siRNA in PLB-WT cells. ROS production was unchanged in PLB-$p67^{phox}$-citrine cells transfected with control siRNA or $p67^{phox}$ siRNA (**Fig. 4E and F**). Imaging by confocal microscopy showed that the time of $p67^{phox}$-citrine disappearance dropped from 14.8 ± 0.8 min to 5.5 ± 0.8 min upon addition of wortmannin after phagosome closure (**Fig. 3** and Supplemental Video 2). To ensure that wortmannin is not exerting an off-target effect, we followed the accumulation of mCherry-Dectin-1 at the phagosome. MCherry-Dectin-1 fluorescence did not decrease after addition of wortmannin: a similar phagosomal accumulation was detected 10 min after phagosomal closure in control or wortmannin treated phagosomes (**Fig. 3D** and **E**). Thus, wortmannin terminated rapidly PI(3)P synthesis in the early phagosome. It also stopped ROS production by triggering the release of $p40^{phox}$ and

p67^{phox} from the phagosome. Moreover, we observed that the time of disappearance was the same for the PI(3)P probe and for both subunits: p67^{phox}-citrine and citrine-p40^{phox}. Using a stable PLB-985 cell line expressing citrine-p40^{phox} (**Fig. 5**) transiently transfected with p67^{phox}-mCherry, we observed that the two subunits stayed at the phagosome for the same amount of time: they both disappeared around 13min after phagosome closure (**Fig. 6** and Supplemental Video 3). Our data suggest that phagosomal p40^{phox} is a late adaptor for p67^{phox} allowing it to stay at the phagosome.

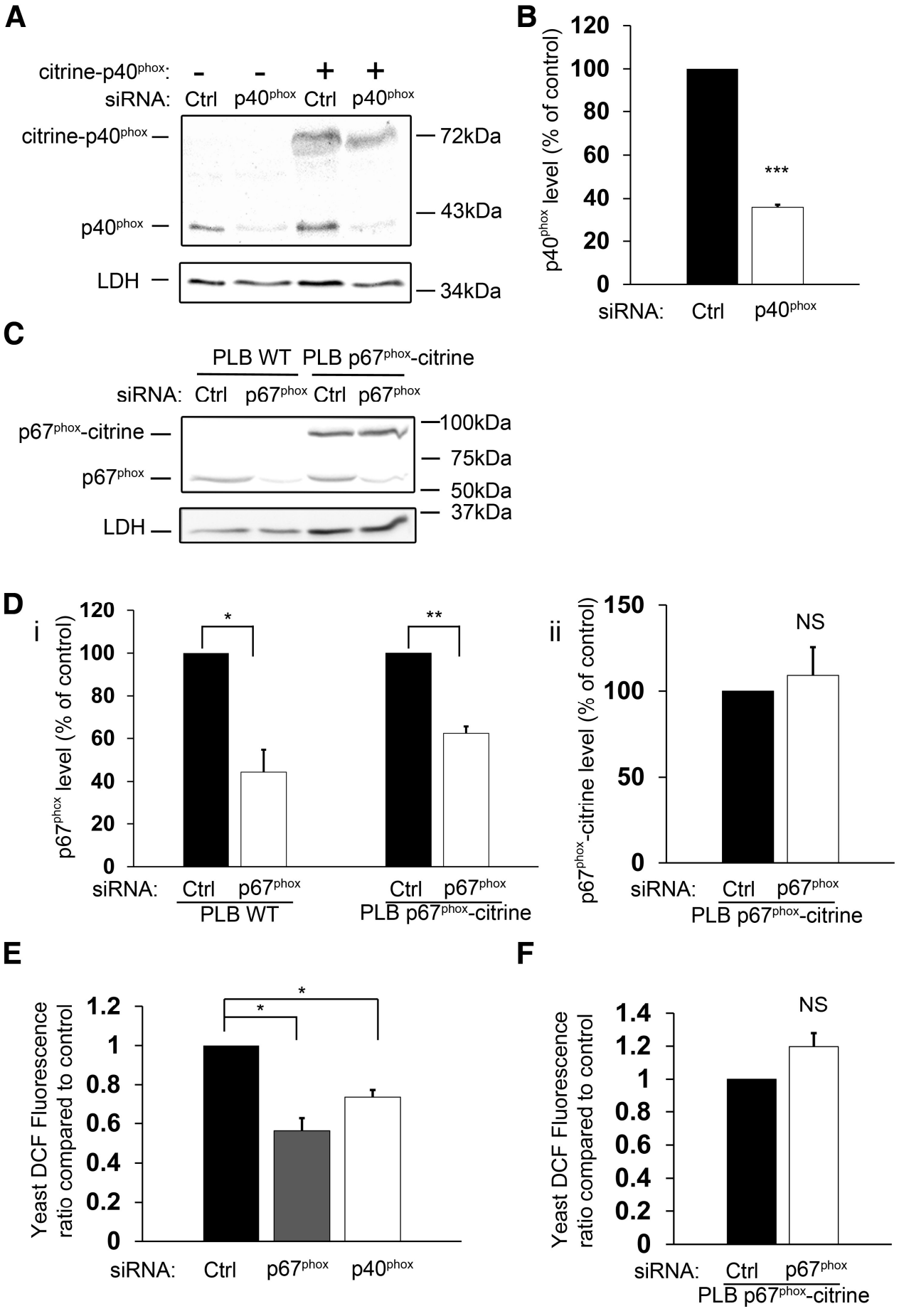
A
citrine-p40phox: - - + +
siRNA: Ctrl p40phox Ctrl p40phox
citrine-p40phox
p40phox
LDH
72kDa
43kDa
34kDa
B
p40phox level (% of control)
120
100
80
60
40
20
0
***
siRNA: Ctrl p40phox
C
PLB WT PLB p67phox-citrine
siRNA: Ctrl p67phox Ctrl p67phox
p67phox-citrine
p67phox
LDH
100kDa
75kDa
50kDa
37kDa
D
i
p67phox level (% of control)
120
100
80
60
40
20
0
*
**
siRNA: Ctrl p67phox Ctrl p67phox
PLB WT
PLB p67phox-citrine
ii
p67phox-citrine level (% of control)
150
100
50
0
NS
siRNA: Ctrl p67phox
PLB p67phox-citrine
E
Yeast DCF Fluorescence ratio compared to control
1.2
1
0.8
0.6
0.4
0.2
0
*
*
siRNA: Ctrl p67phox p40phox
F
Yeast DCF Fluorescence ratio compared to control
1.4
1.2
1
0.8
0.6
0.4
0.2
0
NS
siRNA: Ctrl p67phox
PLB p67phox-citrine

Figure 4. Knockdown of p40^{phox} or p67^{phox} decreases the ROS production at the phagosome.

(A) Western blot analysis of citrine-p40^{phox}, p40^{phox} and LDH in PLB-WT cells transfected with control siRNA or p40^{phox} siRNA with or without citrine-p40^{phox}. Citrine-p40^{phox} and p40^{phox} were detected with anti-p40^{phox} antibody. (B) Quantification of the p40^{phox} protein level. Data are mean ± SEM. *n=3*. ***, P < 0.001 (Ratio paired *t* test). (C) Western blot analysis of p67^{phox}-citrine, p67^{phox} and LDH in PLB-WT cells or PLB-p67^{phox}-citrine cells transfected with control siRNA or p67^{phox} siRNA. P67^{phox}-citrine and p67^{phox} were detected with anti-p67^{phox} Ab. (D) (i) Quantification of the p67^{phox} protein level. PLB-WT cells, *n=3*. PLB-p67^{phox}citrine cells, *n=3*. *P < 0.05; **P < 0.01 (Ratio paired *t* test). (ii) Quantification of the p67^{phox}-citrine protein level. *n=3*. Data are mean ± SEM. (E and F) ROS production was assessed by flow cytometry by evaluating $DCFH_2$-labelled yeast fluorescence in PLB-WT cells transfected with control siRNA, p40^{phox} siRNA or p67^{phox} siRNA (E, *n=3. *P < 0.05 (student's *t* test)) or in PLB-p67^{phox}-citrine cells transfected with control siRNA or p67^{phox} siRNA (F, *n=3*). Data are mean ± SEM.

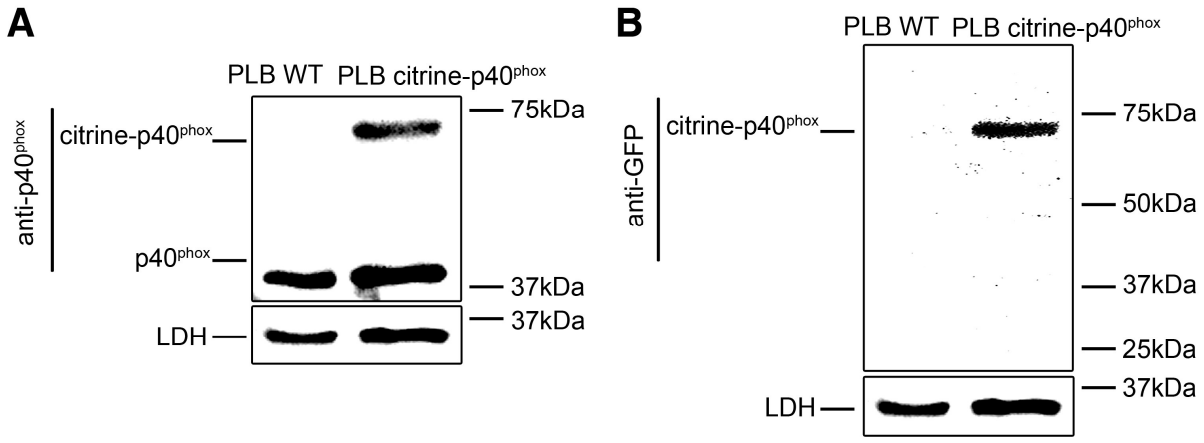

Figure 5. Generation of a stable PLB-citrine-p40^{phox} cell line.

(A, B) Western blot analysis of citrine-p40^{phox} and p40^{phox} in PLB-WT cells and PLB-citrine-p40^{phox} cells using an anti-p40^{phox} antibody (A) or an anti-GFP antibody (B). LDH was immunodetected with an anti-LDH antibody.

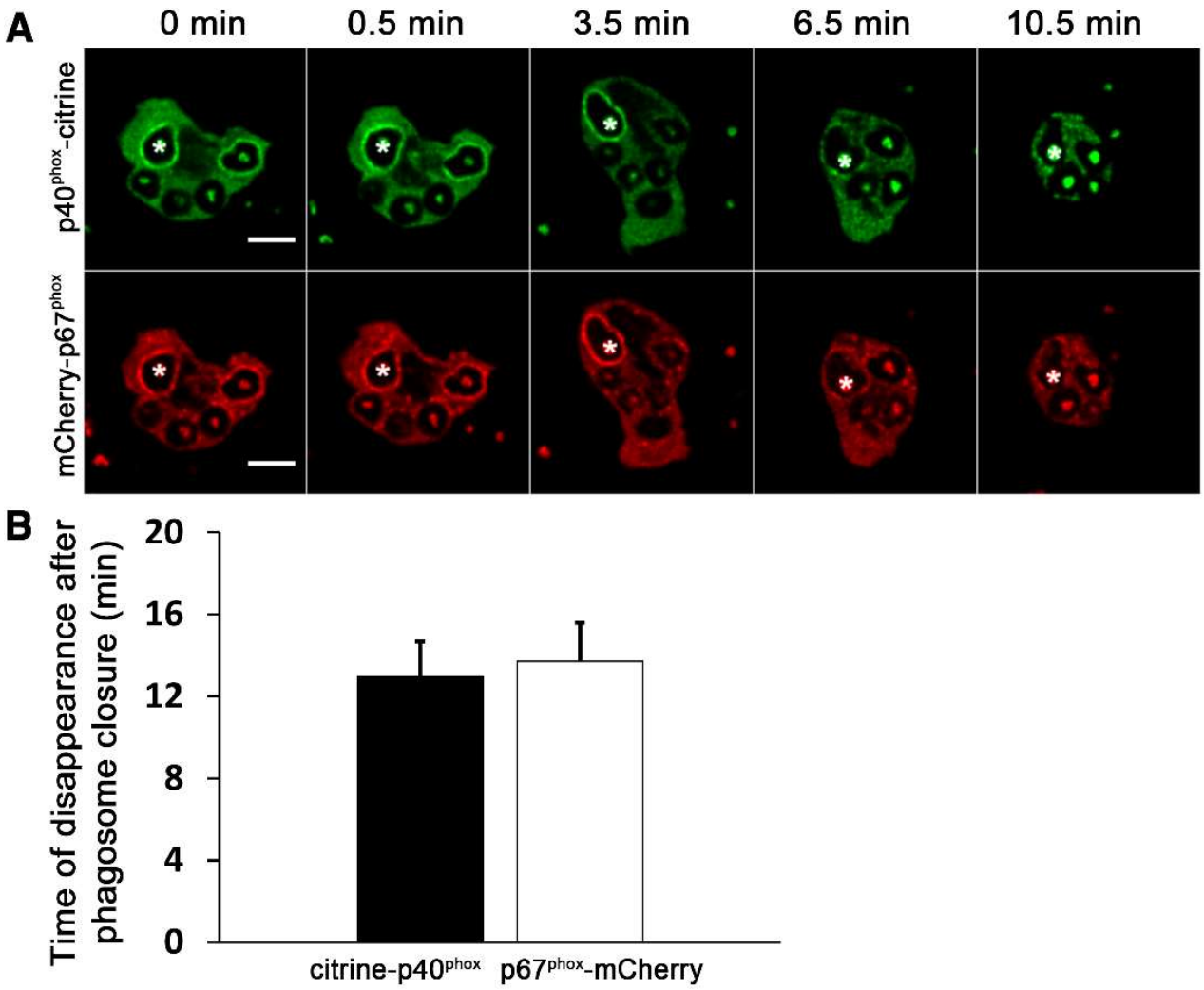

Figure 6. Accumulation of citrine-p40^{phox} and p67^{phox}-citrine at the phagosome.

(A) Representative images of zymosan (*) phagocytosis by transfected cells acquired by spinning disk confocal video microscopy. PLB-citrine-p40^{phox} cells were transfected with p40^{phox}siRNA, p67^{phox}siRNA and mCherry-p67^{phox}. Time 0 represents the closure of the phagosome. The images shown are one plane from a deconvoluted stack. For each of them, a modification of γ=0.85 was applied. Supplemental video 3 is related to the images shown. (B) Quantification of the time of disappearance of mCherry-p67^{phox} and citrine-p40^{phox} at the phagosome. Data are means ± SEM. *n=10.* Scale bar = 5 μm.

MTM1 and Rubicon negatively regulate the PI(3)P level at the phagosome

To further examine whether PI(3)P could regulate the accumulation of $p40^{phox}$ and $p67^{phox}$ as well as the ROS production during phagocytosis, we decided to modulate the PI(3)P level at the phagosome with genetic tools. To increase the PI(3)P level at the phagosome, we knocked down *MTM1* and *Rubicon*. MTM1-GFP is recruited to *Mycobacterium tuberculosis* phagosomes in RAW 264.7 cells [41]. Using immunofluorescence, we also detected MTM1 at the phagosome of PLB-985 cells after 7 min of incubation with opsonized Texas-Red Zymosan (**Fig. 7A and B**). To examine whether MTM1 participates in the regulation of PI(3)P at the phagosome, we knocked down *MTM1* by using siRNA. According to the immunoblotting results, the MTM1 protein level decreased to 38 ± 6.8 % with MTM1 targeted-siRNA as compared with control siRNA in PLB-WT cells (**Fig. 8A and B**). Imaging the PI(3)P probe YFP-$p40^{phox}$PX by confocal microscopy showed an increased and prolonged accumulation at the phagosome (**Fig. 9A and B**) in PLB-WT cells knocked down for *MTM1*. The time of disappearance (mean ± SEM) of YFP-$p40^{phox}$PX from the phagosome was 13.5 ± 1.0 min (**Fig. 9A**) with control siRNA and increased to 25.8 ± 2.6 min with MTM1 targeted-siRNA (**Fig. 9A and C**). These data indicate that MTM1 downregulates the phagosomal level of PI(3)P. Because Rubicon was reported to inhibit hVps34 [20], we wondered whether it regulated PI(3)P on serum opsonized phagosomes. Rubicon-EGFP was recruited to the phagosome of opsonized zymosan in PLB-985 cells (**Fig. 7C**) around 1min after phagosome closure and disappeared 12.4 ± 0.9 min after phagosome closure (**Fig. 7D**). We then knocked down *Rubicon* in PLB-985 cells. The Rubicon protein level was decreased to 49 ± 9.4 % with Rubicon targeted-siRNA in PLB-WT cells (**Fig. 8C and D**). As for *MTM1* knocked-down cells, an increased and prolonged accumulation (26.5 ± 2.5 min) of YFP-$p40^{phox}$PX was observed at the phagosome of PLB-WT cells deficient for Rubicon (Fig. 9). Decreasing both MTM1 and Rubicon increased the time of disappearance (mean ± SEM) of YFP-$p40^{phox}$PX

from the phagosome to 30.4 ± 3.6 min (**Fig. 9A and C** and Supplemental Video 4), which was not significantly longer than in single-knockdown cells. These data indicate that MTM1 and Rubicon increase and prolong PI(3)P accumulation at the phagosome.

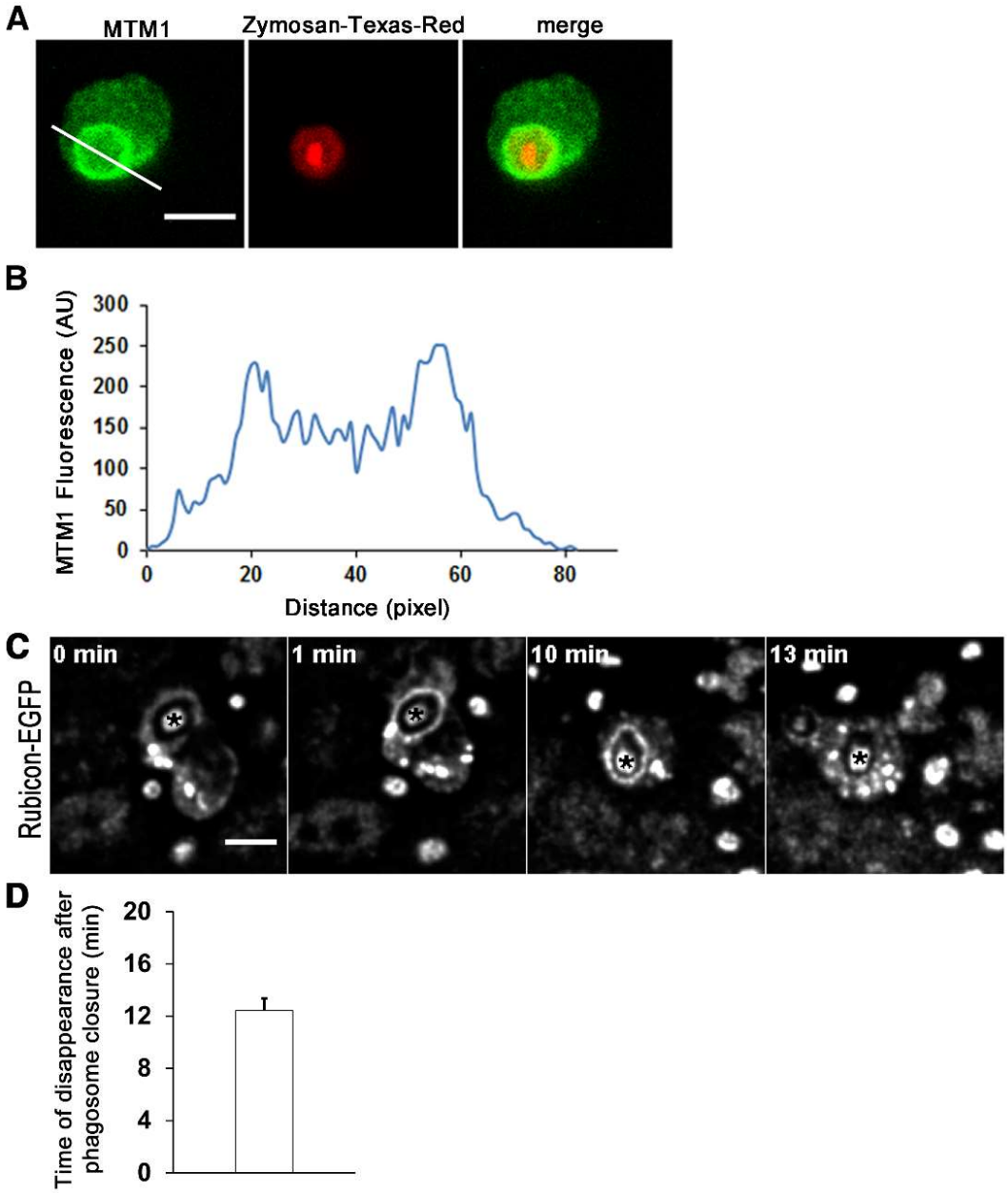

Figure 7. Recruitment of MTM1 and Rubicon during phagocytosis of opsonized zymosan.

(A) Immunofluorescence experiments were performed to detect MTM1 at 7 min after incubation of PLB-WT cells with opsonized zymosan-Texas-Red. (B) Quantification of the fluorescence intensity on the line shown in panel A of the MTM1 signals. (C) Representative images of zymosan (*) phagocytosis by PLB-WT cells transfected with Rubicon-EGFP. Images were acquired by spinning disk confocal video-microscopy. Time 0 represents the closure of the phagosome. The images shown are one plane from a deconvoluted stack. For each image, a modification of γ=0.75 was applied. (D) Quantification of the time of disappearance of Rubicon-EGFP at the phagosome. Data are mean ± SEM. *n=12.* Scale bars = 5 μm.

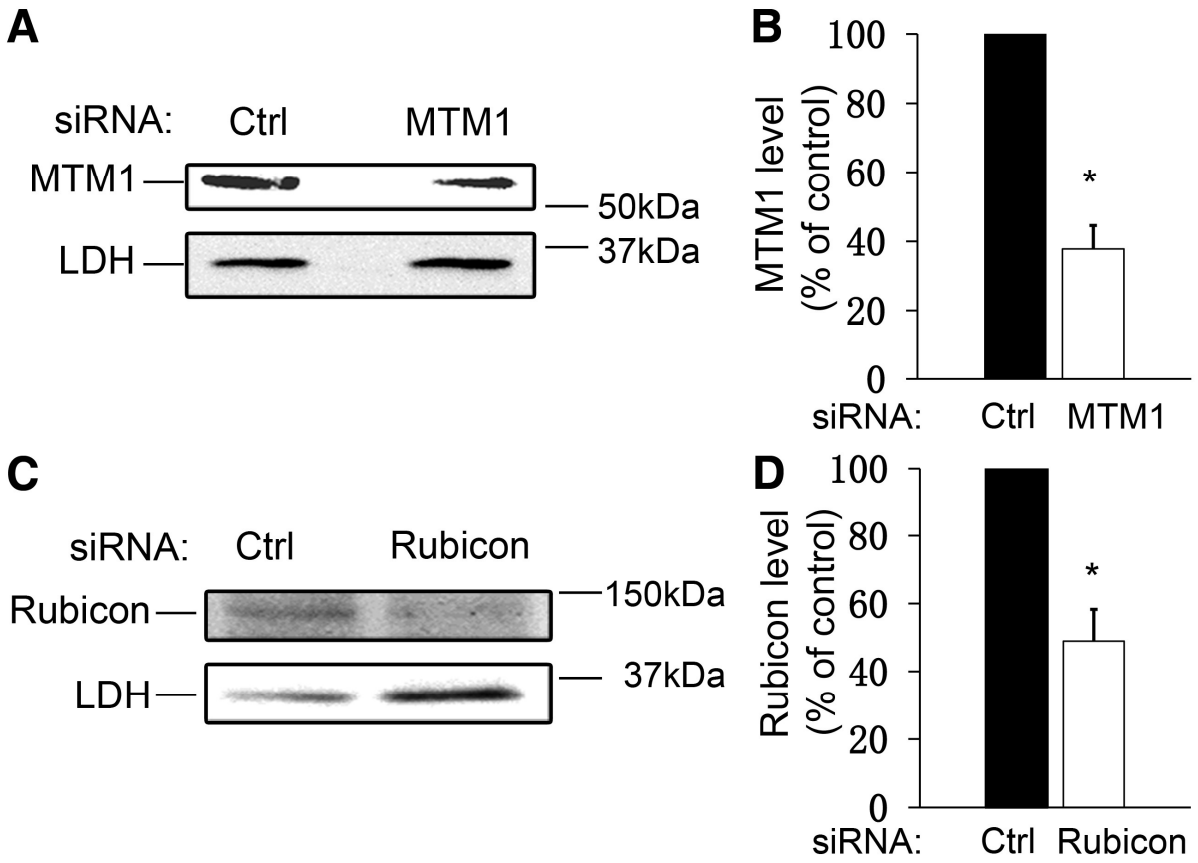

Figure 8. Knockdown of MTM1 and Rubicon in PLB cells.

(A) Western blot analysis of MTM1 and LDH in PLB-WT cells transfected with control siRNA or MTM1 siRNA. MTM1 was detected with anti-MTM1 antibody and LDH with anti-LDH antibody (B) Quantification of the MTM1 protein level. Data are mean ± SEM; *n=3*. **P* < 0.05 (Ratio paired *t* test). (C) Western blot analysis of Rubicon and LDH in PLB-WT cells transfected with control siRNA or Rubicon siRNA. Rubicon was detected with anti-Rubicon antibody. (D) Quantification of the Rubicon protein level. Data are mean ± SEM; *n=5*. **P* < 0.05 (Ratio paired *t* test).

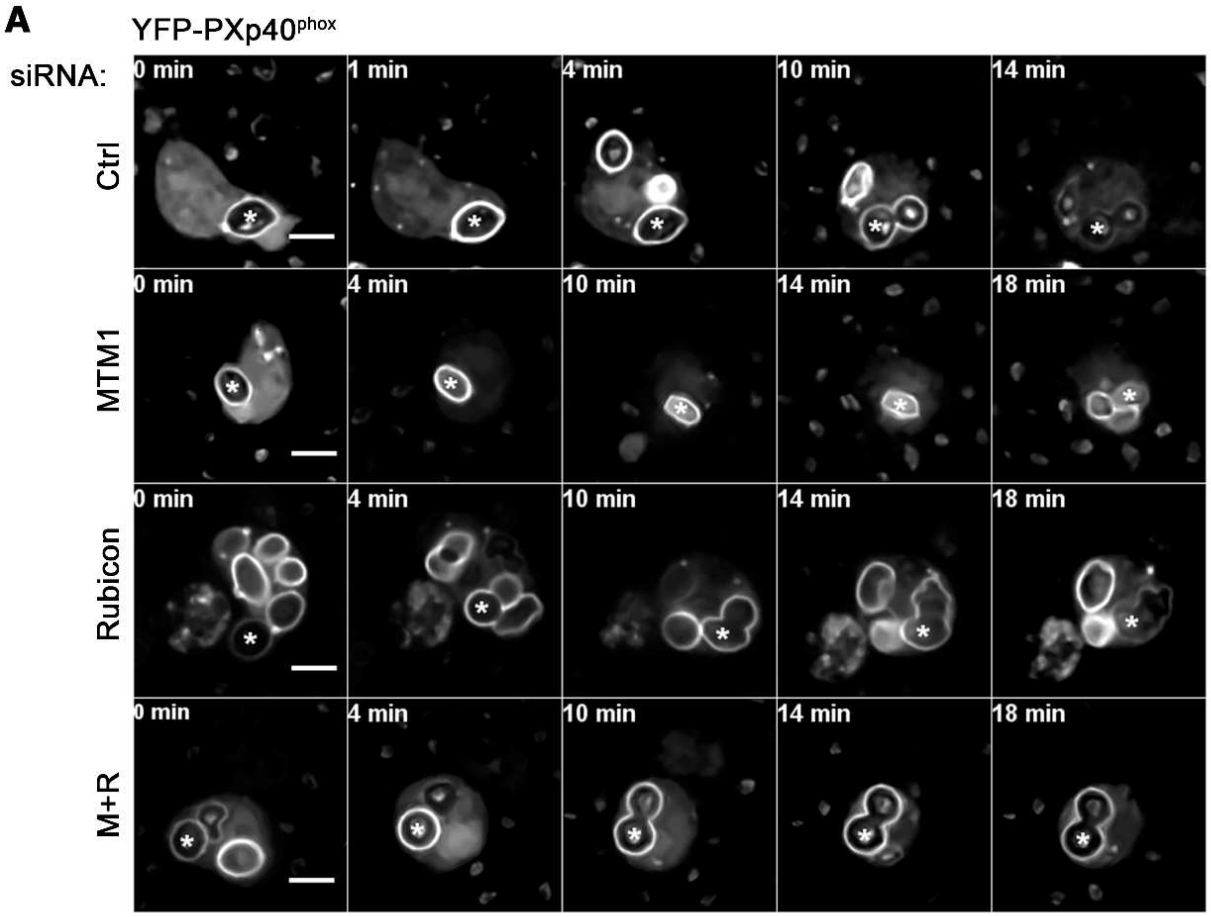
A
YFP-PXp40phox
siRNA:
Ctrl
MTM1
Rubicon
M+R
0 min
1 min
4 min
10 min
14 min
18 min

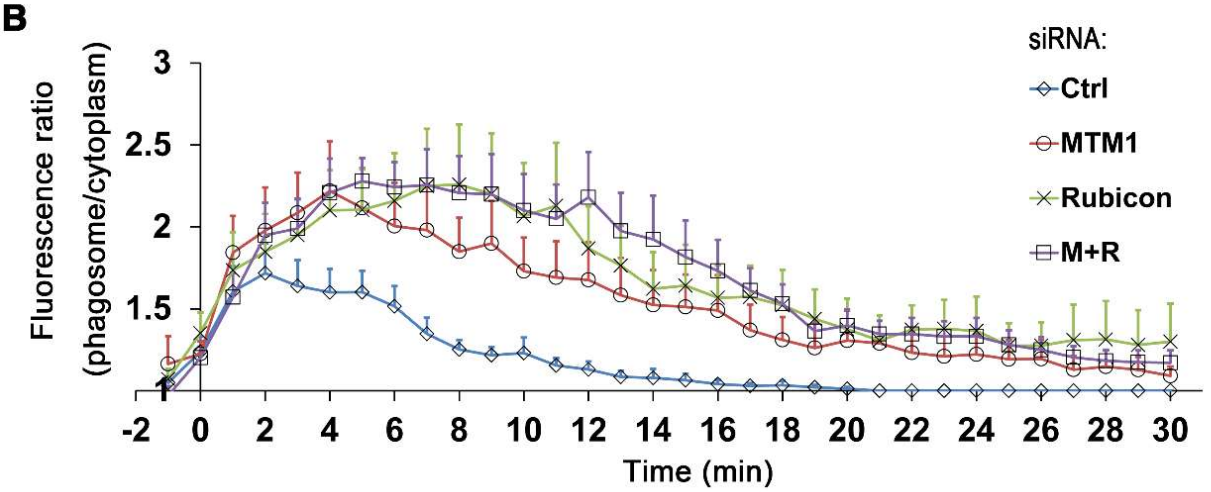
B
Fluorescence ratio
(phagosome/cytoplasm)
siRNA:
Ctrl
MTM1
Rubicon
M+R
Time (min)

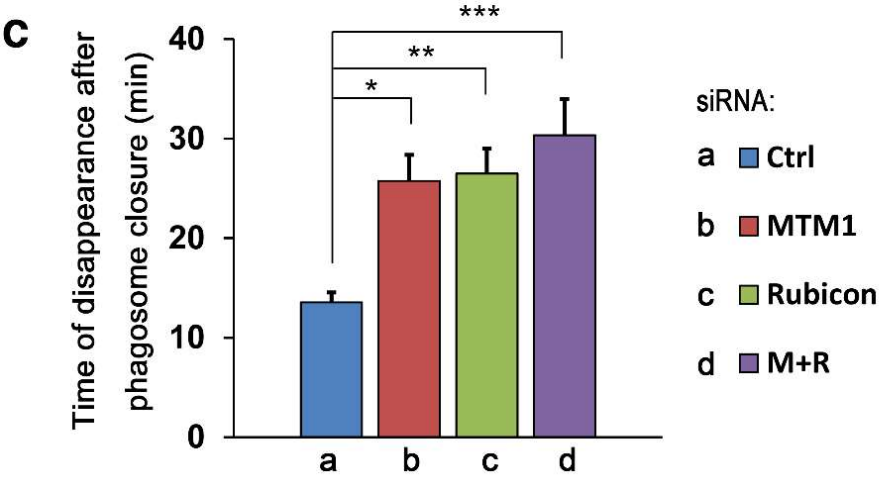
C
Time of disappearance after
phagosome closure (min)
siRNA:
a Ctrl
b MTM1
c Rubicon
d M+R

Figure 9. Knockdown of MTM1 and/or Rubicon increase the PI(3)P level at the phagosome.

(A) Representative images of zymosan (*) phagocytosis by transfected cells acquired by spinning disk confocal video-microscopy. PLB-WT cells were transfected with YFP-PXp40^{phox} and control siRNA, MTM1siRNA, Rubicon siRNA or M+R siRNA (MTM1 siRNA and Rubicon siRNA). After quantification, the images shown have were processed with ND-SAFIR software. The Supplemental videos 4 is related to the images shown. (B) Kinetics of the YFP-p40^{phox}PX accumulation at the phagosome. Data are mean ± SEM. (C) Quantification of the time of disappearance of YFP-p40^{phox}PX at the phagosome. Data are mean ± SEM. control siRNA, *n=11;* MTM1 siRNA, *n=12*; Rubicon siRNA, *n=17*; M+R siRNA, *n=14*. *** $P < 0.001$ (student's *t* test); Scale bar = 5 µm.

Up-regulation of PI(3)P increases ROS production and prolongs the time of presence of $p67^{phox}$ at the phagosome

To examine whether an increased and prolonged PI(3)P signal at the phagosome affects the NADPH oxidase activation, we measured the ROS production and phagocytosis inside the phagosome by flow cytometry. The PLB cells were transfected with control siRNA or Rubicon siRNA and/or MTM1 siRNA and were then incubated with $DCFH_2$-Alexa405-yeasts for 30 minutes. No difference in the percentage of phagocyting cells was detected (data not shown). The yeast DCF fluorescence ratio, as compared to control, increased by 16.5 ± 1.2 % for *MTM1* knockdown cells, 23.1 ± 3.0 % for *Rubicon* knockdown cells and 52.8 ± 4.0 % for *MTM1* plus *Rubicon* double knock-down cells (**Fig. 10A**). The increase in ROS production may be due to a greater accumulation of the assembled NADPH oxidase at the phagosome because of an increased or prolonged accumulation of $p40^{phox}$ and $p67^{phox}$. So we investigated $p67^{phox}$-citrine accumulation at the phagosome in PLB-$p67^{phox}$-citrine cells knocked down for endogenous $p67^{phox}$ gene and *MTM1* or *Rubicon*. We did not see any increase in the accumulation of $p67^{phox}$-citrine; however, its accumulation was significantly prolonged. In PLB $p67^{phox}$-citrine cells transfected with control siRNA, the mean time of disappearance of $p67^{phox}$-citrine was 11.2 ± 0.7 min. When *MTM1* or *Rubicon* was knocked down, the mean time of disappearance of $p67^{phox}$-citrine increased to 22.8 ± 2.6 min and 22.5 ± 2.3 min respectively (**Fig. 10B and C**). We also found a prolonged accumulation of citrine-$p40^{phox}$ at the phagosome in siRNA MTM1 cells as compared to siRNA control cells (data not shown). These data indicate that up-regulation of PI(3)P lengthens the time of presence of $p40^{phox}$ and $p67^{phox}$ at the phagosome during phagocytosis.

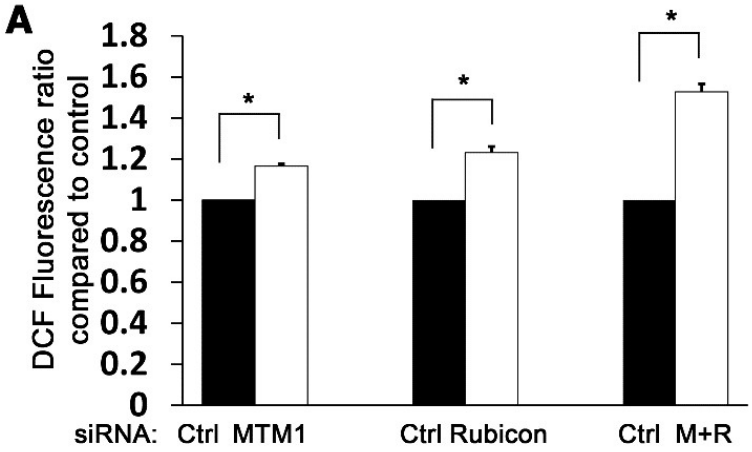
A
DCF Fluorescence ratio compared to control
1.8
1.6
1.4
1.2
1
0.8
0.6
0.4
0.2
0
*
*
*
siRNA: Ctrl MTM1
Ctrl Rubicon
Ctrl M+R

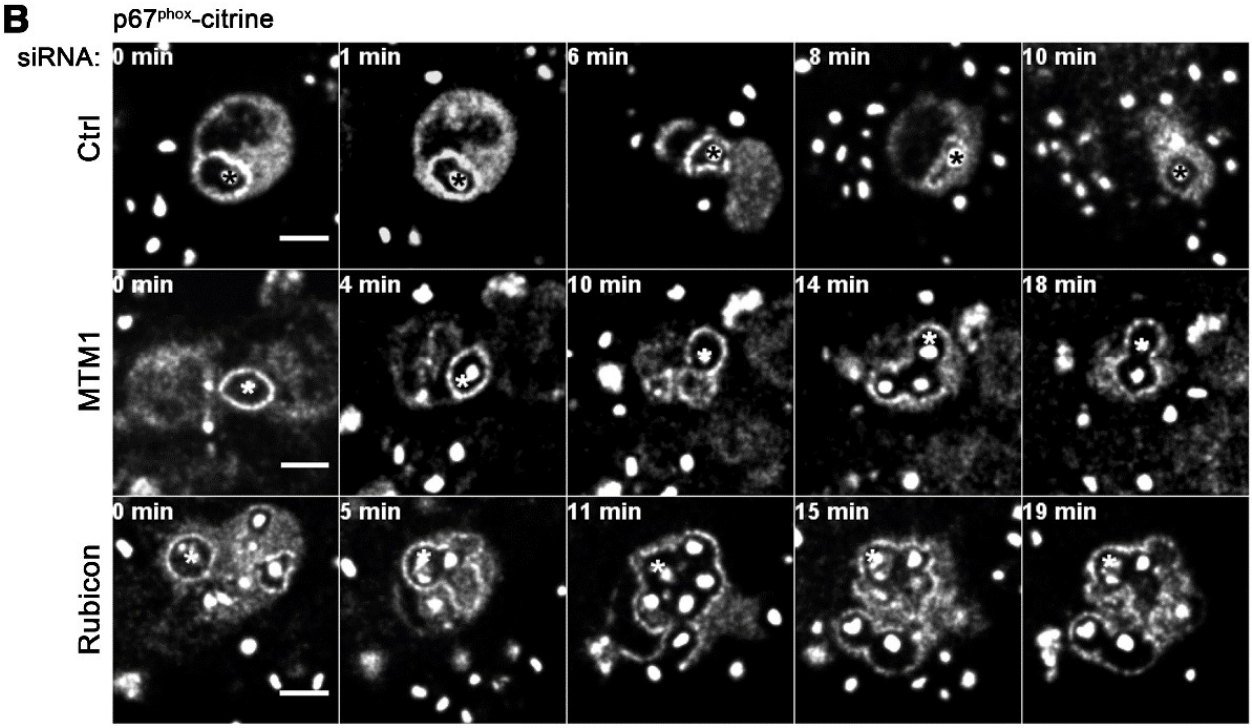
B
p67phox-citrine
siRNA:
Ctrl
0 min
1 min
6 min
8 min
10 min
MTM1
0 min
4 min
10 min
14 min
18 min
Rubicon
0 min
5 min
11 min
15 min
19 min

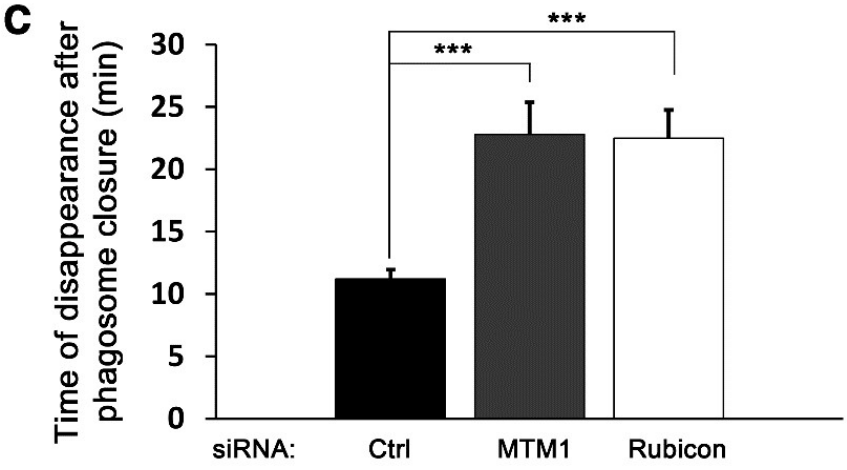
C
Time of disappearance after phagosome closure (min)
30
25
20
15
10
5
0
***
***
siRNA:
Ctrl
MTM1
Rubicon

Figure 10. Knockdown of MTM1 or/and Rubicon increases ROS production and extends the time of presence of p67^{phox} at the phagosome.

(A) ROS production and was assessed by flow cytometry by evaluating $DCFH_2$ and Alexa405-labeled yeast fluorescence in PLB-WT cells transfected with control siRNA, MTM1 siRNA, Rubicon siRNA, or M+R siRNA. Results are presented as the ratio of yeast-DCF fluorescence cells knockdown for MTM or/and Rubicon as compared with control cells. Data are mean ± SEM. (B) Representative images of zymosan (*) phagocytosis by transfected cells acquired by spinning disk confocal video microscopy. PLB-p67^{phox}-citrine cells were transfected with p67^{phox} siRNA and control siRNA or MTM1 siRNA or Rubicon siRNA. Time 0 represents the closure of the phagosome. The images shown are one plane from a deconvoluted stack. For each image, a modification of γ=0.85 was applied. (C) Quantification of the time of disappearance of p67^{phox}-citrine at the phagosome. Data are mean ± SEM. control siRNA, *n=10*; MTM1 siRNA, *n=10*; Rubicon siRNA, *n=11*; ****P*< 0.001 (student's t test). Scale bar = 5 μm.

Down-regulation of PI(3)P prevents ROS production and the accumulation of p67^{phox} at the phagosome

To confirm that PI(3)P could regulate NADPH oxidase activation at the phagosome during phagocytosis, we down-regulated PI(3)P at the phagosomal membrane by overexpressing MTM1. We used a rapamycin-mediated heterodimerization system in PLB-985 cells. Two components are expressed in this system, Lyn11-targeted FKBP rapamycin binding domain (LDR) and mCherry-FK506 binding protein (FKBP)-MTM1 [29, 30]. LDR localized at the plasma membrane because of the N terminus of Lyn. We used mCherry-FKBP as a control. MCherry-FKBP or mCherry-FKBP-MTM1 are distributed in the cytoplasm and cannot be detected on the plasma membrane without adding rapamycin. Addition of 0.25 µg/ml of rapamycin, triggers mCherry-FKBP or mCherry-FKBP-MTM1 recruitment at the plasma membrane in two minutes (data not shown). Then we added opsonized zymosan and examined the recruitment of the PI(3)P probe YFP-p40^{phox}PX to the phagosome. The recruitment of YFP-p40^{phox}PX was not affected by the presence of mCherry-FKBP at the phagosome (**Fig. 11A** and Supplemental Video 5) as indicated by the YFP-p40^{phox}PX fluorescence ratio of phagosome to cytoplasm above 1 at 1, 2 and 6 minutes after phagosome closure (Fig. 11C). In the LDR/mCherry-FKBP-MTM1 transfected cells, no accumulation of YFP-p40^{phox}PX at the phagosome could be detected (**Fig. 11B and C** and Supplemental Video 6; fluorescence ratio<1). Thus, overexpression of MTM1 targeted at the phagosome prevents the PI(3)P accumulation. We next performed video microscopy experiments using $DCFH_2$-zymosan to find out whether down-regulation of PI(3)P affects the ROS production inside the phagosome. We followed the increase in $DCFH_2$ fluorescence from oxidation by ROS over time. In mCherry-FKBP phagosomes, the DCF fluorescence increased and reached a plateau 400 s after phagosome closure, as previously observed (**Fig. 12A**). This plateau is due to a lack of probe on the zymosan, which are smaller than yeast [34]. However, inside the

mCherry-FKBP-MTM1 phagosomes, there was almost no increase in zymosan-DCF fluorescence 700s after phagosome closure (**Fig. 12A**). We further investigated whether decreasing the PI(3)P level at the phagosome affected $p67^{phox}$ recruitment. Indeed, the percentage of mCherry-FKBP phagosomes that were also positive for $p67^{phox}$-citrine was 47.3 ± 2.0 % at five minutes after addition of serum opsonized zymosan. Whereas the percentage of $p67^{phox}$-citrine positive phagosomes dropped to 1.6 ± 0.8 % when mCherry-FKBP-MTM1 was present at the phagosomal membrane (**Fig. 12B and C**). Our data suggest that down-regulation of PI(3)P at the phagosome prevents a sustained ROS production because of the loss of $p67^{phox}$ at the phagosome.

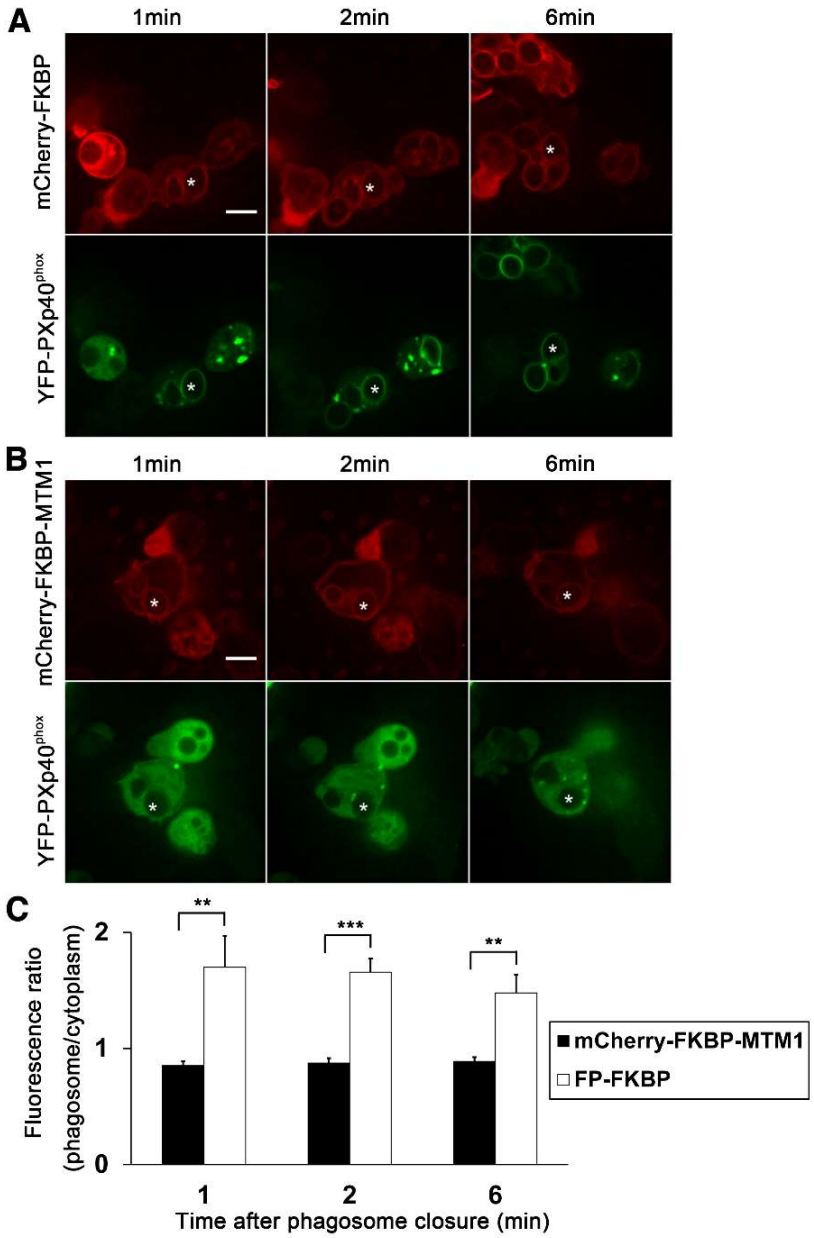

Figure 11. MTM1 overexpression at the phagosomal membrane prevents YFP-p40^{phox}PX recruitment.

(A and B) Representative images of zymosan (*) phagocytosis by transfected cells, at time 1, 2 and 6 min after phagosome closure, acquired by spinning disk confocal video microscopy. PLB-WT cells were transfected with LDR, mCherry-FKBP (A) or mCherry-FKBP-MTM1 (B) and YFP-PXp40^{phox}. After quantification, the images shown were processed with ND-SAFIR software. The Supplemental videos 5 and 6 are related to the images shown. (C) Quantification of the accumulation of YFP-p40^{phox}PX at the phagosome in cells transfected with mCherry-FKBP-MTM1 (*n=12*) or YFP-FKBP / mCherry-FKBP (*n=12*) at times 1, 2 and 6 min after phagosome closure. Data are mean ± SEM. ***P*< 0.01, ****P*< 0.001 (student's *t* test). Scale bars = 5 µm.

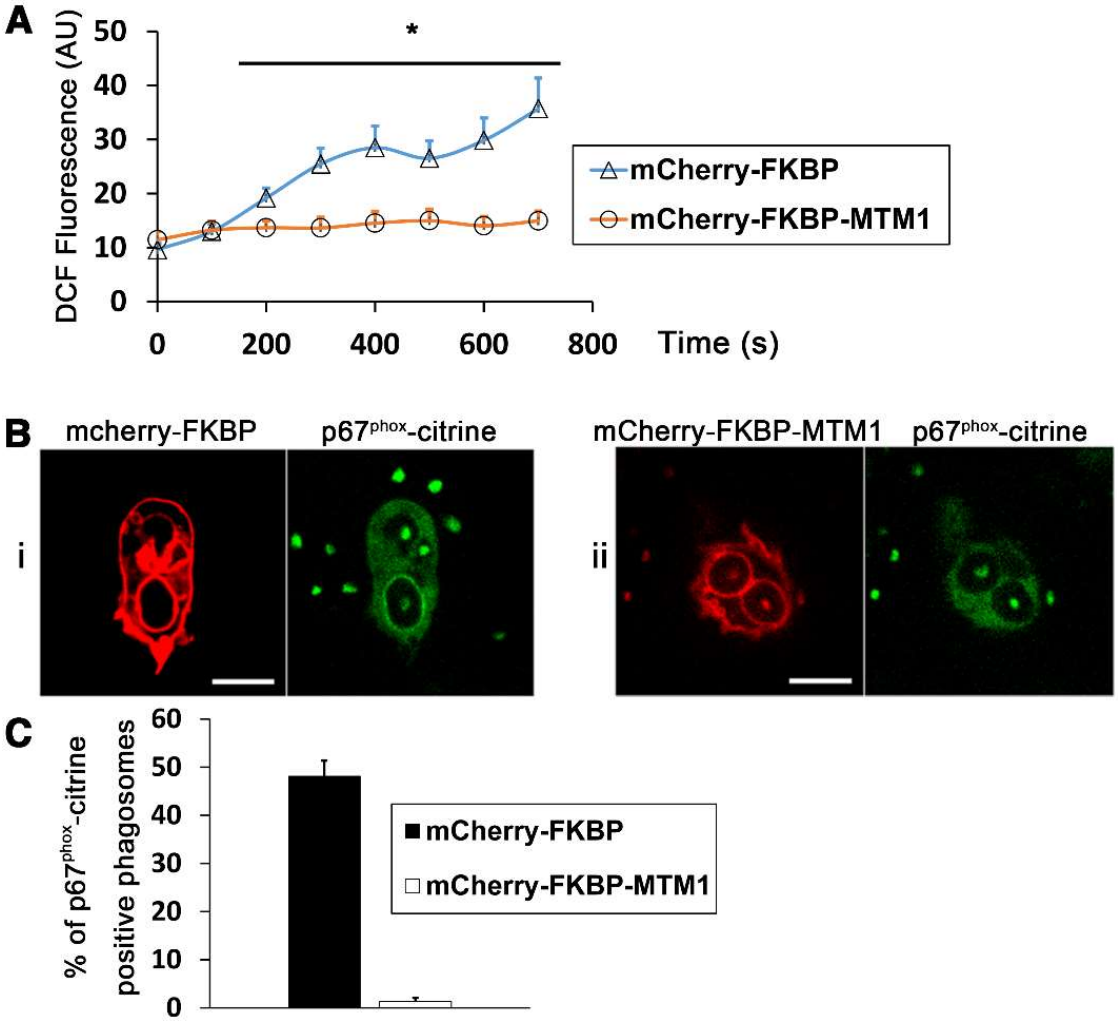

Figure 12. MTM1 overexpression at the phagosomal membrane prevents ROS production and the accumulation of p67^{phox}

(A) The kinetics of ROS production was assessed by video microscopy by quantifying $DCFH_2$-labelled zymosan fluorescence in PLB-WT cells transfected with LDR and mCherry-FKBP (*n=13*) or mCherry-FKBP-MTM1 (*n=11*). Time 0 represents the closure of the phagosome. Data are mean ± SEM. *P< 0.05 (student's t test). (B) PLB p67^{phox}-citrine cells were transfected with LDR, p67^{phox}siRNA and mCherry-FKBP (i) or mCherry-FKBP-MTM1 (ii) and were incubated with opsonized zymosan. Images were taken by spinning disk confocal microscopy after 5 min incubation. (C) Quantification of percentage of p67^{phox}-citrine positive phagosomes at 5 min after the addition of zymosan. Data are mean ± SEM of at least three independent experiments.

Discussion

We have shown here that the regulation of PI(3)P modulates ROS production by controlling the extent of $p67^{phox}$ accumulation at the phagosome. Changes in phagosomal PI(3)P lead to corresponding changes of $p40^{phox}$ and $p67^{phox}$ on the phagosome, which appear to be responsible for the altered ROS production. We used pharmacological tools as well as the expression and targeting of phosphoinositide modulating proteins to address this highly dynamic interaction.

We first observed a decrease in ROS production, in differentiated PLB cells and human neutrophils of ~40% with a recently reported inhibitor of class III PI3K hVps34 [37]. We still observed a slight and transient accumulation of the PI(3)P probe mCherry-PX$p40^{phox}$ at the phagosome, thus some PI(3)P was still generated. This PI(3)P could be generated by Class II PI3K. Although the presence of any of the three isoforms at the phagosome of mammalian cells has not been investigated, the Class II PI3K generates PI(3)P in *Coenorhabditis elegans* phagosomes [16]. Moreover, PI(3)P could be produced upon dephosphorylation of $PI(3,4)P_2$ or $PI(3,4,5)P_3$. These lipids accumulate at the phagosomal cup and soon disappear after sealing [42, 43] (Fig. 1A). SHIP-1 is involved in dephosphorylation of $PI(3,4,5)P_3$ to $PI(3,4)P_2$ [44, 45]. The dephosphorylation of $PI(3,4)P_2$ to PI(3)P is also made by the type I inositol-3,4-bisphosphate4-phosphatase [46, 47]. In RAW 264.7 macrophages, the generation of ROS is also dependent on the level of diacylglycerol [48]. In phagosomes lacking PI(3)P, ROS production may start, but it is not sustained.

The PI3K-inhibitor wortmannin terminates PI(3)P synthesis when added after phagosome sealing, as previously described [40]. We show that this PI(3)P decreases ROS production by inducing the release of citrine-$p40^{phox}$ and $p67^{phox}$-citrine from the phagosome, which is consistent with previous data showing that the PX domain of $p40^{phox}$ binds PI(3)P and stabilizes $p40^{phox}$ at the phagosome [11-13]. Our data indicate that PI(3)P is necessary to

maintain $p67^{phox}$ at the phagosomal membrane, allowing sustained ROS production. Thus $p40^{phox}$ and $p67^{phox}$ are not only recruited together at the phagosome (with $p47^{phox}$) [12] but also leave the phagosome at the same time (**Fig. 6**). This strongly suggests that $p40^{phox}$ is a late adaptor for $p67^{phox}$, although we cannot rule out that another protein that binds PI(3)P, stabilizes $p67^{phox}$ at the phagosome.

To test whether an increased level of PI(3)P at the phagosome would enhance the NADPH oxidase, we decreased the level of the PI3-phosphatase MTM1 and/or the regulatory protein Rubicon. Both proteins are present at the phagosome of serum opsonized zymosan in PLB cells. Our data indicate that they both contribute to the downregulation of PI(3)P at the phagosome. Rubicon binds the protein UVRAG (ultraviolet radiation resistance-associated gene protein) and hVps34 [21, 22]. Rubicon has been shown to antagonize UVRAG activation of hVps34, *in vitro* [20]. On endosomal membranes, the Class III PI3K core complex (hVsp34, hVps15 and Beclin1) can be associated with UVRAG alone or Rubicon and UVRAG [22]. In the Rubicon-UVRAG-Class III PI3K complex, Rubicon downregulates hVps34 activation [21]. This may be also the case at the phagosome. In contrast, upon phagocytosis of non-opsonized zymosan, which stimulates the Toll-like receptor 2 pathway, Rubicon interacts with $p22^{phox}$ and is required for hVps34 activity [24, 25]. The Rubicon-$p22^{phox}$ interaction was not observed upon phagocytosis with IgG-zymosan [25]. This opposite role of Rubicon may be explained by competing interactions of Rubicon. Interaction of Rubicon with UVRAG may prevent the binding of $p22^{phox}$. Indeed, UVRAG binds to a large region of the Rubicon protein, involving amino acids 300-972, that overlaps with the SR domain (serine rich domain aa 558-625) responsible for $p22^{phox}$ binding [20, 25]. Thus we hypothesize that if Rubicon binds $p22^{phox}$, then UVRAG can activate hVps34. Whereas if Rubicon interacts with UVRAG, it prevents hVps34 activation. Upon phagocytosis of serum-opsonized zymosan, the second scenario is supported by our data. Indeed, when we knocked

down Rubicon, we observed an extended PI(3)P accumulation at the phagosome of opsonized zymosan. Which factors determine the binding of Rubicon to $p22^{phox}$ versus UVRAG still need to be investigated. According to Yang *et al*. different signaling pathways modulate Rubicon interactions [25, 49].

The double knockdown of *MTM1* and *Rubicon* did not significantly increase PI(3)P at the phagosome as compared to single knockdown. PI(3)P is phosphorylated to $PI(3,5)P_2$ by PIKfyve (FYVE finger-containing phosphoinositide kinase), and this probably starts a few minutes after phagosome closure [50]. Thus when PI(3)P increases at the phagosome, more $PI(3,5)P_2$ is generated, limiting PI(3)P accumulation. Moreover, other phosphatases belonging to the myotubularin family may participate in the dephosphorylation of PI(3)P.

Upregulation of PI(3)P at the phagosome by knocking down *MTM1* and/or *Rubicon*, increases ROS production and the time until the disappearance of $p67^{phox}$ at the phagosome. Furthermore, overexpression of MTM1 at the phagosome prevents a sustained ROS production and the accumulation of $p67^{phox}$ at the phagosome, demonstrating that PI(3)P has a key role in maintaining the ROS production during phagocytosis.

Previous work has demonstrated that Rac2 and the cytosolic NADPH oxidase subunits $p47^{phox}$, $p67^{phox}$ and $p40^{phox}$ are recruited at the same time at the phagosomal cup just before phagosome sealing [12, 26]. Rac2 and $p47^{phox}$ detach a few minutes after phagosome closure [26] whereas $p67^{phox}$ stays until the end of ROS production [27]. We can now complete the model: PI(3)P regulates the presence of $p40^{phox}$ at the NADPH oxidase complex. $P40^{phox}$ works as an adaptor to maintain the $p67^{phox}$ at the complex sustaining the ROS production. When PI(3)P declines, $p40^{phox}$ and $p67^{phox}$ detach from the membrane at the same time, and the ROS production ends. Of course, additional factors may influence $p40^{phox}$ and $p67^{phox}$ detachment from the phagosome.

PI(3)P is also a target for pathogens like *Mycobacterium tuberculosis* [51]. *M. tuberculosis*

secretes the toxin lipoarabinomannan to inhibit the activation of phagosomal hVps34 and the lipid phosphatase SapM to dephosphorylate PI(3)P. The decrease in phagosomal PI(3)P contributes to arresting phagosomal maturation [41, 52]. Another bacterial pathogen *Legionella pneumophila,* is reported to encode the phosphatase SidP, which hydrolyzes PI(3)P and PI(3,5)P_2 *in vitro* [53]. A study in *Dictyostelium discoideum* showed that PI(3)P is lost from *L. pneumophila* phagosomes, preventing fusion with the endocytic pathway and allowing the formation of *legionella*-containing vacuoles [54]. Controlling the host PI(3)P level at the phagosome is, thus, a common survival strategy for these two pathogens. In both cases, it would be interesting to determine whether the decrease in PI(3)P contributes to a decrease ROS production.

In conclusion, our data provide a possible explanation how PI(3)P could act as a timer for ROS production in the phagosome: stabilization of $p40^{phox}$ at the phagosomal membrane is regulated by the availability of PI(3)P. $P40^{phox}$ functions as an adaptor for $p67^{phox}$, which is indispensable for ROS production.

Authorship

Z.M.S. and S.D.-C. designed, performed and analyzed the experiments. L.B. and E.H. performed experiments. R.L.B. contributed to the imaging experiments. O.N. contributed to the design of the experiments and the writing of the paper. S.D.-C. designed the study and wrote the paper, with the help of Z.M.S.

Acknowledgements

Z.M.S. is the recipient of a fellowship from the Chinese Scholarship Council. L.B. is a recipient of a doctoral grant from Region Île-de -France (DIM Malinf). This work was partly funded by the French program "Investissement d'avenir" run by the "Agence Nationale pour la Recherche"; the grant reference 'Infrastructure d'avenir en Biologie Santé-ANR-11INBS-0006'. This work was also supported by a FRM grant (Fondation for medical research, DCM20121225747). cDNA for human $p40^{phox}$ was a kind gift from Marie-Claire Dagher. We thank My-Chan Dang and Jamel El Benna for providing us human neutrophils. This work has benefited from the facilities and expertise of the I2BC platforms of photonic microscopy and cytometry as well as the flow cytometry facility SpICy. We thank Michael Bourge and Laetitia Besse for their help on these platforms. We also thank Marie Noelle Soler, Isabelle Garcin, Marie Erard and Sylvie Prigent for their help.

Conflict of Interest Disclosure

The authors declare no conflict of interest.

References

1. Mayadas, T. N., Cullere, X., Lowell, C. A. (2014) The multifaceted functions of neutrophils. *Annu. Rev. Pathol.* **9**, 181-218.
2. Kuijpers, T. and Lutter, R. (2012) Inflammation and repeated infections in CGD: two sides of a coin. *Cell. Mol. Life Sci.* **69**, 7-15.
3. Groemping, Y. and Rittinger, K. (2005) Activation and assembly of the NADPH oxidase: a structural perspective. *Biochem. J.* **386**, 401-416.
4. Quinn, M. T., Evans, T., Loetterle, L. R., Jesaitis, A. J., Bokoch, G. M. (1993) Translocation of Rac correlates with NADPH oxidase activation. Evidence for equimolar translocation of oxidase components. *J. Biol. Chem.* **268**, 20983-20987.
5. Cachat, J., Deffert, C., Hugues, S., Krause, K. H. (2015) Phagocyte NADPH oxidase and specific immunity. *Clin. Sci. (Lond.)* **128**, 635-648.
6. Nisimoto, Y., Motalebi, S., Han, C. H., Lambeth, J. D. (1999) The p67(phox) activation domain regulates electron flow from NADPH to flavin in flavocytochrome b(558). *J. Biol. Chem.* **274**, 22999-23005.
7. Bravo, J., Karathanassis, D., Pacold, C. M., Pacold, M. E., Ellson, C. D., Anderson, K. E., Butler, P. J., Lavenir, I., Perisic, O., Hawkins, P. T., Stephens, L., Williams, R. L. (2001) The crystal structure of the PX domain from p40(phox) bound to phosphatidylinositol 3-phosphate. *Mol. Cell* **8**, 829-839.
8. Ellson, C., Davidson, K., Anderson, K., Stephens, L. R., Hawkins, P. T. (2006) PtdIns3P binding to the PX domain of p40phox is a physiological signal in NADPH oxidase activation. *EMBO J.* **25**, 4468-4478.
9. Ellson, C. D., Gobert-Gosse, S., Anderson, K. E., Davidson, K., Erdjument-Bromage, H., Tempst, P., Thuring, J. W., Cooper, M. A., Lim, Z. Y., Holmes, A. B., Gaffney, P. R., Coadwell, J., Chilvers, E. R., Hawkins, P. T., Stephens, L. R. (2001) PtdIns(3)P regulates the neutrophil oxidase complex by binding to the PX domain of p40(phox). *Nat. Cell Biol.* **3**, 679-682.
10. Ellson, C. D., Davidson, K., Ferguson, G. J., O'Connor, R., Stephens, L. R., Hawkins, P. T. (2006) Neutrophils from p40phox-/- mice exhibit severe defects in NADPH oxidase regulation and oxidant-dependent bacterial killing. *J. Exp. Med.* **203**, 1927-1937.
11. Matute, J. D., Arias, A. A., Wright, N. A., Wrobel, I., Waterhouse, C. C., Li, X. J., Marchal, C. C., Stull, N. D., Lewis, D. B., Steele, M., Kellner, J. D., Yu, W., Meroueh, S. O., Nauseef, W. M., Dinauer, M. C.

(2009) A new genetic subgroup of chronic granulomatous disease with autosomal recessive mutations in p40 phox and selective defects in neutrophil NADPH oxidase activity. *Blood* **114**, 3309-3315.

12. Tian, W., Li, X. J., Stull, N. D., Ming, W., Suh, C. I., Bissonnette, S. A., Yaffe, M. B., Grinstein, S., Atkinson, S. J., Dinauer, M. C. (2008) Fc R-stimulated activation of the NADPH oxidase: phosphoinositide-binding protein p40phox regulates NADPH oxidase activity after enzyme assembly on the phagosome. *Blood* **112**, 3867-3877.
13. Anderson, K. E., Chessa, T. A., Davidson, K., Henderson, R. B., Walker, S., Tolmachova, T., Grys, K., Rausch, O., Seabra, M. C., Tybulewicz, V. L., Stephens, L. R., Hawkins, P. T. (2010) PtdIns3P and Rac direct the assembly of the NADPH oxidase on a novel, pre-phagosomal compartment during FcR-mediated phagocytosis in primary mouse neutrophils. *Blood* **116**, 4978-4989.
14. Anderson, K. E., Boyle, K. B., Davidson, K., Chessa, T. A., Kulkarni, S., Jarvis, G. E., Sindrilaru, A., Scharffetter-Kochanek, K., Rausch, O., Stephens, L. R., Hawkins, P. T. (2008) CD18-dependent activation of the neutrophil NADPH oxidase during phagocytosis of Escherichia coli or Staphylococcus aureus is regulated by class III but not class I or II PI3Ks. *Blood* **112**, 5202-5211.
15. Vieira, O. V., Botelho, R. J., Rameh, L., Brachmann, S. M., Matsuo, T., Davidson, H. W., Schreiber, A., Backer, J. M., Cantley, L. C., Grinstein, S. (2001) Distinct roles of class I and class III phosphatidylinositol 3-kinases in phagosome formation and maturation. *J. Cell Biol.* **155**, 19-25.
16. Lu, N., Shen, Q., Mahoney, T. R., Neukomm, L. J., Wang, Y., Zhou, Z. (2012) Two PI 3-kinases and one PI 3-phosphatase together establish the cyclic waves of phagosomal PtdIns(3)P critical for the degradation of apoptotic cells. *PLoS Biol.* **10**, e1001245.
17. Amoasii, L., Hnia, K., Chicanne, G., Brech, A., Cowling, B. S., Muller, M. M., Schwab, Y., Koebel, P., Ferry, A., Payrastre, B., Laporte, J. (2013) Myotubularin and PtdIns3P remodel the sarcoplasmic reticulum in muscle in vivo. *J. Cell Sci.* **126**, 1806-1819.
18. Cao, C., Backer, J. M., Laporte, J., Bedrick, E. J., Wandinger-Ness, A. (2008) Sequential actions of myotubularin lipid phosphatases regulate endosomal PI(3)P and growth factor receptor trafficking. *Mol. Biol. Cell* **19**, 3334-3346.
19. Cao, C., Laporte, J., Backer, J. M., Wandinger-Ness, A., Stein, M. P. (2007) Myotubularin lipid phosphatase binds the hVPS15/hVPS34 lipid kinase complex on endosomes. *Traffic* **8**, 1052-1067.
20. Sun, Q., Zhang, J., Fan, W., Wong, K. N., Ding, X., Chen, S., Zhong, Q. (2011) The RUN domain of rubicon is important for hVps34 binding, lipid kinase inhibition, and autophagy suppression. *J. Biol.*

Chem. **286**, 185-191.

21. Zhong, Y., Wang, Q. J., Li, X., Yan, Y., Backer, J. M., Chait, B. T., Heintz, N., Yue, Z. (2009) Distinct regulation of autophagic activity by Atg14L and Rubicon associated with Beclin 1-phosphatidylinositol-3-kinase complex. *Nat. Cell Biol.* **11**, 468-476.
22. Matsunaga, K., Saitoh, T., Tabata, K., Omori, H., Satoh, T., Kurotori, N., Maejima, I., Shirahama-Noda, K., Ichimura, T., Isobe, T., Akira, S., Noda, T., Yoshimori, T. (2009) Two Beclin 1-binding proteins, Atg14L and Rubicon, reciprocally regulate autophagy at different stages. *Nat. Cell Biol.* **11**, 385-396.
23. Sun, Q., Westphal, W., Wong, K. N., Tan, I., Zhong, Q. (2010) Rubicon controls endosome maturation as a Rab7 effector. *Proc. Natl. Acad. Sci. U. S. A.* **107**, 19338-19343.
24. Martinez, J., Malireddi, R. K., Lu, Q., Cunha, L. D., Pelletier, S., Gingras, S., Orchard, R., Guan, J. L., Tan, H., Peng, J., Kanneganti, T. D., Virgin, H. W., Green, D. R. (2015) Molecular characterization of LC3-associated phagocytosis reveals distinct roles for Rubicon, NOX2 and autophagy proteins. *Nat. Cell Biol.* **17**, 893-906.
25. Yang, C. S., Lee, J. S., Rodgers, M., Min, C. K., Lee, J. Y., Kim, H. J., Lee, K. H., Kim, C. J., Oh, B., Zandi, E., Yue, Z., Kramnik, I., Liang, C., Jung, J. U. (2012) Autophagy protein Rubicon mediates phagocytic NADPH oxidase activation in response to microbial infection or TLR stimulation. *Cell Host Microbe* **11**, 264-276.
26. Faure, M. C., Sulpice, J. C., Delattre, M., Lavielle, M., Prigent, M., Cuif, M. H., Melchior, C., Tschirhart, E., Nusse, O., Dupre-Crochet, S. (2013) The recruitment of p47(phox) and Rac2G12V at the phagosome is transient and phosphatidylserine dependent. *Biol. Cell.* **105**, 501-518.
27. Tlili, A., Erard, M., Faure, M. C., Baudin, X., Piolot, T., Dupre-Crochet, S., Nusse, O. (2012) Stable accumulation of p67phox at the phagosomal membrane and ROS production within the phagosome. *J. Leukoc. Biol.* **91**, 83-95.
28. Benna, J. E., Dang, P. M., Gaudry, M., Fay, M., Morel, F., Hakim, J., Gougerot-Pocidalo, M. A. (1997) Phosphorylation of the respiratory burst oxidase subunit p67(phox) during human neutrophil activation. Regulation by protein kinase C-dependent and independent pathways. *J. Biol. Chem.* **272**, 17204-17208.
29. Inoue, T., Heo, W. D., Grimley, J. S., Wandless, T. J., Meyer, T. (2005) An inducible translocation strategy to rapidly activate and inhibit small GTPase signaling pathways. *Nat Methods* **2**, 415-418.
30. Hammond, G. R., Machner, M. P., Balla, T. (2014) A novel probe for phosphatidylinositol 4-phosphate

reveals multiple pools beyond the Golgi. *J. Cell Biol.* **205**, 113-126.

31. Kanai, F., Liu, H., Field, S. J., Akbary, H., Matsuo, T., Brown, G. E., Cantley, L. C., Yaffe, M. B. (2001) The PX domains of p47phox and p40phox bind to lipid products of PI(3)K. *Nat. Cell Biol.* **3**, 675-678.
32. Varnai, P. and Balla, T. (1998) Visualization of phosphoinositides that bind pleckstrin homology domains: calcium- and agonist-induced dynamic changes and relationship to myo-[3H]inositol-labeled phosphoinositide pools. *J. Cell Biol.* **143**, 501-510.
33. Tlili, A., Dupre-Crochet, S., Erard, M., Nusse, O. (2011) Kinetic analysis of phagosomal production of reactive oxygen species. *Free Radic. Biol. Med.* **50**, 438-447.
34. Nault, L., Bouchab, L., Dupre-Crochet, S., Nusse, O., Erard, M. (2016) Environmental Effects on Reactive Oxygen Species Detection-Learning from the Phagosome. *Antioxid Redox Signal* **25**, 564-576.
35. Boulanger, J., Kervrann, C., Bouthemy, P., Elbau, P., Sibarita, J. B., Salamero, J. (2010) Patch-based nonlocal functional for denoising fluorescence microscopy image sequences. *IEEE Trans. Med. Imaging* **29**, 442-454.
36. Balla, T. (2013) Phosphoinositides: tiny lipids with giant impact on cell regulation. *Physiol. Rev.* **93**, 1019-1137.
37. Bago, R., Malik, N., Munson, M. J., Prescott, A. R., Davies, P., Sommer, E., Shpiro, N., Ward, R., Cross, D., Ganley, I. G., Alessi, D. R. (2014) Characterization of VPS34-IN1, a selective inhibitor of Vps34, reveals that the phosphatidylinositol 3-phosphate-binding SGK3 protein kinase is a downstream target of class III phosphoinositide 3-kinase. *Biochem. J.* **463**, 413-427.
38. Domin, J., Pages, F., Volinia, S., Rittenhouse, S. E., Zvelebil, M. J., Stein, R. C., Waterfield, M. D. (1997) Cloning of a human phosphoinositide 3-kinase with a C2 domain that displays reduced sensitivity to the inhibitor wortmannin. *Biochem. J.* **326 (Pt 1)**, 139-147.
39. Foster, J. G., Blunt, M. D., Carter, E., Ward, S. G. (2012) Inhibition of PI3K signaling spurs new therapeutic opportunities in inflammatory/autoimmune diseases and hematological malignancies. *Pharmacol. Rev.* **64**, 1027-1054.
40. Yeung, T., Heit, B., Dubuisson, J. F., Fairn, G. D., Chiu, B., Inman, R., Kapus, A., Swanson, M., Grinstein, S. (2009) Contribution of phosphatidylserine to membrane surface charge and protein targeting during phagosome maturation. *J. Cell Biol.* **185**, 917-928.
41. Vergne, I., Chua, J., Lee, H. H., Lucas, M., Belisle, J., Deretic, V. (2005) Mechanism of phagolysosome biogenesis block by viable Mycobacterium tuberculosis. *Proc. Natl. Acad. Sci. U. S. A.* **102**, 4033-4038.

42. Levin, R., Grinstein, S., Schlam, D. (2015) Phosphoinositides in phagocytosis and macropinocytosis. *Biochim. Biophys. Acta* **1851**, 805-823.

43. Minakami, R., Maehara, Y., Kamakura, S., Kumano, O., Miyano, K., Sumimoto, H. (2010) Membrane phospholipid metabolism during phagocytosis in human neutrophils. *Genes Cells* **15**, 409-424.

44. Kamen, L. A., Levinsohn, J., Cadwallader, A., Tridandapani, S., Swanson, J. A. (2008) SHIP-1 increases early oxidative burst and regulates phagosome maturation in macrophages. *J. Immunol.* **180**, 7497-7505.

45. Kamen, L. A., Levinsohn, J., Swanson, J. A. (2007) Differential association of phosphatidylinositol 3-kinase, SHIP-1, and PTEN with forming phagosomes. *Mol. Biol. Cell* **18**, 2463-2472.

46. Ferron, M. and Vacher, J. (2006) Characterization of the murine Inpp4b gene and identification of a novel isoform. *Gene* **376**, 152-161.

47. Nigorikawa, K., Hazeki, K., Sasaki, J., Omori, Y., Miyake, M., Morioka, S., Guo, Y., Sasaki, T., Hazeki, O. (2015) Inositol Polyphosphate-4-Phosphatase Type I Negatively Regulates Phagocytosis via Dephosphorylation of Phagosomal PtdIns(3,4)P2. *PLoS One* **10**, e0142091.

48. Schlam, D., Bohdanowicz, M., Chatgilialoglu, A., Steinberg, B. E., Ueyama, T., Du, G., Grinstein, S., Fairn, G. D. (2013) Diacylglycerol kinases terminate diacylglycerol signaling during the respiratory burst leading to heterogeneous phagosomal NADPH oxidase activation. *J. Biol. Chem.* **288**, 23090-23104.

49. Yang, C. S., Rodgers, M., Min, C. K., Lee, J. S., Kingeter, L., Lee, J. Y., Jong, A., Kramnik, I., Lin, X., Jung, J. U. (2012) The autophagy regulator Rubicon is a feedback inhibitor of CARD9-mediated host innate immunity. *Cell Host Microbe* **11**, 277-289.

50. Kim, G. H., Dayam, R. M., Prashar, A., Terebiznik, M., Botelho, R. J. (2014) PIKfyve inhibition interferes with phagosome and endosome maturation in macrophages. *Traffic* **15**, 1143-1163.

51. Steinberg, B. E. and Grinstein, S. (2008) Pathogen destruction versus intracellular survival: the role of lipids as phagosomal fate determinants. *J. Clin. Invest.* **118**, 2002-2011.

52. Vergne, I., Chua, J., Deretic, V. (2003) Tuberculosis toxin blocking phagosome maturation inhibits a novel Ca2+/calmodulin-PI3K hVPS34 cascade. *J. Exp. Med.* **198**, 653-659.

53. Toulabi, L., Wu, X., Cheng, Y., Mao, Y. (2013) Identification and structural characterization of a Legionella phosphoinositide phosphatase. *J. Biol. Chem.* **288**, 24518-24527.

54. Weber, S., Wagner, M., Hilbi, H. (2014) Live-cell imaging of phosphoinositide dynamics and

membrane architecture during Legionella infection. *MBio* **5**, e00839-00813.

CHAPTER THREE: Class I PI3K is required for sustaining β2-integrin dependent ROS production at neutrophil plasma membrane

This article needs to be completed before publication. Some stars in the text indicated the work that still needs to be done to complete some experiments presented in the results part. In the discussion, the experiments that will be done to complete the article are mentioned *in italic*.

Abstract

Reactive oxygen species (ROS) are produced by the NADPH oxidase (NOX2), which is activated when the cytosolic subunits assemble with the membrane subunits. Phosphatidylinositol (3,4)-bisphosphate ($PI(3,4)P_2$) can bind directly to the PX domain of $p47^{phox}$. $PI(3,4)P_2$ and Phosphatidylinositol (3,4,5)-trisphosphate ($PI(3,4,5)P_3$) are formed at the plasma membrane upon neutrophil activation by phosphorylation of PI4P and $PI(4,5)P_2$ by Class I PI3K respectively. However, the relevance of this interaction for sustaining the NADPH oxidase activation at the plasma membrane still needs to be investigated. We aim at investigating if class I PI3K and PX domain of $p47^{phox}$ are involved in sustaining NADPH oxidase activation at the plasma membrane. We found that adherent neutrophil-like PLB cells and human neutrophils, stimulated or not by the bacterial product fMLF, produce ROS for more than forty minutes on fibrinogen coated wells. The addition of LY294002 (a Class I PI3K inhibitor) terminates this integrin dependent ROS production. $P47^{phox}$, $p67^{phox}$ and $p40^{phox}$ are distributed on puncta at the plasma membrane. These puncta disappear after the addition of DPI (a flavocytochrome inhibitor) and LY294002. ROS production is enhanced in neutrophil-like PLB cells expressing constitutively active form GFP-Rac1G12V but is still totally inhibited by adding LY294002. In neutrophil-like PLB cells expressing a $p47^{phox}$ mutant, which can not bind to PI (3,4) P2, integrin stimulation via fibrinogen binding does not induce ROS production. In conclusion, class I PI3K activity is required to maintain the integrin-dependent activation of NADPH oxidase.

Introduction

Circulating neutrophils need to migrate to the infection or inflammation site to fulfil their functions. During this process, neutrophils need to adhere to endothelial cells and extracellular matrix. The adhesion between neutrophils and endothelial cells or extracellular matrix is mainly dependent on the integrins on the neutrophils surface membrane [1]. αMβ2 integrin (CD11b/CD18, Mac-1, complement receptor 3 (CR3)) is the most abundant integrin on neutrophils, involved in adhesion, phagocytosis and ROS production [2, 3]. Fibrinogen is a vascular extracellular matrix glycoprotein which is important for haemostasis, wound healing, inflammation and angiogenesis [4]. Studies show that immobilized fibrinogen, but not soluble fibrinogen, binds to αMβ2 integrin with great affinity [5, 6].This binding to fibrinogen has been shown to be important for neutrophil activation [7]. Bacterial peptide, fMLF, can trigger two phases of ROS production by adherent neutrophils on fibrinogen. The first phase is rapid, transient, and independent of cell adhesion. The second phase of ROS production occurs few minutes after the first phase and last up to 30-40 minutes [8]. The ROS production in the second phase is dependent on the engagement of neutrophil integrins [9]. Cytokines, such as TNF, can also trigger an extended ROS production (more than 40min) by adherent neutrophils on fibrinogen [8, 10]. The ROS production is due to NADPH oxidase activation. NADPH oxidase is composed of the membrane subunits $gp91^{phox}$ and $p22^{phox}$, the cytosolic subunits $p40^{phox}$, $p47^{phox}$ and $p67^{phox}$, and small GTPase Rac. Upon activation by soluble stimuli or activated integrins, all the subunits of the NADPH oxidase are recruited to the plasma membrane [11]. The NADPH oxidase catalyzes the production of $O_2^{\cdot-}$, which is immediately dismutated to H_2O_2. H_2O_2 can give rise to other ROS: hydroxyl radical (HO•) and HOCl in the presence of myeloperoxidase [12].

Class I PI3Ks, which are activated upon stimulation of the cell by FMLF and also by activated integrins, regulates the ROS production by neutrophils [8]. Class I PI3K phosphorylates the 3'-OH position of the inositol ring of PI4P and $PI(4,5)P_2$, generating the products $PI(3,4,5)P_3$ and $PI(3,4)P_2$ [13]. Class I PI3K can induce the activation of NADPH oxidase. Indeed $PI(3,4,5)P_3$ recruits several Guanine Exchange Factors (GEFs) (e.g. Vav, P-Rex), which further activate Rac [14]. $PI(3,4,5)P_3$ also activates AKT, PKCζ and PKCλ [15]. AKT and PKCζ are able to phosphorylate $p47^{phox}$ [16], although other signalling pathway triggered by integrins can activate other PKCs that phosphorylate $p47^{phox}$.

Class I PI3K is necessary to turn on NADPH oxidase activation at the plasma membrane, however whether Class I PI3K is required for sustaining the NADPH oxidase activation has not been investigated. In this study, we found that Class I PI3K is required to sustain integrin dependent NADPH oxidase activation. The reason for this requirement can be due to the need for maintaining Rac in an activated state, although previous study suggests that Rac is only needed to turn on the oxidase [17]. Another possible explanation is that product of the Class I PI3K may be necessary to maintain $p47^{phox}$ at the plasma membrane.

Indeed $p47^{phox}$ bears a PX domain that has two binding pockets: one binds to $PI(3,4)P_2$ and the other binds to phosphatidylserine (PS) and phosphatidic acid (PA) [18]. $p47^{phox}$ also contains two tandem Src homolog 3 (SH3) domains, an auto-inhibitory region (AIR), and a proline-rich region (PRR). In the resting state, the tandem SH3s interact intra-molecularly with AIR [19-21] and the second SH3 (SH3B) interacts intra-molecularly with the PX domain [22, 23]. During activation, these domains are believed to be unmasked. This enable the tandem SH3s to interact with the $p22^{phox}$ C-terminus [24, 25] and brings the $p40^{phox}$-$p47^{phox}$-$p67^{phox}$ complex to the plasma membrane. This also allows the PX domain of $p47^{phox}$ to bind membrane anionic phospholipids [18, 26]. It has been shown that a mutation in the PX domain $p47^{phox}$ leads to a decreased ROS production at the plasma membrane of neutrophils in suspension upon activation by fMLF or PMA [27]. However, whether the PX domain is necessary to sustain ROS production by maintaining the complex at the plasma membrane is not known.

In this study, we found that unprimed adherent neutrophil-like PLB cells and human neutrophils produce ROS on fibrinogen coated wells. The integrin-mediated ROS production is enhanced after treatment with bacterial peptide fMLF in human neutrophils. Class I PI3K plays a critical role in sustaining the integrin-mediated ROS production. Cytosolic subunit $p47^{phox}$, $p67^{phox}$ and $p40^{phox}$ participate in the process of integrin-mediated ROS production. Expression of active Rac1 cannot prevent the decrease in ROS production triggered by Class I PI3K inhibition. However mutation of the PX domain which is responsible for the $PI(3,4)P_2$ binding totally blocked the integrin-mediated ROS production.

Materials and methods

Chemical Products

fMLF, Fibrinogen (F3879) and HRP (horseradish peroxidase, P6782) were from Sigma-Aldrich (St. Louis, MO, USA). L-012 (8-Amino-5-chloro-7-phenylpyrido [3,4-d] pyridazine-1,4(2H,3H)dione Sodium Salt, 120-04891) was from Wako Pure Chemical Industries, Ltd (Osaka, Japan). LY294002 (S1105) was from Selleck chemicals (Houston, TX, USA).

Cell culture

The human myeloid leukaemia cell line PLB-985 was a generous gift from Dr. Marie-José Stasia. The stable PLB cell line expressing GFP tagged $p47^{phox}$, citrine tagged $p40^{phox}$ or citrine tagged $p67^{phox}$ subunit were described previously [17, 28, 29]. For all the experiments, PLB-985 cells were differentiated into neutrophil-like cells by adding 1.25% DMSO in exponentially growing condition for 5 or 6 days. For all the experiments, the differentiated cells were centrifuged 3 min at 2000 rpm and resuspended in Hepes buffer containing 140 mM NaCl, 5 mM KCl, 1 mM $MgCl_2$, 2 mM $CaCl_2$, 10 mM Hepes (pH 7.4), 1.8 mg/ml glucose and 1% heat inactivated foetal bovine serum.

Neutrophil preparation

Neutrophils were withdrawn from healthy donor whole blood by means of dextran sedimentation and Ficoll centrifugation as previously described [30]. The blood was mixed with an equal volume of 2% Dextran T-500 in 0.9% NaCl to sediment erythrocytes. After 45 min at room temperature, the leukocyte rich supernatant was collected and centrifuged at 400 g for 10 min. The cell pellets were resuspended in PBS and centrifuged through Ficoll-Hypaque (cell suspension: Ficoll-hypaque = 2:1) at 400g for 30 min at room temperature. The resulting pellets were re-suspended in ice-cold distilled H_2O for 30 s to lyse the erythrocytes and osmolarity was restored with an equal volume of 1.8% NaCl. The granulocytes were pelleted at 400 g for 10 min at 4°C and then the cells were resuspended in ice-cold PBS before use.

Plasmids

The plasmids pmCherryC1 was constructed as previously described [17]. Lyn11-targeted FRB (LDR) (Addgene plasmid # 20147) and YFP-FKBP (Addgene plasmid # 20175) were provided by Tobias Meyer [31]. MCherry-FKBP-MTM1 (Addgene plasmid # 51614) was provided by Tamas Balla [32]. To obtain mCherry-FKBP, YFP-FKBP cDNA was cut from YFP-FKBP plasmid and replaced by mCherry-FKBP cDNA using AgeI and SalI restriction sites. pCRY2PHR-mCherryN1 (Addgene plasmid # 26866) and pCIBN(deltaNLS)-pmGFP (Addgene plasmid # 26867) were provided from Chandra Tucker [33]. GFP-PTEN (Addgene plasmid # 10759) was provided by William Sellers [34]. The human PTEN cDNA was amplified from GFP-PTEN by PCR using the following primers: GCATGAAGCGCTATGACAGCCATCATCAAAGAG (sense) and GCATGACTCGAGGACTTTTGTAATTTGTGTATGCTGATCTTC (antisense) and then inserted in XhoI and AfeI restriction sites in plasmid pCRY2PHR-mcherryN1 to generate the plasmid PTENf-CRY2PHR-mcherryN1. The phosphatase domain of human PTEN cDNA was amplified from GFP-PTEN by PCR using the following primers: TCGAGCTAGCATGACAGCCATCATCAAAGAG (sense) and GCGCCTCGAGATGATTCTTTAACAGGTAGC (antisense) to generate the plasmid PTENp-CRY2PHR-mcherryN1. iRFP-N1 was provided by Michael Davidson (Addgene plasmid # 54787). P47phox-GFP was cut by HindIII and AgeI sites and P47phox cDNA was inserted at the same restriction sites in iRFP-N1 to generate the plasmid p47phox-iRFP. In order to obtain p47phox(R43Q)-GFP, we introduced mutation R43Q with the Quickchange II Site Directed Mutagenesis kit (Stratagene, La Jolla, CA, USA) using the following primers:5'-AAG GTG GTC TAC CGG CAG TTC ACC GAG ATC TAC G-3'. GFP-Rac1G12V was constructed as previously described [17], GFP-Rac1G12V was cut by HindIII and SacII and Rac1G12V was inserted at the same restriction sites in pmCherryC1 to generate the plasmid mCherry-Rac1G12V. All of the constructs were confirmed by sequencing.

Transient and stable transfection

Differentiated PLB cells, PLB p47phox-GFP stable cell lines were transiently transfected using the 4D-Nucleofector (Lonza, Switzerland) according to the manufacturer's protocol. For each condition, using the SF Cell Line Kit and the EH-100 program, 2×10^6 to 4×10^6 cells

were transfected with 1 µM siRNA or/and 3 µg of vector and incubated in culture medium without antibiotics. GFP, GFP-Rac1G12V, mCherry-Rac1G12V plasmids were transfected 4 hours before the experiment.

PLB p47phox(R43Q)-GFP and PLB p47phox-iRFP stable cell lines were generated by electroporation using a Bio-Rad Gene Pulser II apparatus as previously described [29]. These cell lines were cultured constantly in the presence of 0.5 mg/ml of G418 to maintain the selection.

RNA interference

All the siRNAs were purchased from Eurogenetec (Eurogenetec, Belgium). For each gene knockdown, three siRNA have been tested. The sequence of the selected siRNAs were as followes: SiRNA control (SR-CL000-005), p47phox siRNA (Forward sequence (FS) :5' CGGCUCCCGCCACCCUCAA 3') . 1 µM siRNA was transiently transfected using the 4D-Nucleofector (Lonza, Switzerland) with the SF Cell Line Kit and the EH-100 program. P47phox siRNA were transfected in PLB cells after 2 days of differentiation with DMSO. Then we added DMSO again to the transfected cells to allow complete differentiation and used the cells 2 days after transfection.

Measurement of ROS production

ROS production was measured using a L-012 based chemiluminescence assay in white polystyrene 96-well plates, which were precoated with 250µg/ml human fibrinogen or heat-inactivated Fetal Bovine Serum (50 µl in each well, 37 ℃ for 1 hour, then the liquid was withdrawn and the plate was incubated at 37 ℃ for another 1 hour). 2×10^5 Neutrophil-like PLB cells or human neutrophils were added into the wells and were incubated at 37C° for 30 min, then 100 µM L-012 and 20 U/ml HRP (final concentration) were added and the wells were incubated for 3 min. Light emission was recorded by a plate reader Wallac 1420 VICTOR3™ (Perkin¬Elmer, Waltham). 1 µM fMLF, 10 µM DPI or 10 µM LY294002 was added at different time points according to the experiments. After adding fMLF, light emission was recorded every 10 s for 5-10 min. For other time periods, light emission was recorded every 1 or 2 min.

Immunoblotting analysis

Differentiated PLB cells were incubated on ice with lysis buffer (4×10^4 cells/µl) containing Hepes-Na 25 mM, NaCl 150 mM, $MgCl_2$ 5 mM, EGTA 0.5 mM, TritonX100 0.5%, NaF 10 mM and supplemented with a protease inhibitor cocktail complete mini EDTA-free (Roche, Switzerland). Then lysates were centrifuged at 14000g at 4°C for 30 min. Protein concentration was measured using BioRad Protein assay. Samples were diluted in 6× Laemmli buffer and boiled 5 min at 95°C. Proteins were separated on a 10% SDS-PAGE gel and transferred onto a nitrocellulose membrane (BioRad, USA). The membrane was saturated with 3% milk at room temperature for 30 min (0.05% tween in PBS). The primary antibodies (mouse anti-$p47^{phox}$ antibody 1:1000, BD Biosciences, USA; rabbit anti-LDH antibody 1:5000, AbCam, UK; mouse anti-GFP antibody 1:400, Roche, Germany) were incubated at 37°C for 1h. HRP-labeled secondary antibodies (anti-mouse IgG or anti-rabbit IgG 1:2000, GE healthcare, UK) were incubated at room temperature for 1h. Proteins were detected by using ECL reagent (GE healthcare, UK) and quantification was analysed by using BioD1 software (Fisher scientific, USA).

Immunofluorescence

The immunofluorescence experiments were performed as described before [29]. The cells were immunostained with goat anti-$p40^{phox}$ antibody (Santa Cruz Biotechnology, USA; 1:100), rabbit anti-$p67^{phox}$ antibody (upstate, USA; 1:100) or mouse anti-$p47^{phox}$ antibody (BD Biosciences, USA, 1:100) followed by Alexa 488 goat anti-mouse (Life Technologies, USA; 1:500) or, Alexa 568 goat anti-rabbit (Life Technologies, USA; 1:500)or, Alexa 633 goat anti-rabbit (Life Technologies, USA; 1:500)or Alexa 568 rabbit anti-goat (Life Technologies, USA; 1:500)or Alexa 633 rabbit anti-goat (Life Technologies, USA; 1:500). Cells were imaged at room temperature by TIRF microscopy.

TIRF microscopy

To follow the dynamics of fluorescent tagged-proteins in the cells plated on fibrinogen-coated coverslips, we used a motorized Ti-TIRF arm (Nikon), mounted on a Nikon Eclipse Ti E

inverted microscope, equipped with a 100× plan Apo TIRF 1.49 oil immersion objective (Nikon) and a scientific CMOS camera (ORCA-Flash 4.0 LT, Hamamatsu), driven by MetaMorph 7.7 software (Molecular Devices). Cells were resuspended in Hepes buffer and allowed to adhere to the coverslips (ibidi 160630/3 glass bottom dish) for 30 min precoated with 250 µg/ml fibrinogen. All the experiments were performed at 37°C (microscope incubation chamber, Okolab). Images were recorded with a time-lapse from 1 min to 5 min depending on the different experiments. GFP and citrine were excited at 491 nm using a 0.3 s laser illumination. MCherry was excited at 561 nm using a laser illumination of 0.2 s. iRFP was excited at 642 nm using a laser illumination of 0.3 s. The fluorescence was detected with a four bands beamsplitter, a 525/50 nm (Chroma) emission filter for YFP, GFP and citrine, a 605/52 nm (Chroma) emission filter for mCherry, a 700/75 nm (Chroma) nm emission filter for iRFP.

Image processing and analysis

The image J software was used to analyse all the images and quantify the fluorescence. The ratio of the fluorescence intensity of the fluorescent protein at a given time point of the measurement to that at the first time point was calculated. When the ratio was lower than 1, we considered that the fluorescence at the plasma membrane decreased.

Data analysis

To compare the ratio values between two experiments, ratio paired T-test was analysed by using graphpad prism6 software (GraphPad Software, USA). All the others values were analysed by Students' T test.

Results

ROS production is triggered by immobilized fibrinogen in differentiated neutrophil-like PLB-985 cells and human neutrophils

ROS generation was measured with a highly sensitive chemiluminescence assay, L-012 [35], which is widely used *in vitro* and *in vivo* to detect ROS production (H_2O_2). Neutrophil-like PLB-985 cells plated on fibrinogen-coated wells presented a substantial ROS production that reached a peak at 40-60 min and lasted around 120 min (**Figure 1A and 2A**). As previously shown [36], cells plated on heat-inactivated Fetal Bovine Serum (FBS) coated wells did not produce ROS (**Figure 1A**). Detection of ROS by this assay was completely suppressed by adding the flavocytochrome inhibitor diphenyleneiodonuim (DPI) (**Figure 1A**). The total ROS production integrated over 30 min after adding DPI was sharply decreased as compared to control cells without DPI (2.0 ± 0.8% versus 100% for the control) (**Figure 1B**). The result indicates that the ROS detected are mainly produced by the NADPH oxidase. Similar ROS generation kinetics was observed in human neutrophils plated on fibrinogen-coated wells (**Figure 4**). However the maxima were reached faster (upon 15-20 min) and this ROS production lasted around 60 minutes. The peak value of ROS production in human neutrophils was similar to that in neutrophil-like PLB cells plated on fibrinogen-coated wells.

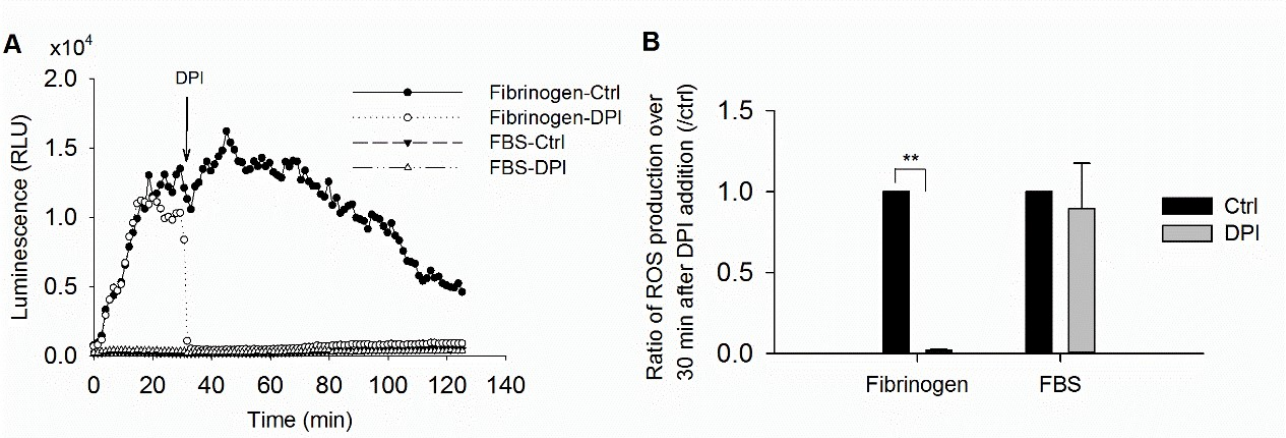

Figure 1. DPI inhibits the ROS production by differentiated PLB cells in response to fibrinogen.

(A and B) Differentiated PLB cells were plated on fibrinogen-coated or heat-inactivated FBS-coated wells. Chemiluminescence was measured every 1 min and up to 125 min. (A) 10 μM DPI was added at 30 min. (B) Ratio of ROS production over 30 min after the addition of DPI compared to the control without DPI. Data are means ± SEM. *n*=3, ***P*<0.01(ratio paired *t* test).

ROS production triggered by fibrinogen is enhanced in response to fMLF in human neutrophils but not in neutrophil-like PLB cells

fMLF-stimulated ROS production in PLB cells and human neutrophils plated on fibrinogen-coated wells occurred in two phases as previously observed (**Figure 2A and 5A**) [8]. The first one was rapid and lasted 2 min. The second phase was similar to the one without fMLF stimulation, reached a peak at ~60 minutes and lasted around 120 minutes. The total ROS production over the first phase after adding fMLF was increased by a factor of 6.2 ± 1.5 as compared to control cells. In the second adhesion-dependent phase, there was no difference in the ROS production with or without fMLF stimulation (**Figure 2**). Interestingly, the peak value of the ROS production in the first phase is lower than that in the second phase. In human neutrophils plated in fibrinogen, fMLF triggered a robust ROS generation, which also occurred also in two phases (**Figure 5**). The first rapid phase after the addition of fMLF lasted around 3 min. The second phase reached a peak at ~15 min after fMLF addition and lasted 60 min. The dynamic of ROS generation in the second phase was quite similar with or without

fMLF stimulation, but the peak value of the ROS production with fMLF was almost 20 times higher than without fMLF (**Figure 4A and 5A**). Thus, stimulation by fMLF enhances the second adhesion-dependent phase of ROS production in human neutrophils.

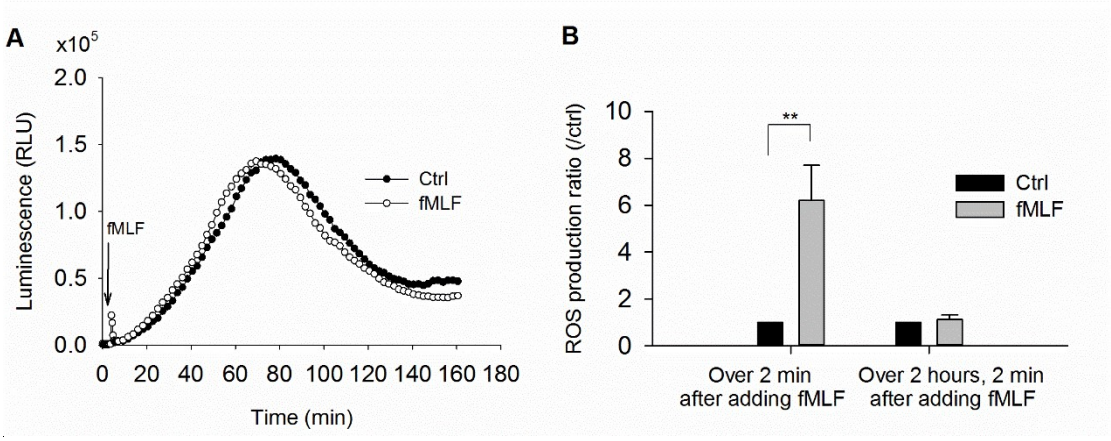

Figure 2. fMLF does not change the fibrinogen induced ROS production by differentiated PLB cells.

(A and B) Differentiated PLB cells were plated on fibrinogen-coated wells. Chemiluminescence was measured every 0.4 min and up to 7 min, then it was recorded every 2 min and up to 160 min. (A) 1 μM fMLF was added at 4 min. (B) Graph represents ROS production ratio over 2 min after the addition of fMLF compared to control without fMLF or ratio over 2 h, 2 min after the addition of fMLF. Data are means ± SEM. n=4, $^{**}P$<0.01 (ratio paired t test).

Sustained ROS production in response to fibrinogen requires Class I PI3K

To better understand the role of Class I PI3K in the regulation of ROS generation triggered by fibrinogen, we used a class I PI3K inhibitor LY294002. In both neutrophil-like PLB cells and human neutrophils, addition of LY294002 terminated the ROS production triggered by fibrinogen (**Figure 3 and 4**). The total ROS production of the PLB cells or human neutrophil integrated over 30 min after adding LY294002 was strikingly decreased as compared to untreated cells (**Figure 3B and 4B**). LY294002 also inhibited the second phase of ROS production in fibrinogen adherent human neutrophils stimulated by fMLF: the total ROS generation of human neutrophils integrated over 30 min after adding LY294002 was decreased to 7.8 +/- 2.7% as compared with untreated neutrophils (**Figure 5B**). Therefore, we

conclude that Class I PI3K sustains adhesion-dependent ROS production in response to fibrinogen both in neutrophil-like PLB cells and human neutrophils.

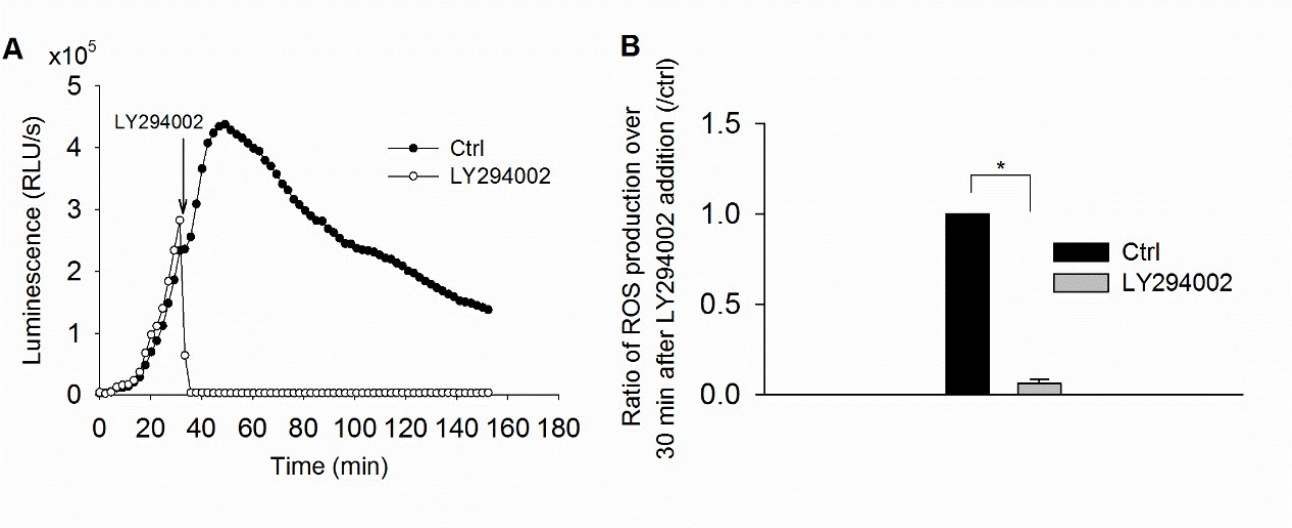

Figure 3. LY294002 inhibits the fibrinogen induced ROS production in differentiated PLB cells.

(A and B) Differentiated PLB cells were plated on fibrinogen-coated wells. Chemiluminescence was measured every 2 min and up to 152 min. (A) 10 μM LY294002 was added at 30 min. (B) Ratio of ROS production over 30 min after the addition of LY294002 compared to the control without LY294002. Data are means ± SEM. *n*=3, **P*<0.05 (ratio paired *t* test).

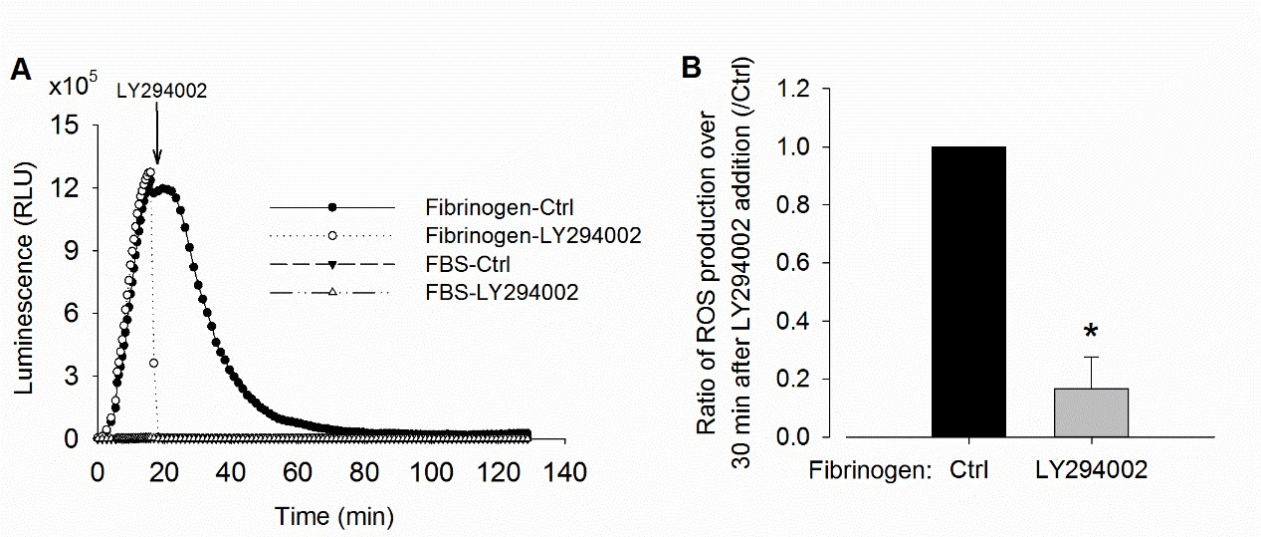

Figure 4. LY294002 inhibits the fibrinogen induced ROS production in human neutrophils.

(A and B) human neutrophils were plated on fibrinogen-coated or heat-inactivated FBS-coated wells. Chemiluminescence was measured every 1 min and up to 128 min. (A) 10 μM LY294002 was added at 16 min. (B) Ratio of ROS production over 30 min after the addition of LY294002 compared to the control without LY294002. Data are means ± SEM. *n*=3, **P*<0.05 (ratio paired *t* test).

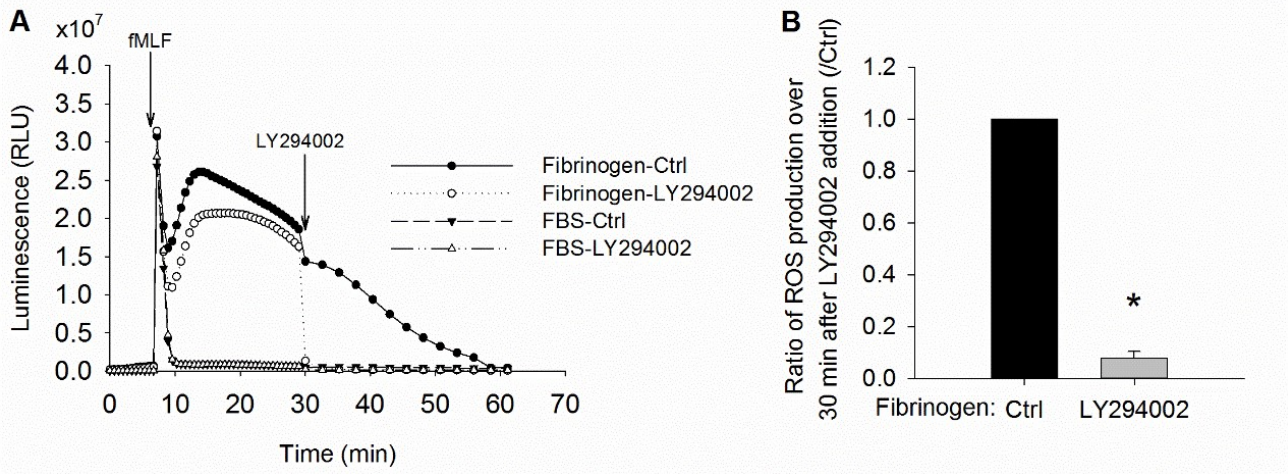

Figure 5. fMLF enhances the fibrinogen dependent ROS production.

(A and B) Human neutrophils were plated on fibrinogen-coated wells or heat-inactivated FBS-coated wells. Chemiluminescence was recorded every 0.7 min and up to 30 min, then it was recorded every 2.5 min and up to 61 min. (A) 1 μM fMLF was added at 7 min and 10 μM LY294002 was added at 30 min. (B) Ratio of ROS production over 30 min after the addition of LY294002 compared to the control without LY294002. Data are means ± SEM. *n*=3, **P*<0.05 (ratio paired *t* test).

Cytosolic NOX subunits p40^{phox}, p47^{phox}, p67^{phox} are recruited to the plasma membrane in cells adherent to fibrinogen.

The stimulation of neutrophils (adherent or in suspension) by soluble cytokines, triggered ROS production by NADPH oxidase at the plasma membrane. Therefore we wanted to examine the localization, in the fibrinogen-adherents cells, of the cytosolic subunits of the NADPH oxidase**.**

We wondered whether all the cytosolic subunits contribute to the ROS generation. We checked the endogenous cytosolic NOX subunits distribution in neutrophil-like PLB cells adherent to fibrinogen by immunofluorescence. We used total internal reflection fluorescence (TIRF) microscopy to detect their localization at the plasma membrane. P40^{phox}, p47^{phox} and p67^{phox} were distributed into puncta at the plasma membrane. P40^{phox} /p67^{phox}, p40^{phox} / p47^{phox} were co-localized together (**Figure 6**). P47^{phox} and p67^{phox} co-localized in human neutrophils with or without fMlF stimulation (**Figure 7**)*

**These results are preliminary. We are currently analyzing all the data with a new macro in image J. The macro, written by Romain Le Bars (IR CNRS, plateforme imagerie Gif), is able to detect the puncta (figure 6). Then, the colocalization between the puncta is evaluated with the JACoP plugin in image J.*

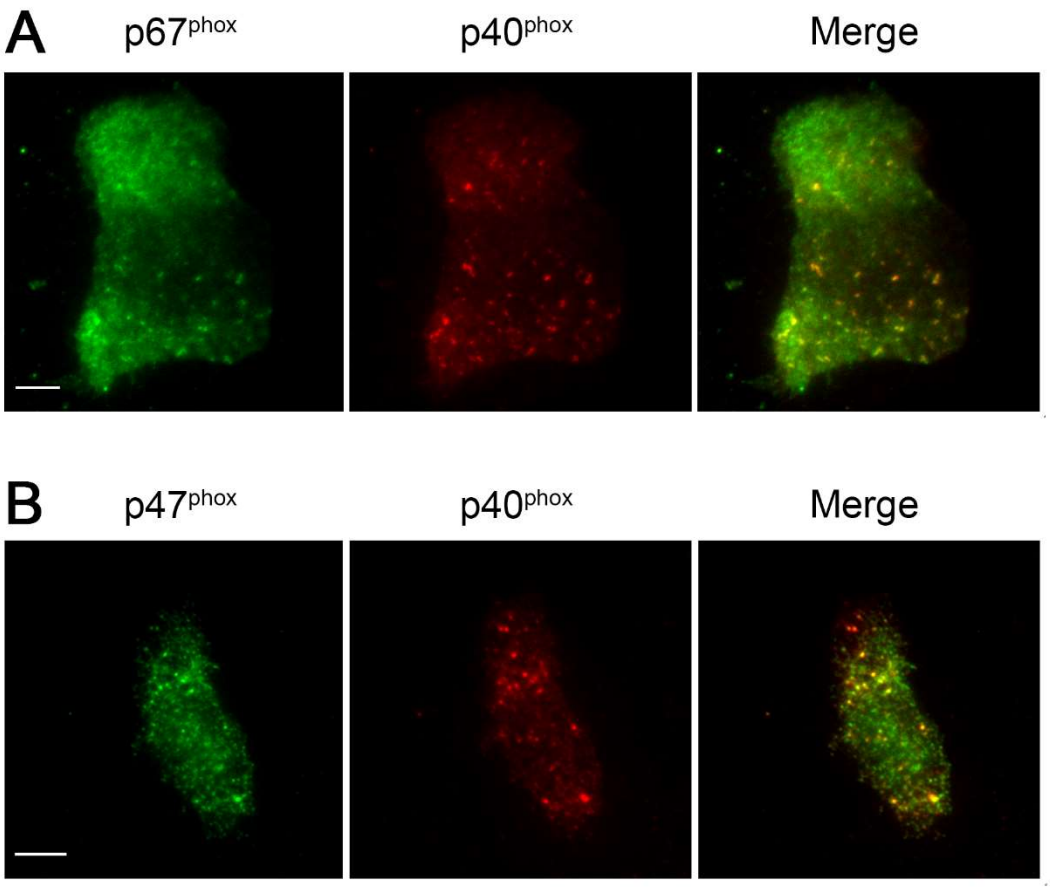

Figure 6. Distribution of the cytosolic NOX subunits in differentiated PLB cells adherent to fibrinogen.

(A and B) Immunofluorescence experiments were performed to detect $p40^{phox}$, $p47^{phox}$ and $p67^{phox}$. Before fixation, differentiated PLB cells were plated on fibrinogen-coated coverslips and incubated 30 min at 37C°. Images were acquired by TIRF microscopy. (A) Immunofluorescence images of PLB cells stained for $p40^{phox}$ and $p67^{phox}$. (B) Immunofluorescence images of PLB cells stained for $p40^{phox}$ and $p47^{phox}$. Scale bar = 5 µm.

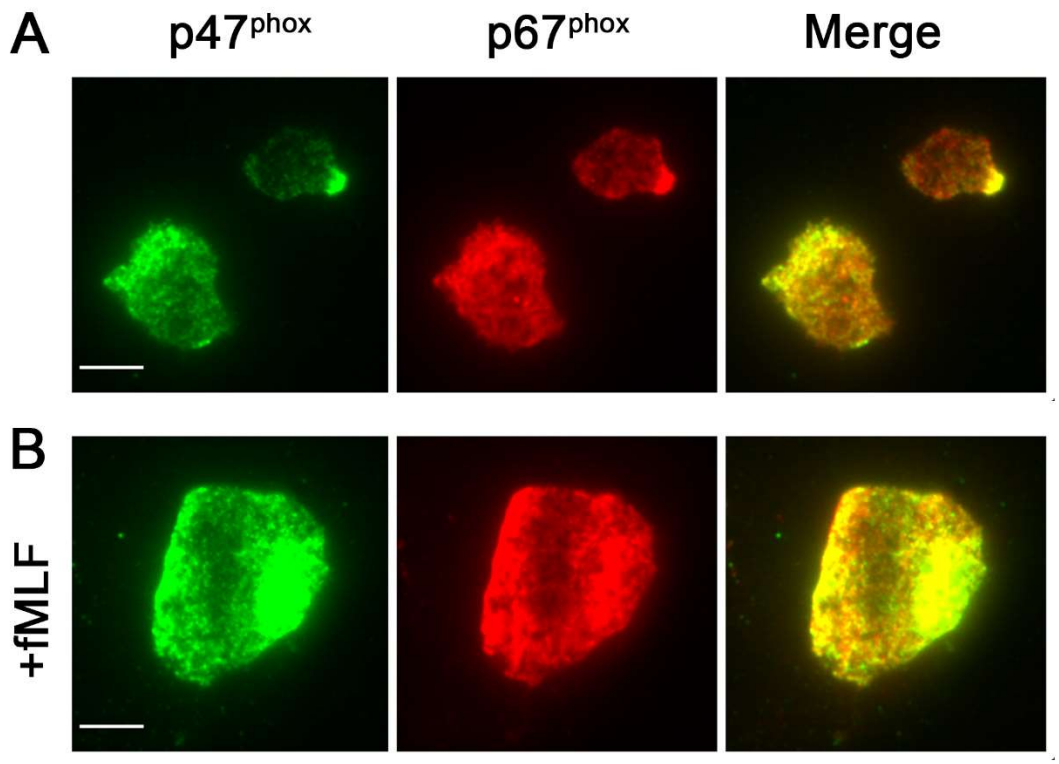

Figure 7. Distribution of the cytosolic NOX subunits in human neutrophils plated on fibrinogen and stimulated with fMLF.

(A and B) Immunofluorescence experiments were performed to detect $p47^{phox}$ and $p67^{phox}$. Before fixation, human neutrophils were plated on fibrinogen-coated coverslips and incubated 30 min at 37°C. Images were acquired by TIRF microscopy. (A) Immunofluorescence images of human neutrophils stained for $p40^{phox}$ and $p67^{phox}$. (B) Immunofluorescence images of human neutrophills stained for $p47^{phox}$ and $p67^{phox}$. 1 µM fMLF was added 10 min before fixation. Scale bar = 5 µm.

We further observed the NADPH oxidase localization at the plasma membrane using TIRF microscopy in neutrophil-like PLB stable cell lines, PLB citrine-$p40^{phox}$, PLB $p67^{phox}$-citrine and PLB $p47^{phox}$-GFP, which stably express fluorescent protein tagged NOX subunits. We observed that $p47^{phox}$-GFP (**Figure 8A and 9A**), $p67^{phox}$-citrine (**Figure 10A**) and citrine-$p40^{phox}$ (**Figure 11A**) distributed into puncta at the plasma membrane*. The addition of DPI triggered the disappearance of the puncta of $p47^{phox}$-GFP (**Figure 8A**). The mean fluorescence of $p47^{phox}$-GFP in the cells decreased from 100% (without DPI) to 72.6 ± 5.0 %, 5 min after the addition of DPI (**Figure 8B**). These results suggest that the DPI induces the release of $p47^{phox}$ as previously observed [29]. This result confirms that ROS generation triggered by adhesion to fibrinogen is NOX dependent.

** For this experiments, we need a negative control We will use PLB KO cells, that do not express gp91^{phox}, transfected with p67^{phox}-GFP. P67^{phox}-GFP should not be at the plasma membrane in these cells*.

The above data demonstrate that the NOX cytosolic subunits $p40^{phox}$, $p47^{phox}$ and $p67^{phox}$ participate in the ROS production at the plasma membrane in neutrophil-like PLB cells in response to fibrinogen.

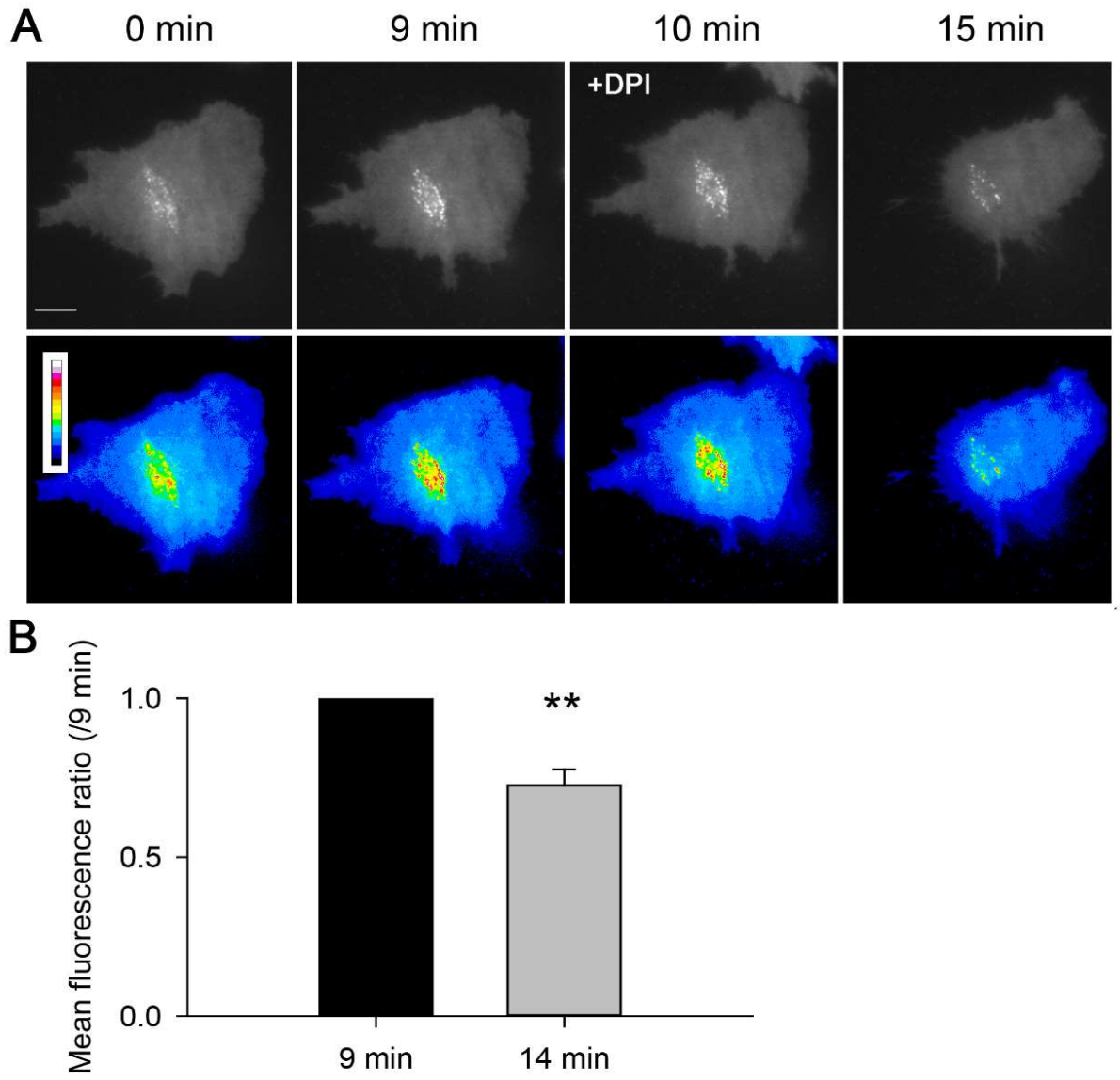

Figure 8. DPI triggers the release of p47^{phox}-GFP from the plasma membrane in differentiated PLB p47^{phox}-GFP cells plated on fibrinogen.

(A-B) Differentiated PLB p47^{phox}-GFP cells were plated on fibrinogen-coated coverslips and incubated 30 min at 37C°. Images were acquired by TIRF video-microscopy. (A) Representative images of cells expressing p47^{phox}-GFP. 10 µM DPI was added after 9 min. (B) Ratio of the mean fluorescence of p47^{phox}-GFP cells at 14 min (5 min after addition of 10 µM DPI) compared to that at 9 min (i.e. just before addition of DPI). *n*=10, ***P*<0.01 (ratio paired *t* test).Scale bar = 5 µm.

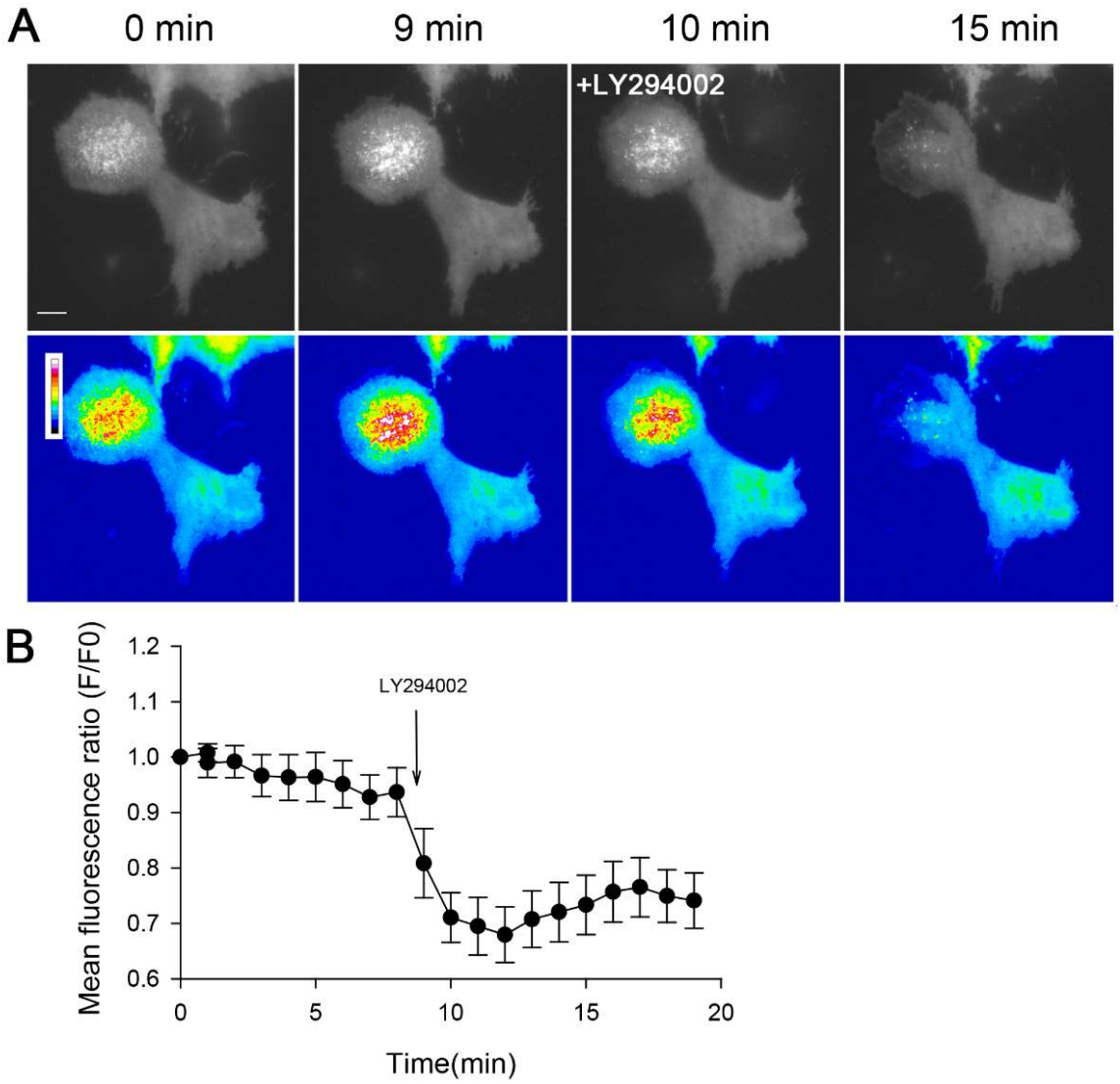

Figure 9. LY294002 releases p47^{phox}-GFP from the plasma membrane of differentiated PLB p47^{phox}-GFP cells plated on fibrinogen.

(A-B) Differentiated PLB p47^{phox}-GFP cells were plated on fibrinogen-coated coverslips and incubated 30 min at 37C°. Images were acquired by TIRF video-microscopy. 10 µM LY294002 was added at time 9 min after the beginning of the video. (A) Representative images of PLB cells expressing p47^{phox}-GFP (B) The Graph represents the ratio of the mean fluorescence of p47^{phox}-GFP cells (F) at different time compared to that at time zero (F0). *n*=17. Scale bar = 5 µm.

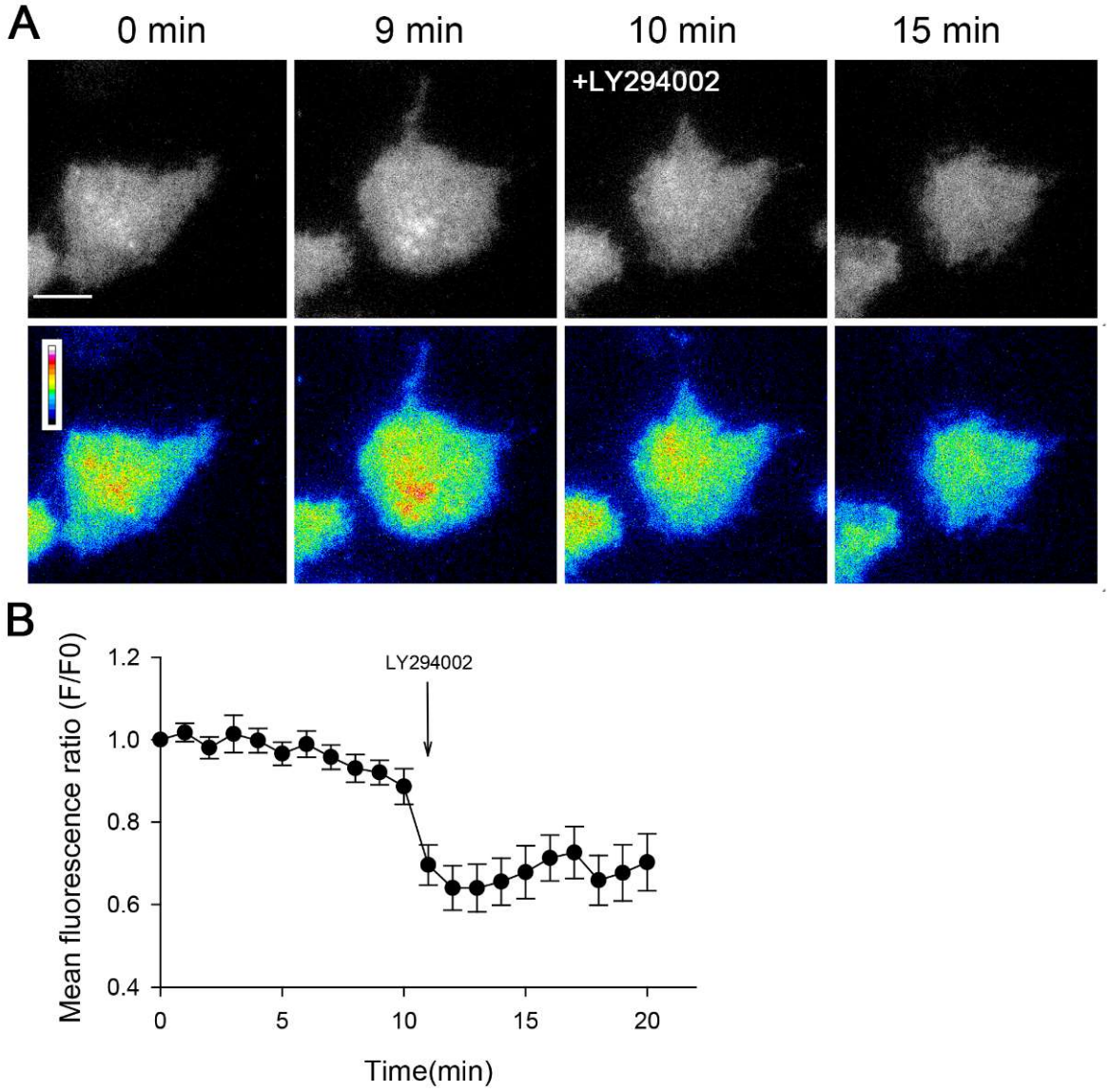

Figure 10. LY294002 releases p67^{phox}-citrine from the plasma membrane of differentiated PLB p67^{phox}-citrine cells plated on fibrinogen.

(A-B) Differentiated PLB p67^{phox}-citrine cells were plated on fibrinogen-coated coverslips and incubated 30 min at 37C°. Images were acquired by TIRF video-microscopy. 10 µM LY294002 was added at time 9 min after the beginning of the video. (A) Representative images of PLB cells expressing p67^{phox}-citrine. (B) The Graph represents the ratio of the mean fluorescence of p67^{phox}-citrine cells (F) at different time compared to that at time zero (F0). *n*=12. Scale bar = 5 µm.

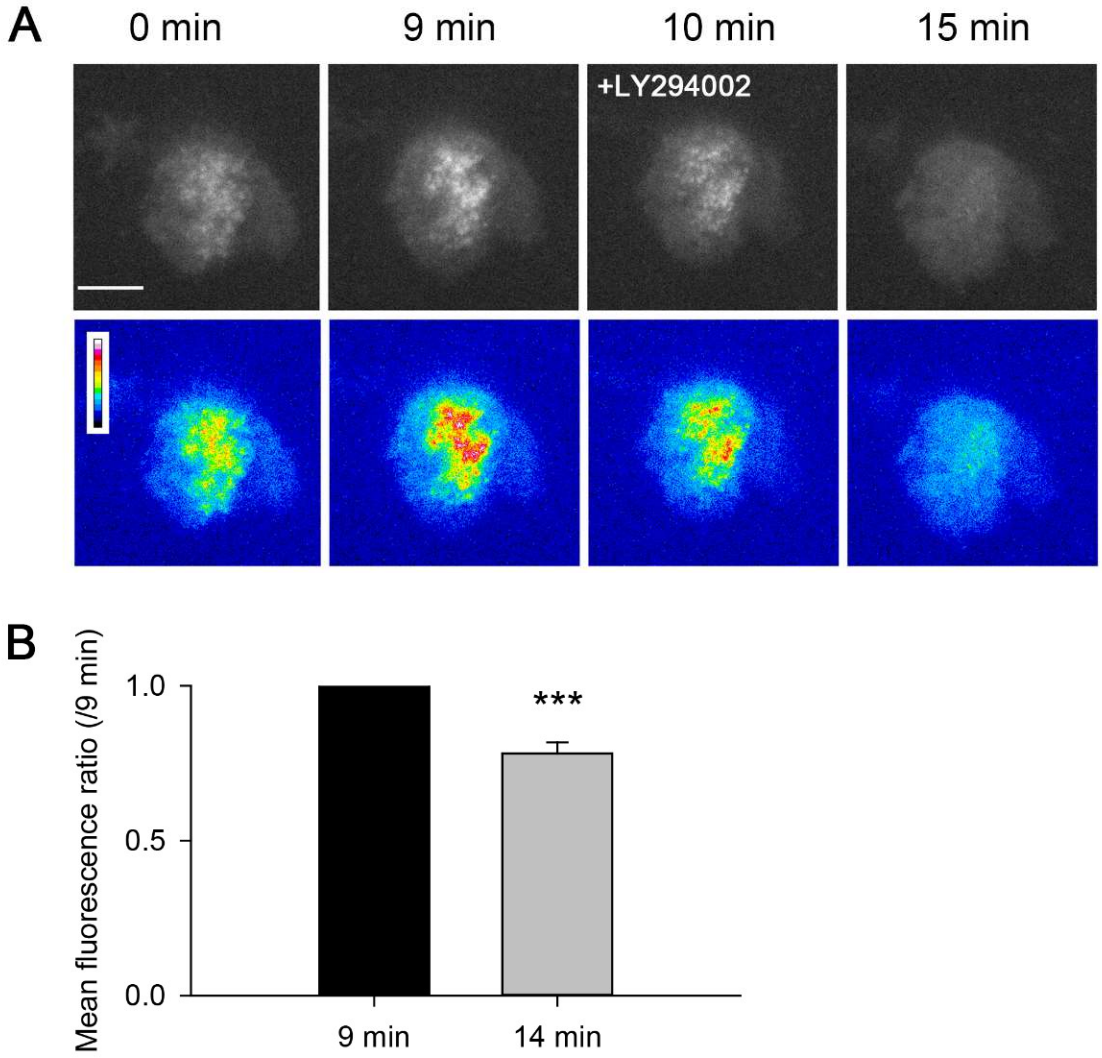

Figure 11. LY294002 releases p40^{phox}-citrine from the plasma membrane of differentiated PLB p40^{phox}-citrine cells plated on fibrinogen.

(A-B) Differentiated PLB p40^{phox}-citrine cells were plated on fibrinogen-coated coverslips and incubated 30 min at 37C°. Images were acquired by TIRF video-microscopy. (A)Representative images of cells expressing p40^{phox}-citrine. 10 µM LY294002 was added after 9 min. (B) Ratio of the mean fluorescence of p40^{phox}-citrine cells at 14 min (5 min after addition of 10 µM DPI) compared to that at 9 min (i.e. just before addition of DPI). *n*=13, ***P<0.001 (ratio paired *t* test). Scale bar = 5 µm.

Accumulation of cytosolic NOX subunits p40^{phox}, p47^{phox}, p67^{phox} at the plasma membrane requires Class I PI3K

We examined the response to LY294002 of neutrophil-like PLB cells plated on fibrinogen. Puncta of citrine-p40^{phox}, p67^{phox}-citrine and p47^{phox}-GFP begun to disappear just after the addition of LY290042. The mean fluorescence of p67^{phox}-citrine and p47^{phox}-GFP cells both decreased after the addition of LY294002. The mean fluorescence of citrine-p40^{phox} cells after incubation with LY294002 also significantly decreased to 78.1+/-3.65% compared to that before LY294002 addition. *The remaining fluorescence we observed after LY294002 addition, was probably the cytosolic fluorescence just beneath the plasma membrane. We will check this with the negative control.* We further checked in human neutrophils whether the addition of LY94002 decreases the plasma membrane localization p47^{phox} and p67^{phox}. P47^{phox} and p67^{phox} were detected by immunofluorescence and their plasma membrane localization was assessed by TIRF microscopy. As expected the fluorescence of p47^{phox} and p67^{phox} cells, at or near the plasma membrane, was respectively decreased to 50% and 54% after the addition of LY294002 (**Figure12**). All these results demonstrate that the localization of the NOX subunits at the plasma membrane in fibrinogen-adherent neutrophils requires Class I PI3K.

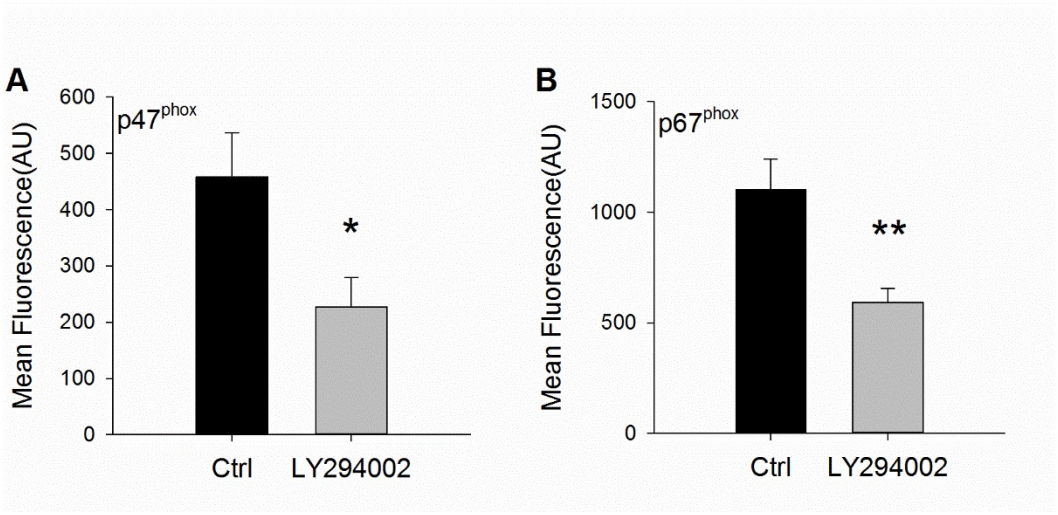

Figure 12. LY294002 addition induces a decrease in p47^{phox} and p67^{phox} plasma membrane fluorescence of differentiated PLB cells.

(A and B) Immunofluorescence experiments were performed to detect p47^{phox} and p67^{phox}. Before fixation, differentiated PLB cells were plated on fibrinogen-coated coverslips and incubated 30 min at 37C°, then 10 µM LY294002 was added 10 min before fixation. Images were acquired by TIRF microscopy. (A) Quantification of the mean cell fluorescence of

p47^{phox} with or without LY294002. (B) Quantification of the mean fluorescence of p67^{phox} with or without LY294002. More than 20 cells were analyzed in each condition. *P<0.05, **P<0.01 (Student t test).

Active rac1 enhances fibrinogen-dependent NADPH oxidase activation but cannot prevent its decrease upon PI3K inhibition

Neutrophil adhesion to fibrinogen is mediated by integrins, which can trigger the activation of PI3K. PI(3,4,5)P_3, the product of PI3K, can recruit GEFs and further activate Rac. Rac is essential to activate the NADPH oxidase. To identify whether active Rac1 is responsible for the downregulation of NADPH oxidase upon Class I PI3K inhibitor addition, we used neutrophil-like PLB cells transiently transfected with constitutively active Rac: GFP-Rac1G12V. A GFP plasmid was used as a control. Differentiated PLB cells expressing GFP-Rac1G12V produced 2 times more ROS compared to those expressing GFP, suggesting that Rac1 may enhance the NOX activity (**Figure 13A and B**). ROS generation integrated over 30 min after the addition of LY294002 in cells expressing GFP or GFP-Rac1G12V was decreased to 16.0+/-6.7% or to 28.8+/-10.9% respectively compared to the control cells without LY294002 (**Figure 13C and D**). Moreover, there was no difference of ROS production after adding LY294002 between cells expressing GFP and cells expressing GFP-Rac1G12V. These data indicate that overexpression of active Rac1 cannot prevent the drop in ROS production induced by Class I PI3K inhibitor. We then wanted to see if the presence of active Rac could prevent the plasma membrane release of NADPH oxidase cytosolic subunit upon addition of LY294002. We expressed mcherry-Rac1G12V in the differentiated PLB stable cell line PLB p47^{phox}-GFP. P47^{phox}-GFP was distributed in puncta at the plasma membrane of neutrophil-like cells expressing mcherry-Rac1G12V (**Figure 13E**). These puncta began to disappear 5 minutes after the addition LY294002 (**Figure 13F**) as observed before without active Rac. These results suggest that active Rac1 enhances fibrinogen dependent NADPH oxidase activation but cannot prevent its de-activation by Class I PI3K inhibitor.

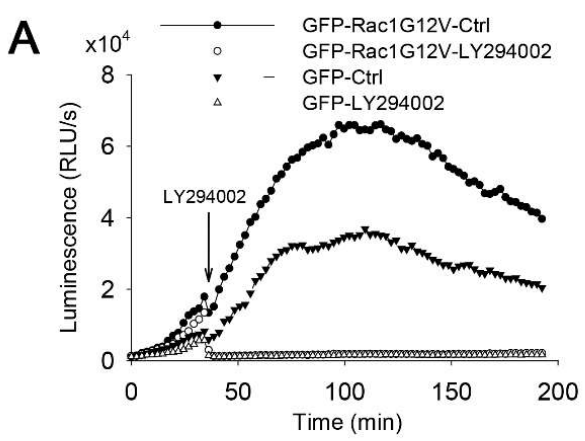
A
x10^4
GFP-Rac1G12V-Ctrl
GFP-Rac1G12V-LY294002
GFP-Ctrl
GFP-LY294002
Luminescence (RLU/s)
LY294002
Time (min)

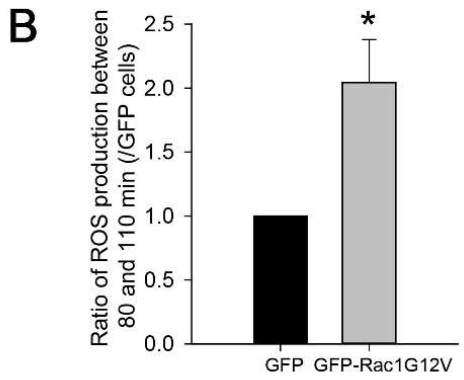
B
Ratio of ROS production between 80 and 110 min (/GFP cells)
*
GFP
GFP-Rac1G12V

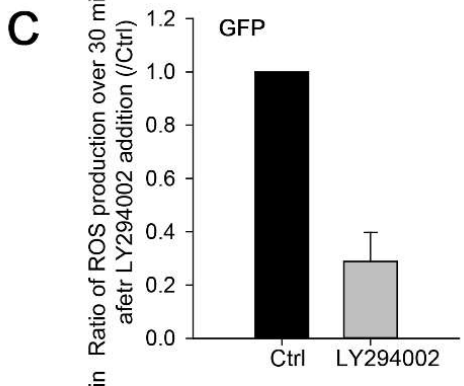
C
GFP
Ratio of ROS production over 30 min afetr LY294002 addition (/Ctrl)
Ctrl
LY294002

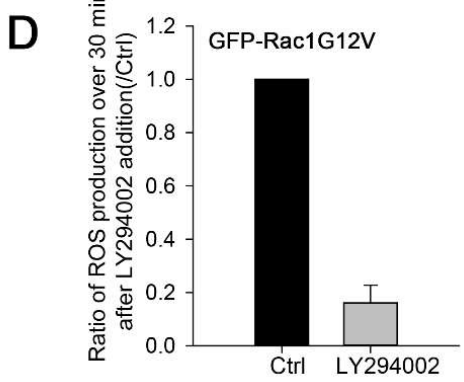
D
GFP-Rac1G12V
Ratio of ROS production over 30 min after LY294002 addition(/Ctrl)
Ctrl
LY294002

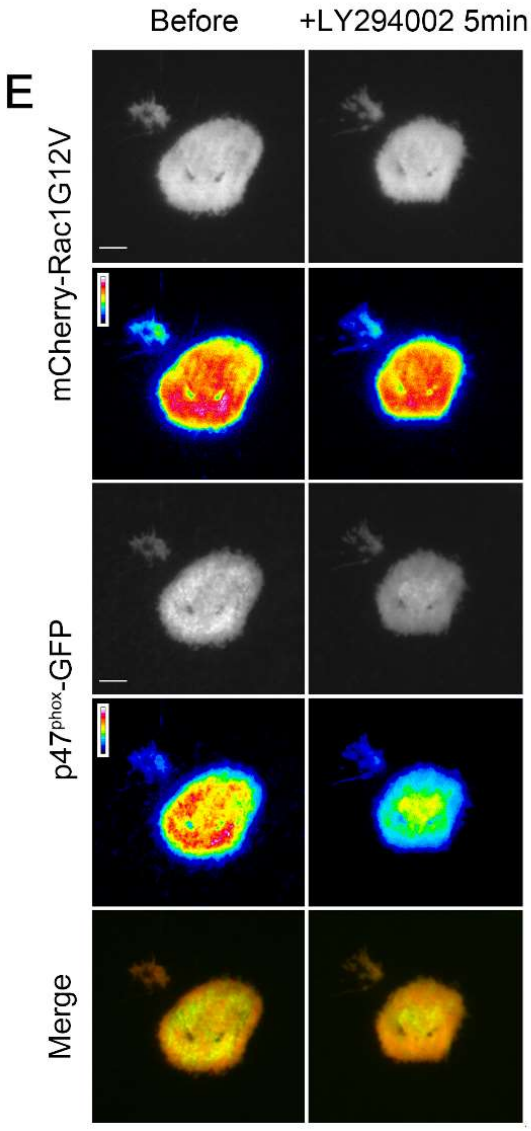
E
Before
+LY294002 5min
mCherry-Rac1G12V
p47phox-GFP
Merge

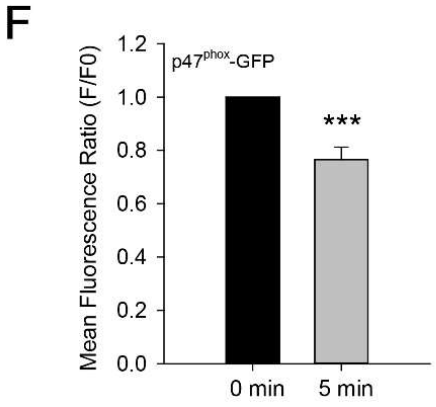
F
p47phox-GFP
Mean Fluorescence Ratio (F/F0)
***
0 min
5 min

Figure 13. Rac1G12V cannot prevent the drop of ROS production and the release of p47^{phox} at the plasma membrane induced by LY294002 in neutrophil-like cells plated on fibrinogen.

(A-D) Differentiated PLB cells transiently transfected with GFP or GFP-Rac1G12V were plated on fibrinogen-coated wells. Chemiluminescence was recorded every 2 min and up to 192 min. (A) 10 µM LY294002 was added at 36 min. (B) Ratio of the ROS production in PLB cells expressing GFP-Rac1G12V over 30 min around the peak value (80-110 min) compared to PLB cells expressing GFP. *n*=3, **P*<0.05. (C) Ratio of the ROS production in PLB cells expressing GFP over 30 min after the addition of LY294002 compared to the control without LY294002. *n*=3. (D) Ratio of the ROS production in PLB cells expressing GFP-Rac1G12V over 30 min after the addition of LY294002 compared to the control without LY294002. *n*=3. (E-F) Differentiated PLB p47^{phox}-GFP cells transiently transfected with mCherry-Rac1G12V were plated on fibrinogen-coated coverslips and incubated 30 min at 37C°. Images were acquired by TIRF video microscopy. (E) Representative images of PLB cells expressing p47^{phox}-GFP and mCherry-Rac1G12V. Images were taken at 0 min (before adding LY294002) and 5 min after adding LY294002. Scale bar = 5 µm. (F) The graph represents the ratio of the mean fluorescence of p47^{phox}-GFP cells 5 min after adding LY294002 (F) compared to that at time zero (F0). Data are means ± SEM. *n*=19, ****P*<0.001 (ratio paired *t* test).

The p47^{phox} PX domain is involved in sustaining NADPH oxidase activation triggered by fibrinogen

To examine the role of phosphoinositide binding of the p47^{phox} PX domain in the process of adhesion dependent NADPH oxidase activation, we mutated one amino acid, Arginine 43 to Glutamine, which is critical for the interactions with the 3-phosphate of PI(3,4)P2 [18]. Then, we generated a stable cell line PLB p47^{phox}(R43Q)-GFP which expressed p47^{phox}(R43Q)-GFP. The immunoblots (**Figure 14**) show that with the anti-GFP antibody only the tagged proteins are expressed in the PLB p47^{phox}(R43Q) cells as well as PLB p47^{phox}-GFP cells. Surprisingly, the mutated form of p47^{phox}(R43Q)-GFP can not be recognized by anti-p47^{phox} antibody (Immunogen: human p47^{phox} aa.18-197). The antibody recognizes the fusion protein p47^{phox}-GFP or p47^{phox}-iRFP. We checked the ROS generation in PLB p47^{phox}(R43Q)-GFP cells plated on fibrinogen as well as PLB citrine cells which were used as control. Without fMLF stimulation, the ROS production was totally suppressed in PLB p47^{phox}(R43Q)-GFP cells, but not in PLB citrine cells (**Figure 15A**). These results suggest that the PX domain is necessary for the NADPH oxidase activation in cells plated on to fibrinogen. Upon fMLF stimulation, there was still a first phase of ROS production (i.e. over 2min after the addition of fMLF) in PLB p47^{phox}(R43Q)-GFP cells. This ROS production was even 5.2 ± 2.8 times higher than in PLB citrine cells, but not significantly different (**Figure 15C**). However, the second phase of ROS production, which is integrin dependent, was suppressed in PLB p47^{phox}(R43Q)-GFP cells with/without fMLF stimulation (**Figure 15B and D**). These results suggest that PI(3,4)P_2-p47^{phox} binding is critical to sustain the adhesion dependent ROS production.

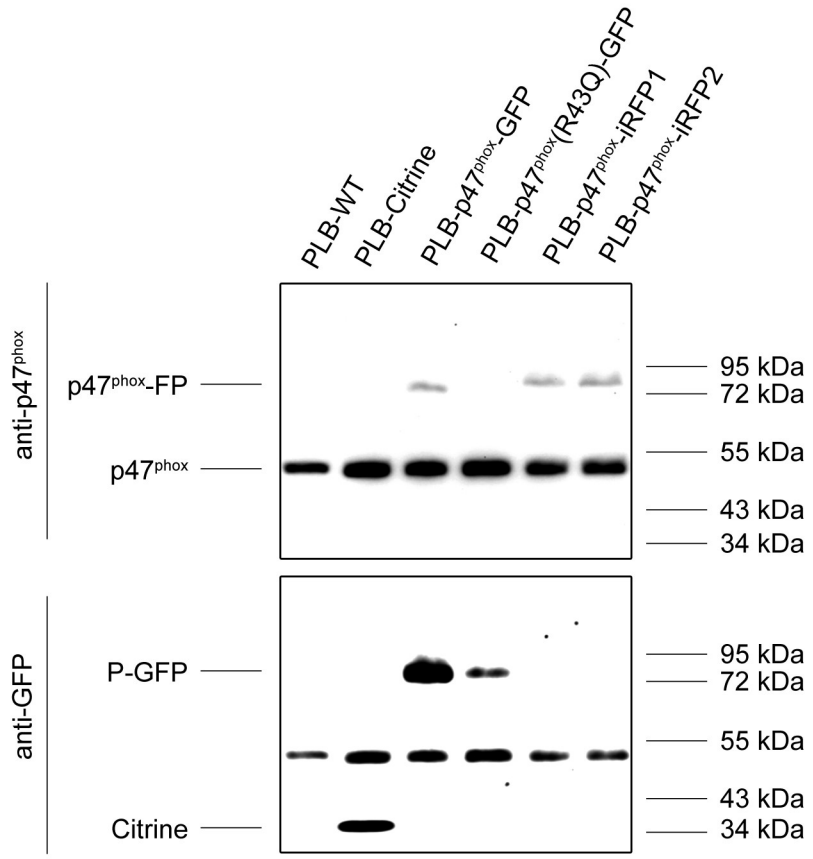

Figure 14. Generation of the stable PLB p47^{phox}(R43Q)-GFP cell line and the PLB p47^{phox}-iRFP cell line.

Western blot analysis of p47^{phox}, p47^{phox}-FP (P47^{phox} tagged with fluorescent protein), P-GFP (protein tagged with GFP), citrine (GFP) in PLB WT, PLB Citrine, PLB p47^{phox}-GFP, PLB p47^{phox}(R43Q)-GFP, PLB p47phox-iRFP1 and PLB p47^{phox}-iRFP2 cells using an anti-p47phox Ab and an anti-GFP Ab. ** The Band of p47^{phox} that appears in the anti-GFP membrane is due to the fact that the immunodetection with anti-GFP antibody was performed in the same membrane as the anti-p47^{phox} Ab. The stripping buffer did not completely remove the anti-p47^{phox} Ab.*

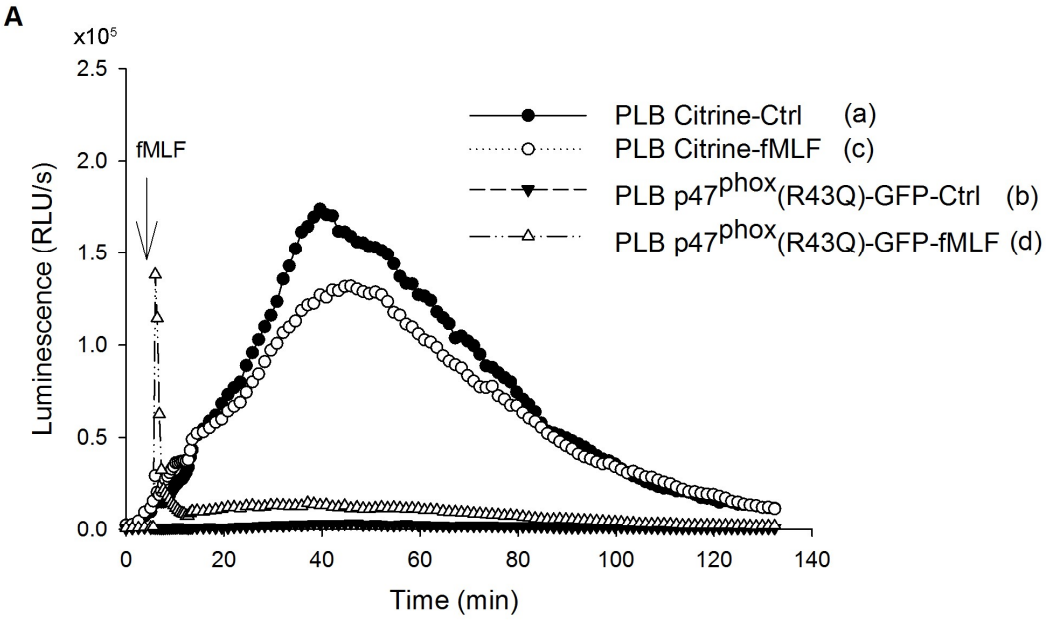
A
x10⁵
2.5
2.0
1.5
1.0
0.5
0.0
Luminescence (RLU/s)
fMLF
PLB Citrine-Ctrl (a)
PLB Citrine-fMLF (c)
PLB p47phox(R43Q)-GFP-Ctrl (b)
PLB p47phox(R43Q)-GFP-fMLF (d)
0
20
40
60
80
100
120
140
Time (min)

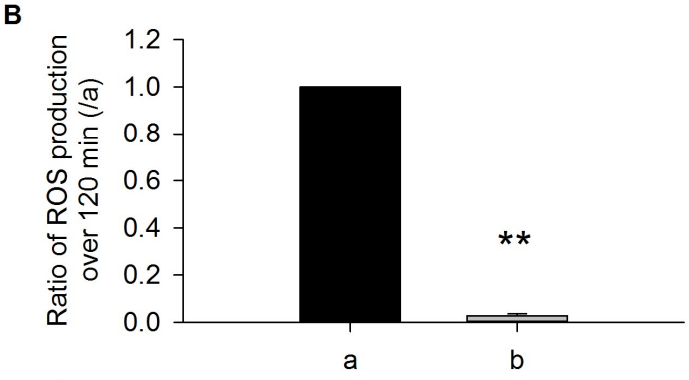
B
Ratio of ROS production over 120 min (/a)
1.2
1.0
0.8
0.6
0.4
0.2
0.0
**
a
b

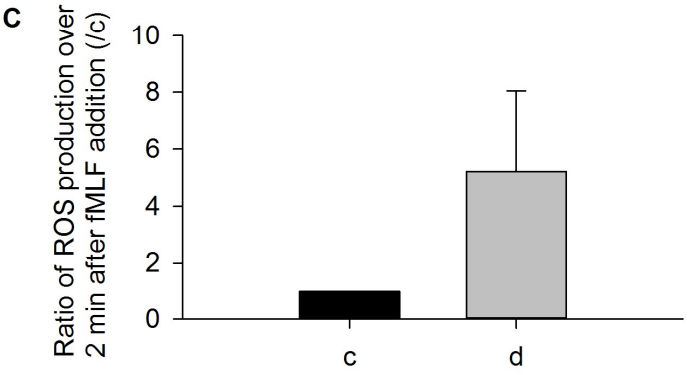
C
Ratio of ROS production over 2 min after fMLF addition (/c)
10
8
6
4
2
0
c
d

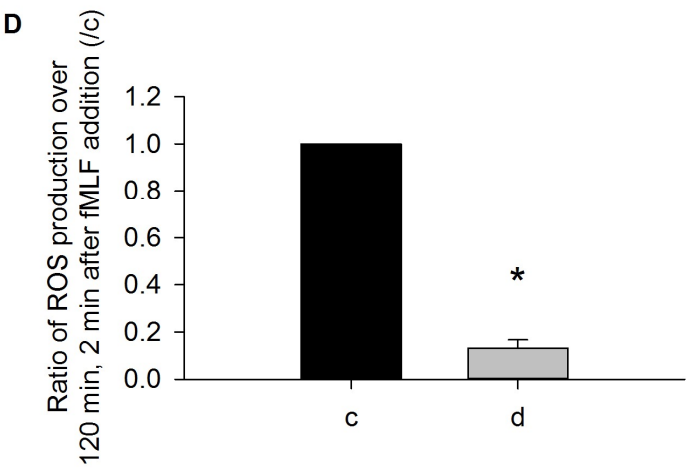
D
Ratio of ROS production over 120 min, 2 min after fMLF addition (/c)
1.2
1.0
0.8
0.6
0.4
0.2
0.0
*
c
d

Figure 15. Differentiated PLB p47^{phox}(R43Q)-GFP cells does not produce ROS in response to fibrinogen.

(A-C) Differentiated PLB p47^{phox}(R43Q)-GFP cells or PLB citrine cells were plated in fibrinogen-coated wells. Chemiluminescence was measured every 1 min except between 6 and 22 min, where it was measured every 0,4min. (A) 1 µM fMLF was added at 6 min. a) PLB citrine cells without fMLF addition. b) PLB p47^{phox}(R43Q)-GFP cells without fMLF addition. c) PLB citrine cells with fMLF addition. d) PLB p47^{phox}(R43Q)-GFP cells with fMLF addition. (B) Ratio of ROS production in the second phase, i.e. over 120 min in PLB p47^{phox}(R43Q)-GFP cells (b) compared to that in PLB citrine cells (a). (C) Ratio of ROS production during the first phase, i.e. over 2 min with the addition of fMLF in PLB p47^{phox}(R43Q)-GFP cells (d) compared to that in PLB citrine cells (c). (D) Ratio of ROS production in the second phase, i.e. over 120 min in PLB p47^{phox}(R43Q)-GFP cells (d) compared to that in PLB citrine cells (c). Data are means ± SEM. n=3, *P<0.01, ** P<0.01. (ratio paired t test).

Discussion

In this study, we investigated the role of Class I PI3K in adhesion (fibrinogen) dependent ROS production by neutrophils. Neutrophil adhesion to fibrinogen is mediated by integrin. A previous study shows that Class I PI3K is essential for the activation of the integrin-mediated ROS production [8]. Our findings show that Class I PI3K plays an important role in sustaining the integrin-mediated NADPH oxidase activation by neutrophils.

We found that immobilized fibrinogen triggers the ROS production by neutrophil-like PLB cells and human neutrophils. It has been shown that immobilized fibrinogen, but not soluble fibrinogen, has a high affinity for leukocytes, and that the interaction is mediated by αMβ2 integrin, poorly binds to leukocytes [5, 6, 37]. Fibrinogen is made of two sets of three polypeptide chains named Aα, Bβ and γ, which form two outer D-domain and a central E-domain. αMβ2 integrin binds to the D-domain at a site corresponding to γ190-202 (which is called P1) and γ377-395 (which is called P2) [38]. It has been hypothesized that immobilized fibrinogen undergoes a conformational change, which exposes the P2 domain for higher binding to αMβ2 integrin [39-42]. As Fibrinogen is normally present in human blood plasma at 1.5-3.5 g/l [43], the conformational change between immobilized fibrinogen and soluble fibrinogen may play an important role to prevent the formation of clot leading to thrombosis. Immobilized fibrinogen can trigger the ROS production by human monocytes [44] and murine neutrophils [10]. We also detected ROS production by un-primed neutrophil-like PLB cells (**Figure 1 and 2**) and human neutrophils (**Figure 4**). The level of integrin-mediated ROS production (**Figure 4**) was strikingly lower (~20 fold lower) than that upon pre-activation by fMLF human neutrophils (**Figure 5**). The low level of integrin-mediated ROS production may be important for neutrophils signalling, as ROS are important second messengers. ROS modulate the specific and reactive cysteine residues of low pKa in redox-sensitive target proteins leading to reversible or irreversible modifications of the enzymatic activity. Then, this low level of ROS may also be important to sustain the cell adhesion in neutrophils and regulate integrin signalling. It has been shown that ROS are able to promote adhesion of neutrophils by triggering β2 integrins expression on the surface of neutrophils [45]. ROS can also regulate integrin signalling through the oxidation of Src that is activated by oxidation [46].

The stimulation by fMLF of neutrophil-like PLB cells did not increase the integrin-mediated ROS, whereas, fMLF stimulation triggered a great increase in ROS production for human

neutrophils. Several hypothesis may explain this difference between neutrophils and PLB cells: 1) The αMβ2 integrins are the most abundant integrins in neutrophils, however other integrins may also contribute to the integrin-mediated ROS production. αVβ3 integrins also mediate the adhesion between neutrophils and fibrinogen (or fibronectin). It has been reported that neutrophil adhesion suppresses ROS production, which was αVβ3-dependent [48]. These integrins may be different between PLB cells and human neutrophils. 2) It has been reported that the expression of primary granules was increased after DMSO mediated differentiation in PLB cells [49]. But less information is available about the expression of peroxidase-negative granules (secondary and tertiary granules) and secretory vesicles. αMβ2 integrins, fMLF receptors and the NADPH oxidase membrane subunits are stored in these peroxidase-negative granules and secretory vesicles. The granules and vesicles fuse with the membrane upon fMLF activation [50]. There may be less granules positive for αMβ2 integrins, fMLF receptors and the NADPH oxidase membrane subunits in neutrophil-like PLB cells compared to human blood neutrophils. So the neutrophils, activated by fMLF, have an higher capacity to mobilize αMβ2 integrins, fMLF receptors and the NADPH oxidase at the plasma membrane.

It has been shown that the activation of integrin-mediated ROS production is dependent on Class I PI3K [8]. During the process of integrin-mediated ROS production, we added a class IA PI3K inhibitor, LY294002, which completely blocked the integrin-mediated ROS production by neutrophil-like PLB cells (**Figure 3**) and human neutrophils (**Figure 4 and 5**) with or without fMLF stimulation. This suggests that Class IA PI3K is essential to maintain the integrin-mediated ROS production. Class I PI3K works as heterodimer including a 110 kDa catalytic subunit (p110α, p110β, p110γ, or p110δ) and a regulatory subunit. P110α, p110β, and p110δ are classified to Class IA PI3K and p110γ belongs to Class IB PI3K. This classification is based on sequence similarity [13]. There are two phases of ROS production in adherent neutrophils upon fMLF activation. The ROS production of the second phase is adhesion dependent. Experiments based with selective inhibitors have shown that both phase of ROS production triggered by fMLF are dependent on Class IA PI3K p110α and p110δ in human neutrophils. Deficiency of p110γ in murine neutrophils leads to a total suppression of early ROS production in response to fMLF but does not affect the adhesion dependent ROS production [8]. Thus different isoforms of Class I PI3K may have different roles in the NADPH oxidase activation, however the function of the different isoforms in maintaining the ROS production still need further investigation.

We will use inhibitors against specific isoform of Class IA PI3K to investigate which isoform is required in maintaining the integrin-mediated ROS production: Alpelisib (BYL719) against p110α, TGX-221 against p110β, and Idelalisib (CAL-101, GS-1101) or GSK2269557 against p110δ.

We found that all the cytosolic subunits contributed to the integrin-mediated ROS production. They are distributed in puncta at the plasma membrane (**Figure 6-11**). It has been reported that $p40^{phox}$ is not needed to induce a high level of NADPH oxidase activity on the plasma membrane or in cell-free system [51-53]. We found that $p40^{phox}$ participated in the integrin-mediated ROS production at the plasma membrane (**Figure 6 and 11**). Previous studies also show that $p40^{phox}$ enhance the recruitment of $p47^{phox}$ and $p67^{phox}$ to the plasma membrane after PMA stimulation [54]. We have reported that PI3P play an important role to maintain the $p67^{phox}$ at the phagosomal membrane to sustain the ROS production via the binding of PI3P to the PX domain of $p40^{phox}$ [28]. However, there is low (or no) PI3P at the plasma membrane (unpublished data). Thus the presence of $p40^{phox}$ in the NADPH oxidase complex at the plasma membrane may be due to the interaction with $p67^{phox}$, which forms a very tight complex by their respective PB1 (Phox and Bem1) domain [55, 56]. The role of $p40^{phox}$ in integrin-mediated NADPH oxidase activation still needs further investigation. *The experiments that we plan to do are described in the general discussion part.* After adding the Class I PI3K inhibitor LY294002, immunofluorescence experiment showed that the levels of endogenous $p47^{phox}$ and $p67^{phox}$ at the plasma membrane decreased (**Figure 12**). In the TIRF experiment, all three fluorescence-tagged cytosolic subunits left the plasma membrane after the addition of the inhibitor LY294002 (**Figure 9-11**). These results suggest that Class IA PI3K is critical to maintain the cytosolic subunits at the plasma membrane. Thus we next investigated how Class I PI3K sustains the cytosolic subunits at the plasma membrane.

Class I PI3K generates $PI(3,4,5)P_3$ and $PI(3,4)P_2$ at the plasma membrane. $PI(3,4,5)P_3$ recruits or activates GEFs for Rac, which is essential for NADPH oxidase activation. It has been reported that GEFs such as P-Rex1, Vav1 and DOCK2 are important for the NADPH oxidase activation [57, 58]. The ability of Rac1 and Rac2 to support $O_2^{\cdot-}$ production is similar in reconstituted cell-free systems using purified proteins [11]. Our results indicate that active Rac1 enhances integrin-dependent NADPH oxidase activation but cannot prevent its de-activation by Class IPI3K inhibitor. R43 and R90 in the PX domain of $p47^{phox}$, which bind to 3-phosphate and 4-phosphate respectively, are critical for the $PI(3,4)P_2$ binding [18]. Li *et al.* show that the PX domain of $p47^{phox}$ is important for the NADPH activation at the plasma

membrane. The $p47^{phox}$ R43A and R90A mutations induce a reduction of PMA stimulated ROS production by respectively 50% and 70% in K562 cells. Suspended neutrophils, from a $p47^{phox}$ KO mouse expressing $p47^{phox}$-R90K, showed, upon stimulation by fMLF, a reduction of NADPH oxidase activity by 37% compared to $p47^{phox}$ KO mouse expressing $p47^{phox}$ WT [27]. However, the role of the PX domain of $p47^{phox}$ in integrin-mediated ROS production has not been investigated. The $p47^{phox}$ PX mutant totally blocked the integrin-mediated ROS production, which suggests the binding between $PI(3,4)P_2$ and PX domain of $p47^{phox}$ is critical to maintain the ROS production. Surprisingly, R43Q mutation didn't inhibit the first phase of fMLF stimulated ROS production but the second one which is adhesion-dependent. The first phase of ROS production is very rapid and may not need a stabilization of the NOX complex at the plasma membrane. *We plan to modify the $PI(3,4)P_2$ level at the plasma membrane using molecular tool to study the role of $PI(3,4)P_2$ in maintaining the integrin-mediated ROS production. The experiments are described in general discussion.* .

Phosphorylation of $p47^{phox}$ is also required for the NADPH oxidase activation. Hoyal *et al.* found that Akt (protein kinase B) activated the NADPH oxidase *in vitro* by phosphorylating serine S304 and S328 of $p47^{phox}$ [59]. It is well known that the activation of Akt depends on PI3K. However, another study showed that Akt was unable to catalyze $p47^{phox}$ *in vitro* kinase assay, they suggested that the phosphorylation of $p47^{phox}$ was dependent on the cPKC and PKCδ after fMLF stimulation [60]. Moreover, it is still not clear if the integrin-mediated ROS production needs persistent phosphorylation of $p47^{phox}$ dependent or not on PI3K. *In order to investigate this, we plan to check the phosphorylation states of Akt and $p47^{phox}$ with or without adding Class IA inhibitor LY294002.*

The acute phase of the inflammatory response involves an increased concentration of fibrinogen and multiple pro-inflammatory mediators. A pro-inflammatory role for fibrinogen has been reported in vascular wall disease, stroke, spinal cord injury, brain trauma, multiple sclerosis, Alzheimer's disease, rheumatoid arthritis, bacterial infection, colitis, lung and kidney fibrosis, Duchenne muscular dystrophy, and several types of cancer. Fibrinogen is considered as an acute-phase reactant. The concentration of fibrinogen in plasma range from 2 to 4 g/l under physiological conditions. However, the blood concentration of fibrinogen increases several fold in pathological conditions, such as after injury or disease associated with vascular disruption, infection, or inflammation [61]. Thus it is important to understand the pro-inflammatory role of fibrinogen. In this study, we find that immobilized fibrinogen can trigger integrin-mediated ROS production by neutrophils, the low level ROS signal may

be an important inflammation signal to recruit or activate other immune cells. In conclusion, our work suggests that Class I PI3K is essential to maintain the integrin-mediated NADPH oxidase activation through $p47^{phox}$ PX domain binding to $PI(3,4)P_2$.

References

1. Borregaard, N. (2010) Neutrophils, from marrow to microbes. Immunity 33, 657-70.
2. Mayadas, T. N. and Cullere, X. (2005) Neutrophil beta2 integrins: moderators of life or death decisions. Trends Immunol. 26, 388-95.
3. Arnaout, M. A. (2016) Biology and structure of leukocyte beta 2 integrins and their role in inflammation. F1000Res 5.
4. Weisel, J. W. (2005) Fibrinogen and fibrin. Adv. Protein Chem. 70, 247-99.
5. Loike, J. D., Silverstein, R., Wright, S. D., Weitz, J. I., Huang, A. J., Silverstein, S. C. (1992) The role of protected extracellular compartments in interactions between leukocytes, and platelets, and fibrin/fibrinogen matrices. Ann. N. Y. Acad. Sci. 667, 163-72.
6. Lishko, V. K., Kudryk, B., Yakubenko, V. P., Yee, V. C., Ugarova, T. P. (2002) Regulated unmasking of the cryptic binding site for integrin alpha M beta 2 in the gamma C-domain of fibrinogen. Biochemistry 41, 12942-51.
7. Rubel, C., Gómez, S., Fernández, G. C., Isturiz, M. A., Caamaño, J., Palermo, M. S. (2003) Fibrinogen-CD11b/CD18 interaction activates the NF-κB pathway and delays apoptosis in human neutrophils. Eur. J. Immunol. 33, 1429-1438.
8. Fumagalli, L., Campa, C. C., Germena, G., Lowell, C. A., Hirsch, E., Berton, G. (2013) Class I Phosphoinositide-3-Kinases and Src Kinases Play a Nonredundant Role in Regulation of Adhesion-Independent and -Dependent Neutrophil Reactive Oxygen Species Generation. The Journal of Immunology 190, 3648-3660.
9. Berton, G., Laudanna, C., Sorio, C., Rossi, F. (1992) Generation of signals activating neutrophil functions by leukocyte integrins: LFA-1 and gp150/95, but not CR3, are able to stimulate the respiratory burst of human neutrophils. J. Cell Biol. 116, 1007-17.
10. McMillan, S. J., Sharma, R. S., Richards, H. E., Hegde, V., Crocker, P. R. (2014) Siglec-E Promotes 2-Integrin-dependent NADPH Oxidase Activation to Suppress Neutrophil Recruitment to the Lung. J. Biol. Chem. 289, 20370-20376.
11. Groemping, Y. and Rittinger, K. (2005) Activation and assembly of the NADPH oxidase: a structural perspective. Biochem. J. 386, 401-16.
12. Robinson, J. M. (2009) Phagocytic leukocytes and reactive oxygen species. Histochem. Cell Biol. 131, 465-9.

13. Balla, T. (2013) Phosphoinositides: tiny lipids with giant impact on cell regulation. Physiol. Rev. 93, 1019-137.

14. Campa, C. C., Ciraolo, E., Ghigo, A., Germena, G., Hirsch, E. (2015) Crossroads of PI3K and Rac pathways. Small GTPases 6, 71-80.

15. Garvey, W. T. (2004) Mechanisms of Insulin Signal Transduction.

16. El-Benna, J., Dang, P. M., Gougerot-Pocidalo, M. A., Marie, J. C., Braut-Boucher, F. (2009) p47phox, the phagocyte NADPH oxidase/NOX2 organizer: structure, phosphorylation and implication in diseases. Exp. Mol. Med. 41, 217-25.

17. Faure, M. C., Sulpice, J. C., Delattre, M., Lavielle, M., Prigent, M., Cuif, M. H., Melchior, C., Tschirhart, E., Nusse, O., Dupre-Crochet, S. (2013) The recruitment of p47(phox) and Rac2G12V at the phagosome is transient and phosphatidylserine dependent. Biol. Cell. 105, 501-18.

18. Karathanassis, D., Stahelin, R. V., Bravo, J., Perisic, O., Pacold, C. M., Cho, W., Williams, R. L. (2002) Binding of the PX domain of p47phox to phosphatidylinositol 3,4-bisphosphate and phosphatidic acid is masked by an intramolecular interaction. The EMBO Journal 21, 5057-5068.

19. Groemping, Y., Lapouge, K., Smerdon, S. J., Rittinger, K. (2003) Molecular basis of phosphorylation-induced activation of the NADPH oxidase. Cell 113, 343-55.

20. Yuzawa, S., Ogura, K., Horiuchi, M., Suzuki, N. N., Fujioka, Y., Kataoka, M., Sumimoto, H., Inagaki, F. (2004) Solution structure of the tandem Src homology 3 domains of p47phox in an autoinhibited form. J. Biol. Chem. 279, 29752-60.

21. Yuzawa, S., Suzuki, N. N., Fujioka, Y., Ogura, K., Sumimoto, H., Inagaki, F. (2004) A molecular mechanism for autoinhibition of the tandem SH3 domains of p47phox, the regulatory subunit of the phagocyte NADPH oxidase. Genes Cells 9, 443-56.

22. Ago, T., Kuribayashi, F., Hiroaki, H., Takeya, R., Ito, T., Kohda, D., Sumimoto, H. (2003) Phosphorylation of p47phox directs phox homology domain from SH3 domain toward phosphoinositides, leading to phagocyte NADPH oxidase activation. Proc. Natl. Acad. Sci. U. S. A. 100, 4474-9.

23. Hiroaki, H., Ago, T., Ito, T., Sumimoto, H., Kohda, D. (2001) Solution structure of the PX domain, a target of the SH3 domain. Nat. Struct. Biol. 8, 526-30.

24. Nobuhisa, I., Takeya, R., Ogura, K., Ueno, N., Kohda, D., Inagaki, F., Sumimoto, H. (2006) Activation of the superoxide-producing phagocyte NADPH oxidase requires co-operation between the tandem SH3

domains of p47phox in recognition of a polyproline type II helix and an adjacent alpha-helix of p22phox. Biochem. J. 396, 183-92.

25. Ogura, K., Nobuhisa, I., Yuzawa, S., Takeya, R., Torikai, S., Saikawa, K., Sumimoto, H., Inagaki, F. (2006) NMR solution structure of the tandem Src homology 3 domains of p47phox complexed with a p22phox-derived proline-rich peptide. J. Biol. Chem. 281, 3660-8.
26. Ago, T., Takeya, R., Hiroaki, H., Kuribayashi, F., Ito, T., Kohda, D., Sumimoto, H. (2001) The PX domain as a novel phosphoinositide- binding module. Biochem. Biophys. Res. Commun. 287, 733-8.
27. Li, X. J., Marchal, C. C., Stull, N. D., Stahelin, R. V., Dinauer, M. C. (2010) p47phox Phox Homology Domain Regulates Plasma Membrane but Not Phagosome Neutrophil NADPH Oxidase Activation. J. Biol. Chem. 285, 35169-35179.
28. Song, Z. M., Bouchab, L., Hudik, E., Le Bars, R., Nusse, O., Dupre-Crochet, S. (2017) Phosphoinositol 3-phosphate acts as a timer for reactive oxygen species production in the phagosome. J. Leukoc. Biol.
29. Tlili, A., Erard, M., Faure, M. C., Baudin, X., Piolot, T., Dupre-Crochet, S., Nusse, O. (2012) Stable accumulation of p67phox at the phagosomal membrane and ROS production within the phagosome. J. Leukoc. Biol. 91, 83-95.
30. Benna, J. E., Dang, P. M., Gaudry, M., Fay, M., Morel, F., Hakim, J., Gougerot-Pocidalo, M. A. (1997) Phosphorylation of the respiratory burst oxidase subunit p67(phox) during human neutrophil activation. Regulation by protein kinase C-dependent and independent pathways. J. Biol. Chem. 272, 17204-8.
31. Inoue, T., Heo, W. D., Grimley, J. S., Wandless, T. J., Meyer, T. (2005) An inducible translocation strategy to rapidly activate and inhibit small GTPase signaling pathways. Nature methods 2, 415-8.
32. Hammond, G. R., Machner, M. P., Balla, T. (2014) A novel probe for phosphatidylinositol 4-phosphate reveals multiple pools beyond the Golgi. J. Cell Biol. 205, 113-26.
33. Kennedy, M. J., Hughes, R. M., Peteya, L. A., Schwartz, J. W., Ehlers, M. D., Tucker, C. L. (2010) Rapid blue-light–mediated induction of protein interactions in living cells. Nature Methods 7, 973-975.
34. Vazquez, F., Grossman, S. R., Takahashi, Y., Rokas, M. V., Nakamura, N., Sellers, W. R. (2001) Phosphorylation of the PTEN Tail Acts as an Inhibitory Switch by Preventing Its Recruitment into a Protein Complex. J. Biol. Chem. 276, 48627-48630.
35. Nishinaka, Y., Aramaki, Y., Yoshida, H., Masuya, H., Sugawara, T., Ichimori, Y. (1993) A New Sensitive Chemiluminescence Probe, L-012, for Measuring the Production of Superoxide Anion by Cells. Biochem. Biophys. Res. Commun. 193, 554-559.

36. Nathan, C. F. (1987) Neutrophil activation on biological surfaces. Massive secretion of hydrogen peroxide in response to products of macrophages and lymphocytes. J. Clin. Invest. 80, 1550-1560.

37. Mosesson, M. W. (2005) Fibrinogen and fibrin structure and functions. J. Thromb. Haemost. 3, 1894-904.

38. Ugarova, T. P., Solovjov, D. A., Zhang, L., Loukinov, D. I., Yee, V. C., Medved, L. V., Plow, E. F. (1998) Identification of a novel recognition sequence for integrin alphaM beta2 within the gamma-chain of fibrinogen. J. Biol. Chem. 273, 22519-27.

39. Yakovlev, S., Zhang, L., Ugarova, T., Medved, L. (2005) Interaction of fibrin(ogen) with leukocyte receptor alpha M beta 2 (Mac-1): further characterization and identification of a novel binding region within the central domain of the fibrinogen gamma-module. Biochemistry 44, 617-26.

40. Yakovlev, S., Litvinovich, S., Loukinov, D., Medved, L. (2000) Role of the beta-strand insert in the central domain of the fibrinogen gamma-module. Biochemistry 39, 15721-9.

41. Yakovlev, S., Makogonenko, E., Kurochkina, N., Nieuwenhuizen, W., Ingham, K., Medved, L. (2000) Conversion of fibrinogen to fibrin: mechanism of exposure of tPA- and plasminogen-binding sites. Biochemistry 39, 15730-41.

42. Yakovlev, S., Loukinov, D., Medved, L. (2001) Structural and functional role of the beta-strand insert (gamma 381-390) in the fibrinogen gamma-module. A "pull out" hypothesis. Ann. N. Y. Acad. Sci. 936, 122-4.

43. Pulanic, D. and Rudan, I. (2005) The past decade: fibrinogen. Coll. Antropol. 29, 341-9.

44. Trezzini, C., Jungi, T. W., Maly, F. E., Vittoz, M., Peterhans, E. (1989) Low-affinity interaction of fibrinogen carboxy-gamma terminus with human monocytes induces an oxidative burst and modulates effector functions. Biochem. Biophys. Res. Commun. 165, 7-13.

45. Serrano, C. V., Mikhail, E. A., Wang, P., Noble, B., Kuppusamy, P., Zweier, J. L. (1996) Superoxide and hydrogen peroxide induce CD18-mediated adhesion in the postischemic heart. Biochimica et Biophysica Acta (BBA) - Molecular Basis of Disease 1316, 191-202.

46. Giannoni, E. and Chiarugi, P. (2014) Redox Circuitries Driving Src Regulation. Antioxidants & Redox Signaling 20, 2011-2025.

47. Ashkenazi, A. and Marks, R. S. (2009) Luminol-dependent chemiluminescence of human phagocyte cell lines: comparison between DMSO differentiated PLB 985 and HL 60 cells. Luminescence 24, 171-177.

48. Kim, H.-Y., Skokos, E. A., Myer, D. J., Agaba, P., Gonzalez, A. L. (2014) αVβ3 Integrin Regulation of Respiratory Burst in Fibrinogen Adherent Human Neutrophils. Cell. Mol. Bioeng. 7, 231-242.

49. Tucker, K. A., Lilly, M. B., Heck, L., Jr., Rado, T. A. (1987) Characterization of a new human diploid myeloid leukemia cell line (PLB-985) with granulocytic and monocytic differentiating capacity. Blood 70, 372-8.

50. Borregaard, N., Kjeldsen, L., Sengelov, H., Diamond, M. S., Springer, T. A., Anderson, H. C., Kishimoto, T. K., Bainton, D. F. (1994) Changes in subcellular localization and surface expression of L-selectin, alkaline phosphatase, and Mac-1 in human neutrophils during stimulation with inflammatory mediators. J. Leukoc. Biol. 56, 80-7.

51. Matute, J. D., Arias, A. A., Dinauer, M. C., Patino, P. J. (2005) p40phox: the last NADPH oxidase subunit. Blood Cells Mol. Dis. 35, 291-302.

52. de Mendez, I. and Leto, T. L. (1995) Functional reconstitution of the phagocyte NADPH oxidase by transfection of its multiple components in a heterologous system. Blood 85, 1104-10.

53. Price, M. O., McPhail, L. C., Lambeth, J. D., Han, C. H., Knaus, U. G., Dinauer, M. C. (2002) Creation of a genetic system for analysis of the phagocyte respiratory burst: high-level reconstitution of the NADPH oxidase in a nonhematopoietic system. Blood 99, 2653-61.

54. Kuribayashi, F., Nunoi, H., Wakamatsu, K., Tsunawaki, S., Sato, K., Ito, T., Sumimoto, H. (2002) The adaptor protein p40(phox) as a positive regulator of the superoxide-producing phagocyte oxidase. EMBO J. 21, 6312-20.

55. Ito, T., Matsui, Y., Ago, T., Ota, K., Sumimoto, H. (2001) Novel modular domain PB1 recognizes PC motif to mediate functional protein-protein interactions. EMBO J. 20, 3938-46.

56. Nakamura, R., Sumimoto, H., Mizuki, K., Hata, K., Ago, T., Kitajima, S., Takeshige, K., Sakaki, Y., Ito, T. (1998) The PC motif: a novel and evolutionarily conserved sequence involved in interaction between p40phox and p67phox, SH3 domain-containing cytosolic factors of the phagocyte NADPH oxidase. Eur. J. Biochem. 251, 583-9.

57. Lawson, C. D., Donald, S., Anderson, K. E., Patton, D. T., Welch, H. C. (2011) P-Rex1 and Vav1 cooperate in the regulation of formyl-methionyl-leucyl-phenylalanine-dependent neutrophil responses. J. Immunol. 186, 1467-76.

58. Kunisaki, Y., Nishikimi, A., Tanaka, Y., Takii, R., Noda, M., Inayoshi, A., Watanabe, K., Sanematsu, F., Sasazuki, T., Sasaki, T., Fukui, Y. (2006) DOCK2 is a Rac activator that regulates motility and polarity

during neutrophil chemotaxis. J. Cell Biol. 174, 647-52.

59. Hoyal, C. R., Gutierrez, A., Young, B. M., Catz, S. D., Lin, J. H., Tsichlis, P. N., Babior, B. M. (2003) Modulation of p47PHOX activity by site-specific phosphorylation: Akt-dependent activation of the NADPH oxidase. Proceedings of the National Academy of Sciences 100, 5130-5135.

60. Yamamori, T., Inanami, O., Nagahata, H., Kuwabara, M. (2004) Phosphoinositide 3-kinase regulates the phosphorylation of NADPH oxidase component p47phox by controlling cPKC/PKCδ but not Akt. Biochem. Biophys. Res. Commun. 316, 720-730.

61. Davalos, D. and Akassoglou, K. (2012) Fibrinogen as a key regulator of inflammation in disease. Semin. Immunopathol. 34, 43-62.

CHAPTER FOUR: General discussion and perspectives

In this study, we investigate the role of phosphoinositides in the regulation of NADPH oxidase at the phagosomal or plasma membrane. We found that PI3P is critical to sustain the ROS production at the phagosomal membrane and PI(3,4)P_2 is essential to maintain the integrin-mediated ROS production at the plasma membrane. Our findings demonstrate that phosphoinositides could accurately regulate the activation of the NADPH oxidase during infection or inflammation. Our work explains how the ROS production is maintained and suggests possible targets in medical treatment and new drug development. In the first and second section of the discussion, additional observations are discussed about the first and second studies. In the third section, modulations of the phosphoinositides are discussed. The fourth section consists of an integrated discussion about the whole study.

4.1 ROS production in the phagosome

4.1.1 Not all phagosomes produce ROS

The mechanism between phagocytosis and activation of the NADPH oxidase is still not clear. In our study, we found that only half of the serum opsonized zymosan phagosomes are $p67^{phox}$-citrine or $p40^{phox}$-citrine positive. In the immunofluorescence experiment with MTM1, we also found that only half of these phagosomes are MTM1 positive phagosomes. These results suggest that phagocytosis does not always activate the NADPH oxidase. Li *et al.* showed that only 52 or 53% of internalized IgG-zymosan phagosomes exhibited accumulation of $p67^{phox}$-YFP or YFP-p47PRR, respectively, whereas the PI(3)P probe YFP-p40PX was present on 65% of IgG-zymosan phagosomes in neutrophil-like PLB cells (Li et al., 2009b). Tlili *et al.* observed the same percentage (~50%) of $p67^{phox}$-citrine accumulation on decomplemented human serum opsonized zymosan phagosomes (Tlili et al., 2012). Underhill *et al.* observed that although nearly all IFN-γ activated macrophages (~80%) internalized zymosan particles, only some cells (~40%) were stained with anti–phospho-Syk by using flow cytometry (Underhill, 2005). This suggests not all macrophages can activate the NADPH oxidase. Heterogeneity among phagosomes may be due to the receptor clustering or density, which may be sufficient for ligands to trigger phagocytosis but not NADPH oxidase activity (Nunes et al., 2013). Another question is about the communication between the phagosomes. In our experiment, we observed that some phagosomes fused with other phagosomes. Whether the fusion of the NADPH oxidase active phagosomes will trigger the

activation of the NADPH oxidase of the non-active phagosomes is still not known. Several hypothesis can be made: 1) If the NADPH oxidase of the active phagosome is still assembled at the time of the fusion, then it can pursue the ROS production in the new phagosome. 2) The flavocytochrome b_{558} that already works in active phagosome may be oxidized and removed by formation of inward or outward vesicles after fusion, so the cytosolic subunits may be used by flavocytochrome b_{558} of previously non active phagosome. Phagosomes heterogeneity also raises a problem: during infection, are all the pathogens effectively killed? Anyway, a multiple number of microbes have special strategies to escape killing by phagocytosis.

4.1.2 Phagosome, endosome and generation of PI3P

For all eukaryotic cells, endocytosis is essential to internalize macromolecules and proteins including receptors, channels and transporters from plasma membrane. Thus endocytosis controls the levels of receptors at the cell surface and regulates their signalling (Watanabe and Boucrot, 2017). Early endosomes are characterized by several markers such as the early endosomal antigen 1 (EEA1), the Class III PI3K Vps34 and the small GTPase Rab5. Late endosomes, which are also known as multivesicular bodies (MVBs), are marked by another small GTPase Rab7 (Spang, 2009). Lysosomes are membrane-bound organelles which can be distinguished from endosomes by the lack of mannose-6-phosphate receptors (MPRs). Lysosomes contain acid hydrolases, and proton-pumping vacuolar ATPases, which maintain the luminal environment at a pH of 4.6-5.0. Lysosomes are regarded as the terminal degradative compartment of the endocytic pathway (Luzio et al., 2007). Phagosomes are able to fuse with early endosomes, late endosomes and lysosomes *in vitro* (Jahraus et al., 1998; Mayorga et al., 1991; Peyron et al., 2001). PI3P is mostly found on the cytosolic leaflet of early endosome membranes. PI3P is generated mainly by a class III PI3K Vps34. Vps34-Vps15 complex is recruited to the early endosomes via direct binding between Rab5 and Vps15 (Christoforidis et al., 1999; Murray et al., 2002). Vps34-Vps15 complex is associated with Beclin and UVRAG, a positive regulator of Vps34 (Backer, 2016). The Vps34-Vps15 complex also interacts with Rab7 in the late endosomes (Stein et al., 2003).Rubicon can bind UVRAG and Vps34. Rubicon has been shown to inhibit UVRAG dependent activation of Vps34 (Sun et al., 2011). Active Rab7 competes for Rubicon binding, which causes the release of UVRAG. When active Rab7 links Rubicon then UVRAG can activate Vps34 in the Beclin, Vps34, Vps15 complex and can also link the HOPS complex to activate more Rab7 (Stein et al., 2003). In mouse RAW 264.7 macrophages, GFP–Rab5 translocated to the

nascent and early phagosomes. However, GFP–Rab5 has not been shown to be accumulated at the phagosomes of serum opsonized zymosan in human and mouse neutrophils (Minakami et al., 2010). GFP–Rab7, in human and mouse neutrophils, is accumulated at the early phagosome, whereas it is absent from the phagocytic cup or nascent phagosome (Minakami et al., 2010). How Vps34 is recruited to the phagosome in neutrophils: is it directly or via fusion with endosome, or in both way? The direct recruitment of Vps34 to the phagosome could be via Rab7. Neutrophil granules also contain Rab7 (Lominadze, 2005), which provide, upon fusion with the phagosome, Rab7 to the phagosomal membrane.

4.1.3 Downregulation of the PI3P and the NADPH oxidase

We found that the stay time of $p67^{phox}$ and $p40^{phox}$ is the same as time of PI3P presence, and we have shown that PI3P acts as a timer for the ROS production. Recently, Bagaitkar *et al.* reported that mice expressing $p40^{phox}$ R58A (deficient in PI3P binding) had impaired macrophage NADPH oxidase activity. $P40^{phox}$R58A/R58A macrophages exhibited diminished phagosome ROS in response to IgG-opsonized particles (Bagaitkar et al., 2017). So the regulation of NADPH oxidase activity seems to be dependent of the regulation of PI3P. We observed that both MTM1 and Rubicon accumulated at the phagosome and demonstrated that the two proteins participate in the downregulation of PI3P at the phagosome. PI3P is also phosphorylated by PIKFYVE to generate $PI(3,5)P_2$ (Balla, 2013). Moreover, PI3P can bind and regulate a numerous proteins (**Table 6**). So, there may be others proteins that play a role in its downregulation. The investigation of the PI3P regulation at the phagosome membrane will be a challenging work.

4.2 ROS production in adherent neutrophils

4.2.1 Neutrophils and biomaterials

Biomaterials are widely used in implant and surgery. Neutrophils and other immune cells have key functions in the devastating inflammatory reactions associated with rejection of transplanted grafts and foreign bodies (Liu et al., 1997). During neutrophil purification, in general, it is better to use polypropylene than polystyrene, because polystyrene is more sticky (*from laboratory page of John R. Gordon, Ph.D.* http://homepage.usask.ca/~jrg426/manualrbclysis.html) and may activate the neutrophils (Bulger et al., 2001). We used polypropylene materials for the neutrophils purification.

During adhesion assay, most laboratories use polystyrene plate. In order to avoid the artificial effect of the materials (polystyrene) and in order to set up better conditions, we tested both plates (polystyrene and polypropylene). We did not observe ROS production of neutrophil-like PLB cells incubated in uncoated polypropylene plates and polystyrene plates. However, we did observe ROS production of human neutrophils incubated in uncoated polypropylene plates and polystyrene plates but not plates coated with heat-inactivated serum. It has been reported that neutrophil adhesion to uncoated or plasma-coated polytetrafluoroethylene (ePTFE) and Dacron surfaces, but not to uncoated or protein-coated polystyrene surfaces, triggered ROS production and non-apoptotic cell death *in vitro* and *in vivo.* Nadzam *et al.* observed increased membrane permeability and cytoplasmic degeneration without DNA fragmentation. This process was named "snyxenatosis" (Nadzam et al., 2000). Then Chang *et al.* found that neutrophil adhesion to roughened polystyrene triggered rapid ROS production and precipitated a non-apoptotic cell death. This suggested that neutrophils survival and ROS production on biomaterials is determined by surface topography and materials (Chang et al., 2003). "Snyxenatosis" may be NETosis, which was discovered by Brinkmann *et al.* later (Brinkmann et al., 2004). Recently, Jhunjhunwala *et al.* demonstrated that neutrophils respond to sterile implant materials. They implanted microcapsules in the peritoneal cavity of mice. These microcapsules (more than 200 μm in diameter) were too large to be taken up by neutrophils. They observed neutrophil extracellular traps on the surface of polystyrene or poly (methyl-methacrylate) or alginate microcapsules (Palaniyar et al., 2015). However, to perform an experiment *in vitro*, people cannot avoid using biomaterials. Polystyrene and polypropylene are still the most frequently used materials in biological research. The mechanism of how neutrophils interact with different materials are still unknown. Even which receptor mediate the adhesion event is not sure, as neither β2 integrins nor Fc receptor inhibitory antibodies prevent neutrophil adhesion to the uncoated surfaces of polytetrafluoroethylene, Dacron, glass, or polystyrene (Chang et al., 2003). Biomaterials are covered with a layer of plasma proteins, predominately albumin, fibrinogen, IgG, fibronectin, and von Willebrand factor shortly after implantation (Thevenot et al., 2008). Thus studing the interaction between the biomaterials and neutrophils may be quite important for surgery and implant, because biomaterials affect the ROS production and survival of neutrophils.

4.2.2 What is the function of the integrin mediated ROS?

In our study, we observed that the production of ROS, triggered by fibrinogen, lasted as long

as 1 hour. What is the role of this integrin mediated ROS production? Does it maintain the neutrophil adhesion as it has been shown for other cells like fibroblasts? Does it participate in the killing of pathogens? The article of Flick *et al.* supports this hypothesis. Indeed Flick *et al.* generated mice carrying the Fibγ390–396A allele, in which the αMβ2-binding motif within the fibrinogen γ chain ($N^{390}RLSIGE^{396}$) was converted to a series of alanine residues, that cannot bind integrin. These mice had a dramatic defect in *Staphylococcus aureus* clearance by leukocyte, although neutrophils were still recruited to the site of infections. The authors postulated that this effect could be explained by the lack of fibrinogen induced activation of neutrophils (Flick et al., 2004). Several articles reported neutrophil activation upon fibrinogen engagement, this activation involved calcium mobilization, upregulation of some surface membrane proteins, increased phagocytic activation, activation of NFκB and delayed apoptosis (Rubel et al., 2001; Shi et al., 2001). The ROS production triggered by fibrinogen can modulate the NFκB signalling pathway. Activation of leukocytes by fibrinogen may however be detrimental in disease such as atherosclerosis or rheumatoid arthritis in which fibrin(ogen) is accumulated (Davalos and Akassoglou, 2012). Indeed, the $Fib\gamma^{390–396A}$ mice in which an inflammatory joint disease was induced, showed a reduction in pro-inflammatory cytokines (Davalos and Akassoglou, 2012). A sustained ROS production, in this context, may also contribute to tissue damage.

The integrin-mediated ROS production was enhanced by fMLF in human neutrophils. It has also been reported that cytokine such as TNF-α can trigger the ROS production by neutrophils on fibrinogen coated plates. This process is mediated by αMβ2 integrins and dependent on Class IA PI3K (Fumagalli et al., 2013; Gao et al., 2006). We also checked the role of TNF-α in integrin-mediated ROS production. The ROS production by neutrophil-like PLB cells on fibrinogen-coated plates did not change with or without treatment with TNF-α. In our preliminary experiments, TNF-α did not enhance the integrin-mediated ROS production by human neutrophils. The discrepancy between our results and the literature may be due to the difference in the concentrations of TNF-α: we used 40 ng/ml TNF-α, while Fumagalli *et al.* used 10ng/ml TNF-α. TNF-α has been described to either induce or decrease neutrophils apoptosis. Van den Berg *et al.* found that the effects of TNF-α were dose dependent: low doses (0.1-1 ng/ml) increased neutrophils survival, higher doses (10 ng/ml) have proapoptotic effects on human neutrophils (van den Berg et al., 2001). However, 10 ng/ml of TNF-α stimulation of neutrophils in patients with LAD-1 and CGD triggered a reduced apoptosis

(van den Berg et al., 2001). This suggest that TNF-α induced apoptosis required both αMβ2 integrins and ROS.

4.3 Modulation of the phosphoinositides to regulate NADPH oxidase

In order to investigate the role of phosphoinositides in the regulation of the NADPH oxidase, we need to modulate the level of phosphoinositides at the phagosomal or plasma membrane. Normally, researchers use pharmacological or molecular tools to modulate the phosphoinositides level.

4.3.1 Pharmacological tools

Pharmacological PI3K inhibitors are widely used in the PI3K related studies. In our study, we used the pan PI3K inhibitor wortmannin, the Vps34 inhibitor VPS34 IN1, which is the only Vps34 specific inhibitor, and the Class IA PI3K inhibitor LY294002. All the PI3K inhibitors are summarized in **Table 1**. Actually, there is no specific Class II PI3K inhibitor and VPS34 IN1 is the only Vps34 inhibitor. In human cancers, there are frequent gain-of-function mutations of PI3Ks and loss-of-function mutations of PTEN, suggesting that PI3Ks are involved in tumorigenesis, so PI3K inhibitors are expected to be promising anticancer drug candidates (Zhao et al., 2017). In 2014, Idelalisib, a p110δ inhibitor, was approved for therapy of relapsed chronic lymphocytic leukemia (CLL) in combination with rituximab (which destroys both normal and malignant B cells and is used to treat diseases which are characterized by having too many B cells, overactive B cells, or dysfunctional B cells). It is the first PI3K inhibitor licensed for cancer treatment (Furman et al., 2014; Zhao et al., 2017). Numerous PI3K inhibitors are in different phase of clinical trials for therapy of different cancers. These inhibitors are in orange in **Table 7**. Thus studies using PI3K inhibitors also can provide useful data for clinical application. In our experiment, Class IA PI3K inhibitor totally inhibits integrin-mediated ROS production. We want to further investigate the role of the different Class IA PI3K isoforms in maintaining the integrin-mediated ROS production by using different inhibitors.

Table 7. PI3K inhibitors

Inhibitor Name	PI3K	p110α	p110β	p110δ	p110γ	C2α	C2β	Vps34	Other Targets
GSK1059615		++++	++++	++++	++++				mTOR
Omipalisib (GSK2126458, GSK458)		++++	++++	++++	++++				mTORC1,mTORC2
PF-04691502		++++	++++	++++	++++				P-Akt (S473),P-Akt (T308),mTOR
Copanlisib (BAY 80-6946)		++++	++++	++++	+++				
PI-103		++++	++++	++++	+++				DNA-PK,mTOR
GDC-0032		++++	+++	++++	++++		++	++	mTOR
VS-5584 (SB2343)		++++	+++	++++	++++				mTOR
Pictilisib (GDC-0941)		++++	+++	++++	++		+		mTOR,DNA-PK
Apitolisib (GDC-0980, RG7422)		++++	+++	+++	+++				mTOR
PKI-402		++++	+++	+++	+++				mTOR
GDC-0084		++++	++	++++	+++				mTOR
PF-4989216		++++	++	++++	++			++	
Dactolisib (BEZ235, NVP-BEZ235)		++++	++	+++	++++				mTOR (p70S6K),ATR
BGT226 (NVP-BGT226)		++++	++		+++				mTOR
Gedatolisib (PF-05212384, PKI-587)		++++			++++				mTOR
Alpelisib (BYL719)		++++							
HS-173		++++							
Duvelisib (IPI-145, INK1197)		+++	++++	++++	++++				
AZD8186		+++	++++	+++	+				
Pilaralisib (XL147)		+++	+++	+++	+++				
ZSTK474	+++	+++	++	++++	++				
AZD8835		+++	++	++++	++				
XL147 analogue		+++	++	+++	+++			+	DNA-PK
CUDC-907		+++	++	+++	++				HDAC1,HDAC3,HDAC10
PIK-90		+++	++	++	+++				
Voxtalisib (SAR245409, XL765) Analogue		+++	++	++	+++				DNA-PK,mTOR
Voxtalisib (XL765, SAR245409)		+++	++	++	+++				DNA-PK,mTOR
CH5132799		+++	++	+	+++		+		mTOR

PIK-93		+++	+	++	+++	+	++	++	PI4KIIIβ,DNA-PK,ATM
PIK-75		+++	+	+	++				DNA-PK
A66		+++			+		++		PI4Kβ
TG100713		++	++	+++	++				
AS-605240		++	++	++	+++				
Buparlisib (BKM120, NVP-BKM120)		++	++	++	++			+	mTOR
TGX-221		+	++++	++					
AZD6482		+	+++	++	+				DNA-PK
Idelalisib (CAL-101, GS-1101)		+	+	++++	++			+	DNA-PK
AMG319		+	+	+++	+				
PI-3065		+	+	+++	+				mTOR
TG100-115		+	+	++	++				
PIK-293		+	+	++	+				
LY294002		+	+	+					
PIK-III		+		+	+			+++	PI4Kβ
AS-252424		+			+++				Casein Kinase 2
AS-604850		+			++				
YM201636		+							PIKfyve
GSK2636771			√						
PIK-294			++	+++	++				
CZC24832			+	+	+++				
IC-87114			+	+	+				
Quercetin			+	+	+				PKC,Src,Sirtuin
GSK2292767				√					
GSK2269557				++++					
CAY10505					√				
3-Methyladenine (3-MA)					+			+	
GNE-317	√								
Wortmannin	++++								DNA-PK,ATM,MLCK
NU7441 (KU-57788)	+								DNA-PK,mTOR
Collapse									
VPS34-IN1								+++	

Data are summarized from **Selleckchem.com**. "+" indicates inhibitory effect. Increased inhibition is marked by a multiple "+" designation. More details, such as half maximal inhibitory concentrations (IC50s) and working concentrations of each inhibitor can be found in selleckchem.com. "√" refers to compounds which have inhibitory effects on the related

isoform, but without specific value. Blue indicates a specific isoform of the PI3K inhibitor. Green indicates the inhibitors used in this study. Red indicates the inhibitor licensed for cancer treatment. Orange indicates the inhibitors which are in clinical trails.

4.3.2 Molecular tools

There are numerous methods and technologies to modulate the phosphoinositides level by using molecular tools. There are numerous kinases, phosphatases or regulatory proteins that are related with the metabolism of phosphoinositides. Modulation of the level of these enzymes or proteins leads to the regulation of the phosphoinositides. We used siRNA against *MTM1* or/and *Rubicon* in our experiment to modulate the PI3P level.

Another powerful tool to modulate the phosphoinositides level is chemically induced dimerization (CID), which brings two proteins in close proximity. Compared to traditional genetic perturbations, they can be operated at defined cellular compartments and desired time points (Voß et al., 2015). Rapamycin induced FKBP-FRB system is one of the commonly used CID. Rapamycin binds with high affinity (Kd=0.2 nM) to the 12-kDa FK506 binding protein (FKBP12, hereafter called FKBP) as well as to a 100-amino acid domain (E2015 to Q2114) of the mammalian target of rapamycin (mTOR) known as the FKBP-rapamycin binding domain (FRB) (Banaszynski et al., 2005). However, the system present some disadvantages. FKBP and FRB fusion proteins compete with endogenous FKBP and mTOR for rapamycin binding, resulting in non productive interactions. The rapamycin binding and inhibition of mTOR leads to cell-cycle arrest. However, we performed the experiment in a short time frame in which the phenomenon can be neglected. Despite its cytotoxic properties, the rapamycin mediated FKBP-FRB system is still the most widely used CID (Rakhit et al., 2014). We used this system in our first study to bring MTM1 to the phagosome membrane to modulate PI3P. This system worked well in neutrophil-like PLB cells. After adding rapamycin, target proteins were quickly recruited to membrane (in two minutes).

Recently, light-induced dimerization has been used to manipulate the phosphoinositides. The optogenetic tools significantly improve the spatiotemporal precision and are less toxic. The interaction is reversibly controlled by light of specific wavelengths (Idevall-Hagren and De Camilli, 2015). CRY2 (cryptochrome 2)-CIB1 (cryptochrome-interacting basic-helix-loop-helix 1) system is one of the most used optogenetic tools. Upon brief blue-light illumination, CRY2-CIB1 association occurred within 300 ms and the disassociation was spontaneously

reversible within minutes (Kennedy et al., 2010). We expressed the CRY2-CIB1 system in neutrophil-like PLB cells and confirmed that the system could be used in our cell line. In order to modulate PI(3,4)P2 at the plasma membrane, we expressed PTEN in the CRY2-CIB1 system, however, we could not detect the expression of the PTEN protein fused with CRY2-mCherry. These results suggest that PTEN-CRY2-mCherry may be not well expressed in our PLB cell line or degraded. Das *et al.* claimed that PTEN-GFP was not stable and used a C124A mutant of PTEN (mutation in the phosphatase domain) because it showed an improved cellular stability (Das et al., 2003). However, Yang *et al.* succeded to express PTEN-GFP (Yang et al., 2015). We are currently trying to express PTEN in the FKBP-FRB system. We will also use the 4'-phosphatase INPP4 to modulate the $PI(3,4)P_2$ level. Firstly, we want to investigate whether decreased level of $PI(3,4)P_2$ will affect the $p47^{phox}$ accumulation at the plasma membrane. Secondly, we want to see whether decreased level of $PI(3,4)P_2$ will affect the integrin mediated ROS production.

4.4 Regulation of NADPH oxidase at phagosomal versus plasma membrane

We propose an assembly model of the NADPH oxidase at the phagosomal membrane based on my Ph.D. results and the previous data from the laboratory: upon activation, all the cytosolic subunits are recruited to the membrane together with the membrane subunits, as well with the small GTPase Rac. A few minutes later, $p47^{phox}$ and Rac detach from the phagosomal membrane (Faure et al., 2013). But $p67^{phox}$ stays at the phagosome until the termination of ROS production (Tlili et al., 2012). Our results suggest that PI3P and $p40^{phox}$ play an important role in sustaining the ROS production at the phagosomal membrane (**Figure 32**). However, the mechanism of assembly of NADPH oxidase at the plasma membrane may be different. $P47^{phox}$ stays at the plasma membrane thanks to its binding to $PI(3,4)P_2$, which may maintain $p67^{phox}$ at the plasma membrane. $P40^{phox}$ also stays at the plasma membrane, although there is no PI3P. What is the role of $p40^{phox}$ in the oxidase complex assembled at the plasma membrane during integrin-mediated ROS production? Does $p40^{phox}$ enhance the recruitment of $p47^{phox}$/$p67^{phox}$ as it was observed with PMA? We planned to express the PB1 domain of $p40^{phox}$, which can bind to $p67^{phox}$. Expression of this domain should decrease the binding of $p40^{phox}$ to $p67^{phox}$. We will observe this by FRET (Förster resonance energy transfer) in Cos-7 cells transfected with the PB1 domain and tagged $p40^{phox}$

and $p67^{phox}$. We then want to see whether the expression of this domain will affect the ROS production in PLB cells and the recruitment/stability of $p67^{phox}$. How is $p40^{phox}$ maintained at the plasma membrane? Is it thanks to its interaction with $p67^{phox}$ or/and actin by its PX domain? We planned to express $p40^{phox}$ protein without PX domain to investigate whether this protein is still at the plasma membrane in cells plated on fibrinogen. We also want to add Cytochalasin D, which inhibits actin polymerization and induce depolymerization of actin, after cells adhesion to fibrinogen and look if $p40^{phox}$ stays at the plasma membrane.

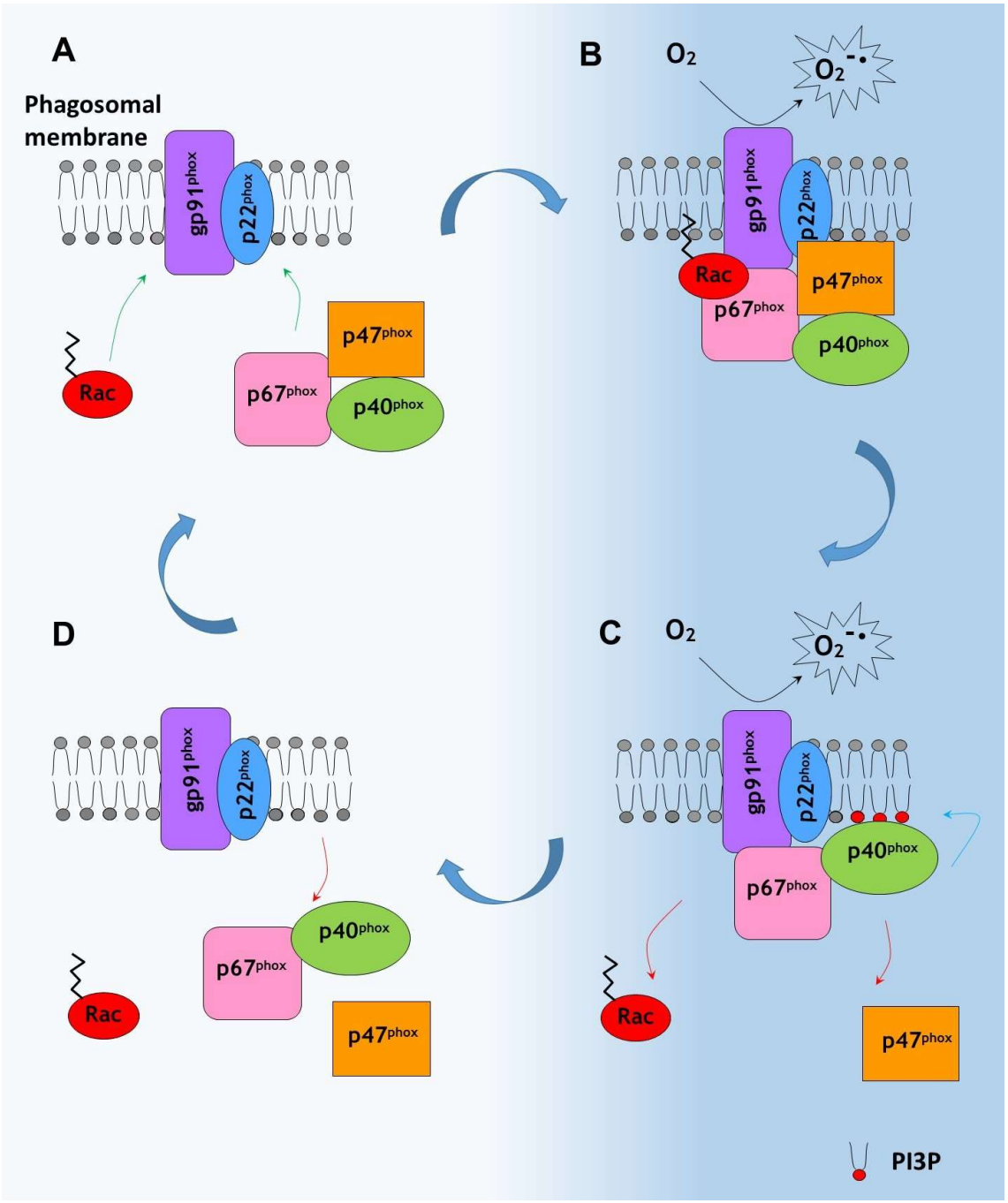

Figure 32. Model of NADPH oxidase assembly and PI3P involvement during phagocytosis

A-B, Upon activation, all the cytosolic subunits, membrane subunits and small GTPase Rac assemble at the phagosome membrane and produce ROS. C, Few minutes later, $p47^{phox}$ and Rac leave the phagosomal membrane, PI3P is synthetised at the phagosomal membrane and binds to p40phox to stabilize $p67^{phox}$, and thus sustain the ROS production. D, When PI3P disappears at the phagosomal membrane, $p40^{phox}$ and $p67^{phox}$ leave the membrane together and the ROS production is terminated.

We summarized the possible pathways involved in integrin-mediated ROS production (**Figure 33**). Our results showed that mutation in the PX domain of $p47^{phox}$ inhibited the integrin-mediated ROS production and the second phase of ROS production after the stimulation of adherent neutrophils by fMLF. It has been reported that small molecule antagonists (PITenins, PITs) of $PI(3,4,5)P_3$–PH domain interactions inhibit interactions of a number of $PI(3,4,5)P_3$-binding PH domains such as Akt and PDK1, but do not affect $PI(4,5)P_2$ selective PH domains such as PLC-δ, TAPP1, and TAPP2. PITs suppress the PI3K-PDK1-Akt pathway and trigger metabolic stress and apoptosis (Miao et al., 2010). Thus small molecules interfering with protein binding domains may be interesting inhibitors. As an excessive production of ROS by neutrophils in the extracellular medium can damage tissue, it would be interesting in some cases to decrease the activity of the NADPH oxidase at the plasma membrane. We should look for small molecules that can bind to the PX domain of $p47^{phox}$ and prevent its binding to the $PI(3,4)P_2$. This may destabilize the NADPH complex at the plasma membrane thus reducing ROS production.

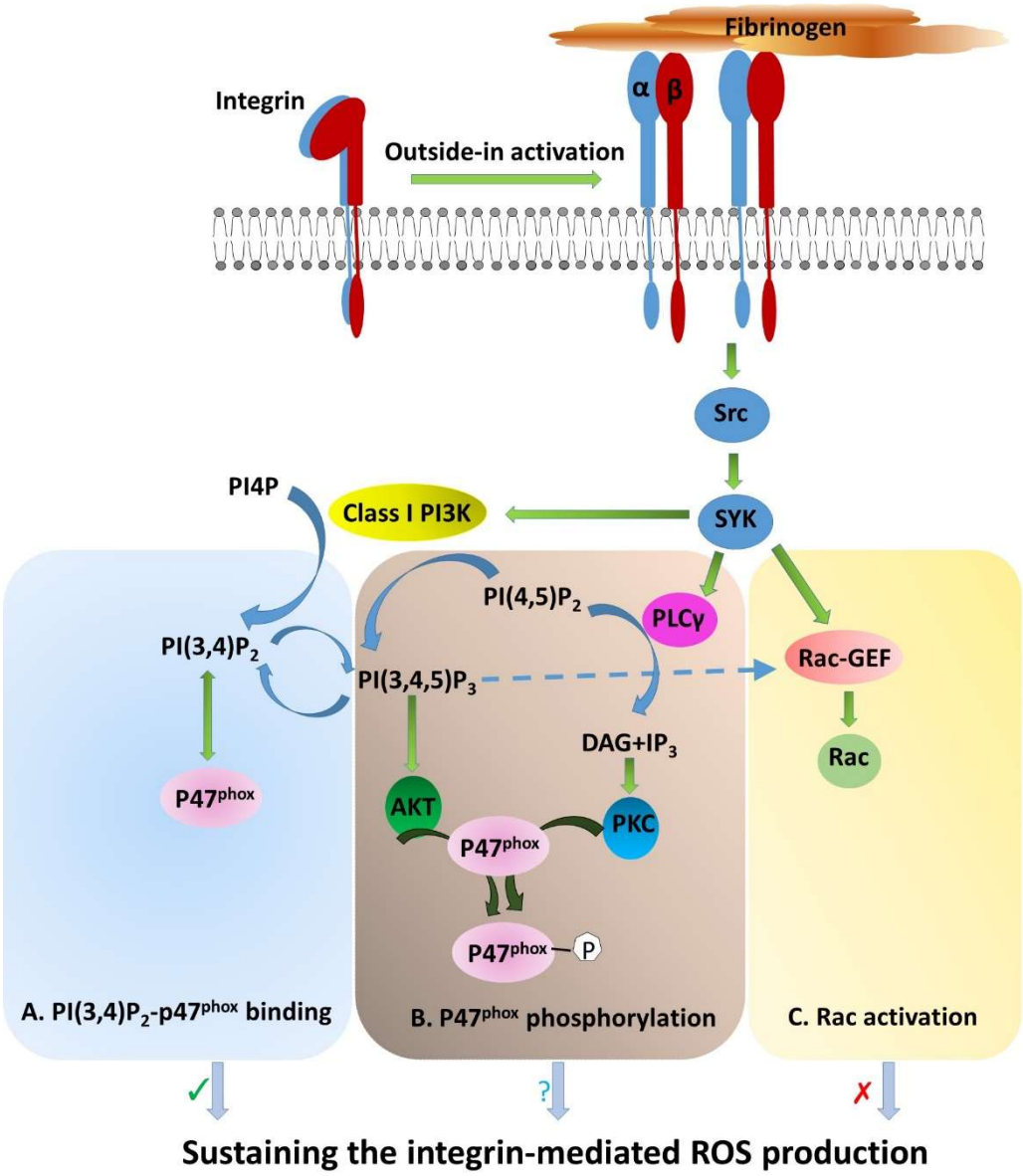

Figure 33. Pathways in sustaining the integrin-mediated ROS production

Possible pathways in maintaining the integrin-mediated ROS production: Immobilized fibrinogen binding with neutrophils leads to outside-in activation of neutrophils integrins. Src-family kinases participate in this signaling pathway. Src kinases phosphorylate the ITAM motif of DAP12 and FcRγ, which recruit and activate Syk. Syk can activate Class I PI3K, which can produce $PI(3,4)P_2$ and $PI(3,4,5)P_3$. A, $PI(3,4)P_2$ and $p47^{phox}$ binding may sustain the ROS production. B, Phosphorylation of $p47^{phox}$ may sustain the ROS production. C, Syk can activate Rac-GEF, $PI(3,4,5)P_3$ can also recruit and activate Rac-GEF. Rac-GEF further activate Rac. Rac activation may sustain the ROS production.

References

Aderem, A., and Underhill, D.M. (1999). Mechanisms of phagocytosis in macrophages. Annu Rev Immunol *17*, 593-623.

Ago, T., Kuribayashi, F., Hiroaki, H., Takeya, R., Ito, T., Kohda, D., and Sumimoto, H. (2003). Phosphorylation of p47phox directs phox homology domain from SH3 domain toward phosphoinositides, leading to phagocyte NADPH oxidase activation. Proc Natl Acad Sci U S A *100*, 4474-4479.

Ago, T., Takeya, R., Hiroaki, H., Kuribayashi, F., Ito, T., Kohda, D., and Sumimoto, H. (2001). The PX domain as a novel phosphoinositide- binding module. Biochem Biophys Res Commun *287*, 733-738.

Allen, L.A.H., Beecher, B.R., Lynch, J.T., Rohner, O.V., and Wittine, L.M. (2005). Helicobacter pylori Disrupts NADPH Oxidase Targeting in Human Neutrophils to Induce Extracellular Superoxide Release. The Journal of Immunology *174*, 3658-3667.

Amulic, B., Cazalet, C., Hayes, G.L., Metzler, K.D., and Zychlinsky, A. (2012). Neutrophil Function: From Mechanisms to Disease. Annu Rev Immunol *30*, 459-489.

Anderson, D.C., and Springer, T.A. (1987). Leukocyte adhesion deficiency: an inherited defect in the Mac-1, LFA-1, and p150,95 glycoproteins. Annu Rev Med *38*, 175-194.

Arnaout, M.A. (2016). Biology and structure of leukocyte beta 2 integrins and their role in inflammation. F1000Res *5*.

Ayres-Sander, C.E., and Gonzalez, A.L. (2012). Approaches in extracellular matrix engineering for determination of adhesion molecule mediated single cell function. Frontiers in Biology *8*, 32-49.

Azizova, O.A., Aseichev, A.V., Piryazev, A.P., Roitman, E.V., and Shcheglovitova, O.N. (2007). Effects of oxidized fibrinogen on the functions of blood cells, blood clotting, and rheology. Bull Exp Biol Med *144*, 397-407.

Backer, J.M. (2016). The intricate regulation and complex functions of the Class III phosphoinositide 3-kinase Vps34. Biochem J *473*, 2251-2271.

Bagaitkar, J., Barbu, E.A., Perez-Zapata, L.J., Austin, A., Huang, G., Pallat, S., and Dinauer, M.C. (2017). PI(3)P-p40phox binding regulates NADPH oxidase activation in mouse macrophages and magnitude of inflammatory responses in vivo. J Leukoc Biol *101*, 449-457.

Bagaitkar, J., Pech, N.K., Ivanov, S., Austin, A., Zeng, M.Y., Pallat, S., Huang, G., Randolph, G.J., and Dinauer, M.C. (2015). NADPH oxidase controls neutrophilic response to sterile inflammation in mice by regulating the IL-1 /G-CSF axis. Blood *126*, 2724-2733.

Bagheri, F., Khori, V., Alizadeh, A.M., Khalighfard, S., Khodayari, S., and Khodayari, H. (2016). Reactive oxygen species-mediated cardiac-reperfusion injury: Mechanisms and therapies. Life Sci *165*, 43-55.

Balla, T. (2013). Phosphoinositides: tiny lipids with giant impact on cell regulation. Physiol Rev *93*, 1019-1137.

Banaszynski, L.A., Liu, C.W., and Wandless, T.J. (2005). Characterization of the FKBP.rapamycin.FRB ternary complex. J Am Chem Soc *127*, 4715-4721.

Barczyk, M., Carracedo, S., and Gullberg, D. (2010). Integrins. Cell Tissue Res *339*, 269-280.

Becatti, M., Emmi, G., Silvestri, E., Bruschi, G., Ciucciarelli, L., Squatrito, D., Vaglio, A., Taddei, N., Abbate, R., Emmi, L*., et al.* (2015). Neutrophil Activation Promotes Fibrinogen Oxidation and Thrombus Formation in Behçet's Disease. Circulation, CIRCULATIONAHA.115.017738.

Berger, M., Hsieh, C.Y., Bakele, M., Marcos, V., Rieber, N., Kormann, M., Mays, L., Hofer, L., Neth, O., Vitkov, L*., et al.* (2012). Neutrophils express distinct RNA receptors in a non-canonical way. J Biol Chem *287*, 19409-19417.

Bianchi, M., Hakkim, A., Brinkmann, V., Siler, U., Seger, R.A., Zychlinsky, A., and Reichenbach, J. (2009). Restoration of NET formation by gene therapy in CGD controls aspergillosis. Blood *114*, 2619-2622.

Bloes, D.A., Kretschmer, D., and Peschel, A. (2015). Enemy attraction: bacterial agonists for leukocyte chemotaxis receptors. Nat Rev Microbiol *13*, 95-104.

Bohdanowicz, M., and Grinstein, S. (2013). Role of phospholipids in endocytosis, phagocytosis, and macropinocytosis. Physiol Rev *93*, 69-106.

Bonnans, C., Chou, J., and Werb, Z. (2014). Remodelling the extracellular matrix in development and disease. Nature Reviews Molecular Cell Biology *15*, 786-801.

Borregaard, N. (2010). Neutrophils, from marrow to microbes. Immunity *33*, 657-670.

Borregaard, N., and Cowland, J.B. (1997). Granules of the human neutrophilic polymorphonuclear leukocyte. Blood *89*, 3503-3521.

Borregaard, N., Kjeldsen, L., Sengelov, H., Diamond, M.S., Springer, T.A., Anderson, H.C., Kishimoto, T.K., and Bainton, D.F. (1994). Changes in subcellular localization and surface expression of L-selectin, alkaline phosphatase, and Mac-1 in human neutrophils during stimulation with inflammatory mediators. J Leukoc Biol *56*, 80-87.

Botelho, R.J., Teruel, M., Dierckman, R., Anderson, R., Wells, A., York, J.D., Meyer, T., and Grinstein, S. (2000). Localized biphasic changes in phosphatidylinositol-4,5-bisphosphate at sites of phagocytosis. J Cell Biol *151*, 1353-1368.

Bouaouina, M., Lad, Y., and Calderwood, D.A. (2008). The N-terminal domains of talin cooperate with the phosphotyrosine binding-like domain to activate beta1 and beta3 integrins. J Biol Chem *283*, 6118-6125.

Boura, E., and Nencka, R. (2015). Phosphatidylinositol 4-kinases: Function, structure, and inhibition. Exp Cell Res *337*, 136-145.

Boyle, K.B., Gyori, D., Sindrilaru, A., Scharffetter-Kochanek, K., Taylor, P.R., Mocsai, A., Stephens, L.R., and Hawkins, P.T. (2011). Class IA phosphoinositide 3-kinase beta and delta regulate neutrophil oxidase activation in response to Aspergillus fumigatus hyphae. J Immunol *186*, 2978-2989.

Bravo, J., Karathanassis, D., Pacold, C.M., Pacold, M.E., Ellson, C.D., Anderson, K.E., Butler, P.J., Lavenir, I., Perisic, O., Hawkins, P.T.*, et al.* (2001). The crystal structure of the PX domain from p40(phox) bound to phosphatidylinositol 3-phosphate. Mol Cell *8*, 829-839.

Brinkmann, V., Reichard, U., Goosmann, C., Fauler, B., Uhlemann, Y., Weiss, D.S., Weinrauch, Y., and Zychlinsky, A. (2004). Neutrophil extracellular traps kill bacteria. Science *303*, 1532-1535.

Brinkmann, V., and Zychlinsky, A. (2007). Beneficial suicide: why neutrophils die to make NETs. Nat Rev Microbiol *5*, 577-582.

Brinkmann, V., and Zychlinsky, A. (2012). Neutrophil extracellular traps: is immunity the second function of chromatin? J Cell Biol *198*, 773-783.

Brown, G.D., and Gordon, S. (2001). Immune recognition. A new receptor for beta-glucans. Nature *413*, 36-37.

Brown, J.R., and Auger, K.R. (2011). Phylogenomics of phosphoinositide lipid kinases: perspectives on the evolution of second messenger signaling and drug discovery. BMC Evol Biol *11*, 4.

Bulger, E.M., Nathens, A.B., and Maier, R.V. (2001). The Immuno-Inflammatory Response. 893-908.

Cachat, J., Deffert, C., Hugues, S., and Krause, K.H. (2015). Phagocyte NADPH oxidase and specific immunity. Clin Sci (Lond) *128*, 635-648.

Campanelli, D., Detmers, P.A., Nathan, C.F., and Gabay, J.E. (1990). Azurocidin and a homologous serine protease from neutrophils. Differential antimicrobial and proteolytic properties. J Clin Invest *85*, 904-915.

Campbell, I.D., and Humphries, M.J. (2011). Integrin Structure, Activation, and Interactions. Cold Spring Harb Perspect Biol *3*, a004994-a004994.

Cantrell, D.A. (2001). Phosphoinositide 3-kinase signalling pathways. J Cell Sci *114*, 1439-1445.

Cao, C., Laporte, J., Backer, J.M., Wandinger-Ness, A., and Stein, M.-P. (2007). Myotubularin Lipid Phosphatase Binds the hVPS15/hVPS34 Lipid Kinase Complex on Endosomes. Traffic *8*, 1052-1067.

Carlyon, J.A., Chan, W.T., Galan, J., Roos, D., and Fikrig, E. (2002). Repression of rac2 mRNA Expression by Anaplasma phagocytophila Is Essential to the Inhibition of Superoxide Production and Bacterial Proliferation. The Journal of Immunology *169*, 7009-7018.

Casbon, A.J., Long, M.E., Dunn, K.W., Allen, L.A., and Dinauer, M.C. (2012). Effects of IFN-gamma on intracellular trafficking and activity of macrophage NADPH oxidase flavocytochrome b558. J Leukoc Biol *92*, 869-882.

Chagpar, R.B., Links, P.H., Pastor, M.C., Furber, L.A., Hawrysh, A.D., Chamberlain, M.D., and Anderson, D.H. (2010). Direct positive regulation of PTEN by the p85 subunit of phosphatidylinositol 3-kinase. Proceedings of the National Academy of Sciences *107*, 5471-5476.

Chang, S., Popowich, Y., Greco, R.S., and Haimovich, B. (2003). Neutrophil survival on biomaterials is determined by surface topography. J Vasc Surg *37*, 1082-1090.

Christoforidis, S., Miaczynska, M., Ashman, K., Wilm, M., Zhao, L., Yip, S.-C., Waterfield, M.D., Backer, J.M., and Zerial, M. (1999). Phosphatidylinositol-3-OH kinases are Rab5 effectors. Nat Cell Biol *1*, 249-252.

Condliffe, A.M. (2005). Sequential activation of class IB and class IA PI3K is important for the primed respiratory burst of human but not murine neutrophils. Blood *106*, 1432-1440.

Conradt, B., Lu, N., Shen, Q., Mahoney, T.R., Neukomm, L.J., Wang, Y., and Zhou, Z. (2012). Two PI 3-Kinases and One PI 3-Phosphatase Together Establish the Cyclic Waves of Phagosomal PtdIns(3)P Critical for the Degradation of Apoptotic Cells. PLoS Biol *10*, e1001245.

Corbin, B.D., Seeley, E.H., Raab, A., Feldmann, J., Miller, M.R., Torres, V.J., Anderson, K.L., Dattilo, B.M., Dunman, P.M., Gerads, R.*, et al.* (2008). Metal chelation and inhibition of bacterial growth in tissue abscesses. Science *319*, 962-965.

Corcoran, A., and Cotter, T.G. (2013). Redox regulation of protein kinases. FEBS J *280*, 1944-1965.

Cowland, J.B., and Borregaard, N. (2016). Granulopoiesis and granules of human neutrophils. Immunol Rev *273*, 11-28.

Cox, D., Dale, B.M., Kashiwada, M., Helgason, C.D., and Greenberg, S. (2001). A regulatory role for Src homology 2 domain-containing inositol 5'-phosphatase (SHIP) in phagocytosis mediated by Fc gamma receptors and

complement receptor 3 (alpha(M)beta(2); CD11b/CD18). J Exp Med *193*, 61-71.
Cross, A.R., and Curnutte, J.T. (1995). The cytosolic activating factors p47phox and p67phox have distinct roles in the regulation of electron flow in NADPH oxidase. J Biol Chem *270*, 6543-6548.
Dahan, I., Smith, S.M.E., and Pick, E. (2015). A Cys-Gly-Cys triad in the dehydrogenase region of Nox2 plays a key role in the interaction with p67phox. J Leukoc Biol *98*, 859-874.
Das, S., Dixon, J.E., and Cho, W. (2003). Membrane-binding and activation mechanism of PTEN. Proceedings of the National Academy of Sciences *100*, 7491-7496.
Davalos, D., and Akassoglou, K. (2012). Fibrinogen as a key regulator of inflammation in disease. Semin Immunopathol *34*, 43-62.
de Rezende, F.F., Martins Lima, A., Niland, S., Wittig, I., Heide, H., Schröder, K., and Eble, J.A. (2012). Integrin α7β1 is a redox-regulated target of hydrogen peroxide in vascular smooth muscle cell adhesion. Free Radic Biol Med *53*, 521-531.
DeLeo, F.R. (2000). Processing and Maturation of Flavocytochrome b558 Include Incorporation of Heme as a Prerequisite for Heterodimer Assembly. J Biol Chem *275*, 13986-13993.
Di Carlo, F.J., and Fiore, J.V. (1958). On the composition of zymosan. Science *127*, 756-757.
Di Paolo, G., and De Camilli, P. (2006). Phosphoinositides in cell regulation and membrane dynamics. Nature *443*, 651-657.
Dinauer, M.C. (2014). Disorders of Neutrophil Function: An Overview. *1124*, 501-515.
Dinauer, M.C., Pierce, E.A., Bruns, G.A., Curnutte, J.T., and Orkin, S.H. (1990). Human neutrophil cytochrome b light chain (p22-phox). Gene structure, chromosomal location, and mutations in cytochrome-negative autosomal recessive chronic granulomatous disease. J Clin Invest *86*, 1729-1737.
Domin, J., Pages, F., Volinia, S., Rittenhouse, S.E., Zvelebil, M.J., Stein, R.C., and Waterfield, M.D. (1997). Cloning of a human phosphoinositide 3-kinase with a C2 domain that displays reduced sensitivity to the inhibitor wortmannin. Biochem J *326 (Pt 1)*, 139-147.
Dou, Z., Chattopadhyay, M., Pan, J.-A., Guerriero, J.L., Jiang, Y.-P., Ballou, L.M., Yue, Z., Lin, R.Z., and Zong, W.-X. (2010). The class IA phosphatidylinositol 3-kinase p110-β subunit is a positive regulator of autophagy. The Journal of Cell Biology *191*, 827-843.
Dumler, J.S., Choi, K.-S., Garcia-Garcia, J.C., Barat, N.S., Scorpio, D.G., Garyu, J.W., Grab, D.J., and Bakken, J.S. (2005). Human Granulocytic Anaplasmosis andAnaplasma phagocytophilum. Emerg Infect Dis *11*, 1828-1834.
Dupre-Crochet, S., Erard, M., and Nubetae, O. (2013). ROS production in phagocytes: why, when, and where? J Leukoc Biol *94*, 657-670.
Dusi, S., Donini, M., and Rossi, F. (1995). Mechanisms of NADPH oxidase activation in human neutrophils: p67phox is required for the translocation of rac 1 but not of rac 2 from cytosol to the membranes. Biochem J *308 (Pt 3)*, 991-994.
Eble, J.A., and de Rezende, F.F. (2014). Redox-relevant aspects of the extracellular matrix and its cellular contacts via integrins. Antioxid Redox Signal *20*, 1977-1993.
Edimo, W.s.E., Janssens, V., Waelkens, E., and Erneux, C. (2012). Reversible Ser/Thr SHIP phosphorylation: A new paradigm in phosphoinositide signalling? Bioessays *34*, 634-642.
El-Benna, J., Dang, P.M., Gougerot-Pocidalo, M.A., Marie, J.C., and Braut-Boucher, F. (2009). p47phox, the phagocyte NADPH oxidase/NOX2 organizer: structure, phosphorylation and implication in diseases. Exp Mol Med *41*, 217-225.
El Benna, J., Dang, P.M., Andrieu, V., Vergnaud, S., Dewas, C., Cachia, O., Fay, M., Morel, F., Chollet-Martin, S., Hakim, J*., et al.* (1999). P40phox associates with the neutrophil Triton X-100-insoluble cytoskeletal fraction and PMA-activated membrane skeleton: a comparative study with P67phox and P47phox. J Leukoc Biol *66*, 1014-1020.
el Benna, J., Ruedi, J.M., and Babior, B.M. (1994). Cytosolic guanine nucleotide-binding protein Rac2 operates in vivo as a component of the neutrophil respiratory burst oxidase. Transfer of Rac2 and the cytosolic oxidase components p47phox and p67phox to the submembranous actin cytoskeleton during oxidase activation. J Biol Chem *269*, 6729-6734.
Ellson, C.D., Davidson, K., Ferguson, G.J., O'Connor, R., Stephens, L.R., and Hawkins, P.T. (2006). Neutrophils from p40phox-/- mice exhibit severe defects in NADPH oxidase regulation and oxidant-dependent bacterial killing. J Exp Med *203*, 1927-1937.
Evans, R., Patzak, I., Svensson, L., De Filippo, K., Jones, K., McDowall, A., and Hogg, N. (2009). Integrins in immunity. J Cell Sci *122*, 215-225.
Falasca, M., and Maffucci, T. (2012). Regulation and cellular functions of class II phosphoinositide 3-kinases. Biochem J *443*, 587-601.
Falkenburger, B.H., Jensen, J.B., Dickson, E.J., Suh, B.-C., and Hille, B. (2010). SYMPOSIUM REVIEW:

Phosphoinositides: lipid regulators of membrane proteins. The Journal of Physiology *588*, 3179-3185.
Fan, W., Nassiri, A., and Zhong, Q. (2011). Autophagosome targeting and membrane curvature sensing by Barkor/Atg14(L). Proceedings of the National Academy of Sciences *108*, 7769-7774.
Faure, M.C., Sulpice, J.C., Delattre, M., Lavielle, M., Prigent, M., Cuif, M.H., Melchior, C., Tschirhart, E., Nusse, O., and Dupre-Crochet, S. (2013). The recruitment of p47(phox) and Rac2G12V at the phagosome is transient and phosphatidylserine dependent. Biol Cell *105*, 501-518.
Faurschou, M., and Borregaard, N. (2003). Neutrophil granules and secretory vesicles in inflammation. Microbes and Infection *5*, 1317-1327.
Fayard, E. (2005). Protein kinase B/Akt at a glance. J Cell Sci *118*, 5675-5678.
Ferguson, G.J., Milne, L., Kulkarni, S., Sasaki, T., Walker, S., Andrews, S., Crabbe, T., Finan, P., Jones, G., Jackson, S.*, et al.* (2007). PI(3)Kgamma has an important context-dependent role in neutrophil chemokinesis. Nat Cell Biol *9*, 86-91.
Finkel, T. (2011). Signal transduction by reactive oxygen species. The Journal of Cell Biology *194*, 7-15.
Flannagan, R.S., Cosio, G., and Grinstein, S. (2009). Antimicrobial mechanisms of phagocytes and bacterial evasion strategies. Nat Rev Microbiol *7*, 355-366.
Flick, M.J., Du, X., Witte, D.P., Jiroušková, M., Soloviev, D.A., Busuttil, S.J., Plow, E.F., and Degen, J.L. (2004). Leukocyte engagement of fibrin(ogen) via the integrin receptor αMβ2/Mac-1 is critical for host inflammatory response in vivo. J Clin Invest *113*, 1596-1606.
Francke, U., Ochs, H.D., Darras, B.T., and Swaroop, A. (1990). Origin of mutations in two families with X-linked chronic granulomatous disease. Blood *76*, 602-606.
Frantz, C., Stewart, K.M., and Weaver, V.M. (2010). The extracellular matrix at a glance. J Cell Sci *123*, 4195-4200.
Freeman, S.A., and Grinstein, S. (2014). Phagocytosis: receptors, signal integration, and the cytoskeleton. Immunol Rev *262*, 193-215.
Fumagalli, L., Campa, C.C., Germena, G., Lowell, C.A., Hirsch, E., and Berton, G. (2013). Class I Phosphoinositide-3-Kinases and Src Kinases Play a Nonredundant Role in Regulation of Adhesion-Independent and -Dependent Neutrophil Reactive Oxygen Species Generation. The Journal of Immunology *190*, 3648-3660.
Furman, R.R., Sharman, J.P., Coutre, S.E., Cheson, B.D., Pagel, J.M., Hillmen, P., Barrientos, J.C., Zelenetz, A.D., Kipps, T.J., Flinn, I.*, et al.* (2014). Idelalisib and Rituximab in Relapsed Chronic Lymphocytic Leukemia. N Engl J Med *370*, 997-1007.
Futosi, K., Fodor, S., and Mocsai, A. (2013a). Reprint of Neutrophil cell surface receptors and their intracellular signal transduction pathways. Int Immunopharmacol *17*, 1185-1197.
Futosi, K., Fodor, S., and Mócsai, A. (2013b). Reprint of Neutrophil cell surface receptors and their intracellular signal transduction pathways. Int Immunopharmacol *17*, 1185-1197.
Gahmberg, C.G., Fagerholm, S.C., Nurmi, S.M., Chavakis, T., Marchesan, S., and Gronholm, M. (2009). Regulation of integrin activity and signalling. Biochim Biophys Acta *1790*, 431-444.
Gao, X.P., Zhu, X., Fu, J., Liu, Q., Frey, R.S., and Malik, A.B. (2006). Blockade of Class IA Phosphoinositide 3-Kinase in Neutrophils Prevents NADPH Oxidase Activation- and Adhesion-dependent Inflammation. J Biol Chem *282*, 6116-6125.
Gazendam, R.P., van de Geer, A., Roos, D., van den Berg, T.K., and Kuijpers, T.W. (2016). How neutrophils kill fungi. Immunol Rev *273*, 299-311.
Grabon, A., Khan, D., and Bankaitis, V.A. (2015). Phosphatidylinositol transfer proteins and instructive regulation of lipid kinase biology. Biochimica et Biophysica Acta (BBA) - Molecular and Cell Biology of Lipids *1851*, 724-735.
Green, J.N., Kettle, A.J., and Winterbourn, C.C. (2014). Protein chlorination in neutrophil phagosomes and correlation with bacterial killing. Free Radic Biol Med *77*, 49-56.
Groemping, Y., Lapouge, K., Smerdon, S.J., and Rittinger, K. (2003). Molecular basis of phosphorylation-induced activation of the NADPH oxidase. Cell *113*, 343-355.
Groemping, Y., and Rittinger, K. (2005). Activation and assembly of the NADPH oxidase: a structural perspective. Biochem J *386*, 401-416.
Hanna, S., and Etzioni, A. (2012). Leukocyte adhesion deficiencies. Ann N Y Acad Sci *1250*, 50-55.
Hato, T., and Dagher, P.C. (2014). How the Innate Immune System Senses Trouble and Causes Trouble. Clin J Am Soc Nephrol *10*, 1459-1469.
Hayashi, F., Means, T.K., and Luster, A.D. (2003). Toll-like receptors stimulate human neutrophil function. Blood *102*, 2660-2669.
Hemmings, B.A., and Restuccia, D.F. (2012). PI3K-PKB/Akt Pathway. Cold Spring Harb Perspect Biol *4*, a011189-a011189.
Henschen, A., Lottspeich, F., Kehl, M., and Southan, C. (1983). Covalent structure of fibrinogen. Ann N Y Acad Sci

408, 28-43.
Herman, P.K., and Emr, S.D. (1990). Characterization of VPS34, a gene required for vacuolar protein sorting and vacuole segregation in Saccharomyces cerevisiae. Mol Cell Biol *10*, 6742-6754.
Hess, J. (2004). AP-1 subunits: quarrel and harmony among siblings. J Cell Sci *117*, 5965-5973.
Hibbs, M.L., Quilici, C., Kountouri, N., Seymour, J.F., Armes, J.E., Burgess, A.W., and Dunn, A.R. (2007). Mice lacking three myeloid colony-stimulating factors (G-CSF, GM-CSF, and M-CSF) still produce macrophages and granulocytes and mount an inflammatory response in a sterile model of peritonitis. J Immunol *178*, 6435-6443.
Hidalgo, A., Peired, A.J., Wild, M.K., Vestweber, D., and Frenette, P.S. (2007). Complete identification of E-selectin ligands on neutrophils reveals distinct functions of PSGL-1, ESL-1, and CD44. Immunity *26*, 477-489.
Hiroaki, H., Ago, T., Ito, T., Sumimoto, H., and Kohda, D. (2001). Solution structure of the PX domain, a target of the SH3 domain. Nat Struct Biol *8*, 526-530.
Hodge, R.G., and Ridley, A.J. (2016). Regulating Rho GTPases and their regulators. Nat Rev Mol Cell Biol *17*, 496-510.
Hoesel, B., and Schmid, J.A. (2013). The complexity of NF-κB signaling in inflammation and cancer. Mol Cancer *12*, 86.
Hoffmann, J.J.M.L. (2009). Neutrophil CD64: a diagnostic marker for infection and sepsis. Clin Chem Lab Med *47*.
Horan, K.A., Watanabe, K., Kong, A.M., Bailey, C.G., Rasko, J.E., Sasaki, T., and Mitchell, C.A. (2007). Regulation of FcgammaR-stimulated phagocytosis by the 72-kDa inositol polyphosphate 5-phosphatase: SHIP1, but not the 72-kDa 5-phosphatase, regulates complement receptor 3 mediated phagocytosis by differential recruitment of these 5-phosphatases to the phagocytic cup. Blood *110*, 4480-4491.
Huysamen, C., and Brown, G.D. (2008). The fungal pattern recognition receptor, Dectin-1, and the associated cluster of C-type lectin-like receptors. FEMS Microbiol Lett *290*, 121-128.
Hynes, R.O. (2002). Integrins: bidirectional, allosteric signaling machines. Cell *110*, 673-687.
Hynes, R.O., and Naba, A. (2012). Overview of the matrisome--an inventory of extracellular matrix constituents and functions. Cold Spring Harb Perspect Biol *4*, a004903.
Idevall-Hagren, O., and De Camilli, P. (2015). Detection and manipulation of phosphoinositides. Biochim Biophys Acta *1851*, 736-745.
Infanger, D.W., Sharma, R.V., and Davisson, R.L. (2006). NADPH Oxidases of the Brain: Distribution, Regulation, and Function. Antioxidants & Redox Signaling *8*, 1583-1596.
Jahraus, A., Tjelle, T.E., Berg, T., Habermann, A., Storrie, B., Ullrich, O., and Griffiths, G. (1998). In Vitro Fusion of Phagosomes with Different Endocytic Organelles from J774 Macrophages. J Biol Chem *273*, 30379-30390.
Jakus, Z., Nemeth, T., Verbeek, J.S., and Mocsai, A. (2008). Critical but overlapping role of FcgammaRIII and FcgammaRIV in activation of murine neutrophils by immobilized immune complexes. J Immunol *180*, 618-629.
Jean, S., and Kiger, A.A. (2014). Classes of phosphoinositide 3-kinases at a glance. J Cell Sci *127*, 923-928.
Jeschke, A., and Haas, A. (2016). Deciphering the roles of phosphoinositide lipids in phagolysosome biogenesis. Commun Integr Biol *9*, e1174798.
Jia, Z., Ghai, R., Collins, B.M., and Mark, A.E. (2014). The recognition of membrane-bound PtdIns3P by PX domains. Proteins *82*, 2332-2342.
Jiang, F., Zhang, Y., and Dusting, G.J. (2011). NADPH oxidase-mediated redox signaling: roles in cellular stress response, stress tolerance, and tissue repair. Pharmacol Rev *63*, 218-242.
Jog, N.R., Rane, M.J., Lominadze, G., Luerman, G.C., Ward, R.A., and McLeish, K.R. (2007). The actin cytoskeleton regulates exocytosis of all neutrophil granule subsets. Am J Physiol Cell Physiol *292*, C1690-1700.
Jones, H.R., Robb, C.T., Perretti, M., and Rossi, A.G. (2016). The role of neutrophils in inflammation resolution. Semin Immunol *28*, 137-145.
Kamen, L.A., Levinsohn, J., and Swanson, J.A. (2007). Differential association of phosphatidylinositol 3-kinase, SHIP-1, and PTEN with forming phagosomes. Mol Biol Cell *18*, 2463-2472.
Kanai, F., Liu, H., Field, S.J., Akbary, H., Matsuo, T., Brown, G.E., Cantley, L.C., and Yaffe, M.B. (2001). The PX domains of p47phox and p40phox bind to lipid products of PI(3)K. Nat Cell Biol *3*, 675-678.
Karathanassis, D., Stahelin, R.V., Bravo, J., Perisic, O., Pacold, C.M., Cho, W., and Williams, R.L. (2002). Binding of the PX domain of p47phox to phosphatidylinositol 3,4-bisphosphate and phosphatidic acid is masked by an intramolecular interaction. The EMBO Journal *21*, 5057-5068.
Kawano, Y., Kaneko-Kawano, T., and Shimamoto, K. (2014). Rho family GTPase-dependent immunity in plants and animals. Frontiers in plant science *5*, 522.
Kennedy, A.D., Willment, J.A., Dorward, D.W., Williams, D.L., Brown, G.D., and DeLeo, F.R. (2007). Dectin-1 promotes fungicidal activity of human neutrophils. Eur J Immunol *37*, 467-478.
Kennedy, M.J., Hughes, R.M., Peteya, L.A., Schwartz, J.W., Ehlers, M.D., and Tucker, C.L. (2010). Rapid blue-light-

mediated induction of protein interactions in living cells. Nature methods *7*, 973-975.
Kleniewska, P., Piechota, A., Skibska, B., and Goraca, A. (2012). The NADPH oxidase family and its inhibitors. Arch Immunol Ther Exp (Warsz) *60*, 277-294.
Kretschmer, D., Gleske, A.K., Rautenberg, M., Wang, R., Koberle, M., Bohn, E., Schoneberg, T., Rabiet, M.J., Boulay, F., Klebanoff, S.J.*, et al.* (2010). Human formyl peptide receptor 2 senses highly pathogenic Staphylococcus aureus. Cell host & microbe *7*, 463-473.
Kuhns, D.B., Alvord, W.G., Heller, T., Feld, J.J., Pike, K.M., Marciano, B.E., Uzel, G., DeRavin, S.S., Priel, D.A., Soule, B.P.*, et al.* (2010). Residual NADPH oxidase and survival in chronic granulomatous disease. N Engl J Med *363*, 2600-2610.
Kulkarni, S., Sitaru, C., Jakus, Z., Anderson, K.E., Damoulakis, G., Davidson, K., Hirose, M., Juss, J., Oxley, D., Chessa, T.A.M.*, et al.* (2011). PI3Kβ Plays a Critical Role in Neutrophil Activation by Immune Complexes. Science Signaling *4*, ra23-ra23.
Kuribayashi, F., Nunoi, H., Wakamatsu, K., Tsunawaki, S., Sato, K., Ito, T., and Sumimoto, H. (2002). The adaptor protein p40(phox) as a positive regulator of the superoxide-producing phagocyte oxidase. EMBO J *21*, 6312-6320.
Kutateladze, T.G. (2010). Translation of the phosphoinositide code by PI effectors. Nat Chem Biol *6*, 507-513.
Kwon, J., Lee, S.R., Yang, K.S., Ahn, Y., Kim, Y.J., Stadtman, E.R., and Rhee, S.G. (2004). Reversible oxidation and inactivation of the tumor suppressor PTEN in cells stimulated with peptide growth factors. Proceedings of the National Academy of Sciences *101*, 16419-16424.
Kwong, C.H., Malech, H.L., Rotrosen, D., and Leto, T.L. (1993). Regulation of the human neutrophil NADPH oxidase by rho-related G-proteins. Biochemistry *32*, 5711-5717.
Lambeth, J.D., and Neish, A.S. (2014). Nox enzymes and new thinking on reactive oxygen: a double-edged sword revisited. Annu Rev Pathol *9*, 119-145.
Lapouge, K., Smith, S.J., Groemping, Y., and Rittinger, K. (2002). Architecture of the p40-p47-p67phox complex in the resting state of the NADPH oxidase. A central role for p67phox. J Biol Chem *277*, 10121-10128.
Lapouge, K., Smith, S.J., Walker, P.A., Gamblin, S.J., Smerdon, S.J., and Rittinger, K. (2000). Structure of the TPR domain of p67phox in complex with Rac.GTP. Mol Cell *6*, 899-907.
Le Cabec, V., Carreno, S., Moisand, A., Bordier, C., and Maridonneau-Parini, I. (2002). Complement receptor 3 (CD11b/CD18) mediates type I and type II phagocytosis during nonopsonic and opsonic phagocytosis, respectively. J Immunol *169*, 2003-2009.
Lemmon, M.A. (2008). Membrane recognition by phospholipid-binding domains. Nat Rev Mol Cell Biol *9*, 99-111.
Levay, P.F., and Viljoen, M. (1995). Lactoferrin: a general review. Haematologica *80*, 252-267.
Leverrier, Y., Okkenhaug, K., Sawyer, C., Bilancio, A., Vanhaesebroeck, B., and Ridley, A.J. (2003). Class I Phosphoinositide 3-Kinase p110β Is Required for Apoptotic Cell and Fcγ Receptor-mediated Phagocytosis by Macrophages. J Biol Chem *278*, 38437-38442.
Levin, R., Grinstein, S., and Canton, J. (2016). The life cycle of phagosomes: formation, maturation, and resolution. Immunol Rev *273*, 156-179.
Levin, R., Grinstein, S., and Schlam, D. (2015). Phosphoinositides in phagocytosis and macropinocytosis. Biochim Biophys Acta *1851*, 805-823.
Levin, R., Hammond, G.R.V., Balla, T., De Camilli, P., Fairn, G.D., Grinstein, S., and Parent, C. (2017). Multiphasic dynamics of phosphatidylinositol 4-phosphate during phagocytosis. Mol Biol Cell *28*, 128-140.
Lewis, E.M., Sergeant, S., Ledford, B., Stull, N., Dinauer, M.C., and McPhail, L.C. (2010). Phosphorylation of p22phox on threonine 147 enhances NADPH oxidase activity by promoting p47phox binding. J Biol Chem *285*, 2959-2967.
Li, X., Utomo, A., Cullere, X., Choi, Myunghwan M., Milner, Danny A., Venkatesh, D., Yun, S.-H., and Mayadas, Tanya N. (2011). The β-Glucan Receptor Dectin-1 Activates the Integrin Mac-1 in Neutrophils via Vav Protein Signaling to Promote Candida albicans Clearance. Cell host & microbe *10*, 603-615.
Li, X.J., Marchal, C.C., Stull, N.D., Stahelin, R.V., and Dinauer, M.C. (2010). p47phox Phox Homology Domain Regulates Plasma Membrane but Not Phagosome Neutrophil NADPH Oxidase Activation. J Biol Chem *285*, 35169-35179.
Li, X.J., Tian, W., Stull, N.D., Grinstein, S., Atkinson, S., and Dinauer, M.C. (2009a). A fluorescently tagged C-terminal fragment of p47phox detects NADPH oxidase dynamics during phagocytosis. Mol Biol Cell *20*, 1520-1532.
Li, X.J., Tian, W., Stull, N.D., Grinstein, S., Atkinson, S., and Dinauer, M.C. (2009b). A Fluorescently Tagged C-Terminal Fragment of p47phox Detects NADPH Oxidase Dynamics during Phagocytosis. Mol Biol Cell *20*, 1520-1532.

Liang, C., Feng, P., Ku, B., Dotan, I., Canaani, D., Oh, B.H., and Jung, J.U. (2006). Autophagic and tumour suppressor activity of a novel Beclin1-binding protein UVRAG. Nat Cell Biol *8*, 688-699.
Liang, C., Lee, J.-s., Inn, K.-S., Gack, M.U., Li, Q., Roberts, E.A., Vergne, I., Deretic, V., Feng, P., Akazawa, C.*, et al.* (2008). Beclin1-binding UVRAG targets the class C Vps complex to coordinate autophagosome maturation and endocytic trafficking. Nat Cell Biol *10*, 776-787.
Lin, L.J., Grimme, J.M., Sun, J., Lu, S., Gai, L., Cropek, D.M., and Wang, Y. (2013). The antagonistic roles of PDGF and integrin alphavbeta3 in regulating ROS production at focal adhesions. Biomaterials *34*, 3807-3815.
Lishko, V.K., Kudryk, B., Yakubenko, V.P., Yee, V.C., and Ugarova, T.P. (2002). Regulated unmasking of the cryptic binding site for integrin alpha M beta 2 in the gamma C-domain of fibrinogen. Biochemistry *41*, 12942-12951.
Lishko, V.K., Podolnikova, N.P., Yakubenko, V.P., Yakovlev, S., Medved, L., Yadav, S.P., and Ugarova, T.P. (2004). Multiple binding sites in fibrinogen for integrin alphaMbeta2 (Mac-1). J Biol Chem *279*, 44897-44906.
Liu, L., Elwing, H., Karlsson, A., Nimeri, G., and Dahlgren, C. (1997). Surface-related triggering of the neutrophil respiratory burst. Characterization of the response induced by IgG adsorbed to hydrophilic and hydrophobic glass surfaces. Clin Exp Immunol *109*, 204-210.
Liu, L., Song, X., He, D., Komma, C., Kita, A., Virbasius, J.V., Huang, G., Bellamy, H.D., Miki, K., Czech, M.P.*, et al.* (2006). Crystal structure of the C2 domain of class II phosphatidylinositide 3-kinase C2alpha. J Biol Chem *281*, 4254-4260.
Loike, J.D., Silverstein, R., Wright, S.D., Weitz, J.I., Huang, A.J., and Silverstein, S.C. (1992). The role of protected extracellular compartments in interactions between leukocytes, and platelets, and fibrin/fibrinogen matrices. Ann N Y Acad Sci *667*, 163-172.
Lominadze, G. (2005). Proteomic Analysis of Human Neutrophil Granules. Mol Cell Proteomics *4*, 1503-1521.
Luo, H.R., and Mondal, S. (2015). Molecular control of PtdIns(3,4,5)P3 signaling in neutrophils. EMBO reports *16*, 149-163.
Luzio, J.P., Pryor, P.R., and Bright, N.A. (2007). Lysosomes: fusion and function. Nature Reviews Molecular Cell Biology *8*, 622-632.
Maehara, Y., Miyano, K., and Sumimoto, H. (2009). Role for the first SH3 domain of p67phox in activation of superoxide-producing NADPH oxidases. Biochem Biophys Res Commun *379*, 589-593.
Marcos, V., Zhou, Z., Yildirim, A.O., Bohla, A., Hector, A., Vitkov, L., Wiedenbauer, E.M., Krautgartner, W.D., Stoiber, W., Belohradsky, B.H.*, et al.* (2010). CXCR2 mediates NADPH oxidase-independent neutrophil extracellular trap formation in cystic fibrosis airway inflammation. Nat Med *16*, 1018-1023.
Marcoux, J., Man, P., Castellan, M., Vivès, C., Forest, E., and Fieschi, F. (2009). Conformational changes in p47phoxupon activation highlighted by mass spectrometry coupled to hydrogen/deuterium exchange and limited proteolysis. FEBS Lett *583*, 835-840.
Markart, P., Korfhagen, T.R., Weaver, T.E., and Akinbi, H.T. (2004). Mouse lysozyme M is important in pulmonary host defense against Klebsiella pneumoniae infection. Am J Respir Crit Care Med *169*, 454-458.
Martinez, J., Malireddi, R.K., Lu, Q., Cunha, L.D., Pelletier, S., Gingras, S., Orchard, R., Guan, J.L., Tan, H., Peng, J.*, et al.* (2015). Molecular characterization of LC3-associated phagocytosis reveals distinct roles for Rubicon, NOX2 and autophagy proteins. Nat Cell Biol *17*, 893-906.
Massenet, C., Chenavas, S., Cohen-Addad, C., Dagher, M.C., Brandolin, G., Pebay-Peyroula, E., and Fieschi, F. (2005). Effects of p47phox C terminus phosphorylations on binding interactions with p40phox and p67phox. Structural and functional comparison of p40phox and p67phox SH3 domains. J Biol Chem *280*, 13752-13761.
Matsunaga, K., Noda, T., and Yoshimori, T. (2009a). Binding Rubicon to cross the Rubicon. Autophagy *5*, 876-877.
Matsunaga, K., Saitoh, T., Tabata, K., Omori, H., Satoh, T., Kurotori, N., Maejima, I., Shirahama-Noda, K., Ichimura, T., Isobe, T.*, et al.* (2009b). Two Beclin 1-binding proteins, Atg14L and Rubicon, reciprocally regulate autophagy at different stages. Nat Cell Biol *11*, 385-396.
Matute, J.D., Arias, A.A., Wright, N.A., Wrobel, I., Waterhouse, C.C., Li, X.J., Marchal, C.C., Stull, N.D., Lewis, D.B., Steele, M.*, et al.* (2009). A new genetic subgroup of chronic granulomatous disease with autosomal recessive mutations in p40 phox and selective defects in neutrophil NADPH oxidase activity. Blood *114*, 3309-3315.
Mayadas, T.N., and Cullere, X. (2005). Neutrophil beta2 integrins: moderators of life or death decisions. Trends Immunol *26*, 388-395.
Mayadas, T.N., Cullere, X., and Lowell, C.A. (2014). The multifaceted functions of neutrophils. Annu Rev Pathol *9*, 181-218.
Mayorga, L.S., Bertini, F., and Stahl, P.D. (1991). Fusion of newly formed phagosomes with endosomes in intact cells and in a cell-free system. J Biol Chem *266*, 6511-6517.
McCaffrey, R.L., Schwartz, J.T., Lindemann, S.R., Moreland, J.G., Buchan, B.W., Jones, B.D., and Allen, L.A.H. (2010). Multiple mechanisms of NADPH oxidase inhibition by type A and type B Francisella tularensis. J Leukoc

Biol *88*, 791-805.
McConnachie, G., Pass, I., Walker, S.M., and Downes, C.P. (2003). Interfacial kinetic analysis of the tumour suppressor phosphatase, PTEN: evidence for activation by anionic phospholipids. Biochem J *371*, 947-955.
Metzler, K.D., Fuchs, T.A., Nauseef, W.M., Reumaux, D., Roesler, J., Schulze, I., Wahn, V., Papayannopoulos, V., and Zychlinsky, A. (2011). Myeloperoxidase is required for neutrophil extracellular trap formation: implications for innate immunity. Blood *117*, 953-959.
Miao, B., Skidan, I., Yang, J., Lugovskoy, A., Reibarkh, M., Long, K., Brazell, T., Durugkar, K.A., Maki, J., Ramana, C.V.*, et al.* (2010). Small molecule inhibition of phosphatidylinositol-3,4,5-triphosphate (PIP3) binding to pleckstrin homology domains. Proceedings of the National Academy of Sciences *107*, 20126-20131.
Minakami, R., Maehara, Y., Kamakura, S., Kumano, O., Miyano, K., and Sumimoto, H. (2010). Membrane phospholipid metabolism during phagocytosis in human neutrophils. Genes Cells *15*, 409-424.
Mitchell, T., Lo, A., Logan, M.R., Lacy, P., and Eitzen, G. (2008). Primary granule exocytosis in human neutrophils is regulated by Rac-dependent actin remodeling. Am J Physiol Cell Physiol *295*, C1354-1365.
Mocsai, A., Ruland, J., and Tybulewicz, V.L. (2010). The SYK tyrosine kinase: a crucial player in diverse biological functions. Nat Rev Immunol *10*, 387-402.
Mocsai, A., Walzog, B., and Lowell, C.A. (2015). Intracellular signalling during neutrophil recruitment. Cardiovasc Res *107*, 373-385.
Mondal, S., Subramanian, K.K., Sakai, J., Bajrami, B., and Luo, H.R. (2012). Phosphoinositide lipid phosphatase SHIP1 and PTEN coordinate to regulate cell migration and adhesion. Mol Biol Cell *23*, 1219-1230.
Mosesson, M.W. (2005). Fibrinogen and fibrin structure and functions. J Thromb Haemost *3*, 1894-1904.
Mosesson, M.W., Siebenlist, K.R., and Meh, D.A. (2001). The structure and biological features of fibrinogen and fibrin. Ann N Y Acad Sci *936*, 11-30.
Mott, J. (2002). Effects of Anaplasma phagocytophila on NADPH Oxidase Components in Human Neutrophils and HL-60 Cells. Infect Immun *70*, 1359-1366.
Murphy, K.J., C.A. ; Travers, P. ; Mowat, A. ; Weaver, C.T. (2012). Janeway's immunobiology 8th edition.
Murray, J.T., Panaretou, C., Stenmark, H., Miaczynska, M., and Backer, J.M. (2002). Role of Rab5 in the recruitment of hVps34/p150 to the early endosome. Traffic *3*, 416-427.
Nadzam, G.S., De La Cruz, C., Greco, R.S., and Haimovich, B. (2000). Neutrophil adhesion to vascular prosthetic surfaces triggers nonapoptotic cell death. Ann Surg *231*, 587-599.
Nagata, M. (2005). Inflammatory cells and oxygen radicals. Curr Drug Targets Inflamm Allergy *4*, 503-504.
Nakatsu, F., Perera, R.M., Lucast, L., Zoncu, R., Domin, J., Gertler, F.B., Toomre, D., and De Camilli, P. (2010). The inositol 5-phosphatase SHIP2 regulates endocytic clathrin-coated pit dynamics. The Journal of Cell Biology *190*, 307-315.
Nash, J.A., Ballard, T.N., Weaver, T.E., and Akinbi, H.T. (2006). The peptidoglycan-degrading property of lysozyme is not required for bactericidal activity in vivo. J Immunol *177*, 519-526.
Nathan, C., Srimal, S., Farber, C., Sanchez, E., Kabbash, L., Asch, A., Gailit, J., and Wright, S.D. (1989). Cytokine-induced respiratory burst of human neutrophils: dependence on extracellular matrix proteins and CD11/CD18 integrins. J Cell Biol *109*, 1341-1349.
Nauseef, W.M. (2008). Biological Roles for the NOX Family NADPH Oxidases. J Biol Chem *283*, 16961-16965.
Nauseef, W.M., and Borregaard, N. (2014). Neutrophils at work. Nat Immunol *15*, 602-611.
Nauseef, W.M., Volpp, B.D., McCormick, S., Leidal, K.G., and Clark, R.A. (1991). Assembly of the neutrophil respiratory burst oxidase. Protein kinase C promotes cytoskeletal and membrane association of cytosolic oxidase components. J Biol Chem *266*, 5911-5917.
Neeli, I., Dwivedi, N., Khan, S., and Radic, M. (2009). Regulation of extracellular chromatin release from neutrophils. J Innate Immun *1*, 194-201.
Nobuhisa, I., Takeya, R., Ogura, K., Ueno, N., Kohda, D., Inagaki, F., and Sumimoto, H. (2006). Activation of the superoxide-producing phagocyte NADPH oxidase requires co-operation between the tandem SH3 domains of p47phox in recognition of a polyproline type II helix and an adjacent alpha-helix of p22phox. Biochem J *396*, 183-192.
Nunes, P., Demaurex, N., and Dinauer, M.C. (2013). Regulation of the NADPH oxidase and associated ion fluxes during phagocytosis. Traffic *14*, 1118-1131.
Ogura, K., Nobuhisa, I., Yuzawa, S., Takeya, R., Torikai, S., Saikawa, K., Sumimoto, H., and Inagaki, F. (2006). NMR solution structure of the tandem Src homology 3 domains of p47phox complexed with a p22phox-derived proline-rich peptide. J Biol Chem *281*, 3660-3668.
Palaniyar, N., Jhunjhunwala, S., Aresta-DaSilva, S., Tang, K., Alvarez, D., Webber, M.J., Tang, B.C., Lavin, D.M., Veiseh, O., Doloff, J.C.*, et al.* (2015). Neutrophil Responses to Sterile Implant Materials. PLoS One *10*, e0137550.
Pan, L., Zhao, Y., Yuan, Z., and Qin, G. (2016). Research advances on structure and biological functions of

integrins. Springerplus *5*, 1094.
Panday, A., Sahoo, M.K., Osorio, D., and Batra, S. (2015). NADPH oxidases: an overview from structure to innate immunity-associated pathologies. Cell Mol Immunol *12*, 5-23.
Papakonstanti, E.A., Ridley, A.J., and Vanhaesebroeck, B. (2007). The p110delta isoform of PI 3-kinase negatively controls RhoA and PTEN. EMBO J *26*, 3050-3061.
Peyron, P., Maridonneau-Parini, I., and Stegmann, T. (2001). Fusion of Human Neutrophil Phagosomes with Lysosomes in Vitro: INVOLVEMENT OF TYROSINE KINASES OF THE Src FAMILY AND INHIBITION BY MYCOBACTERIA. J Biol Chem *276*, 35512-35517.
Plato, A., Willment, J.A., and Brown, G.D. (2013). C-Type Lectin-Like Receptors of the Dectin-1 Cluster: Ligands and Signaling Pathways. Int Rev Immunol *32*, 134-156.
Price, L.S., Langeslag, M., ten Klooster, J.P., Hordijk, P.L., Jalink, K., and Collard, J.G. (2003). Calcium signaling regulates translocation and activation of Rac. J Biol Chem *278*, 39413-39421.
Pulanic, D., and Rudan, I. (2005). The past decade: fibrinogen. Coll Antropol *29*, 341-349.
Raad, H., Paclet, M.H., Boussetta, T., Kroviarski, Y., Morel, F., Quinn, M.T., Gougerot-Pocidalo, M.A., Dang, P.M.C., and El-Benna, J. (2008). Regulation of the phagocyte NADPH oxidase activity: phosphorylation of gp91phox/NOX2 by protein kinase C enhances its diaphorase activity and binding to Rac2, p67phox, and p47phox. The FASEB Journal *23*, 1011-1022.
Raess, M.A., Friant, S., Cowling, B.S., and Laporte, J. (2017). WANTED – Dead or alive: Myotubularins, a large disease-associated protein family. Advances in Biological Regulation *63*, 49-58.
Rakhit, R., Navarro, R., and Wandless, Thomas J. (2014). Chemical Biology Strategies for Posttranslational Control of Protein Function. Chem Biol *21*, 1238-1252.
Riechelmann, H. (2004). Cellular and molecular mechanisms in environmental and occupational inhalation toxicology. GMS Curr Top Otorhinolaryngol Head Neck Surg *3*, Doc02.
Robinson, F.L., and Dixon, J.E. (2006). Myotubularin phosphatases: policing 3-phosphoinositides. Trends Cell Biol *16*, 403-412.
Robinson, J.M. (2008). Reactive oxygen species in phagocytic leukocytes. Histochem Cell Biol *130*, 281-297.
Rosenzweig, S.D., and Holland, S.M. (2004). Phagocyte immunodeficiencies and their infections. J Allergy Clin Immunol *113*, 620-626.
Ross, G.D. (2000). Regulation of the adhesion versus cytotoxic functions of the Mac-1/CR3/alphaMbeta2-integrin glycoprotein. Crit Rev Immunol *20*, 197-222.
Rubel, C., Fernandez, G.C., Dran, G., Bompadre, M.B., Isturiz, M.A., and Palermo, M.S. (2001). Fibrinogen Promotes Neutrophil Activation and Delays Apoptosis. The Journal of Immunology *166*, 2002-2010.
Russell, E.G., and Cotter, T.G. (2015). New Insight into the Role of Reactive Oxygen Species (ROS) in Cellular Signal-Transduction Processes. Int Rev Cell Mol Biol *319*, 221-254.
Sadhu, C., Masinovsky, B., Dick, K., Sowell, C.G., and Staunton, D.E. (2003). Essential Role of Phosphoinositide 3-Kinase in Neutrophil Directional Movement. The Journal of Immunology *170*, 2647-2654.
Sankaran, V.G., and Weiss, M.J. (2015). Anemia: progress in molecular mechanisms and therapies. Nat Med *21*, 221-230.
Schu, P.V., Takegawa, K., Fry, M.J., Stack, J.H., Waterfield, M.D., and Emr, S.D. (1993). Phosphatidylinositol 3-kinase encoded by yeast VPS34 gene essential for protein sorting. Science *260*, 88-91.
Seet, L.F., and Hong, W. (2006). The Phox (PX) domain proteins and membrane traffic. Biochim Biophys Acta *1761*, 878-896.
Sengeløv, H., Kjeldsen, L., Diamond, M.S., Springer, T.A., and Borregaard, N. (1993). Subcellular localization and dynamics of Mac-1 (alpha m beta 2) in human neutrophils. J Clin Invest *92*, 1467-1476.
Serrano, C.V., Mikhail, E.A., Wang, P., Noble, B., Kuppusamy, P., and Zweier, J.L. (1996). Superoxide and hydrogen peroxide induce CD18-mediated adhesion in the postischemic heart. Biochimica et Biophysica Acta (BBA) - Molecular Basis of Disease *1316*, 191-202.
Shacter, E., Williams, J.A., Lim, M., and Levine, R.L. (1994). Differential susceptibility of plasma proteins to oxidative modification: examination by western blot immunoassay. Free Radic Biol Med *17*, 429-437.
Shao, D., Segal, A.W., and Dekker, L.V. (2010). Subcellular localisation of the p40phox component of NADPH oxidase involves direct interactions between the Phox homology domain and F-actin. The International Journal of Biochemistry & Cell Biology *42*, 1736-1743.
Shewan, A., Eastburn, D.J., and Mostov, K. (2011). Phosphoinositides in Cell Architecture. Cold Spring Harb Perspect Biol *3*, a004796-a004796.
Shi, C., Zhang, X., Chen, Z., Robinson, M.K., and Simon, D.I. (2001). Leukocyte integrin Mac-1 recruits toll/interleukin-1 receptor superfamily signaling intermediates to modulate NF-kappaB activity. Circ Res *89*, 859-865.

Smith, R.M., Connor, J.A., Chen, L.M., and Babior, B.M. (1996). The cytosolic subunit p67phox contains an NADPH-binding site that participates in catalysis by the leukocyte NADPH oxidase. J Clin Invest *98*, 977-983.
Song, M.S., Salmena, L., and Pandolfi, P.P. (2012). The functions and regulation of the PTEN tumour suppressor. Nature Reviews Molecular Cell Biology.
Song, X., Xu, W., Zhang, A., Huang, G., Liang, X., Virbasius, J.V., Czech, M.P., and Zhou, G.W. (2001). Phox homology domains specifically bind phosphatidylinositol phosphates. Biochemistry *40*, 8940-8944.
Sorensen, O.E., Follin, P., Johnsen, A.H., Calafat, J., Tjabringa, G.S., Hiemstra, P.S., and Borregaard, N. (2001). Human cathelicidin, hCAP-18, is processed to the antimicrobial peptide LL-37 by extracellular cleavage with proteinase 3. Blood *97*, 3951-3959.
Spang, A. (2009). On the fate of early endosomes. Biol Chem *390*.
Sperandio, M., Gleissner, C.A., and Ley, K. (2009). Glycosylation in immune cell trafficking. Immunol Rev *230*, 97-113.
Stahelin, R.V., Karathanassis, D., Bruzik, K.S., Waterfield, M.D., Bravo, J., Williams, R.L., and Cho, W. (2006). Structural and Membrane Binding Analysis of the Phox Homology Domain of Phosphoinositide 3-Kinase-C2 J Biol Chem *281*, 39396-39406.
Stanley, A., Thompson, K., Hynes, A., Brakebusch, C., and Quondamatteo, F. (2014). NADPH oxidase complex-derived reactive oxygen species, the actin cytoskeleton, and Rho GTPases in cell migration. Antioxid Redox Signal *20*, 2026-2042.
Stasia, M.J. (2016). CYBA encoding p22phox, the cytochrome b558 alpha polypeptide: gene structure, expression, role and physiopathology. Gene *586*, 27-35.
Stein, M.P., Feng, Y., Cooper, K.L., Welford, A.M., and Wandinger-Ness, A. (2003). Human VPS34 and p150 are Rab7 interacting partners. Traffic *4*, 754-771.
Stephens, L., Milne, L., and Hawkins, P. (2008). Moving towards a Better Understanding of Chemotaxis. Curr Biol *18*, R485-R494.
Stoyanova, S., Bulgarelli-Leva, G., Kirsch, C., Hanck, T., Klinger, R., Wetzker, R., and Wymann, M.P. (1997). Lipid kinase and protein kinase activities of G-protein-coupled phosphoinositide 3-kinase gamma: structure-activity analysis and interactions with wortmannin. Biochem J *324 (Pt 2)*, 489-495.
Suh, C.I., Stull, N.D., Li, X.J., Tian, W., Price, M.O., Grinstein, S., Yaffe, M.B., Atkinson, S., and Dinauer, M.C. (2006). The phosphoinositide-binding protein p40phox activates the NADPH oxidase during FcgammaIIA receptor-induced phagocytosis. J Exp Med *203*, 1915-1925.
Suire, S., Condliffe, A.M., Ferguson, G.J., Ellson, C.D., Guillou, H., Davidson, K., Welch, H., Coadwell, J., Turner, M., Chilvers, E.R., *et al.* (2006). Gβγs and the Ras binding domain of p110γ are both important regulators of PI(3)Kγ signalling in neutrophils. Nat Cell Biol *8*, 1303-1309.
Sun, Q., Zhang, J., Fan, W., Wong, K.N., Ding, X., Chen, S., and Zhong, Q. (2010). The RUN Domain of Rubicon Is Important for hVps34 Binding, Lipid Kinase Inhibition, and Autophagy Suppression. J Biol Chem *286*, 185-191.
Sun, Q., Zhang, J., Fan, W., Wong, K.N., Ding, X., Chen, S., and Zhong, Q. (2011). The RUN domain of rubicon is important for hVps34 binding, lipid kinase inhibition, and autophagy suppression. J Biol Chem *286*, 185-191.
Tamura, M., Kai, T., Tsunawaki, S., Lambeth, J.D., and Kameda, K. (2000). Direct interaction of actin with p47(phox) of neutrophil NADPH oxidase. Biochem Biophys Res Commun *276*, 1186-1190.
Tetik, S., Kaya, K., and Yardimci, T. (2011). Effect of oxidized fibrinogen on hemostatic system: in vitro study. Clin Appl Thromb Hemost *17*, 259-263.
Theocharis, A.D., Skandalis, S.S., Gialeli, C., and Karamanos, N.K. (2016). Extracellular matrix structure. Advanced Drug Delivery Reviews *97*, 4-27.
Thevenot, P., Hu, W., and Tang, L. (2008). Surface chemistry influences implant biocompatibility. Curr Top Med Chem *8*, 270-280.
Thorpe, L.M., Yuzugullu, H., and Zhao, J.J. (2015). PI3K in cancer: divergent roles of isoforms, modes of activation and therapeutic targeting. Nat Rev Cancer *15*, 7-24.
Tlili, A., Erard, M., Faure, M.C., Baudin, X., Piolot, T., Dupre-Crochet, S., and Nusse, O. (2012). Stable accumulation of p67phox at the phagosomal membrane and ROS production within the phagosome. J Leukoc Biol *91*, 83-95.
Tridandapani, S., Nigorikawa, K., Hazeki, K., Sasaki, J., Omori, Y., Miyake, M., Morioka, S., Guo, Y., Sasaki, T., and Hazeki, O. (2015). Inositol Polyphosphate-4-Phosphatase Type I Negatively Regulates Phagocytosis via Dephosphorylation of Phagosomal PtdIns(3,4)P2. PLoS One *10*, e0142091.
Turvey, S.E., and Broide, D.H. (2010). Innate immunity. J Allergy Clin Immunol *125*, S24-S32.
Tzenaki, N., and Papakonstanti, E.A. (2013). p110δ PI3 kinase pathway: emerging roles in cancer. Front Oncol *3*.
Ugarova, T.P., Solovjov, D.A., Zhang, L., Loukinov, D.I., Yee, V.C., Medved, L.V., and Plow, E.F. (1998). Identification of a novel recognition sequence for integrin alphaM beta2 within the gamma-chain of fibrinogen. J Biol Chem

273, 22519-22527.
Ugarova, T.P., and Yakubenko, V.P. (2001). Recognition of fibrinogen by leukocyte integrins. Ann N Y Acad Sci *936*, 368-385.
Underhill, D.M. (2005). Dectin-1 activates Syk tyrosine kinase in a dynamic subset of macrophages for reactive oxygen production. Blood *106*, 2543-2550.
Underhill, D.M., and Ozinsky, A. (2002). Phagocytosis of microbes: complexity in action. Annu Rev Immunol *20*, 825-852.
Upchurch Jr, G.R., Ramdev, N., Walsh, M.T., and Loscalzo, J. (1998). Prothrombotic Consequences of the Oxidation of Fibrinogen and their Inhibition by Aspirin. J Thromb Thrombolysis *5*, 9-14.
Urban, C.F., Ermert, D., Schmid, M., Abu-Abed, U., Goosmann, C., Nacken, W., Brinkmann, V., Jungblut, P.R., and Zychlinsky, A. (2009). Neutrophil extracellular traps contain calprotectin, a cytosolic protein complex involved in host defense against Candida albicans. PLoS Pathog *5*, e1000639.
van den Berg, J.M., Weyer, S., Weening, J.J., Roos, D., and Kuijpers, T.W. (2001). Divergent effects of tumor necrosis factor alpha on apoptosis of human neutrophils. J Leukoc Biol *69*, 467-473.
Vanhaesebroeck, B., Guillermet-Guibert, J., Graupera, M., and Bilanges, B. (2010). The emerging mechanisms of isoform-specific PI3K signalling. Nature Reviews Molecular Cell Biology *11*, 329-341.
Vanhaesebroeck, B., Welham, M.J., Kotani, K., Stein, R., Warne, P.H., Zvelebil, M.J., Higashi, K., Volinia, S., Downward, J., and Waterfield, M.D. (1997). P110delta, a novel phosphoinositide 3-kinase in leukocytes. Proc Natl Acad Sci U S A *94*, 4330-4335.
Vanhaesebroeck, B., Whitehead, M.A., and Piñeiro, R. (2016). Molecules in medicine mini-review: isoforms of PI3K in biology and disease. J Mol Med *94*, 5-11.
Velichkova, M., Juan, J., Kadandale, P., Jean, S., Ribeiro, I., Raman, V., Stefan, C., and Kiger, A.A. (2010). Drosophila Mtm and class II PI3K coregulate a PI(3)P pool with cortical and endolysosomal functions. The Journal of Cell Biology *190*, 407-425.
Vieira, O.V., Botelho, R.J., Rameh, L., Brachmann, S.M., Matsuo, T., Davidson, H.W., Schreiber, A., Backer, J.M., Cantley, L.C., and Grinstein, S. (2001). Distinct roles of class I and class III phosphatidylinositol 3-kinases in phagosome formation and maturation. J Cell Biol *155*, 19-25.
Villanueva, E., Yalavarthi, S., Berthier, C.C., Hodgin, J.B., Khandpur, R., Lin, A.M., Rubin, C.J., Zhao, W., Olsen, S.H., Klinker, M.*, et al.* (2011). Netting neutrophils induce endothelial damage, infiltrate tissues, and expose immunostimulatory molecules in systemic lupus erythematosus. J Immunol *187*, 538-552.
Volinia, S., Dhand, R., Vanhaesebroeck, B., MacDougall, L.K., Stein, R., Zvelebil, M.J., Domin, J., Panaretou, C., and Waterfield, M.D. (1995). A human phosphatidylinositol 3-kinase complex related to the yeast Vps34p-Vps15p protein sorting system. EMBO J *14*, 3339-3348.
Voß, S., Klewer, L., and Wu, Y.-W. (2015). Chemically induced dimerization: reversible and spatiotemporal control of protein function in cells. Curr Opin Chem Biol *28*, 194-201.
Vowells, S.J., Fleisher, T.A., Sekhsaria, S., Alling, D.W., Maguire, T.E., and Malech, H.L. (1996). Genotype-dependent variability in flow cytometric evaluation of reduced nicotinamide adenine dinucleotide phosphate oxidase function in patients with chronic granulomatous disease. J Pediatr *128*, 104-107.
Watanabe, S., and Boucrot, E. (2017). Fast and ultrafast endocytosis. Curr Opin Cell Biol *47*, 64-71.
Wegener, K.L., and Campbell, I.D. (2008). Transmembrane and cytoplasmic domains in integrin activation and protein-protein interactions (review). Mol Membr Biol *25*, 376-387.
Weisel, J.W. (2005). Fibrinogen and fibrin. Adv Protein Chem *70*, 247-299.
Winkler, I.G., Barbier, V., Wadley, R., Zannettino, A.C., Williams, S., and Levesque, J.P. (2010). Positioning of bone marrow hematopoietic and stromal cells relative to blood flow in vivo: serially reconstituting hematopoietic stem cells reside in distinct nonperfused niches. Blood *116*, 375-385.
Winterbourn, C.C., Hampton, M.B., Livesey, J.H., and Kettle, A.J. (2006). Modeling the reactions of superoxide and myeloperoxidase in the neutrophil phagosome: implications for microbial killing. J Biol Chem *281*, 39860-39869.
Woodman, R.C., Ruedi, J.M., Jesaitis, A.J., Okamura, N., Quinn, M.T., Smith, R.M., Curnutte, J.T., and Babior, B.M. (1991). Respiratory burst oxidase and three of four oxidase-related polypeptides are associated with the cytoskeleton of human neutrophils. J Clin Invest *87*, 1345-1351.
Woolley, J.F., Stanicka, J., and Cotter, T.G. (2013). Recent advances in reactive oxygen species measurement in biological systems. Trends Biochem Sci *38*, 556-565.
Worby, C.A., and Dixon, J.E. (2014). Pten. Annu Rev Biochem *83*, 641-669.
Wright, H.L., Moots, R.J., Bucknall, R.C., and Edwards, S.W. (2010). Neutrophil function in inflammation and inflammatory diseases. Rheumatology *49*, 1618-1631.
Yaffe, M.B. (2002). The p47phox PX domain: two heads are better than one! Structure *10*, 1288-1290.

Yakovlev, S., Litvinovich, S., Loukinov, D., and Medved, L. (2000a). Role of the beta-strand insert in the central domain of the fibrinogen gamma-module. Biochemistry *39*, 15721-15729.
Yakovlev, S., Loukinov, D., and Medved, L. (2001). Structural and functional role of the beta-strand insert (gamma 381-390) in the fibrinogen gamma-module. A "pull out" hypothesis. Ann N Y Acad Sci *936*, 122-124.
Yakovlev, S., Makogonenko, E., Kurochkina, N., Nieuwenhuizen, W., Ingham, K., and Medved, L. (2000b). Conversion of fibrinogen to fibrin: mechanism of exposure of tPA- and plasminogen-binding sites. Biochemistry *39*, 15730-15741.
Yakovlev, S., Zhang, L., Ugarova, T., and Medved, L. (2005). Interaction of fibrin(ogen) with leukocyte receptor alpha M beta 2 (Mac-1): further characterization and identification of a novel binding region within the central domain of the fibrinogen gamma-module. Biochemistry *44*, 617-626.
Yang, C.S., Lee, J.S., Rodgers, M., Min, C.K., Lee, J.Y., Kim, H.J., Lee, K.H., Kim, C.J., Oh, B., Zandi, E.*, et al.* (2012). Autophagy protein Rubicon mediates phagocytic NADPH oxidase activation in response to microbial infection or TLR stimulation. Cell host & microbe *11*, 264-276.
Yang, J.-M., Nguyen, H.-N., Sesaki, H., Devreotes, P.N., and Iijima, M. (2015). Engineering PTEN function: Membrane association and activity. Methods *77-78*, 119-124.
Ye, R.D., Boulay, F., Wang, J.M., Dahlgren, C., Gerard, C., Parmentier, M., Serhan, C.N., and Murphy, P.M. (2009). International Union of Basic and Clinical Pharmacology. LXXIII. Nomenclature for the formyl peptide receptor (FPR) family. Pharmacol Rev *61*, 119-161.
Yu, L. (1999). Biosynthesis of Flavocytochrome b558. gp91phox IS SYNTHESIZED AS A 65-kDa PRECURSOR (p65) IN THE ENDOPLASMIC RETICULUM. J Biol Chem *274*, 4364-4369.
Yuzawa, S., Ogura, K., Horiuchi, M., Suzuki, N.N., Fujioka, Y., Kataoka, M., Sumimoto, H., and Inagaki, F. (2004a). Solution structure of the tandem Src homology 3 domains of p47phox in an autoinhibited form. J Biol Chem *279*, 29752-29760.
Yuzawa, S., Suzuki, N.N., Fujioka, Y., Ogura, K., Sumimoto, H., and Inagaki, F. (2004b). A molecular mechanism for autoinhibition of the tandem SH3 domains of p47phox, the regulatory subunit of the phagocyte NADPH oxidase. Genes Cells *9*, 443-456.
Zarbock, A., and Ley, K. (2008). Mechanisms and consequences of neutrophil interaction with the endothelium. Am J Pathol *172*, 1-7.
Zhan, S., Vazquez, N., Zhan, S., Wientjes, F.B., Budarf, M.L., Schrock, E., Ried, T., Green, E.D., and Chanock, S.J. (1996). Genomic structure, chromosomal localization, start of transcription, and tissue expression of the human p40-phox, a new component of the nicotinamide adenine dinucleotide phosphate-oxidase complex. Blood *88*, 2714-2721.
Zhang, K., and Chen, J. (2014). The regulation of integrin function by divalent cations. Cell Adhesion & Migration *6*, 20-29.
Zhang, X.C., Piccini, A., Myers, M.P., Van Aelst, L., and Tonks, N.K. (2012). Functional analysis of the protein phosphatase activity of PTEN. Biochem J *444*, 457-464.
Zhao, T., Benard, V., Bohl, B.P., and Bokoch, G.M. (2003). The molecular basis for adhesion-mediated suppression of reactive oxygen species generation by human neutrophils. J Clin Invest *112*, 1732-1740.
Zhao, W., Qiu, Y., and Kong, D. (2017). Class I phosphatidylinositol 3-kinase inhibitors for cancer therapy. Acta Pharmaceutica Sinica B *7*, 27-37.
Zhong, Y., Wang, Q.J., Li, X., Yan, Y., Backer, J.M., Chait, B.T., Heintz, N., and Yue, Z. (2009a). Distinct regulation of autophagic activity by Atg14L and Rubicon associated with Beclin 1-phosphatidylinositol-3-kinase complex. Nat Cell Biol *11*, 468-476.
Zhong, Y., Wang, Q.J., and Yue, Z. (2009b). Atg14L and Rubicon: yin and yang of Beclin 1-mediated autophagy control. Autophagy *5*, 890-891.

Résumé

Les neutrophiles participent à la défense de l'hôte en phagocytant les agents pathogènes et en les détruisant via notamment la production de formes réactives de l'oxygène (FRO). Les FRO sont produites par un complexe multi-protéique : la NADPH oxydase (NOX2). Celle-ci peut s'assembler à la membrane du phagosome lors de la phagocytose mais aussi à la membrane plasmique lors de la stimulation des neutrophiles par des agents bactériens ou des médiateurs de l'inflammation. La NADPH oxydase est une arme à double tranchant; une activation excessive ou inappropriée de la NADPH oxydase génère un stress oxydant, facteur aggravant des nombreuses pathologies. Cette enzyme doit donc être finement régulée. La NADPH oxydase est activée lorsque les sous-unités cytosoliques de NOX2 ($p67^{phox}$, $p47^{phox}$, $p40^{phox}$) et la petite GTPase Rac s'assemblent avec les sous-unités membranaires ($p22^{phox}$ et $gp91^{phox}$). $P67^{phox}$ régule le flux d'électrons qui transite via $gp91^{phox}$ du NADPH à $O_2^{\cdot-}$. Des travaux récents indiquent que les phospholipides anioniques contribueraient à la régulation de la NADPH oxydase. De plus, les protéines organisatrices $p40^{phox}$ et $p47^{phox}$ possèdent des domaines de liaison à ces phosphoinositides : $p40^{phox}$ peut se lier au phosphatidylinositol 3-phosphate (PI(3)P) et $p47^{phox}$ au phosphatidylinositol 3,4-bisphosphate ($PI(3,4)P_2$). Nous avons donc voulu comprendre le rôle de ces phospholipides dans la régulation de la NADPH oxydase.

Dans un premier temps nous avons examiné le rôle du PI(3)P, présent au phagosome après la fermeture de celui-ci, dans l'activation de la NADPH oxydase. Nous avons constaté que Vps34 IN1, un inhibiteur spécifique de la phosphoinositide 3-Kinase (PI3K) de classe 3, qui génère du PI(3)P, diminue la production de FRO à la fois dans une lignée cellulaire différenciée en neutrophile, PLB-985, et dans les neutrophiles humains. L'ajout de

wortmannine, un inhibiteur des PI3K, provoque le disparition prématurée du PI(3)P, de $p40^{phox}$ et $p67^{phox}$ du phagosome. Une augmentation du PI(3)P au niveau du phagosome, dans des cellules transfectées par des siRNA contre Rubicon, une protéine contrôlant l'activité de la PI3K, et / ou contre une phosphoinositide 3-phosphatase, MTM1, augmente la production des FRO à l'intérieur du phagosome et provoque la rétention de $p67^{phox}$ au phagosome. En outre, la régulation négative du PI(3)P au niveau de la membrane du phagosome, par la surexpression de MTM1, empêche la production de FRO et l'accumulation de $p67^{phox}$ au phagosome. Nos données suggèrent que $p40^{phox}$ fonctionne comme un adaptateur, PI(3)P dépendant, permettant de maintenir $p67^{phox}$ dans le complexe de la NADPH oxydase. Le PI(3)P agit donc comme un « timer » pour l'activation de la NADPH oxydase.

Nous avons ensuite voulu examiner le rôle du $PI(3,4)P_2$ dans la régulation de la NADPH oxydase à la membrane plasmique. Ce lipide est formé à la membrane plasmique par phosphorylation du PI(4)P par la PI3K de classe I lors de l'activation des neutrophiles.

Nous avons découvert que les cellules PLB-985 et les neutrophiles humains adhérents au fibrinogène et, stimulés ou non par un peptide bactérien (fmlf), produisaient des FRO de façon soutenue et prolongée. L'addition de LY294002 (un inhibiteur de la PI3K de classe I) met fin à cette production de FRO dépendante des intégrines. $P47^{phox}$, $p67^{phox}$ et $p40^{phox}$ sont distribuées au niveau de la membrane plasmique sous forment de « patches ». Ces patches disparaissent après l'addition de DPI (un inhibiteur de la NADPH oxydase) et de LY294002. La surexpression d'un mutant constitutivement actif de Rac, GFP-Rac1G12V, augmente la production de FRO mais n'empêche pas la diminution de celle-ci suite à l'inhibition de la PI3K. Dans cellules de PLB différenciées exprimant un mutant de $p47^{phox}$, qui ne peut se lier au $PI(3,4)P_2$, la stimulation des intégrines via la liaison au fibrinogène n'induit pas la

production de FRO. En conclusion, l'activité PI3K de classe I est nécessaire pour maintenir l’activation, intégrine-dépendante, de la NADPH oxydase.

université PARIS-SACLAY
ÉCOLE DOCTORALE
Signalisation et réseaux intégratifs en biologie (BIOSIGNE)

Titre : Le rôle des phosphoinositides dans la régulation de la régulation de l'activation de la NADPH oxydase des neutrophiles

Mots clés : Phagocytose, NADPH oxydase, FRO, phosphoinositides

Résumé : Les neutrophiles participent à la défense de l'hôte en phagocytant les agents pathogènes et en les détruisant via notamment la production de formes réactives de l'oxygène (FRO). Les FRO sont produites par un complexe multi-protéique :la NADPH oxydase (NOX2). Celle-ci peut s'assembler à la membrane du phagosome lors de la phagocytose mais aussi à la membrane plasmique lors de la stimulation des neutrophiles par des agents bactériens ou des médiateurs de l'inflammation. La NADPH oxydase est une arme à double tranchant; une activation excessive ou inappropriée de la NADPH oxydase génère un stress oxydant, facteur aggravant des nombreuses pathologies. Cette enzyme doit donc être finement régulée. La NADPH oxydase est activée lorsque les sous-unités cytosoliques de NOX2 ($p67^{phox}$, $p47^{phox}$, $p40^{phox}$) et la petite GTPase Rac s'assemblent avec les sous-unités membranaires ($p22^{phox}$ et $gp91^{phox}$) à la membrane phagosomale ou plasmique. $P67^{phox}$ régule le flux d'électrons qui transite via $gp91^{phox}$ du NADPH à $O_2^{\cdot-}$. Des travaux récents indiquent que les phospholipides anioniques contribueraient à la régulation de la NADPH oxydase. De plus, Les protéines organisatrices $p40^{phox}$ et $p47^{phox}$ possèdent des domaines de liaison à ces phosphoinositides : p40phox peut se lier au phosphatidylinositol 3-phosphate (PI(3)P) et $p47^{phox}$ au phosphatidylinositol 3,4-bisphosphate ($PI(3,4)P_2$).Nous avons donc voulu comprendre le rôle des ces phospholipides dans la régulation de la NADPH oxydase. Dans un premier temps nous nous sommes intéressés au rôle du PI(3)P, présent au phagosome après la fermeture de celui-ci, dans l'activation de la NADPH oxydase. Nos données indiquent que $p40^{phox}$ fonctionne comme un adaptateur, PI(3)P dépendant, permettant de maintenir $p67^{phox}$ dans le complexe de la NADPH oxydase. Le PI(3)P agit comme un « timer » pour l'activation de la NADPH oxydase au phagosome. Nous avons ensuite voulu examiner le rôle du $PI(3,4)P_2$ dans la régulation de la NADPH oxydase à la membrane plasmique. Ce lipide est formé à la membrane plasmique par phosphorylation du PI(4)P par la PI3K de classe I lors de l'activation des neutrophiles. Nous avons montré que, l'activité PI3K de classe I est nécessaire pour maintenir l'activation, intégrine-dépendante, de la NADPH oxydase à la membrane plasmique.

Titre : The role of phosphoinositides in the regulation of NADPH oxidase activation in neutrophils

Mots clés : Phagocytosis, NADPH oxidase, ROS, phosphoinositides

Résumé : The NADPH oxidase of the professional phagocyte is essential for the immune system. The phagocyte NADPH oxidase, NOX2, catalyze the reduction of molecular oxygen to superoxide. Superoxide is transformed rapidly into other reactive oxygen species (ROS) which play a critical role in the killing of pathogens in host defense. Indeed neutrophils, the first cells that arrive at the site of infections, engulf pathogens in a process called phagocytosis. The production of reactive oxygen species is then triggered by the NADPH oxidase in the phagosome. The importance of ROS production is demonstrated by the recurrent bacterial and fungal infections that face patients who lack functional NADPH oxidase as in the rare genetic disorder known as the chronic granulomatous disease (CGD). Upon stimulation by bacterial peptide or in some pathological conditions, NADPH oxidase can also be activated at the phagocyte plasma membrane producing ROS in the extracellular medium. So, an excessive or inappropriate NADPH oxidase activation generates oxidative stress involve in chronic inflammation, cardiovascular disease and neurodegenerative disease. The NADPH oxidase activity should be tightly regulated. The activity of the enzyme is the result of the assembly of cytosolic subunits ($p47^{phox}$, $p67^{phox}$, $p40^{phox}$ and Rac2) with membranous subunits ($gp91^{phox}$ and $p22^{phox}$). $P67^{phox}$ regulates the electron flow through $gp91^{phox}$ from NADPH to oxygen leading to the formation of superoxide. Recent data indicate that the anionic phospholipids are important for the NADPH oxidase regulation. Moreover, p40phox and $p47^{phox}$ bear a PX domain that binds respectively phosphatidylinositol3-phosphate (PI(3)P) and phosphatidylinositol (3,4)-bisphosphate($PI(3,4)P_2$). Our objective was to decipher the importance of these phosphoinositides on the NADPH oxidase activity. We first examined the role of PI(3)P, which is present on the cytosolic leaflet of phagosome after its sealing, in NADPH oxidase activation. Our data indicate that $p40^{phox}$ works as a late adaptor controlled by PI(3)P to maintain p67phox in the NADPH oxidase complex. Thus, PI(3)P acts as a timer for NADPH oxidase assembly. We then examined the role of PI(3,4)P2 in the activation of the NADPH oxidase assembled at the plasma membrane. PI(3,4)P2 and PI(3,4,5)P3 are formed at the plasma membrane, upon neutrophil activation, by phosphorylation by Class I PI3K of respectively PI(4)P and PI(4,5)P2. We found that class I PI3K activity is required to maintain the integrin-dependent activation of NADPH oxidase at the plasma membrane.